Modelling and Control of Agitation-Sedation Dynamics in Critically Ill Patients

Andrew David Rudge

A thesis presented for the degree of
Doctor of Philosophy
in
Mechanical Engineering
at the
University of Canterbury,
Christchurch, New Zealand.

6 November 2005

Acknowledgements

Many people have played an important role in the completion of this thesis, the progress of this research, and my development over the last three years. I would like to thank each one for the role they have played, and the impact they have had on this research and on my life. In particular, I would like to acknowledge my primary supervisors, Associate Professor J. Geoffrey Chase and Dr. Geoffrey Shaw, and thank them for their guidance and support. Not only have they provided excellent supervision, but they have also gone beyond their call of duty to ensure my professional development. Dr Chris Hann's encouragement and technical support was invaluable at critical times in the writing of this thesis, and I wish to thank him specifically for that. I would also like to thank my advisors for their contribution and enthusiasm; Dr. Dominic Lee, Professor Graeme Wake, Associate Professor David Wall, Dr. Lucy Johnston and Dr. Irene Hudson.

This research would not have been possible without the kind help and assistance of the friendly staff at the Christchurch Intensive Care Unit, and I wish to thank them all. In particular, I would like to thank Jenny Barton for her willingness to help out and her enthusiasm for progress, and Gary and Richard for their support of this research. Without the support, understanding, assistance, and feedback of these key people, this project would not have been possible. Many people have also worked alongside this research and provided welcome ideas, support, and encouragement. In particular, my thanks go to the team involved with the agitation-sedation research; Zhuhui, Christina, Steve, and Franck.

There are also many people who have made the last three years so much more enjoyable. I would like to thank all my office mates throughout my time at University for the laughter, fun and jokes (some of them at my expense). In particular, my thanks go to Bram, Zhuhui, Mark Carey, Jamie, and everyone in the Centre for Bioengineering.

The University of Canterbury, and in particular the Department of Mechanical Engineering, has supported me throughout my studies with facilities, computers, and other resources. I would particularly like to thank the faculty members who took the time to support me throughout my studies even though it was not their direct responsibility. I would also like to acknowledge and thank the Foundation for Research Science and Technology for the scholarship and travel expenses that allowed me to undertake this research, and the Todd Foundation for the generous grant towards my research costs.

My friends and family have been an important part of maintaining balance in my life throughout the last three years, and I thank God for providing such critical people in my life and for His leading. I want to thank the guys and gals in Gravitate for accepting me and putting up with my terrible rhythm and timing, especially as the due date for this thesis draws near. Thank you for your energising musical talent, your friendship, and for making me laugh. I also want to thank two of my closest friends, Zhuhui and Maurice, for their friendship, continual support, and always keeping an eye out for me. Without the encouragement, support, and guidance of my family I would not have had the opportunity to do this research. I want to thank my Mum, my Dad, my brothers Bevan and Karl, as well as Chris, Hamish, Noel, Marlene, Duncan and Erica. I especially want to say really big thank you to my Mum and Dad— thank you for your advice, your patience, your love, your encouragement and support.

Most importantly, I would like to thank my wife, Marion, for her warm love, caring encouragement, and amazing support. Right from the beginning she has motivated me, especially recently as I've struggled to pull this thesis together. Somehow, it seems she knows me better than I know myself, and more importantly wants to see me grow. Thank you for challenging me, encouraging me, supporting me, and sharing with me so much of life that cannot be learned, only experienced.

Contents

List of Figures

List of Tables

Nomenclature

$\cdot^a$	Denotes a parameter associated with the analgesic Morphine
$\cdot^s$	Denotes a parameter associated with the sedative Midazolam
$\cdot_c$	Denotes a parameter associated with the central compartment
$\cdot_e$	Denotes a parameter associated with the effect compartment
$\cdot_p$	Denotes a parameter associated with the peripheral compartment
$\dot{A}$	Rate of change of agitation (min^{-1})
ϵ	Cumulative combined effect of sedation over time
κ	Parameter defining the gradient of the linearised surface
$\mathbf{A_{cl}}$	closed-loop system matrix
$\mathbf{A}$	open-loop system matrix
$\mathbf{B_{cl}}$	closed-loop B matrix
$\mathbf{B_1}$	Control input coefficient vector
$\mathbf{B_2}$	Disturbance coefficient vector
$\mathbf{C_1}$	Output matrix
$\mathbf{D_1}$	Output disturbance coefficient vector
$\mathbf{K}$	Control gain vector
$\mathbf{P}$	Positive definite matrix
$\mathbf{v}$	Lyapunov function
$\mathbf{x}$	State vector
$\mathbf{y}$	Output vector
$\mathbf{z}$	Regulated output vector
μ	Mean infusion rate
ω	Kernel weights
$\phi(\cdot\|\mu,\sigma^2)$	denotes the normal density with mean μ and variance σ^2
ψ	Steepness parameter in sigmoidal relationships

τ	Variable of integration
θ	Ratio of drugs
$\tilde{w}_2$	Virtual sedative sensitivity
D_{Bolus}	Dose of drug delivered via bolus infusion (mg)
D_{Cont}	Dose of drug delivered via continuous infusion (mg)
C	Concentration (mg/L)
C_{50}	Concentration at which 50% of maximal effect is achieved (mg/L)
E	Pharmacodynamic effect
E_0	Minimum pharmacodynamic effect
E_{Comb}	Combined sedative effect
E_{max}	Maximum pharmacodynamic effect
$Ex(\cdot)$	Expectation
$f_t(\cdot)$	Marginal density of $\cdot$ at time t
h	Kernel bandwidth
$k(t)$	Kernel
K_{CL}	Rate of clearance (L/min)
K_{ij}	Rate of transfer from compartment i to compartment j (L/min)
K_T	Effect time constant (min^{-1})
K_d	Derivative control gain (mL)
K_p	Proportional control gain (mL/min)
$P(\cdot)$	Denotes probability
q	Order of the MA model
R^a	Morphine concentration in infusion solution (mg/L)
R^s	Midazolam concentration in infusion solution (mg/L)
t	Time (min)
U	Infusion rate (mL/min)
u_o	Potency of Morphine
u_s	Potency of Midazolam
V	Volume of distribution (L)
$Var(\cdot)$	Variance
w_1	Stimulus sensitivity
w_2	Sedative sensitivity
w_3	EAR sensitivity
A	Agitation
AND	Average Normalised Density
AR	Auto Regressive
ARF	Acute Renal Failure
ARMA	Auto Regressive Moving Average

BIS	Bispectral Index
CRF	Chronic Renal Failure
CSF	Cerebro-spinal-fluid
EAR	Endogenous Agitation Reduction
ETT	Endotracheal Tube
ICU	Intensive Care Unit
IV	Intravenous
LQ	Lower Quartile
LOS	Length of Stay
M3G	Morphine-3-glucuronide
M6G	Morphine-6-glucuronide
MA	Moving Average
MAAS	Motor Activity Assessment Scale
Max	Maximum value
MEC	Minimum Effective Concentration
Med	Median value
Min	Minimum value
OAA/S	Observers Assessment of Alertness/Sedation
OCR	Observed Concentration Range
PD	Pharmacodynamic
PK	Pharmacokinetic
RAND	Relative Average Normalised Density
RASS	Richmond Agitation Sedation Scale
RF	Renal Failure
RTD	Relative Total Dose
S	Stimulus
SAS	Sedation Agitation Scale
TCI	Target Controlled Infusion
TIB	Time in Band
TIVA	Total Intravenous Anaesthesia
UQ	Upper Quartile
IQR	Inter-Quartile Range

Abstract

Effective agitation management through sedative delivery is a fundamental activity in the intensive care unit (ICU), and is the basis for providing comfort and relief to the critically ill. The primary goal of sedation management in the ICU is to manage patient agitation, the sometimes violent activity that creates a risk to both patients and clinical staff. Recent statistics show that 71% of critically ill patients experience agitation for 58% of their stay in ICU, so the problem is significant in size and patients affected.

In clinical practice, a lack of understanding of the underlying dynamics, combined with subjective agitation assessment tools, makes effective and consistent agitation management difficult. Quantitative models of agitation-sedation dynamics are developed to enhance understanding of the underlying system, and to create a platform enabling the development of sedative control protocols for improved agitation management. Compartmental pharmacokinetic models are employed to model the transport and elimination of drugs, and response surface modelling is used to represent the pharmacodynamic effect of the drugs on patient agitation. These physiologically-based models incorporate observations of critically ill patients, and are evaluated against recorded infusion data.

The models are then used to evaluate different methods of sedation and patient agitation management. Constant infusion protocols, derivative-focused agitation feedback control protocols, and non-linear agitation feedback protocols are specifically investigated. The results identify physiological effect saturation as a severe limitation on the capacity of sedative control protocols to reduce agitation. In spite of this restriction, significant improvements over current clinical practice are achieved through the use of very simple control protocols. These improvements represent significant benefits for patients and medical staff alike. However, the fundamental outcome of this thesis is that improved agitation management is not determined so much by the class of drug or drug dose, as by the specific drug administration strategy employed.

Chapter 1

Introduction

1.1 Motivation

Critically ill patients are typically admitted to the Intensive Care Unit (ICU) for life support and specialised treatment. Patients commonly experience pain and/or discomfort as a result of the life support systems, combined with their disease, injury, and environment. This pain and discomfort can invoke anxiety and confusion, which may lead to patient agitation, including excessive potentially harmful motion, and increased heart rate and blood pressure. Such agitation reduces the ability of the patient to recover, and if not appropriately managed, increases the length of stay and other potential risks.

To provide comfort and relief, patients are typically given hypnotic drug therapy in the form of intravenous (IV) sedatives and analgesics. Sedative agents induce amnesia and a lowered state of consciousness, while analgesics primarily relieve pain. During surgical operations, sedative and analgesic drugs are used in anaesthesia to induce very deep sedation and remove any appreciation of pain. The goal of sedation in the ICU is to reduce anxiety, control agitation, and produce a patient who is calm, cooperative, and able to communicate [Fragen, 1997]. Hence, (short-term) surgical anaesthesia and ICU (long-term) sedation have very different goals and target outcomes.

Therefore, in the ICU, these drugs are used at different doses than in anaesthesia to induce a state known as ICU sedation. During ideal ICU sedation patients are thus not fully anaesthetised. Instead, they are administered only enough sedative and analgesic agents to adequately relieve their pain, provide

comfort, and ease anxiety enough to prevent agitation.

Effective delivery of sedation is a fundamental activity in the ICU, and is the basis for providing comfort and relief to the critically ill. Insufficient sedation exacerbates anxiety and agitation, and increases the risk of complications such as self-extubation. Over-sedation, on the other hand, is damaging to patient health and increases the length of stay and healthcare costs [Kress et al., 2000]. Altered consciousness is one of the most common side-effects of continuous infusion of sedatives and analgesics and may lead to delayed weaning and prolonged mechanical ventilation [De Jonghe et al., 2005]. For these reasons, it is important that the appropriate dose of sedative and analgesic drugs is delivered at the appropriate time to ensure the best care for the patient.

A Midazolam and Morphine combination, given by intermittent bolus or continuous infusion, is the mainstay of many ICU regimens [Burns et al., 1992]. Midazolam is a sedative agent used to induce amnesia and a lowered state of consciousness, and Morphine is a powerful opioid analgesic with mild sedative effects. While several drug delivery techniques exist, the typical drug therapy approach is for bedside medical staff to adjust the IV infusion rate based upon their observations of the patient. Accordingly, most sedative drugs administered in the Intensive Care Unit are given in response to patient agitation [Fraser and Riker, 2001a], which contributes significantly to the US$0.8-1.2B spent on sedation every year in the United States alone [Kress et al., 2000]. Hence, the target, or control, metric for regulating sedation in critical care is minimal patient agitation utilising minimal drug dose, rather than a given level of consciousness.

Although ICU sedation utilises hypnotic drugs similar to those used in Total IntraVenous Anaesthesia (TIVA), the drug dose and consciousness levels are distinctly different, as are the patients and the environment. More importantly, the overall goal of the therapy is significantly different with anaesthesia applications aiming to induce reduced consciousness for short periods and ICU sedation wanting to simultaneously minimise agitation and over-sedation over extended periods of time. Hence, critical care sedation management is a very different problem that seeks the best trade-off between sedative dose and patient agitation. Therefore, while similarities between the two fields may provide some insight, the differences prevent simple application of anaesthesia delivery methods, measurements and protocols to long-term ICU sedation administration.

The underlying non-linear dynamics of the agitation-sedation system are not well understood, and many complex interactions contribute to observed patient behaviour. Traditional therapeutic treatment methods rely heavily upon the knowledge, experience and intuition of the medical staff, the 'art of medicine', introducing variability and inconsistency [Kress et al., 2000]. While some studies report little benefit in the use of protocols [MacLaren et al., 2000; Devlin et al., 1997], several recent studies have highlighted the cost and healthcare benefits of drug delivery protocols based upon agitation-sedation assessment scales [Brattebo et al., 2002; Smyrnios et al., 2002; Szokol and Vender, 2001; Barr and Donner, 1995]. Very simple protocols minimising over-sedation have reduced the length of stay 28–35%, as well as reducing total drug requirements 46–57% and testing for altered mental status 67% [Kress et al., 2000; Brattebo et al., 2002]. The primary outcome of the studies is that it is not so important which drug is used, or the exact dose delivered, but rather how the drug is employed [De Jonghe et al., 2005; Kress et al., 2002]. In spite of these results, many intensive care units apply no specific, quantified protocol to sedative infusion, relying upon the judgement and experience of the intensive care unit staff [Cohen, 2002].

Computerised sedative infusion protocols that enable consistency of care and minimise fluctuations in treatment could therefore improve patient care, simplify administration, minimise drug consumption and staff effort, and reduce costs. In spite of these significant potential advantages, current computer-assisted infusion feedback control systems in the ICU are still in their infancy [Shaw et al., 2003b; Smith and Reves, 1995]. One major drawback is the lack of a quantified, consistent means of measuring agitation, as current protocols rely on subjective assessment and dosing.

Currently, subjective agitation assessment scoring systems are used to help guide sedation management. Several studies have been conducted to analyse the effect of scoring systems and agitation-sedation scales on patient outcome, length of stay, cost, and healthcare benefits [Smyrnios et al., 2002; Szokol and Vender, 2001; Barr and Donner, 1995]. However, in each case the studies have required large-scale, double-blind clinical trials involving many patients and staff, significant time, and careful ethical consideration. It is clearly not ethical to test the effectiveness of a proposed sedative infusion protocol on critically ill patients if there is a chance that the protocol may hamper recovery. Thus, the development of quantitative models to enhance understanding of the system and provide a

platform for the development and evaluation of control protocols is important.

The primary limitations to the development of automated sedative infusion protocols include the lack of an objective, physiologically-based, quantified agitation scale and limited understanding of the underlying system dynamics. The subjective measures of agitation assessment currently employed introduce significant variability between assessors and inconsistency of care [Szokol and Vender, 2001; Weinert et al., 2001]. While no gold-standard agitation-sedation scale exists, the Riker Sedation Agitation Scale (SAS) is widely accepted [Fraser and Riker, 2001b]. Quantitative agitation sensors being developed [Lam et al., 2003; Lam, 2003; Starfinger et al., 2003; Starfinger, 2003; Shaw et al., 2003b; Chase et al., 2004a], offer the potential to significantly improve agitation management when coupled with dynamic models and control protocols [Chase et al., 2004a].

Recent research has shown that consistent, quantifiable measures of patient agitation can be developed [Chase et al., 2004c,a; Lam et al., 2003; Starfinger et al., 2003; Agogué, 2005; Lam, 2003; Starfinger, 2003], creating the potential for automated, or semi-automated, feedback control approaches to sedation management with patient agitation as the control metric. Automated sedative delivery systems would thus offer the potential to optimally control patient agitation. It would also potentially improve patient care, simplify administration, minimise drug consumption and effort, and reduce costs.

In spite of these advantages, there are no known computer assisted infusion systems utilising feedback control in the ICU [Smith and Reves, 1995; Shaw et al., 2003a,b]. Target Controlled Infusion (TCI) systems aim to deliver drugs at a rate that maintain target plasma concentrations, using a pharmacokinetic (PK) model. This approach is well suited to anaesthesia where short periods of reduced consciousness and well-known pharmacology are common. However, infusion systems that regulate the infusion rate to maintain target agitation levels, and therefore control the primary metric for long-term sedation, are the goal for improving care in the ICU.

This research therefore has two primary aims:

1. To develop physiologically-based models of the agitation-sedation system to enhance understanding of the system and create a platform enabling the development of agitation feedback protocols.

2. To utilise agitation-sedation models as a platform for the design and evaluation of sedative administration control protocols using agitation feedback, for use in medical decision support systems and automated sedation administration.

1.2 Background and Literature Review

While there are many pharmacological models of Morphine and Midazolam, no known models of the interaction of these drugs with patient agitation dynamics exist. However, related studies have investigated the PK and pharmacodynamics (PD) of Morphine [Meineke et al., 2002; Lötsch et al., 2002; Anderson and Kenny, 2003; Faura et al., 1998; Milne et al., 1996] and Midazolam [Platten et al., 1998; Persson et al., 1987; Bolon et al., 2003; Burns et al., 1992; Shafer, 1998; Tuk et al., 1999], and related models have been developed for use in anaesthesia [Kenny and Mantzaridis, 1999; Schwilden et al., 1989; Gentilini et al., 2001]. However, none of these studies attempt to model the effect of sedative and analgesic drugs on agitation in ICU patients.

1.2.1 Agitation Management

Previous attempts to improve agitation management in the ICU have been limited to clinical trials employing constant sedative infusion protocols and subjective agitation assessments [Kress et al., 2000; Smyrnios et al., 2002; Brattebo et al., 2002; Brook et al., 1999]. The use of quantitative modelling to enhance understanding of the system and provide a simulation platform is a recently developed tool in this area [Shaw et al., 2003b; Rudge et al., 2003a,b]. Hence, there is no significant, relevant body of prior art in this field. In particular, the linking of a physical patient symptom, like agitation, to a therapeutic pharmacodynamic, is not common in any area.

1.2.2 General Pharmacology

The study of pharmacology has developed methods for modelling the PKs and PDs of drugs in the body. *Pharmacokinetics* describes the distribution of drugs throughout the body, and their subsequent elimination from the body, while *pharmacodynamics* describes the effect drugs have on the body. Hence, pharmacology represents the physics of transport once delivered, and the physics of utilisation and effect in the body.

Medical experience and empirical studies have shown that the rate of elimination of drugs from the body is proportional to the concentration of the drug itself. Consequently, common PK approaches include the use of rate equations to model the distribution of drugs throughout the body, and their elimination from the body. Differential equations therefore form the backbone of PK studies.

Observations of delayed drug distribution gave rise to the method of compartmental modelling, which represents the body as several vessels in which different drug concentrations can exist. This approach is popular because it is capable of capturing observed drug dynamics, is flexible in terms of complexity and structure, is well-suited to differential equations, and is easily visualised. For example, Figure 1.1 shows a 2-compartment model [Wood and Wood, 1990]. The linear equations describing the drug distribution in Figure 1.1 are defined:

$$V_1 \frac{dC_1}{dt} = -(K_{el} + K_{12})C_1 + Dose + K_{21}C_2 \tag{1.1}$$

$$V_2 \frac{dC_2}{dt} = -K_{21}C_2 + K_{12}C_1 \tag{1.2}$$

where V_1 and V_2 are the volumes of the compartments, C_1 and C_2 are the drug concentrations in the compartments, K_{12} is the transfer rate from compartment 1 to compartment 2, K_{21} is the transfer rate from compartment 2 to compartment 1, K_{El} is the rate of drug elimination from compartment 1 and $Dose$ is the rate of infusion of drug into C_1.

Experimental research has shown that the typical effect of a drug on the body is not linearly proportional to its concentration. Rather, there is a non-linear PD relationship between concentration and effect. The Hill equation is a common representation of the generalised relationship between drug concentration and

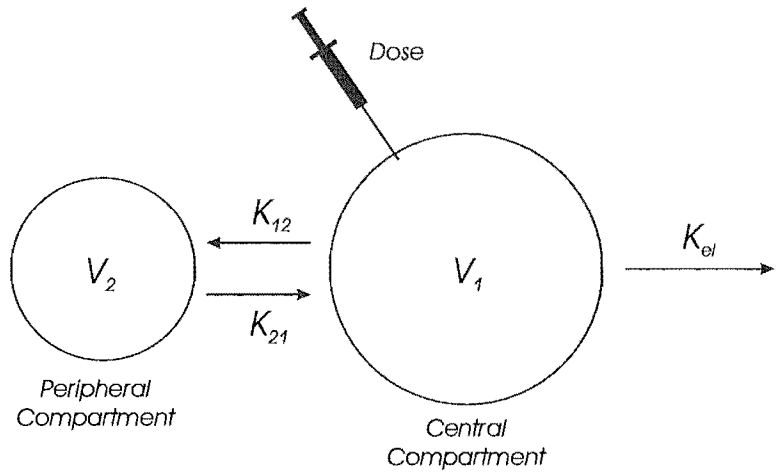

Figure 1.1 Schematic of a basic 2-compartment PK model.

effect, and forms the basis for many PD models. One form of the generalised Hill equation is displayed in Figure 1.2 and defined:

$$E = E_0 + (E_{max} - E_0)\left(\frac{C^{\psi}}{C_{50}^{\psi} + C^{\psi}}\right) \tag{1.3}$$

where E represents the pharmacodynamic drug effect, E_0 is the minimum effect, E_{max} is the maximum possible effect, C is the drug concentration, ψ is the steepness coefficient, and C_{50} is the concentration corresponding to 50% drug effect.

Figure 1.2 shows the non-linear sigmoidal relationship between drug concentration and PD effect per Equation (1.3). As concentration reaches higher levels past point A, the increase in effect gained from increased concentration diminishes. Past point B there is effectively no additional effect for additional drug, indicating a saturation of effect.

In sedation management, saturation past point B means excess drug exists in the system and may be stored in fatty tissue. This stored drug will be released later when the plasma concentrations fall, typically during weaning from sedation [Wagner and O'Hara, 1997]. The result is increased length of effect, and as a result length of stay (LOS) and cost and increase. Thus, saturation

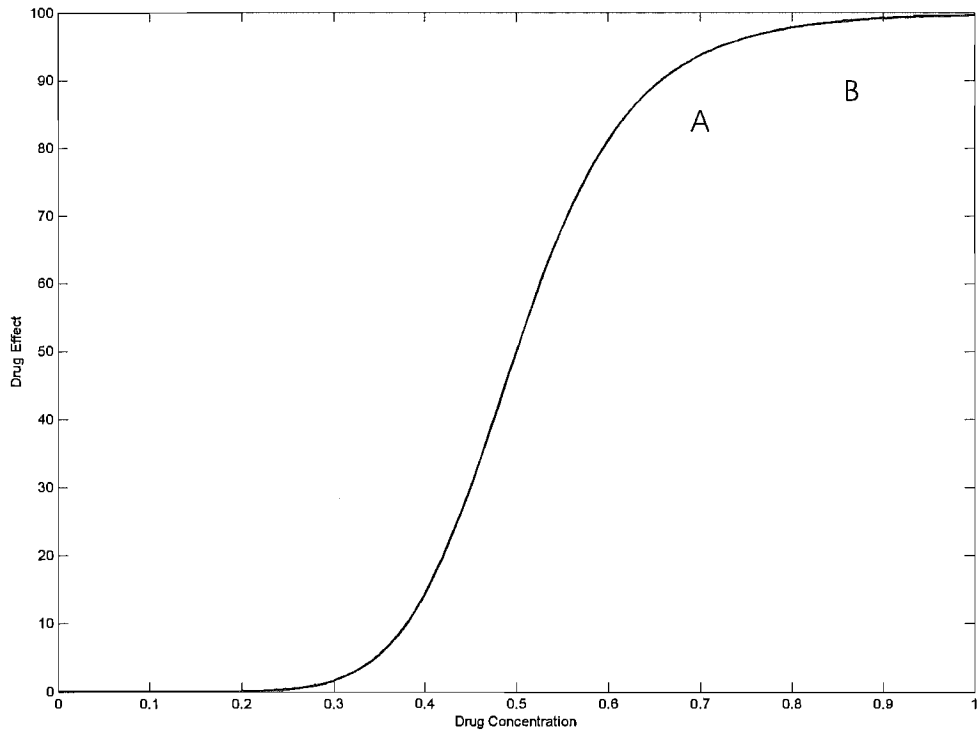

Figure 1.2 Representation of the non-linear PD concentration-effect relationship described by the Hill Equation.

is an important patient-specific parameter to be accounted for in any effective sedation management protocol. Simply identifying and avoiding saturation may significantly reduce the incidence and effect of over-sedation.

Similarly, observations of the effects of interactions between several drugs simultaneously present in the body have shown that the combined effect is not always linear. In particular, it has been shown that different drug combinations interact differently to produce either additive, synergistic (super-additive), or antagonistic (sub-additive) effects. Several techniques have been developed to model the effects of these drug interactions, many of them using response surfaces [Fidler et al., 2003; Minto et al., 2000; Rudge et al., 2005b]. The main goal of all these approaches is a better, more accurate description of saturation that is applicable to common clinical practice of using multiple drugs in combination.

1.2.3 PK and PD Studies

While there have been many pharmacological studies on Morphine and Midazolam, very few, if any, investigate the effect of these drugs on patient agitation in the critically ill. In particular, there have been many PK studies investigating the distribution of Morphine and Midazolam throughout the human body. However, they focus primarily on animal or healthy human subjects. Although there have been fewer studies on the PD of Morphine and Midazolam, they too focus primarily on healthy subjects.

A review of the pharmacology of Morphine and its metabolites in both humans and animals was conducted by Milne et al. [1996]. Further, studies have investigated the PK of Morphine in patients with Acute Renal Failure (ARF) [Bion et al., 1986], Renal Failure (RF) [Osborne et al., 1993], Chronic Renal Failure (CRF) [Aitkenhead et al., 1984], and neurosurgical and neurological ICU patients [Meineke et al., 2002]. A few PK studies employing compartmental modelling to investigate the PK of Morphine for healthy [Lötsch et al., 2002] and ICU patients [Meineke et al., 2002] are also available. There are fewer studies investigating the PD of Morphine, however Barr and Donner [1995] and Levine [1994] present qualitative information regarding the PD effects of Morphine. In particular, the results published by Berger and Waldhorn [1995], Schmidt et al. [2004], and Tverskoy et al. [1989] point to the potent analgesic and mild sedative properties of Morphine.

Studies have investigated the PK of Midazolam in patients with ARF [Driessen et al., 1991], CRF [Vinik et al., 1983], elderly patients [Fragen, 1997], and general ICU patients [Driessen et al., 1991; Malacrida et al., 1992; Oldenhof et al., 1988; Shafer, 1998; Bolon et al., 2003]. A few PK studies employing compartmental modelling to investigate the PK of Midazolam for healthy [Persson et al., 1987] and ICU patients [Bolon et al., 2003] are also available. There are fewer studies investigating the PD of Midazolam, however Fragen [1997] and Platten et al. [1998] present information regarding the PD effects of Midazolam. Perhaps more importantly, several reviews and studies discuss the combined PD effects of Morphine and Midazolam [Tverskoy et al., 1989; Wagner and O'Hara, 1997; Barr and Donner, 1995; Fragen, 1997; Gilliland et al., 1996].

1.2.4 Anaesthesia Models

In general, the body of knowledge of short term anaesthesia is much more advanced than that of ICU sedation and provides a useful clinical and theoretical backdrop. However, its direct application to work with ICU sedation is limited due to distinctly different drug doses, target metrics, end-points, and goals. Specifically, anaesthesia uses volatile, very short acting agents in large doses to induce a deeply anaesthetised state of unconsciousness. However, many of these volatile agents, such as Propofol, are toxic in the long time-frames and doses encountered in ICU sedation management [ADRAC, 2004; Kang, 2002; McKeage and Perry, 2003]. In contrast to anaesthesia, sedation uses longer acting agents in much lower doses to slightly lower the level of consciousness, relieve anxiety, and manage agitation.

Pharmacological models of the opioid Alfentanil have been developed and used in closed-loop feedback control of analgesia [Gentilini et al., 2002]. Similarly, attempts have been made using various anaesthetic drugs to create models for closed-loop control of anaesthesia [Kenny and Mantzaridis, 1999; Schwilden et al., 1989; Gentilini et al., 2001]. However, in most cases, the models focus on the PKs rather than the PDs, and use blood pressure or the Bispectral Index (BIS) as a feedback quantity. One reason for the lack of PD focus is the difficulty of objectively quantifying the resulting level of sedation in a consistent repeatable fashion— very similar to the difficulty in measuring agitation. In addition, while there is some debate in the literature over the clinical usefulness of BIS in the ICU environment, most studies conclude that more trials are required to prove the clinical effectiveness of BIS in the ICU [De Deyne et al., 1998; Simmons et al., 1999; Gilbert et al., 2001; Nasraway et al., 2002; Tonner et al., 2005; Nasraway, 2005; Kress et al., 2002].

While the models and systems developed for anaesthetic applications cannot be directly applied to ICU sedation, they certainly contribute to the methodology and considerations used in developing models and controllers for agitation management. In particular, a focused design approach based upon specific target metrics, similar to current anaesthesia approaches, would provide significant advantages over current approaches to sedation management in the ICU that lack quantified feedback control metrics.

1.2.5 Summary and Preface

Quantitative models of the agitation-sedation dynamics are developed to enhance understanding of the agitation-sedation system and create a platform enabling the development of agitation feedback protocols. The developed models are then used as a platform for the design and evaluation of sedative administration control protocols using agitation feedback, for use in medical decision support systems and automated sedation administration.

Part I of this thesis focuses on the physiology and modelling of the agitation-sedation system. The first chapter covers the construction of the proposed agitation-sedation model, starting with an initial model consisting of two compartments. The next chapter develops the initial model into a more physiologically-representative model by adding separate PKs, a non-linear PD concentration-effect relationship, synergism, endogenous agitation reduction, and effect saturation.

Part II develops the model evaluation metrics and procedures for use with recorded infusion data. The model evaluation technique is explained, followed by the development of several model evaluation metrics. The initial model is evaluated and its capabilities and limitations identified. The more physiologically-based model of Chapter 3 is then evaluated, including the identification of system parameters and analysis of their sensitivities.

Part III develops and evaluates control protocols for use in semi-automated sedative control systems. Control protocol specifications are developed based upon physiological limits and goals of ICU sedation. Simple controllers are used in conjunction with the developed models to assess the effectiveness of the simple control protocols, before developing more advanced controllers. Finally, the robustness of the developed control protocols is assessed.

Part I

Modelling and Physiology

Chapter 2

Physiology and Current Treatment Methods

2.1 Physiology

Critically ill patients are typically admitted to the Intensive Care Unit for critical treatment and life support. As a result of the life support systems, combined with their critical condition, and environment, patients commonly experience pain and/or discomfort during their stay in ICU. This pain and discomfort can invoke anxiety and confusion, which can lead to patient agitation.

Agitation affects 71% of critically ill patients for 58% of their stay in ICU [Fraser and Riker, 2001b]. Anxious and agitated patients may groan and grimace, and in some circumstances attempt to remove the endotracheal tube and other catheters, as well as resist staff [Agogué, 2005; Kress et al., 2000]. This physiological stress on the body increases the chance of complications and prevents speedy recovery.

While many drug administration routes exist, such as the subcutaneous, intra-muscular, and intravenous routes, sedative and analgesic drugs in the ICU are typically administered intravenously into the blood stream. Intravenous administration is selected because the delay between drug delivery and effect is small, and because of the ease of administration through current drug delivery systems.

Although the use of the opioid drug Morphine has a history dating back to the early 19th century [Milne et al., 1996], its pharmacology and the mechanism of action is still not fully understood [Faura et al., 1998; Meineke et al., 2002;

Milne et al., 1996]. Midazolam is part of the benzodiazepine family of sedative drugs, whose popularity has recently increased [Wagner and O'Hara, 1997] due to their application for long-term sedation, consistency of action, and relatively less significant side-effects. While there have been many studies investigating the pharmacology and mechanism of action of benzodiazepines, their exact mode of action is also not fully understood [Crippen, 1990]. Drugs delivered intravenously enter the venous blood stream returning to the heart. After passing through the heart and lungs, the drug is then distributed in the blood throughout the different parts of the body, including the brain and central nervous system, where sedative action occurs.

For hypnotic drugs, the site of action is commonly considered to be the receptors in the brain and the spinal column in the cerebro-spinal fluid (CSF). Studies have detected Morphine and Midazolam in the CSF, although the entry mechanism is still unclear [Faura et al., 1998; Arendt et al., 1983]. Morphine and Midazolam then bind with their respective receptors and assert their PD effects [Milne et al., 1996; Arendt et al., 1983].

The half-life of Morphine and Midazolam is approximately 2.5–8.5 hours [Bion et al., 1986; Aitkenhead et al., 1984; Volles and McGory, 1999] and 3-7 hours [Fragen, 1997; Malacrida et al., 1992; Wagner and O'Hara, 1997], respectively. Morphine is primarily metabolised in the liver and kidneys, and only a small portion is excreted in the urine [Crippen, 1990]. In contrast, Midazolam is metabolised extensively in the liver and conjugated and excreted exclusively in the urine [Crippen, 1990]. During metabolism, Morphine is converted into its major metabolites Morphine-3-glucuronide (M3G) and Morphine-6-glucuronide (M6G) [Milne et al., 1996]. Midazolam is also converted into its major metabolites α-hydroxy-Midazolam and 4-hydroxy-Midazolam [Mandema et al., 1992; Tuk et al., 1999]. While some studies have shown that these Morphine and Midazolam metabolites are pharmacologically active, the extent of their activity and mechanism of action is still under debate [Knoester et al., 2002; Mandema et al., 1992; Milne et al., 1996; Meineke et al., 2002].

The half-life, clearance and PK parameters of Morphine and Midazolam are known to vary between patients, and are particularly influenced by renal and hepatic failure [Knoester et al., 2002; Mandema et al., 1992; Platten et al., 1998; Fragen, 1997; Vinik et al., 1983; Milne et al., 1996; Aitkenhead et al., 1984].

Drug storage in the fatty tissues can result in delayed release of drugs, causing prolonged effect [Crippen, 1990], and effectively increasing the half-life during periods of low infusion, like weaning. Combinations of sedatives and analgesics are synergistic in producing sedation [Wagner and O'Hara, 1997], potentially leading to an unintendedly higher total level of sedation.

Delirium occurs in 20.7–36.8% of ICU patients [Szokol and Vender, 2001], and is defined as "a reversible, global impairment of cognitive processes, usually of sudden onset, coupled with disorientation, impaired short-term memory, altered sensory perceptions (hallucinations), abnormal thought processes, and inappropriate behaviour". Delirium can go unrecognised in more than two-thirds of patients in clinical practice, and may be confused for agitation [Ely et al., 2004], leading to mistreatment in both cases. Delirium is commonly treated with haloperidol, and can be antagonised by Morphine and Midazolam [Crippen, 1994] or similar sedatives. As a result, over-sedation leads to time-consuming and expensive testing for altered mental status, to ensure the appropriate treatment is being given [Kress et al., 2000; Ely et al., 2004].

Finally, the natural response of the body to induced pain or stress is the release of endorphins. Abbreviated from "endogenous Morphine", endorphins are a form of natural analgesic produced is response to pain and physical stress [Kreek, 2002]. Although endorphins form an important part of the physiological system and their qualitative effect can be described, their impact is difficult to quantify. This dynamic, along with the previously mentioned dynamics, may be important in the agitation-sedation system and are significant considerations for the development of a quantitative model of the agitation-sedation system.

2.2 Current Treatment Methods

In the hospitalised adult, agitation is defined as an excessive motor or verbal behavior that interferes with patient care, patient or staff safety, and medical therapies. Current agitation management methods rely on subjective agitation assessment, and an appropriate sedation input response, from bedside medical staff. Bedside medical staff assess patient agitation using subjective agitation scales [Ramsay et al., 1974; Riker et al., 1999; Fraser and Riker, 2001b; Jaarsma

et al., 2001; Sessler et al., 2002], and then select an appropriate infusion rate based upon their evaluation, experience, and intuition [Kress et al., 2002]. This process is depicted in Figure 2.1. Figure 2.2 shows the same situation schematically in block diagram form where bedside medical staff assess agitation and choose the drug infusion rate. Subjectivity, and more particularly subjective assessment, is introduced in this section. The most current subjective agitation scales are presented and discussed to delineate the current state of the art in agitation assessment, and thus sedation management.

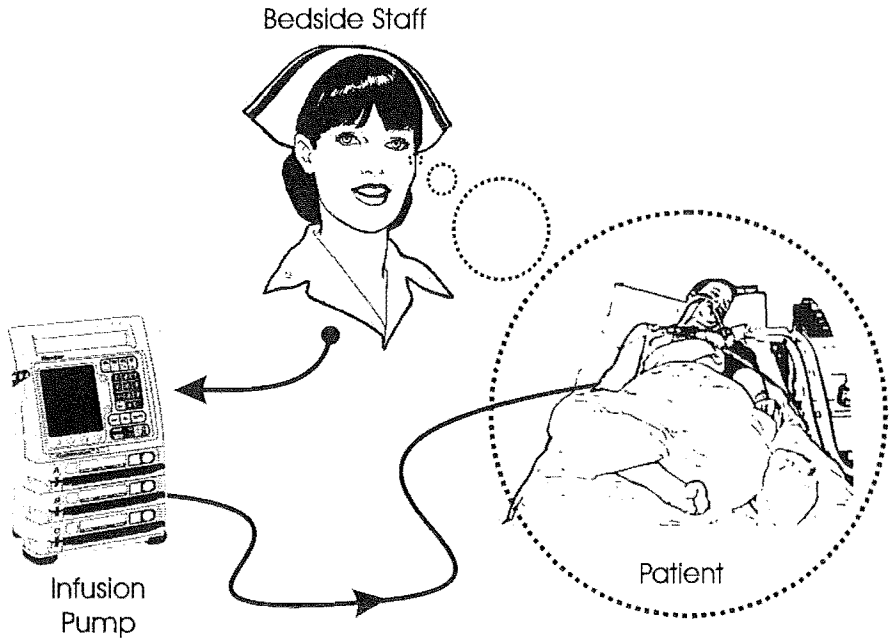

Figure 2.1 Diagram of typical sedative administration method.

Several recent studies have highlighted the cost and healthcare benefits of drug delivery protocols based upon agitation-sedation assessment scales [Brattebo et al., 2002; Smyrnios et al., 2002; Szokol and Vender, 2001; Barr and Donner, 1995]. Very simple protocols minimising over-sedation have reduced the length of stay 28-35%, as well as reducing total drug requirements 46-57%. However, a daily interruption of sedative drug infusion can lead to under-sedation, which results in sudden changes in the level of consciousness due to mental and physical stress. In spite of the obvious benefits of formal sedation protocols, many intensive care units apply no specific, quantified protocol to sedative infusion, relying upon

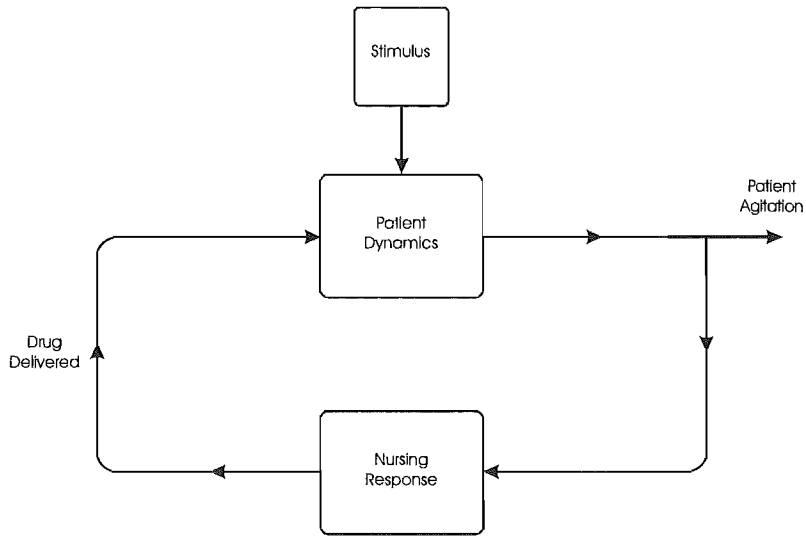

Figure 2.2 Block diagram schematic of typical sedative administration.

the judgement and experience of the intensive care unit staff [Cohen, 2002]. Note that the use of sedative infusion protocols assumes that everything has been done to remove or reduce all obvious sources of stimulus that may lead to agitation [Kress et al., 2002]. Further, it is acknowledged that the removal of all obvious sources of stimulus may be sufficient for some patients, inferring that not all patients require sedation [Kress et al., 2002].

There are many subjective agitation scales available to bedside medical staff for assessing patient agitation. However, their subjectivity means that the resulting assessment, and hence resulting treatment, relies heavily on the experience and intuition of the staff. Further, once bedside staff have assessed the patient agitation, their response also depends upon their experience and intuition. This reliance creates variability and inconsistency in treatment, as ability and experience can vary greatly between staff, and over time for any given clinician. These factors make it difficult to implement a pre-defined agitation management protocol, particularly one that is effective and patient-specific, given the variability also present in patients. A summary of some of the common agitation and sedation scales used in ICUs is presented below.

2.2.1 The Ramsay Scale

The first scale developed to assess the level of agitation and sedation of critically ill patients was the Ramsay scale developed in 1974 [Ramsay et al., 1974]. It consists of a 6-grade scale ranging from 1 (agitated) to 6 (unarousable, over-sedated). These different grades are detailed in Table 2.1.

Table 2.1 Ramsay Scale

Level	Characteristics
1	Patient awake, anxious, agitated or restless
2	Patient awake, cooperative, orientated and tranquil
3	Patient drowsy, with response to commands
4	Patient asleep, brisk response to glabella tap or loud auditory stimulus
5	Patient asleep, sluggish response to stimulus
6	Patient has no response to firm nail-bed pressure or other noxious stimuli

The subjectivity of this scale was first estimated in 1999 [Riker et al., 1999], with an inter-rater agreement ($\kappa = 0.88$). Unfortunately, the Ramsay scale classifies all different levels of agitation into one single level including behaviours from mild anxiety to dangerous agitation [Ramsay et al., 1974]. In spite of this limitation, the Ramsay scale remains one of the most widely used scales for monitoring sedation in daily practice, as well as clinical research [Carrasco, 2000].

2.2.2 The Riker Sedation/Agitation Scale

The Riker Sedation/Agitation Scale (SAS) was first developed in 1994, and subsequently improved in 1999 [Riker et al., 1999]. It provides a symmetric approach of 3 grades each to assess the patient's levels of agitation and sedation, and a middle grade for calm and co-operative patients — a total of 7 possible levels. The Riker SAS has an inter-rater agreement of $\kappa = 0.92$. The intra-rater agreement has not been evaluated. The validity of this scale has also been assessed through agreement with other subjective scales [Riker et al., 1999]. However, there is a key limitation in the Riker SAS, since the patient is classified as either agitated, or sedated, but not both.

Recent research by Shaw et al. [2005] has shown that a patient can be simul-

taneously agitated and sedated. Therefore, it is more consistent to assign the patient with both an agitation index and a sedation index. A modified version of the original Riker SAS, referred to as the modified SAS, is shown in Table 2.2. This scale has been developed and used in the Christchurch Hospital ICU to assess agitation and sedation levels separately, creating two concurrent and independent indices, around the "0" score.

Table 2.2 Modified version of the SAS Scale

Score	Term	Description
Agitation score		
3	Dangerous Agitation	Pulling at Endotracheal Tube (ETT), trying to remove catheters, climbing over bed rail, striking at staff, thrashing side-to-side
2	Very Agitated	Requiring restraint and frequent verbal reminding of limits, biting ETT
1	Agitated	Anxious or physically agitated, calms to verbal instructions
0	Calm	Calm
Sedation score		
0	Cooperative	Easily arousable, follows commands
-1	Sedated	Difficult to arouse but awakens to verbal stimuli or gentle shaking, follows simple commands but drifts off again
-2	Very Sedated	Arouses to physical stimuli but does not communicate or follow commands, may move spontaneously
-3	Unarousable	Minimal or no response to noxious stimuli, does not communicate or follow commands

Guidelines for applying the modified SAS assessment [Riker et al., 1999] help differentiate different levels of sedation and agitation. First, agitated patients are scored by their most severe degree of agitation in the 0–3 range. Then, sedated patients are scored similarly for level of sedation on the -3–0 range. Finally, both scores are reported as concurrent, independent indices.

2.2.3 The Motor Activity Assessment Scale

The Motor Activity Assessment Scale (MAAS) has been developed from the Riker SAS and is also a 7-level scale with three categories for both agitation and sedation, as well as a middle level for calm patients [Fraser and Riker, 2001b]. Behavioural descriptors are provided to assist clinicians in patient assessment, as defined in Table 2.3. The MAAS has an inter-rater agreement of $\kappa = 0.83$, and has been confirmed through comparisons with other subjective scales and clinical parameters, such as changes in vital signs [Fraser and Riker, 2001b]. However, the validity of the MAAS has only been assessed in surgical ICU patients, and further study should be carried out on critically ill patients [Carrasco, 2000].

Table 2.3 The Motor Activity Assessment Scale

Score	Term	Description
6	Dangerously agitated, uncooperative	No external stimulus is required to elicit movement, and patient pulls at tubes or catheters or thrashes side-to-side or strikes at staff or tries to climb out of bed and does not calm down when asked
5	Agitated	No external stimulus is required to elicit movement, and attempts to sit up or moves limbs out of bed and does not consistently follow commands (e.g., will lie down when asked but soon reverts to attempts to sit up or move limbs out of bed)
4	Restless and cooperative	No external stimulus is required to elicit movement and patient picks at sheets or tubes or uncovers self and follow commands
3	Calm and cooperative	No external stimulus is required to elicit movement and patient adjusts sheets or clothes purposefully and follow commands
2	Responsive to touch or name	Opens eyes or raises eyebrows or turns head toward stimulus OR moves limbs when touched or name is loudly spoken
1	Responsive only to noxious stimuli	Opens eyes or raises eyebrows or turns head toward stimulus or moves limbs with noxious stimulus
0	Unresponsive	Does not move with noxious stimulus

There are additional subjective assessment tools available to evaluate the level of sedation and agitation of a patient. Among those are the Harris scale, the Sheffield scale, the Vancouver interaction and calmness scale, the visual analogue

scale [Fraser and Riker, 2001b], the Observer's Assessment of Alertness/Sedation (OAA/S), the COMFORT scale [Jaarsma et al., 2001], and the Richmond Agitation Sedation Scale (RASS)[Sessler et al., 2002]. They all provide a reliable assessment tool with advantages and disadvantages, and they may focus more or less on different aspects. However, these scales are more subjective and they are not presented in more detail in this thesis.

2.2.4 Summary of Subjective Scales

Among the literature concerning agitation and sedation assessment methods, Fraser and Riker [2001b] recommend that each intensive care unit select one scale proven to be valid and reliable, and include that scale in their agitation and sedation protocols. Because of the ease of use, proven reliability and validity, behavioural descriptors to guide patient classification, and the capability of monitoring both agitation and sedation, Christchurch Hospital ICU uses the modified Riker SAS [Shaw et al., 2005, 2003b]. However, no data confirms that this scale is superior to others.

More importantly, all the scales described share the requirement of subjective assessment with relatively limited (3–5) levels of resolution for agitation. In addition, all scales currently available describe agitation and sedation as two ends of a single spectrum, rather than two independent spectrums. The scales therefore fail to separate agitation and sedation, even though the application of sedative agents is the treatment for patient agitation. If sedatives are used to treat agitation, and the sedation and agitation levels are related, then the scales measure a balance of treatment and behaviour. However, the subjective scales previously mentioned are not utilised in this way. Furthermore, social, personal, and professional factors have been shown to influence sedative therapy [Weinert et al., 2001], and intra- and inter-rater scales reported from controlled studies with well trained staff can differ significantly in every day practice [Agogué, 2005].

Given the variation in assessment as well as sedation, implementation of closed-loop feedback control of sedation with agitation as the feedback quantity could well improve patient healthcare and cost. To enable the development of semi-automated systems, quantitative models of the agitation-sedation dynamics are required to gain insight and understanding of the system, and develop

suitable sedative administration controllers. This thesis develops models of the agitation-sedation system and employs the models for the development of sedative controllers to provide improved agitation management through feedback control of patient agitation.

Chapter 3

Agitation-Sedation Modelling

Several quantitative models of the agitation-sedation system have been developed throughout the course of this research, each model building upon the previous model's strengths and improving the weaknesses. The first models developed capture the fundamental dynamics of the agitation-sedation system, but lack physiological resemblance and more advanced dynamics. These first models established a platform from which more physiological models were developed, incorporating more advanced dynamics. The model development process, beginning with the creation of the initial model, and consisting of improvement building on previous models is portrayed in Figure 3.1. The three models presented in this section are:

Initial Model This model was developed to capture the fundamental dynamics of the agitation-sedation system, and employs simple PK relationships and linear PDs. The model is used to establish a fundamental platform for further model development.

Predator-Prey Model This model is a development of the initial model incorporating non-linear PDs. This model is used to investigate the impact of non-linear PDs on the ability of the model to capture the fundamental dynamics.

Physiologically-based Model This model builds upon the understanding gained from the previous models and adds more complex dynamics to the model, capturing synergism, saturation, and a non-linear concentration-effect dynamic. This model captures both the fundamental dynamics of the agitation system captured in the Initial mode, while at the same time being more representative of the physiology.

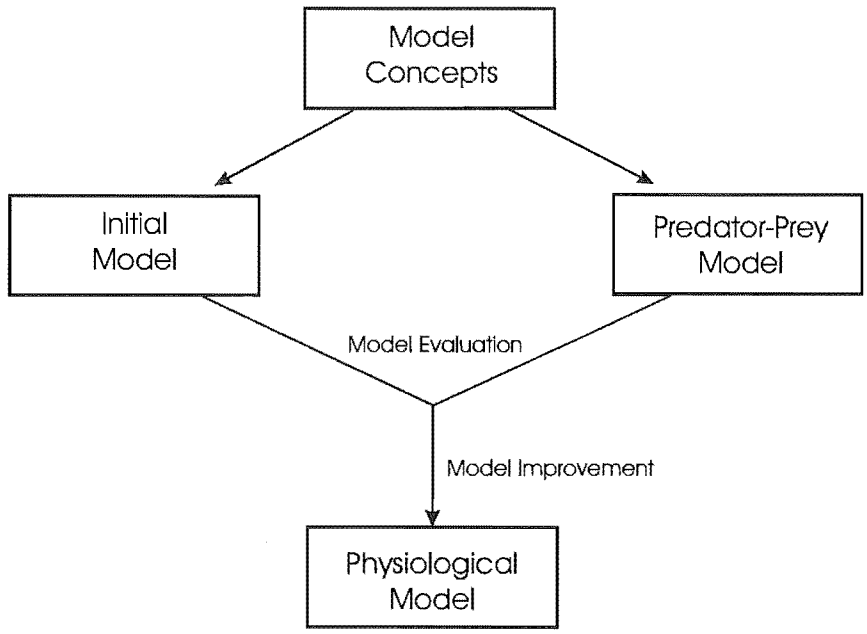

Figure 3.1 Schematic of the model development process.

This chapter presents each of the models and explains the important aspects of each model and their physiological resemblance. Part II of this thesis then proceeds to evaluate the models consecutively. Rather than present only the final physiological model, this thesis presents the three separate models as a progression of the development process to convey the development and improvement of the models, and to help compare and contrast the various aspects of the models. Through explicit comparison between models, the important features within each model can be identified thereby enhancing understanding of the underlying system dynamics.

3.1 Initial Model

An initial model of the agitation-sedation system is presented as a platform from which to develop the agitation-sedation model. The models developed are intended to be the simplest required to capture the fundamental patient dynamics common to ICU patients, rather than represent the detailed and complex mech-

anisms underlying all of the pharmacology. This macroscopic approach to modelling arises out of the overall goal of this research to enhance understanding of the system dynamics and create a platform for controller development.

The initial model presented in this section builds upon a well-known general two-compartment PK model [Wood and Wood, 1990], adding patient agitation as a third state variable. As a simplification, the model treats Morphine and Midazolam as one fixed-ratio drug. Equations (3.1)–(3.3) define the agitation-sedation system model:

$$\frac{dC_1}{dt} = -K_1 C_1 + \frac{U}{V_d} R \tag{3.1}$$

$$\frac{dC_2}{dt} = -K_2 C_2 + K_3 C_1 \tag{3.2}$$

$$\frac{dA}{dt} = w_1 S - w_2 K_T \int_0^t C_2(\tau) e^{-K_T(t-\tau)} d\tau \tag{3.3}$$

where C_1 is the drug concentration in compartment 1 (mg/L), C_2 is the drug concentration in compartment 2 (mg/L), U is the IV infusion rate (mL/min), R is the concentration of the drug in the infusion solution (mg/mL), V_d is the volume of distribution (L), A is an agitation index, S is the stimulus invoking agitation, $K_{1\text{–}3}$ are parameters related to drug elimination and transport (min^{-1}), and K_T is the effect time constant (min^{-1}). Time is represented by t in min, τ is the variable of integration, and the terms w_1 and w_2 are the stimulus and sedative sensitivities, respectively. A and S are assumed unitless.

This initial model is intended to be the simplest necessary to capture the essential dynamics of the agitation-sedation system. Therefore, $K_{1\text{–}3}$ are assumed constant over time, although they can be treated as slow moving functions of time to model more complicated, very long-term phenomena such as tachyphylaxis or fatty tissue distribution [Hughes et al., 1992]. Hence, it also considers Morphine and Midazolam administered concomitantly as a single drug.

Equation (3.1) represents the kinetics of drug infusion and distribution, while Equation (3.2) represents the transport of sedative from the infusion site to the effect site, which for sedative and analgesic drugs is the central nervous system. An acceptable approximation for this effect site concentration is considered by some authors to be the drug concentration in the CSF [Meineke et al., 2002;

Cousins and Mather, 1984]. These kinetics are shown schematically in Figure 3.2 for Equations (3.1)-(3.3).

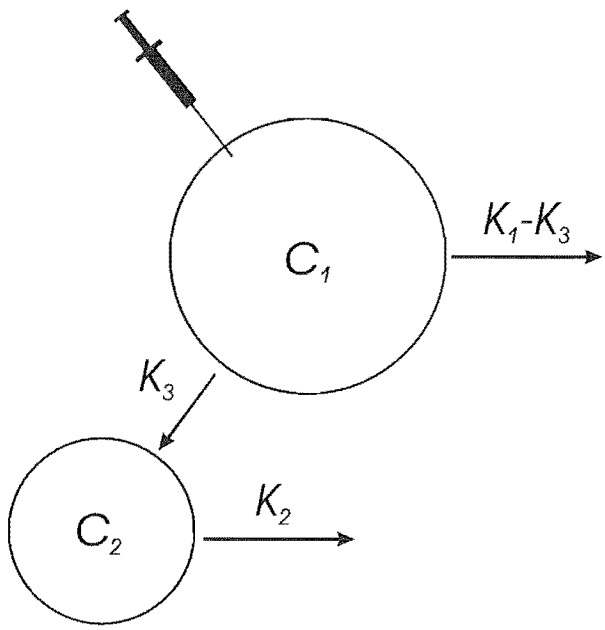

Figure 3.2 Schematic representation of the PK of the initial model.

The non-linear pharmacodynamic Equation (3.3) was developed based upon physiological observations of ICU patient behaviour. Specifically, it states that the rate of change of agitation depends upon the magnitude of the stimulus relative to the cumulative effect of the sedative agent. Stimulus in this context refers to the combined effect of inherent pain, distress, or loss of inhibition caused by the diseased/injured state of the patient, and the therapeutic and diagnostic procedures performed by medical staff [Kress et al., 2002].

Equations (3.1)–(3.3) represent a model of the fundamental dynamics of the ICU patient. In particular, the PD Equation (3.3) is developed to capture the agitation response of the *patient* to external stimuli and drug delivered to the patient. The model, and PD equation in particular, should be independent the nursing response and stimulus inputs. More specifically, the patient PDs are not a function of the nurse or stimulus, but a response to these inputs. Hence, the

models should be patient specific but independent of these external inputs that are administered to the patient.

Under constant stimulus levels, observed agitation typically falls or remains unchanged upon increased infusion of sedative agents. Similarly, patients become more agitated by increased stimulus, due to procedures or condition, if infusion rates are not increased. Patient agitation is therefore modelled as being primarily reduced by the cumulative effect of current and prior sedation administration, as modelled by the convolution term in Equation (3.3). Finally, the K_T term in front of the integral term in Equation (3.3) exists to scale the integral term back to a magnitude of similar order to the terms within the integral.

The introduction of the convolution term in Equation (3.3) creates a simple method of capturing the cumulative effect of Morphine and Midazolam on patient agitation. It represents a novel method of capturing the cumulative effect over time of current and prior sedative administration. While the model is not completely physiological, it creates a good base for the further development of the agitation-sedation model.

Equation (3.3) emphasises the pharmacological effect of the drugs on agitation over time. Specifically, it captures the observed time-lag between drug concentration and drug effect, which may represent the crossing of drugs across the blood brain barrier, or the uptake of drug by receptors. While other forms of Equation (3.3) are explored in Chapter 13, the form presented in this section is physiologically intuitive because of its explicit representation of the effect of pharmacological action over time. Specifically, it emphasises the relatively high impact of recent drug delivery compared to the reduced impact of prior drug delivery, recognising rates of transport and utilisation of drug. The form of Equation (3.3) also has particular advantages in controller formulation, particularly techniques employing the Laplace transform. The presence of the convolution integral in Equation (3.3) simplifies the evaluation of its Laplace transform and thus enables the use of other well known control development and analysis tools.

This initial drug model incorporates the fundamental PK principles, and introduces a simple relationship between drug concentration, stimulus, and patient agitation. However, it lacks the separate PK profiles of Morphine and Midazolam, and assumes a linear relationship between drug concentration and effect. This

model is therefore incapable of capturing saturation or drug interaction dynamics. The model also lacks complete physiological resemblance and is not easily visualised because of the uni-directional transfer and losses, as seen in Figure 3.2. However, it does capture the essential PK transfer of drug and its utilisation to reduce agitation. Hence, it creates a fundamental platform from which to develop more advanced physiologically-based models of the agitation-sedation system.

3.2 Predator-Prey Model

The model presented in this section is identical to the initial model in all respects except for the integral term in Equation (3.3). The predator-prey model incorporates a non-linear dynamic commonly observed in species competing for existence, and often used in pharmacodynamic models, such as for the insulin-glucose system [Lam et al., 2002; Bergman et al., 1985].

Equations (3.4)–(3.6) define the Predator-Prey version of the initial agitation-sedation system model of Equations (3.1)–(3.3):

$$\frac{dC_1}{dt} = -K_1 C_1 + \frac{U}{V_d} R \tag{3.4}$$

$$\frac{dC_2}{dt} = -K_2 C_2 + K_3 C_1 \tag{3.5}$$

$$\frac{dA}{dt} = w_1 S - w_2 K_T A \int_0^t C_2(\tau) e^{-K_T(t-\tau)} d\tau \tag{3.6}$$

where C_1 is the drug concentration in compartment 1 (mg/L), C_2 is the drug concentration in compartment 2 (mg/L), U is the IV infusion rate (mL/min), R is the concentration of the drug in the infusion solution (mg/mL), V_d is the volume of distribution (L), A is an agitation index, S is the stimulus invoking agitation, $K_{1\text{–}3}$ are parameters related to drug elimination and transport (min^{-1}), and K_T is the effect time constant (min^{-1}). Time is represented by t in min, τ is the variable of integration, and the terms w_1 and w_2 are the stimulus and sedative sensitivities, respectively. A and S are assumed unitless.

The distinction between the initial model and the predator-prey model is in

the inclusion of agitation in the integral term in the final pharmacodynamic, third equation. By adding agitation as a factor in the term responsible for reducing patient agitation, the predator-prey framework suggests that the level of agitation affects the ability of the therapeutic drugs to reduce patient agitation. More specifically, it defines a multiplications relationship so that very low agitation limits the drug effect and very high agitation magnifies it.

Observations of agitation in critically ill patients reveal no direct suggestion of the existence of this type of predator-prey dynamic. There is also no known mention of its effects in the published literature. However, the predator-prey model is regularly used to model other drug pharmacodynamics such as those of the insulin-glucose system [Lam et al., 2002]. Hence, it may yet represent a valid (and accepted) modelling framework that at 'central' levels of agitation and drug effect is similar to a calibration constant in w_2.

Therefore, the predator-prey model of agitation-sedation dynamics is retained for further investigation. Its independent representation of patient specific PDs is also used later in the independent selection of the nurse control parameters in Section 6.1. Hence, it provides a second, independent dynamic model of patient agitation-sedation response using a well-known PD modelling structure.

3.3 Physiologically-based Model

Using the initial model as a platform for further development, additional dynamics are added to the model to create a more physiologically representative model. This improved model utilises separate PK models for Midazolam and Morphine, and incorporates a non-linear PD relationship. Displayed schematically in Figure 3.3, the model is a closer representation of the actual physiological system than the initial model and includes delayed distribution, drug synergism, effect saturation and endogenous agitation reduction (EAR). The model is defined in three main portions:

I. Pharmacokinetics of Morphine:

$$V_c^a \frac{dC_c^a}{dt} = -(K_{CL}^a + K_{ce}^a + K_{cp}^a)C_c^a + R^a U + K_{ec}^a C_e^a + K_{pc}^a C_p^a \qquad (3.7)$$

$$V_p^a \frac{dC_p^a}{dt} = -K_{pc}^a C_p^a + K_{cp}^a C_c^a \tag{3.8}$$

$$V_e^a \frac{dC_e^a}{dt} = -K_{ec}^a C_e^a + K_{ce}^a C_c^a \tag{3.9}$$

II. Pharmacokinetics of Midazolam:

$$V_c^s \frac{dC_c^s}{dt} = -(K_{CL}^s + K_{ce}^s) C_c^s + R^s U + K_{ec}^s C_e^s \tag{3.10}$$

$$V_e^s \frac{dC_e^s}{dt} = -K_{ec}^s C_e^s + K_{ce}^s C_c^s \tag{3.11}$$

III. Pharmacodynamics of Morphine and Midazolam:

$$\frac{dA}{dt} = w_1 S - w_2(t) K_T \int_0^t E_{Comb}(\tau) e^{-K_T(t-\tau)} d\tau - w_3 A \tag{3.12}$$

where C_c, C_p and C_e are the drug concentrations (mg/L) in the central, peripheral and effect compartments, V_c, V_p and V_e are the distribution volumes (L) of the central, peripheral and effect compartments, U is the IV infusion rate (mL/min), A is an agitation index, S is the stimulus invoking agitation, K_{ij} is the transfer rate (L/min) from compartment i to compartment j, K_{CL} is the drug clearance (L/min), K_T is the effect time constant (min^{-1}), and R^a and R^s are the concentrations of analgesic ('a') Morphine and sedative ('s') Midazolam in the infusion solution respectively (mg/mL). A and S are assumed unitless. Time is represented by t (min), τ is the variable of integration, and the terms w_1 and $w_2(t)$ are the stimulus and sedative sensitivities respectively. Similarly, w_3 is the sensitivity associated with the endogenous reduction of patient agitation. Finally, E_{Comb} is the combined PD effect of the individual effect site drug concentrations of Morphine and Midazolam, determined using response surface modelling as defined by Minto et al. [2000]. The PD response surface is displayed in the lower portion of Figure 3.3.

To define the PD response surface, the effect concentrations of Morphine and Midazolam are first normalised and expressed in units of potency:

$$u_a = \frac{C_e^a}{C_{50}^a}, \qquad u_s = \frac{C_e^s}{C_{50}^s} \tag{3.13}$$

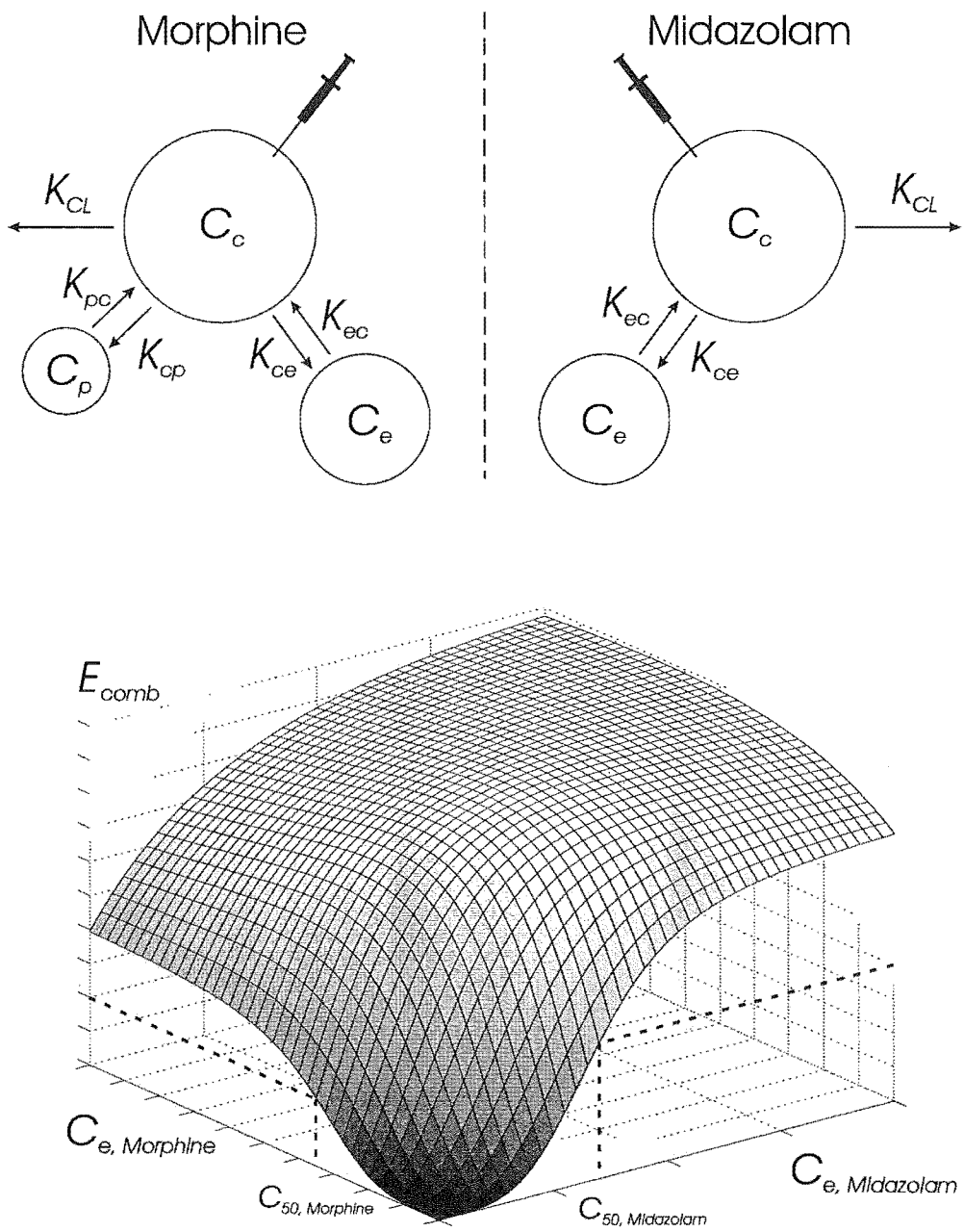

Figure 3.3 Schematic representation of the physiologically-based model, including the compartmental PKs (upper portion) and the PD response surface (lower portion).

where C_{50} (mg/L) represents the concentration that results in 50% of maximal drug effect if administered alone. Hence, u_a and u_s represent the concentrations, which are functions of time, relative to the midpoint of the sigmoidal curves in Figure 3.3.

The PD response surface function, E_{Comb}, can then be defined as a dual-drug version of the Hill equation presented in Section 1.2:

$$E_{Comb} = E_0 + [E_{max}(\theta) - E_0]\frac{\left(\frac{u_a + u_s}{U_{50}(\theta)}\right)^{\psi(\theta)}}{1 + \left(\frac{u_a + u_s}{U_{50}(\theta)}\right)^{\psi(\theta)}} \tag{3.14}$$

where $\theta = \frac{u_s}{u_a+u_s}$ is the ratio of the two drugs, $\psi(\theta)$ is the steepness of the concentration-response relation at ratio θ, $U_{50}(\theta)$ is the number of units (U) associated with 50% of maximum effect at ratio θ, and $E_{max}(\theta)$ is the maximum possible drug effect at ratio θ. The terms $\psi(\theta)$, $U_{50}(\theta)$, and $E_{max}(\theta)$ simply express how the terms they represent change with varying drug ratios, and are each defined in terms of a fourth order polynomial:

$$E_{max}(\theta) = \beta_{E,0} + \beta_{E,1} \cdot \theta + \beta_{E,2} \cdot \theta^2 + \beta_{E,3} \cdot \theta^3 + \beta_{E,4} \cdot \theta^4 \tag{3.15}$$

$$U_{50}(\theta) = \beta_{U,0} + \beta_{U,1} \cdot \theta + \beta_{U,2} \cdot \theta^2 + \beta_{U,3} \cdot \theta^3 + \beta_{U,4} \cdot \theta^4 \tag{3.16}$$

$$\psi(\theta) = \beta_{\psi,0} + \beta_{\psi,1} \cdot \theta + \beta_{\psi,2} \cdot \theta^2 + \beta_{\psi,3} \cdot \theta^3 + \beta_{\psi,4} \cdot \theta^4 \tag{3.17}$$

where $\beta_{E,0}$–$\beta_{E,4}$ are the coefficients of the polynomial defining E_{max} over θ, $\beta_{U,0}$–$\beta_{U,4}$ are the coefficients of the polynomial defining U_{50} over θ, and $\beta_{\psi,0}$–$\beta_{\psi,4}$ are the coefficients of the polynomial defining ψ over θ, as defined by Minto et al. [2000]. The values for these parameters are selected to create the general shape of the desired response surface, and depend on the relative PD effects of the drugs and whether the drug interaction is synergistic or antagonistic [Minto et al., 2000].

As per the initial model of Section 3.1, Equations (3.7)–(3.12) represent a model of the fundamental dynamics of the ICU patient. The physiological model is more detailed in its representation of the PK and PD response of the patient. The model, and PD equation in particular, are also designed to be independent

of the nursing response and stimulus inputs. Hence, the models are capable of being patient specific but independent of these external inputs administered to the patient.

3.3.1 Physiology

This physiologically-based model in Equations (3.7)–(3.12) incorporates some of the major dynamics lacking in the initial model. The model is still intended to be the simplest necessary to capture the essential dynamics of the agitation-sedation system, matching patient observations and published literature with a physiologically representative model. Equations (3.7)–(3.8) represent the pharmacokinetics (PK) of the infusion and distribution of Morphine, and Equation (3.9) represents transport of Morphine to and from the effect site. Similarly, Equation (3.10) represents the PKs of the infusion and distribution of Midazolam, and Equation (3.11) represents transport of Midazolam to and from the effect site.

Although the model compartments are hypothetical, the model is a representation of the physiological system, as presented in Figure 3.4. The central compartment represents the infusion site and local blood vessels such as the heart and lungs. The peripheral compartment can be thought of as the other peripheral parts of the body to which blood flows, such as the legs and arms. The effect site is that region in which the drug exerts its primary effect, which can be considered to be the CSF, or the brain. Finally, the delay induced by K_T can be thought of as crossing of the blood brain barrier, or uptake by receptors in the brain.

The non-linear PD Equation (3.12) is based on physiological observations of patient behaviour, and simply states that the rate of change of agitation depends upon the relative magnitude of the stimulus to the cumulative sedative effect and EAR. Stimulus in this context refers to the combined effect of inherent pain, distress, or loss of inhibition caused by the diseased/injured state of the patient, and the therapeutic and diagnostic procedures performed by medical staff. Observed agitation typically falls upon increased infusion of sedative agents, under (apparently) constant stimulus. Similarly, patients become more agitated by increased stimulus if infusion rates are not increased. Patient agitation is therefore primarily reduced by the cumulative impact of current and prior sedation

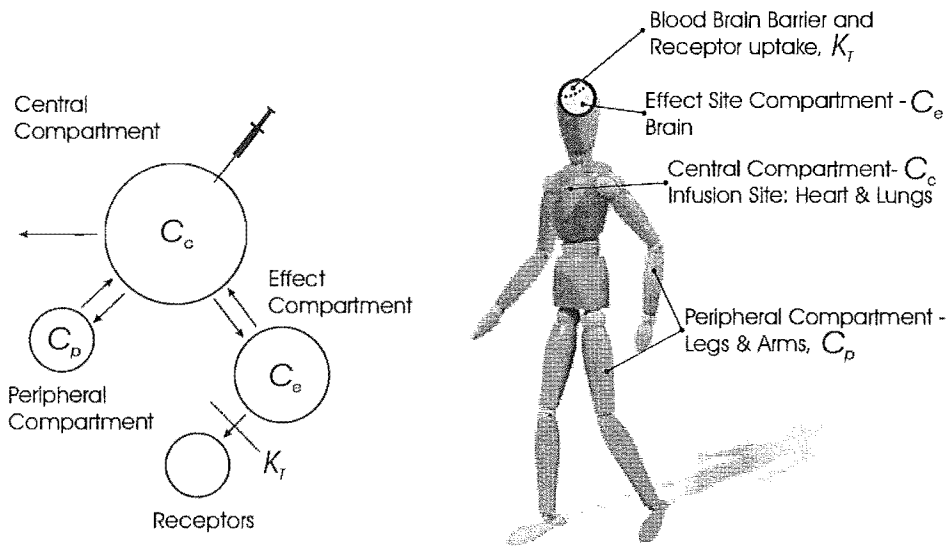

Figure 3.4 Schematic outlining the physiological representation of the hypothetical compartments.

administration, as modelled by the convolution integral in Equation (3.12).

The major development from the initial model is that the combined PD effect of the drugs is captured in Equation (3.12) using a response surface for drug interactions [Minto et al., 2000]. This surface incorporates synergism and effect saturation in its shape, as shown in Figure 3.3. Hence, where the initial model was linear in its drug effect at all levels, this model allows more realistic, saturable behaviours. The ability of this model to capture saturation is essential for capturing over-sedation.

3.3.1.1 Pharmacokinetic (PK) Modelling

The PK compartments in this model, shown in the upper portion of Figure 3.3, are hypothetical, but can be thought of as different regions of the body. The central compartment represents the infusion site and local blood vessels such as the heart and lungs. The peripheral compartment can be thought of as the other

peripheral parts of the body to which blood flows, such as the legs and arms, and incorporating the fatty tissues into which these drugs and/or metabolites can be deposited. The effect site is that region in which the drug exerts its primary effect. For drugs affecting the central nervous system, such as Morphine and Midazolam, an acceptable representation of the effect site can be considered to be the CSF [Meineke et al., 2002; Cousins and Mather, 1984], or the brain [Anderson and Kenny, 2003; Bates et al., 2004].

Clinical trials investigating the PK of Morphine show that concentration profiles in healthy and ICU subjects are best approximated by a 3-compartment model [Meineke et al., 2002; Lötsch et al., 2002]. These studies attempt to model the PK of IV Morphine incorporating the effect of metabolites such as M3G and M6G by employing additional compartments. However, the analgesic and sedative effects of these metabolites are not easily quantified and the details of their pharmacological effect are not yet fully understood [Anderson and Kenny, 2003; Faura et al., 1998; Milne et al., 1996]. Further, metabolite concentrations have been shown to be small when administration techniques bypassing the first-pass effect are used, such as IV administration [Faura et al., 1998]. Therefore, the model employed in this research uses three compartments for Morphine kinetics, as shown in the upper portion of Figure 3.3. In addition, it does not attempt to model the formation, distribution or secondary effects of Morphine metabolites.

Clinical trials investigating the PK of IV Midazolam show that concentration profiles in healthy and ICU subjects are best approximated by a 2-compartment model [Platten et al., 1998; Persson et al., 1987; Bolon et al., 2003]. While the activity of the major metabolite of Midazolam, α-OH Midazolam, has been the subject of much research, its activity has not yet been fully defined [Burns et al., 1992; Shafer, 1998; Tuk et al., 1999]. Therefore, the model employed in this research uses two compartments, as shown in Figure 3.3, and does not model the formation, distribution or secondary effects of metabolites for Midazolam.

3.3.1.2 Pharmacodynamic (PD) Modelling

Many pharmacological models exist for the individual delivery of Morphine or Midazolam. However, in this application Morphine and Midazolam are administered concomitantly. This model therefore utilises separate compartmental PK

equations for each drug, so the combined drug infusion rate results in individual effect site concentrations. In addition, this research seeks to capture their impact on agitation, *not* sedation, which is the focus of all prior PD studies. Hence, it is important to capture the appropriate effect site concentrations.

Midazolam is a commonly used sedative agent that can be used to induce anaesthesia or induce sedation, depending on dose [Persson et al., 1987; Young et al., 2000]. Morphine, while primarily an analgesic, is also a mild sedative [Barr and Donner, 1995; Levine, 1994]. However, Morphine and Midazolam, when administered concomitantly act in a synergistic manner to have an overall combined effect greater than the simple sum of the two individual effects [Wagner and O'Hara, 1997; De Jonghe et al., 2003; Kress et al., 2002]. Furthermore, the effects of Morphine and Midazolam are typically not linearly proportional to drug concentrations, and instead behave like the well-known sigmoid concentration-effect relationship [Minto et al., 2000; Romberg et al., 2004; Koopmans et al., 1988].

A mathematical representation of the combined PD effect of these drugs is created using a response surface for drug interactions [Minto et al., 2000], incorporating synergism and effect saturation, as shown in Figure 3.3. The sedative effect on the vertical axis lowers awareness, relieving anxiety and reducing agitation. Finally, Equation (3.12) captures the cumulative sedative effect of the drugs on the brain over time, and provides the relationship between stimulus invoking agitation and the sedative agents employed to manage agitation.

The non-linear PD Equation (3.12) is based on physiological observations of patient behaviour. It states that the rate of change of agitation depends upon the relative magnitude of the stimulus to the cumulative sedative effect and EAR. Observed agitation typically falls upon increased infusion of sedative agents, under constant stimulus. Similarly, patients become more agitated by increased stimulus if infusion rates are not increased. Patient agitation is therefore primarily reduced by the cumulative impact of current and prior sedation administration, as modelled by the convolution integral in Equation (3.12).

Note that these PD effects are limited by the response surface, E_{comb}, defined in Equation (3.14), at very high and very low concentrations. In between such levels the model behaves somewhat linearly. The major difference is that the

initial model treats the drugs as a single drug, whereas this model treats the drugs separately for PK modelling, and combines them using the PD response surface in Figure 3.3.

The final term in Equation (3.12) represents the effect of the endogenous opioid biochemical compounds endorphins. Abbreviated from "endogenous Morphine", endorphins are a form of natural analgesic produced is response to pain and physical stress [Kreek, 2002; Guyton and Hall, 1996]. An agitated patient may therefore experience a reduction in agitation due to the natural sedative effect of endorphins produced as result of agitation itself, modelled by the EAR term, $-w_3A$, in Equation (3.12). This term is not present in the initial model, and is a further example of additional dynamics added to make the model more physiologically representative.

This physiologically representative model has the capacity to model many dynamics existing in the agitation-sedation system such as saturation, synergism, concomitant administration, and endogenous agitation reduction. However, in general terms the model, or portions of it, creates a platform for modelling the general effects of concomitant administration of combinations of a variety of drugs. In particular, the model may be used to model the effects of different sedatives and analgesics in the ICU. Different drug interactions, such as antagonism and simple addition, may be modelled through different definitions of the shape of the response surface. Different drug profiles can be implemented by changing the drug transfer parameters K_{ij}, and varying numbers of compartments can be used to model different drug types. In this thesis, however, the model will be applied only to the concomitant administration of Morphine and Midazolam to ICU patients.

3.4 Model Summary

The initial model and the Predator-Prey model represent two approaches to capture the same observed fundamental dynamics, and are later used to analyse the appropriateness of the initial models drug/stimulus balance equation. While the initial model employs a simple drug effect as the agitation reduction mechanism, the predator-prey model employs a well-known and non-linear species-competitive

mechanism of agitation reduction. Both models are assumed to capture the fundamental dynamics of the agitation-sedation system and will be employed later for further analysis.

This physiologically-based model builds on the initial model by incorporating some of the major dynamics not present in the initial model. The two major developments from the initial model are the EAR dynamic and the combined PD effect of the drugs captured in the response surface [Minto et al., 2000]. This surface incorporates synergism and effect saturation in its shape, as shown in Figure 3.3. Hence, where the initial model was linear in its drug effect at all levels, this model allows more realistic, saturable behaviours. The ability of this model to capture saturation is essential for capturing over-sedation.

Part II

Model Evaluation and System Identification

Chapter 4

Recorded Data and Model Evaluation Technique

To verify the models presented in Chapter 3, three ingredients are required:

- Recorded patient infusion data
- A model of the fundamental clinical sedation management response to agitation
- A robust simulation platform

These elements enable modelled inputs and outputs to be compared to recorded data. From this comparison a variety of graphical, numerical and statistical conclusions can be drawn.

4.1 Recorded Data and Patient Cohort

The Christchurch Hospital ICU employs a semi-automatic sedative and analgesic adminstration protocol designed to minimise over-sedation. The protocol, administered electronically, delivers a fixed ratio Morphine (1mg/mL) and Midazolam (0.5mg/mL) solution based upon bedside medical staff (subjective) assessment of patient agitation. The fixed ratio sedative/analgesic solution is delivered intravenously using Graseby 3500 electronic infusion pumps (Graseby Medical Limited, Herts, U.K.).

The device, known as the InfuseRite infusion system, facilitates the simple administration of Morphine and Midazolam. It also records all infusion data

[Greenfield et al., 2001]. Figure 4.1 displays the current sedation administration situation in the Christchurch ICU. Note that the InfuseRite is the new element in an otherwise typical sedation management situation, as seen by the difference between Figure 2.1 and Figure 4.1.

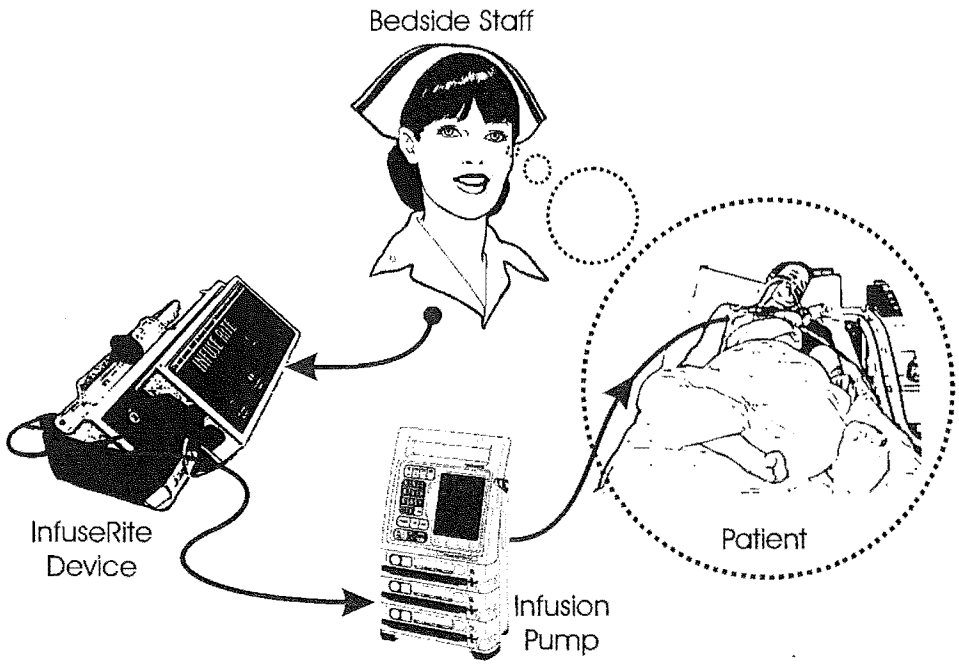

Figure 4.1 Schematic of the infusion protocol employed in the Christchurch ICU.

The semi-automated infusion protocol employed in the ICU at Christchurch Hospital utilises bedside nursing staff as a form of patient agitation sensor and feedback controller. Under this system, bedside medical staff observe the patient and deliver a fixed-dose bolus infusion in response to observed agitation, by pressing the 'bolus' button on the InfuseRite interface. An Infinite Impulse Response (IIR) filter [Rorabaugh, 1998] is employed to ensure the sedation infusion rate is minimised in the absence of agitation and reduce variability due to errors and inconsistencies in subjective clinical assessment of agitation. The IIR filter is defined:

$$D_{Cont}(n) = \frac{1}{6} \sum_{i=n-4}^{n-1} [D_{Cont}(i) + D_{Bolus}(i)] \tag{4.1}$$

where $D_{Cont}(i)$ and $D_{Bolus}(i)$ represent the dose of drug (mg) delivered per hour through continuous and bolus infusion respectively in the i^{th} hour. The amount

delivered via continuous infusion, $D_{Cont}(i)$, is the ongoing constant level of input. The amount delivered via bolus infusion, $D_{Bolus}(i)$, is the amount given beyond this input in response to observed patient agitation. Safety limits, determined by patient age and condition, are also placed on the range of allowable drug delivery rates, and the infusion rate is updated hourly.

Equation (4.1) represents a low-pass filter and titrates sedation to the minimum required, thereby minimising over-sedation and reducing vulnerability to assessment variability and error response. If more than one-third of the hourly total is given as bolus, indicative of significant agitation, the amount delivered via continuous infusion, D_{Cont}, rises. Less, and the amount falls. Note that the one-third limit is arbitrary and based on clinical experience [Shaw et al., 2003a]. It is important to know that with this definition oscillations below 1-2 times per day have a gain greater than 0dB, increasing the mean infusion rate and reflecting a potential instability.

Importantly, the protocol is effectively a closed-loop feedback controller, where nursing staff close the loop by providing agitation sensing and feedback via the electronic infusion controller, as shown in Figure 4.1. Staff assess the agitation levels using the modified Riker SAS in Table 2.2, and respond to agitation with additional bolus sedation. Boluses are provided in response to agitation and lead to modifications of the continuous infusion rate via Equation (4.1). The infusion rate is therefore representative of efforts to control agitation, and is not influenced by any specific efforts to induce sedation, which is in general a minimal amount of the total sedation administered and required [Fraser and Riker, 2001a].

Examples of sedation administration profiles in critically ill patients for whom the nurse control protocol has been employed are presented in Figure 4.2. Solid dark areas in Figure 4.2 represent bolus drug delivery, and lighter filled areas represent the resulting continuous infusion rate. Note that the continuous infusion rate increases after large volumes of bolus delivery, and declines rapidly in the absence of boluses to minimise over-sedation due to unnecessary sedation administration.

The presence of sudden spikes and apparent over-shoots are likely a result of the variability and subjectivity of nursing staff assessment of agitation [Agogué, 2005]. Figure 4.2 shows that the infusion rate varies considerably for each of the

four patients. Further, it can be seen that boluses tend to occur in regular clusters. In this control system, intensive care staff respond to heightened or depressed levels of agitation with increased or reduced volumes of boluses respectively.

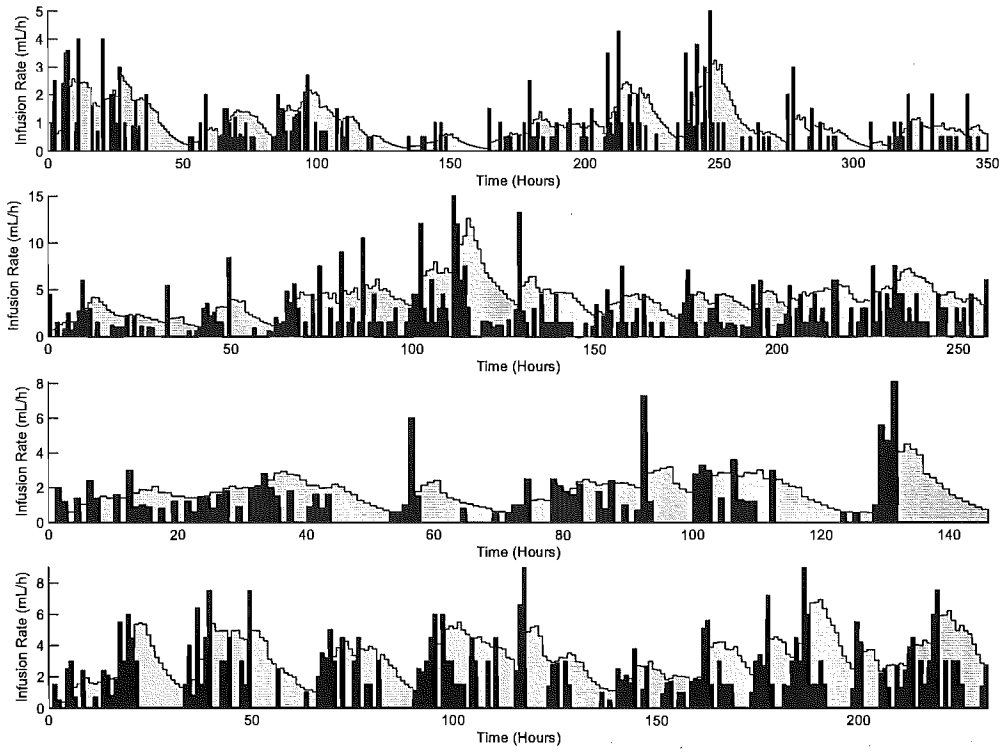

Figure 4.2 Examples of sedative administration profiles recorded using the InfuseRite infusion device.

In addition to the standard boluses and continuous infusion delivered to the patients, independent procedural boluses are given to patients in anticipation of painful or uncomfortable procedures. Examples of typical procedures include bathing, turning, or changing the patient, inserting new feed or arterial lines, applying new dressings, suctioning, and diagnostic procedures such as x-rays, MRIs, and cognitive testing. The procedural boluses are intended to be delivered entirely independent of the standard boluses and continuous infusion, and are designed to be given in preparation for a painful or uncomfortable procedure. Procedural boluses are delivered approximately 10-30 minutes prior to the procedure, typically last for 10-30 minutes, and are electronically recorded by the infusion device [Shaw et al., 2003b].

Sedative drug infusion data was recorded using the InfuseRite infusion de-

vice [Greenfield et al., 2001; Shaw et al., 2003a; Rudge et al., 2003a; Shaw et al., 2003b] for all ICU patients admitted to the ICU during a nine month observation period and requiring more than 24hrs of sedation. Over this period, infusion data equivalent to 377 days of continuous data was recorded from a total of 114 patients. Infusion data containing less than 48hrs of continuous data, or data from patients with severe brain injuries, trauma or excessive sedation requirements were excluded from further analysis. The remaining patient cohort after exclusions therefore consists of 37 ICU patients. The results in this thesis, unless otherwise stated, are for this cohort of 37 ICU patients. Approval was obtained from the Canterbury Ethics Committee for this research.

4.2 Nurse Control Model Capturing the Clinical Response

Bedside intensive care staff rely on monitored autonomous parameters (e.g. blood pressure, heart rate etc) and physical indicators (e.g. sweat, rapid motion etc) to subjectively gauge agitation levels [Riker et al., 1999; Kress et al., 2000; Cohen, 2002]. Many primary indicators of agitation are qualitative in nature, and sometimes contradictory, and therefore difficult to assess consistently over time and between assessors [Lam, 2003; Starfinger, 2003; Agogué, 2005].

As early as 1959 Helson showed perception to be relative to the mean or "adaptation level" in the whole environment [Helson, 1959]. The perception of many properties of objects such as weight, colour and odour, accordingly, become subjective [Helson, 1959; Wallach, 1963; Pol et al., 1998]. For example, the evaluation of pain level varies as a function of past pain levels experienced [Dar et al., 1995]. This subjective adaptation level will lead to small changes in odour, colour, weight or pain having little impact on subjective experiences. Minor changes in agitation over long periods of time are therefore often overlooked, while more rapid changes, or derivatives, are more readily assessed. More specifically, the primary changes noticed are relative changes rather than absolute magnitudes.

This form of observational sensing and feedback can be modelled as a proportional-derivative feedback controller. Hence, the fundamental sedation management response of bedside medical staff in the control loop of Figure 4.1 can

be simply modelled as a proportional-derivative controller with agitation as the feedback quantity. The output, U, can then be combined with the IIR filter in Equation (4.1). The infusion rate, U, in the form of a proportional-derivative controller using agitation, A, as the feedback quantity can be defined:

$$U = K_p A + K_d \dot{A} \tag{4.2}$$

where U is the feedback-controlled infusion rate, A is the agitation level, $\dot{A}$ is the rate of change of agitation, and K_p and K_d are the proportional and derivative gains, respectively. the relative values of these gains are left to be identified via recorded infusion data.

The feedback-controlled infusion, U, in Equation (4.2) represents the nursing response to agitation, and is updated once each hour, as per clinical practice in the Christchurch ICU, creating a piecewise constant infusion. The infusion rate, U, is then put through the filter in Equation (4.1) via $D_{Bolus}(i)$, implementing the filtered protocol used in Christchurch Hospital to minimise over-sedation. The simulated nursing sedative administration input, U, with the IIR filter, is substituted into Equation (3.1) or Equations (3.7) and (3.10) to model the feedback loop created by their response to subjectively assessed patient agitation for model evaluation. Note that negative infusion rates are not allowed.

4.3 Stimulus Input Generation

The unknown nature of pain and anxiety, combined with disease state and painful diagnostic procedures makes the direct recording of stimulus profiles impossible. A surrogate is therefore required for simulations using Equations (3.1)–(3.3) and (3.7)–(3.12). The stimulus, S, invoking agitation in Equations (3.3) and (3.12) is an important term in the agitation-sedation system. As mentioned in Sections 3.1 and 3.3.1, stimulus in this context refers to the combined effect of inherent pain, distress, or loss of inhibition caused by the diseased/injured state of the patient, and the therapeutic and diagnostic procedures performed by medical staff.

The semi-automated sedation infusion system implemented in the ICU, and described in Section 4.1 has as its input the bedside medical staff's indications of observed agitation, via the demand for additional bolus sedation. These bolus

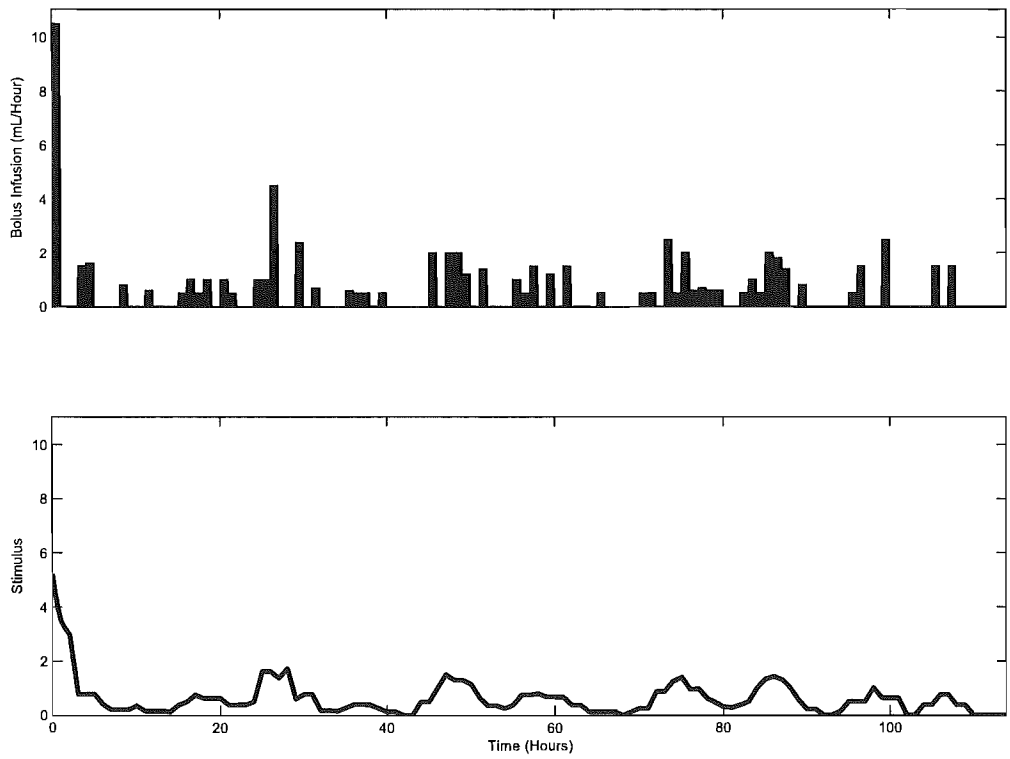

Figure 4.3 Example of the bolus and stimulus profiles for Patient 3.

recordings indicate periods where the patient's agitation levels increased enough to warrant additional sedative, implying the presence of stimulus. This bolus recording thus forms the basis for a surrogate measure of stimulus for the purpose of fundamental dynamic model evaluation. Obtaining the 4-hour moving average of this record retains the underlying structure of the recording, while creating a smooth stimulus profile with minimal subjective noise. All simulations in this thesis employ the 4-hour moving average of the recorded bolus profile as the stimulus profile. Figures 4.3–4.4 show examples of the recorded bolus profile, and resulting stimulus profile for Patients 3 and 37.

Note that clinical implementation of agitation feedback control of sedation would not require this input profile, requiring only measured agitation to determine the infusion needed. Hence, this surrogate is used only for evaluation of the fundamental dynamics. While this approach is less than perfect, it is one of the best options available.

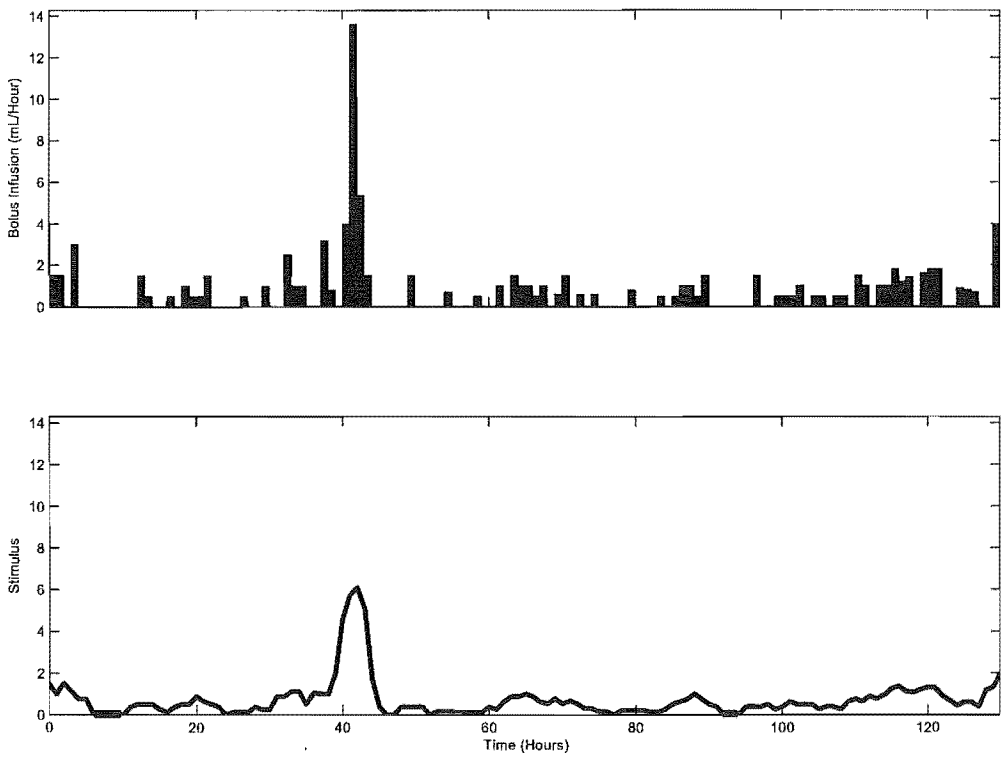

Figure 4.4 Example of the bolus and stimulus profiles for Patient 37.

4.4 Model Simulation Methods

Combining Equations (3.1)–(3.3), (3.4)–(3.6), or (3.7)–(3.12) with the nurse control model in Equation (4.2) creates a system for simulating the patient dynamics and nursing staff response, respectively. Figure 4.5 presents the block diagram in which the nursing response control model and the InfuseRite IIR filter close the loop by providing feedback control of sedation using agitation as the feedback quantity.

Sedative drug infusion data, recorded through the electronic infusion system, provides a basis for comparison and model evaluation. Using the stimulus profiles developed in Section 4.3, a simulation is conducted for each patient using an identical procedure for all patients. Although quantitative agitation sensors are under development, they are not currently available. This limits the data available for model evaluation, and necessitates the use of these alternative methods. Numerical and graphical approaches are used to provide statistical measures of tracking to assess the model's ability to capture the fundamental dynamics of the

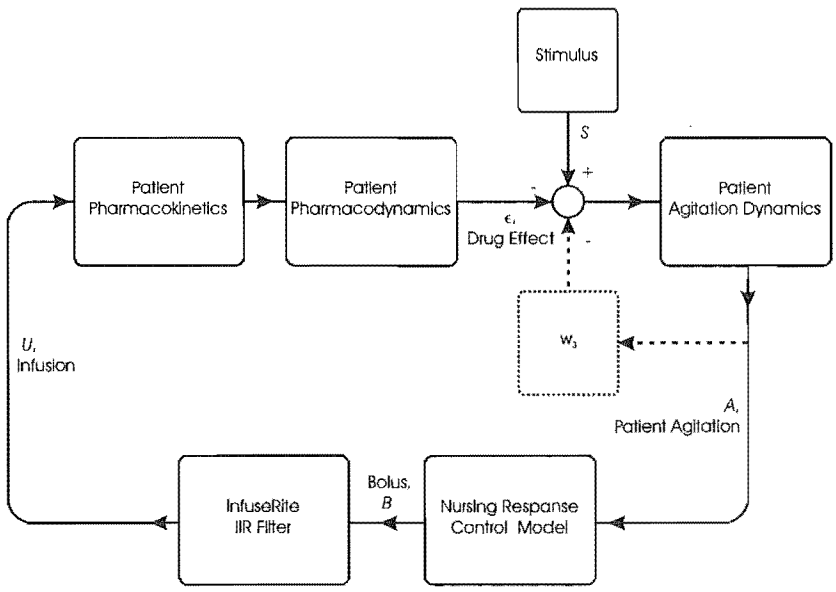

Figure 4.5 Simulation block diagram.

agitation-sedation system.

The systems of equations presented in Sections 3.1 and 3.3 represent differential equations that can be solved using an ODE solver. These equations are implemented and solved in MATLAB using $\Delta t = 1\text{min}$. This implementation creates the platform for analysis of the physiological system, and is the final ingredient required for model evaluation.

Chapter 5

Model Evaluation Metrics

Quantitative research and problem-solving in any field of study invariably proceed with the aid of mathematical models. An important aspect of model development for practical applications is validating the proposed model against empirical data. A good model is usually the result of an arduous, iterative process involving incremental steps of improvement and refinement, guided by empirical data via goodness-of-fit diagnostics. Such diagnostic tools constitute an essential part of the model development process and good tools can go a long way toward shortening the process or improving the quality of the resulting model.

Using the model equations in Sections 3.1 and 3.3 with the method described in Section 4.4 results in simulated total infusion profiles, generated from the nurse-control feedback model and IIR filter. These are compared to the recorded total infusion profiles. For each of the 37 patients, a comparison between the simulated and recorded infusion profile provides an indication of the model's ability to capture the fundamental observed dynamics.

Overlaying the simulated and recorded infusion profiles allows a simple visual comparison between simulated and recorded infusion data. However, objective comparison methods are required for more rigorous model evaluation. To objectively assess how well Equations (3.1)–(3.3) and (3.7)–(3.12) model the agitation-sedation system, two general methods of comparing the recorded and simulated infusion profiles are utilised: a graphical approach and a numerical approach. Both methods, based on accepted statistical analyses, are developed to provide an objective, quantified understanding of the model's ability to capture essential dynamics present in the recorded infusion data. These approaches also examine both the local and global measures of model validity.

The approach to model assessment has two parts:

Graphical Approach Use of local linear kernel regression and Chebyshev's inequality to construct a non-parametric probability band for qualitative visual assessment. This band can also be used to quantify the time in band.

Numerical Approach Use of local linear kernel regression and weighted kernel density estimation to construct a density profile that provides quantitative statistical measures of compatibility between model output and empirical data. This approach more rigorously quantifies the likelihood of the model dynamics being the same as those observed clinically.

The non-parametric character of the overall approach avoids making unnecessary simplifying assumptions about the data. In many applications, including the one in this research, it can be difficult to impose a parametric model on the data, or perhaps even undesirable to do so. Equally importantly, it overcomes the difficulty of comparing the outputs of a continuous model with discrete recorded data.

5.1 Model Evaluation Metrics

A simple indication of the similarity between the recorded and simulated infusion profiles is the total drug dose delivered. If two infusion profiles are similar, then the total drug dose is also similar. Therefore, the total drug dose of the simulated infusion profile, relative to the recorded total drug dose, represents the Relative Total Dose (RTD).

$$RTD = \frac{\text{Total Simulated Dose}}{\text{Total Recorded Dose}} \tag{5.1}$$

RTD is clearly a useful, but not sufficient, measure of similarity between the simulated and recorded profiles. For instance, a simulated infusion equal to a constant infusion at the rate equal to the average recorded infusion rate would result in a RTD=1.0, yet is not a good fit with the recorded data. However, it is a good overall measure of global matching of the model and recorded data.

Deterministic dynamic models represented by differential equations are very popular in many areas of research for modelling all kinds of phenomena that vary over time or space. Empirical data for model evaluation, on the other hand, are almost inevitably discrete measurements of some kind, hence imperfect and noise-corrupted. The goal is to develop a way to assess the models against empirical data, without introducing yet another (parametric) model for the data, so as to avoid imposing an inadequate model onto the data. One way to proceed is to consider non-parametric regression of the recorded data.

Non-parametric regression has been suggested for assessing a parametric statistical model by constructing a confidence band for the proposed model and then checking whether the non-parametric regression curve lies within the band [Azzalini et al., 1989]. For instance, a confidence band may be created for a statistical model of population growth or financial market fluctuations. The regression curve from the measured data can then be overlaid to see whether it falls within the confidence band.

However, in the case of a deterministic model, there is no confidence band. Hence a reversal of roles is suggested – construct a probability band for the non-parametric regression curve and check whether the proposed model lies within the band. This novel approach extends the utility of non-parametric regression for model assessment to deterministic models.

5.2 Probability Band Formulation

A graphical method of identifying instances in time where the model and nurse-controller are less than adequate serves to identify regions of differing performance within a patient's simulated profile. The development of a probability band for the recorded infusion profile [Lee et al., 2005, 2003; Rudge et al., 2005b] enables a visual assessment of the performance of the simulation. The band is constructed using Chebychev's inequality, and represents the target region of the simulated infusion controller. A simulated infusion profile that lies entirely within the probability band represents good performance, while regular departures from the band illustrate where the model does not effectively capture behaviour.

Let U_1, U_2, ..., U_n be the observed time series of the infusion rate over the

time interval $(0, T)$. Assuming the signal includes noise due to error in subjective assessment or response results in the following additive noise model:

$$U_t = \mu_t + \varepsilon_t \tag{5.2}$$

where μ_t is the underlying mean infusion rate and ε is a zero-mean noise process. For $t \in T$, we wish to estimate μ_t from the recorded data using local linear kernel regression with a compact kernel. Centering the kernel at t, let $U_{[t-m]}, U_{[t-m+1]}, U_{[t-m+2]}, \ldots, U_{[t+m-2]}, U_{[t+m-1]}, U_{[t+m]}$ be the observations that are within the support of the $(2m+1)$ long kernel.

An estimate of μ_t, the regression function, obtained using local linear kernel regression with a compactly supported kernel with bandwidth m, can be expressed in the form of a weighted average as [Wand and Jones, 1995]:

$$\hat{\mu}_t = \sum_{i=-m}^{m} \omega_{t,i} U_{t+i} \tag{5.3}$$

where $\omega_{t,i}$ are the normalised effective kernel weights such that, for each t

$$\sum_{i=-m}^{m} \omega_{t,i} = 1 \tag{5.4}$$

and $\omega_{t,i} = 0$ if $t + i < 1$ or $t + i > n$. Note that Equations (5.3)–(5.4) are effectively a finite impulse response filter (FIR) reducing higher frequency content depending on the weights, $\omega_{t,i}$. The estimated regression function, $\hat{\mu}_t$, therefore forms a smoothed profile of the recorded data, representing the underlying mean recorded infusion rate.

The recorded infusion data, U_1, U_2, ..., U_n, are smoothed using local linear kernel regression with the Epanechnikov kernel, according to Equation (5.3), to give smoothed infusion rates, $\hat{\mu}_{1:n}$. The $w_i(t)$ values for the kernel regression are evaluated using:

$$\omega_{t,i} = \sum_{i=-m}^{m} \frac{\{\hat{s_2}(t;h) - \hat{s_1}(t;h)(t_{[i]} - t)\}k_h(t_{[i]} - t)}{\hat{s_2}(t;h)\hat{s_0}(t;h) - \hat{s_1}(t;h)^2}, \tag{5.5}$$

where $t_{[i]}$ is the time index corresponding to $U_{[i]}$, $k_h(t_{[i]} - t)$ is the kernel function

centered about point t with bandwidth h, and $\hat{s_r}(t;h)$ is defined:

$$\hat{s_r}(t;h) = \sum_{i=-m}^{m} (t_{[i]} - t)^r k_h(t_{[i]} - t) \tag{5.6}$$

In this application the Epanechnikov kernel used is defined in Wand and Jones [1995]:

$$k(t) = \begin{cases} 0.75(1-t^2) & \text{if } -1 < t < 1 \\ 0 & \text{otherwise} \end{cases} \tag{5.7}$$

This kernel is selected because it has compact support, meaning that it has a finite number of points within its support, and enjoys certain asymptotic optimality properties [Hardle, 1990; Wand and Jones, 1995], which give it a theoretical edge over other kernel shapes. The amount of smoothing is controlled by the bandwidth of the kernel. The kernel including bandwidth h is defined by

$$k_h(t) = \frac{1}{h} k(\frac{t}{h}) \tag{5.8}$$

Kernel smoothing refers to a general methodology for recovery of the underlying structure in data sets. Kernel smoothing offers a means of estimating the underlying function without the need to specify a parametric model, and has the advantage of mathematical and intuitive simplicity. This application of kernel smoothing utilises local linear kernel regression with a compactly supported kernel. Local linear kernel regression is chosen for its balanced combination of good practical performance and theoretical properties. A compact, or finite, kernel is used to simplify computations and to facilitate the construction of probability bands for the smoothed estimates.

Bandwidth selection is extremely important. An excessively narrow bandwidth results in an under-smoothed estimate that removes little of the random fluctuations from the underlying data structure. An over-sized bandwidth on the other hand results in an over-smoothed estimate that removes part of the underlying structure within the data set. From an engineering perspective, this process is effectively a filtering process to remove noise and recover the underlying systematic dynamics in the data. A suitable bandwidth is one in which the kernel estimate is not overly noisy, yet the essential structure of the underlying function has been recovered. The bandwidth is therefore potentially partly subjective in choice.

A variety of methods exist to select an appropriate bandwidth based upon the properties of the data set. However, for this application in which a fixed bandwidth is used to smooth the infusion profiles for a variety of time series with different total lengths, no obvious objective method of selecting the bandwidth presents itself.

There are many situations where it is satisfactory to choose the bandwidth subjectively by eye, especially when the user has reason to believe that there is certain underlying structure in the data [Wand and Jones, 1995; Silverman, 1986]. The process used in this research involves looking at several estimates over a range of bandwidths and selecting the estimate that recovers the essential structure of the underlying function by removing unwanted noise, without losing important features. In this application, a 4-hour bandwidth was found to achieve these objectives. Moreover, it matches the ~4-hour half-life of the drugs and the 4-hour window in the IIR filter in Equation (4.1).

Let $Ex(\hat{\mu}_t)$ and $Var(\hat{\mu}_t)$ denote the expectation (mean) and variance, respectively, of the regression function estimate $\hat{\mu}_t$. For $0 < p < 1$ and by Chebyshev's inequality, a probability equation can be written:

$$P\left[|\hat{\mu}_t - Ex(\hat{\mu}_t)| < \sqrt{\frac{Var(\hat{\mu}_t)}{1-p}}\right] \geq p \tag{5.9}$$

Thus, if $Ex(\hat{\mu}_t)$ and $Var(\hat{\mu}_t)$ can be estimated, a $100p\%$ probability band for $\hat{\mu}_t$ is defined:

$$Ex(\hat{\mu}_t) \pm \sqrt{\frac{Var(\hat{\mu}_t)}{1-p}} \tag{5.10}$$

Moreover, since Chebyshev's inequality holds regardless of the underlying distribution of $U_{1:n}$, Equation (5.10) is a non-parametric probability band for the mean recorded infusion rate.

The proof in Appendix A shows that $Ex(\hat{\mu}_t)$ and $Var(\hat{\mu}_t)$ can be estimated as defined:

$$\hat{Ex}(\hat{\mu}_t) = \sum_{i=-m}^{m} \omega_{t,i}\hat{\mu}_{t+i} \tag{5.11}$$

$$\begin{aligned}\hat{Var}(\hat{\mu}_t) &= \hat{\sigma}_0^2 \sum_{i=-m}^{m} \omega_{t,i}^2 + 2\hat{\sigma}_1^2 \sum_{i=-m}^{m-1} \omega_{t,i}\omega_{t,i+1} + 2\hat{\sigma}_2^2 \sum_{i=-m}^{m-2} \omega_{t,i}\omega_{t,i+2} + \ldots \\ &\quad \ldots + 2\hat{\sigma}_{2m}^2 \omega_{t,-m}\omega_{t,m} \end{aligned} \tag{5.12}$$

respectively, where $\hat{\sigma}_\lambda^2$ is defined:

$$\hat{\sigma}_\lambda^2 = \frac{1}{n-\lambda} \sum_{k=1}^{n-\lambda} (U_k - \hat{\mu}_k)(U_{k+\lambda} - \hat{\mu}_{k+\lambda}) \quad \forall \ \lambda = 0, 1, \ldots, 2m \tag{5.13}$$

Note that the estimator for $Ex(\hat{\mu}_t)$ in Equation (5.11) has the same form as the local linear kernel estimator for μ_t in Equation (5.3), except with smoothed values replacing recorded data values. Thus, the mean of the regression curve is estimated by the same local linear kernel regression on the regression curve itself.

To summarise, a non-parametric probability band can be constructed using Equations (5.5)–(5.13). After determining $\hat{\mu}_{1:n}$ through kernel smoothing, the means and variances of $\hat{\mu}_{1:n}$ are computed using Equations (5.11) and (5.12). The probability band is then obtained using Equation (5.10). A 99% probability band constructed using this method implies that for at least 99% of the time, the estimated mean value of the recorded infusion rate lies within the band.

Figure 5.1 contains three graphs showing the 99% probability bands for three patients. The probability band is shown as the grey shaded region in each graph. Note that the bands widen automatically near the boundaries where the kernel is truncated and less data points are available to use. Each graph also contains the recorded infusion data (darker solid line).

As a graphical assessment tool, the probability band is useful for model development and refinement. In addition to providing an overall visual indication of model performance, it also draws attention to specific regions of good or poor performance, which is extremely useful for diagnosing model error. However, as yet, it does not provide a quantifiable metric.

A useful numeric metric based upon the probability band is the amount of time that the simulated infusion profile lies within the band, relative to the total recorded time. This metric is denoted as the Time In Band (TIB):

$$TIB = \frac{\text{Time in Band}}{\text{Total Time of Series}} \tag{5.14}$$

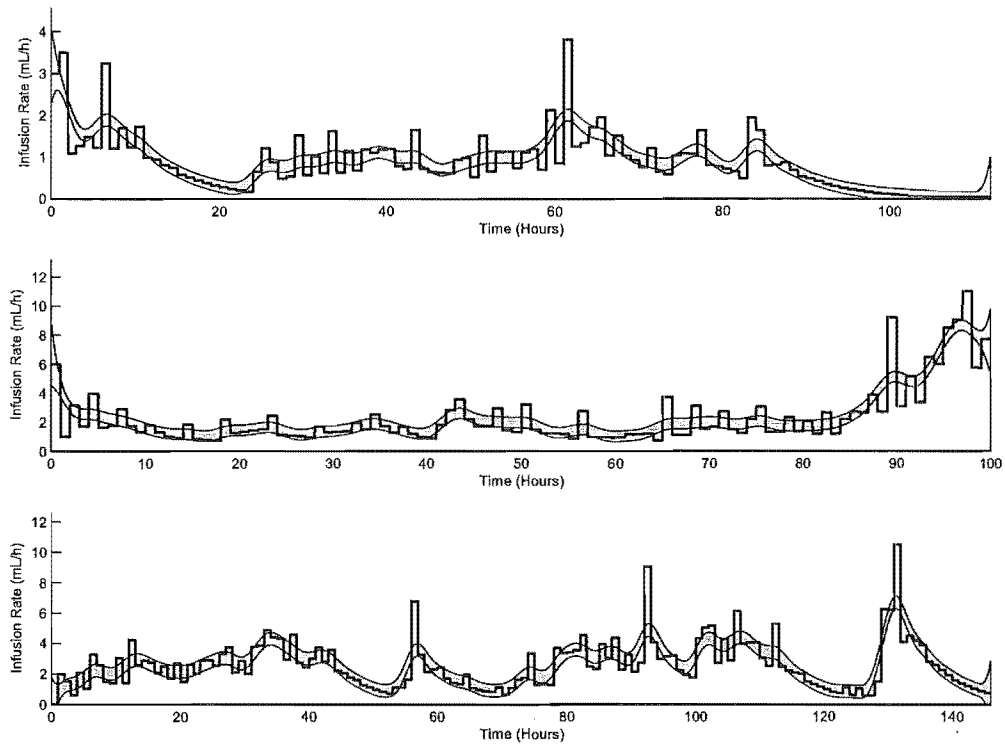

Figure 5.1 Examples of the 99% probability band for three patients.

TIB quantifies a global measure of model validity. However, the TIB does not provide any guidance locally as to where the model may not be valid, as the probability band does visually. Hence, numerically the TIB is a global evaluation metric, while graphically the probability band is both a local and global evaluation metric.

The probability band forms an excellent visual tool for testing and developing improved models. Inspection of a recorded profile and probability band with simulated infusion profile overlaid depicts, in a simple manner, the closeness of fit of the simulated and recorded profiles. Further, locations where the simulated profile departs from the probability band highlight instances where there is a poor fit. Globally, the TIB metric provides a numerical indication of the ability of the model to capture the dynamics present in the agitation-sedation system. Overall this information is extremely useful in identifying dynamics in the agitation-sedation system that are not captured by the model, and provides an invaluable tool for model improvement.

5.3 RAND Metric for Model Evaluation

The form of the mean estimator from Equation (5.3) is also used to define a weighted kernel density estimator that gives an estimate of the marginal density for each smoothed value. Taken together, the set of marginal densities defines a density profile from which numerical measures of compatibility between the proposed model and the empirical data can be defined and computed. Two such measures are presented in this section – average normalised density (AND) and relative average normalised density (RAND).

Intuitively, the AND of the proposed model measures how close the simulated output is to regions of high probability in the recorded infusion profile as determined by the recorded data. RAND calibrates the AND of the proposed model by the AND of the smoothed curve, allowing assessment of the closeness of the model relative to a typical realisation in the form of the smoothed curve. Plotting the density profile using constant density contours would also provide another visual assessment tool that could potentially be more informative than the original probability band.

Let $f_t(\hat{\mu})$ be the marginal density of $\hat{\mu}$ at time t, which describes the density of the infusion rate at time t. Consider a weighted kernel estimator for $f_t(\hat{\mu})$, motivated by the form of $\hat{Ex}(\hat{\mu}_t)$ in Equation (5.11), where each $\hat{\mu}_{t+i}$ is replaced by a normal kernel with variance s_t^2 and centered at $\hat{\mu}_{t+i}$:

$$\tilde{f}_t(\hat{\mu}) = \sum_{i=-m}^{m} \omega_{t,i}\phi(\hat{\mu}|\hat{\mu}_{t+i}, s_t^2) \tag{5.15}$$

where $\phi(\cdot|\mu, \sigma^2)$ denotes the normal density with mean μ and variance σ^2.

It is important to note that the estimated marginal density, $\tilde{f}_t(\hat{\mu})$, should contain the same information expressed by the mean and variance, $\hat{Ex}(\hat{\mu}_t)$ and $\hat{Var}(\hat{\mu}_t)$, in Equations (5.11) and (5.12). It is therefore important that the mean and variance of the marginal density are equivalent to the mean and variance, $\hat{Ex}(\hat{\mu}_t)$ and $\hat{Var}(\hat{\mu}_t)$, in Equations (5.11) and (5.12). To ensure the estimated marginal density, $\tilde{f}_t(\hat{\mu})$, has the same mean and variance as $\hat{Ex}(\hat{\mu}_t)$ and $\hat{Var}(\hat{\mu}_t)$,

the following form of estimator is proposed:

$$\tilde{f}_t(\hat{\mu}) = \sum_{i=-m}^{m} \omega_{t,i}\phi(\hat{\mu}|\alpha_t\hat{\mu}_{t+i} + (1-\alpha_t)\hat{Ex}(\hat{\mu}_t), \alpha_t^2 s_t^2) \tag{5.16}$$

Note that with $\alpha_t = 1$, Equation (5.16) becomes Equation (5.15). More importantly, the presence of α_t gives the added flexibility for matching the mean and variance to $\hat{Ex}(\hat{\mu}_t)$ and $\hat{Var}(\hat{\mu}_t)$.

There are two ways to see how α_t facilitates this matching. First, α_t may be thought of as a shrinkage factor on the locations of the normal kernels and a scale factor on their variance. More specifically, $\hat{\mu}_{t+i}$ is "shrunk" towards $\hat{Ex}(\hat{\mu}_t)$ when $0 < \alpha_t < 1$ and "stretched" away from $\hat{Ex}(\hat{\mu}_t)$ when $\alpha > 1$. Controlling the variance of a kernel density estimator by "shrinking" the kernel locations was first suggested by West [1993]. Here, the kernel locations may also be "stretched". Second, suppose that a random variable is generated from Equation (5.15), multiplied by α_t and then added to $(1-\alpha_k)\hat{Ex}(\hat{\mu}_t)$. The resulting random variable will have density $\tilde{f}_t$.

It is shown in Appendix B at the end of this thesis that the following equalities are valid:

$$Ex(\tilde{f}_t) = \hat{Ex}(\hat{\mu}_t) \tag{5.17}$$

$$Var(\tilde{f}_t) = \alpha_t^2[s_t^2 + \sum_{i=-m}^{m} \omega_{t,i}\hat{\mu}_{t+i}^2 - \hat{Ex}(\hat{\mu}_t)^2] \tag{5.18}$$

With the appropriate selection of α_t and s_t, Equation (5.18) yields:

$$Var(\tilde{f}_t) = \hat{Var}(\hat{\mu}_t) \tag{5.19}$$

Therefore, Equation (5.16) with the appropriate choice of α_t and s_t, represents an estimate of the marginal density of the estimated mean recorded infusion rate at time t, or $\hat{\mu}_t$.

It is observed that near a data boundary, where the regression kernel is truncated, some of the effective kernel weights, $\omega_{t,i}$, can become negative [Wand and Jones, 1995]. These negative values can upset the definition of the weighted kernel estimator in Equation (5.16). To remedy this problem, the following variables

can be defined:

$$\rho_t = \sum_{i=-m}^{m} |\omega_{t,i}| \tag{5.20}$$

$$\omega^{\star}_{t,i} = \frac{|\omega_{t,i}|}{\rho_t} \tag{5.21}$$

so that $0 \leq \omega^{\star}_{t,i} \leq 1$ and

$$\sum_{i=-m}^{m} \omega^{\star}_{t,i} = 1 \tag{5.22}$$

Defining:

$$\hat{\mu}^{\star}_{t+i} = sgn(\omega_{t,i})\rho_t \hat{\mu}_{t+i} \tag{5.23}$$

where $sgn(x)$ denotes the sign of x, and using $\omega_{t,i} = sgn(\omega_{t,i})|\omega_{t,i}|$ and Equations (5.21) and (5.23) yields

$$\sum_{i=-m}^{m} \omega^{\star}_{t,i}\hat{\mu}^{\star}_{t+i} = \sum_{i=-m}^{m} \frac{|\omega_{t,i}|}{\rho_t} sgn(\omega_{t,i})\rho_t \hat{\mu}_{t+i} = \sum_{i=-m}^{m} \omega_{t,i}\hat{\mu}_{t+i} \tag{5.24}$$

showing the equivalence of $\sum_{i=-m}^{m} \omega_{t,i}\hat{\mu}_{t+i}$ and $\sum_{i=-m}^{m} \omega^{\star}_{t,i}\hat{\mu}^{\star}_{t+i}$. Therefore, the modified weighted kernel estimator can be defined:

$$\tilde{f}_t(\hat{\mu}) = \sum_{i=-m}^{m} \omega^{\star}_{t,i}\phi(\hat{\mu}|\alpha_t\hat{\mu}^{\star}_{t+i} + (1-\alpha_t)\hat{Ex}(\hat{\mu}_t), \alpha_t^2 s_t^2) \tag{5.25}$$

As a result, $\tilde{f}_t(\hat{\mu})$ remains well-defined even when some of the effective kernel weights become negative. Moreover, Equation (5.25) is equivalent to Equation (5.16) when all of the effective kernel weights are non-negative.

To summarise, the density profile is the collection of marginal densities computed from Equation (5.25). It enables the definition of an objective, numerical measure of fit between the recorded and simulated infusion rates using the estimated marginal density. These marginal densities can be thought of as the local density of the smoothed infusion profile at the point in time of interest.

Let $U_{1:n} = \{U_1, U_2, ...U_n,\}$ be the sequence of output values produced by a proposed model. The average normalised density (AND) value for the data series

of $U_{1:n}$ is defined:

$$AND(U_{1:n}) = \frac{1}{n}\sum_{t=1}^{n}\frac{\tilde{f}_t(U_t)}{\max_{\hat{\mu}}\tilde{f}_t(\hat{\mu})} \tag{5.26}$$

where AND($U_{1:n}$) is an average of normalised densities, and each component in the sum is the value of $\tilde{f}_t$ at U_t, normalised by the maximum value of $\tilde{f}_t$. A normalised density value equals 1 when U_t occurs at a point where $\tilde{f}_t$ has a maximum value. Therefore, AND($U_{1:n}$) equals 1 if and only if the simulated values coincide exactly with the maximum density at every time point. On the other hand, AND($U_{1:n}$) approaches 0 if the simulated values are all far away from regions of high density. Hence it is a strict statistical representation of how well the model correlates globally, by examining the normalised density for each point in the data series.

Clearly, the interpretation of the values AND($U_{1:n}$) is easy for values near 0 or 1, but less so for values in between. For example, how good is AND($U_{1:n}$) = 0.7 or how bad is AND($U_{1:n}$) = 0.2? To remedy this issue, a calibrated version of AND($U_{1:n}$) using $\hat{\mu}_{1:n}$ is defined:

$$RAND = \frac{AND(U_{1:n})}{AND(\hat{\mu}_{1:n})} \tag{5.27}$$

Equation (5.27) defines RAND as the relative average normalised density (RAND) of ($U_{1:n}$). It tells us what AND($U_{1:n}$) is, relative to a typical realization (in the form of $\hat{\mu}_{1:n}$) from $\tilde{f}_t$. Intuitively, RAND=0.6 may be interpreted as being 60% similar (on average) to a typical realization from $\tilde{f}_t$, where greater similarity means greater compatibility between the simulated values and the empirical ones.

The bottom panel in Figure 5.2 shows the marginal density estimate at t =55 hours, $\tilde{f}_{55}$, for the density profile in the top panel. The simulated hourly infusion rates are indicated by the superimposed dots, and the dot on the x-axis indicates the value of the deterministic simulated infusion rate for t =55. From this plot, it can be seen that for t =55, the value of the marginal density at the simulated infusion rate is approximately 1.0 and the maximum density value is approximately 2.5, giving a normalised density of approximately 0.4.

The AND for the simulated infusion rates is the average of these normalised density values over all time points for a given patient. Similarly, the AND for the smoothed infusion rates is obtained by superimposing the smoothed values onto

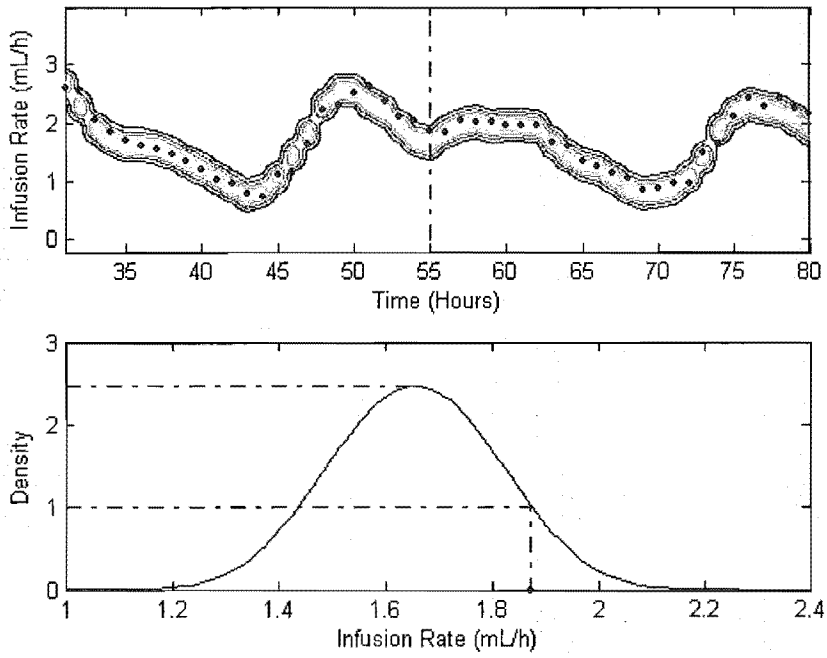

Figure 5.2 Example of the density profile (upper portion) and the marginal density at time point 55 (lower portion).

the same density profile, after which RAND can be computed. Recall that RAND measures how probabilistically similar the model outputs are to the smoothed data, and hence the degree of compatibility between the model and the recorded clinical data. RAND is a global measure of model performance as it does not indicate where (in time) any lack of compatibility may exist.

Since the models in Chapter 3 are deterministic, their outputs do not come from the same probabilistic mechanism that generated the data. As a result, RAND is an extremely stringent measure. Consequently, consistently high RAND values that are close to 1.0 are not expected, even for a good model. A reasonable and practical threshold for adequate model performance is RAND$>$ 0.5, which implies that the model outputs are more similar than not, to the smoothed data. If comparing two models then the higher valued model, assumed to be greater than 0.5 as well, would be selected.

The statistical model evaluation metric, RAND, complements and completes the other statistical tools previously employed for model evaluation. The proba-

bility band with hard boundaries developed previously allows visual assessment and numerical TIB evaluation, which is useful during model development and refinement. RAND provides an objective, calibrated measure of statistical compatibility between the simulated infusion profile and the recorded data. It thus provides a statistical measure of how well the model captures the essential dynamics of the agitation-sedation system. Together, RAND, TIB and the RTD metrics presented in Sections (5.1)–(5.3) cover a range of model evaluation criteria.

Chapter 6

Model Evaluation: Initial Model

This chapter presents the evaluation method, results and discussion for the initial model of Section 3.1. Section 6.1 outlines the procedure used in the simulations and presents the parameters employed in the model. Section 6.2 presents the results and discusses their implications with regard to model evaluation. The overall goal is to analyse the initial and predator-prey models and their parameters.

6.1 Model Evaluation Methods

In this chapter, the initial and predator-prey basic model structures outlined in Chapter 3 are axiomatically assumed to be appropriate representations of observed agitation-sedation dynamics. They are both used to evaluate the available data to provide additional insight in contrasting their results. Given their contrasting linear and non-linear pharmacodynamics the comparison also ensures that results of the linear model are not simply an artefact of loop gain, as discussed. This section introduces the known quantities and measurements for the initial and predator-prey models, and what variables yet remain to be identified.

6.1.1 Elements for Model Analysis

The information available to identify the system consists of two strings of recorded infusion data from 37 patients:

1. Recorded infusion profiles consisting of standard boluses and continuous infusion related by the IIR filter of Equation (4.1).

2. Procedural bolus data.

The elements of the agitation-sedation system model that must be identified for patient specific simulation and analysis are:

1. Stimulus profile, $S(t)$, for input.

2. PD model parameters (ratio w_1/w_2, yielding w_2 for a fixed w_1).

3. Nurse control model parameters (K_p and K_d) for Equation (4.2), or specifically their ratio for a fixed or calibrated K_p.

Table 6.1 summarises this information.

Table 6.1 Summary of information available and elements required for simulation

Model	Information Available	Elements Required
Initial	Standard bolus data Procedural bolus data	Stimulus PD parameters (w_1 and w_2) Nurse control model (K_p and K_d)
Predator-prey	Standard bolus data Procedural bolus data	Stimulus PD parameters (w_1 and w_2) Nurse control model (K_p and K_d)

Because only two independent strings of data are available for determining three elements of the system, a complete system identification is not possible using a single model without an added measurement, such as agitation, which does not fully exist yet [Agogué, 2005]. However using both the initial and predator-prey models, a method is developed for independently determining the required elements of the system.

The main idea of the construction is to show that for the given model structure, the agitation-sedation mechanism chosen is independent of the nurse model

and is fundamentally important for optimal model evaluation metrics. That is, a slightly inferior agitation mechanism cannot be compensated for by changing the nurse model parameters, and the nurse model is independent of the particular agitation mechanism chosen. The nurse model parameters can then be effectively separated from the agitation parameters.

This approach makes the agitation mechanism mathematically identifiable, as it consists of two unknown parameters Stimulus and PD parameters which can be identified from two pieces of recorded data: the standard bolus and infusion data, and the procedural bolus data. The third unknown, parameters K_p and K_d, are accounted for and independently identified by requiring their invariance with respect to two independent models containing two different agitation mechanisms. This invariance property across both models provides the third independent condition required to identify the three unknowns of stimulus, PD parameters and nurse model.

Note that the initial and predator-prey models are expected to capture the same essential PK and PD of the patient, though one model may be slightly inferior to the other. Hence, the external stimulus, S, and nurse model gains, K_p and K_d, must remain unaffected by the choice of model. Both models can therefore be expected to capture the patient dynamic using the same stimulus input and nurse response model across both models. More specifically, given the same stimulus across both models, the identified nurse model gains over all patients and entire patient records should be the same for both models, and largely invariant between patients. Such a result would indicate that the nurse control model obtained is independent of the model and any linear loop gain.

It is also important to note that if the identified nurse control model was different for each of the two patient models, it would indicate that the nurse gains are in fact model-dependant. A model-dependant nurse response would directly imply that one or both patient models did not accurately capture the dynamics in the data. Alternatively, it might equally well indicate an inaccurate model for nursing control response for that model, which implies a model-dependent nursing controller. Such a result would thus be a failure of the modelled patient dynamics to be independent of, and invariant to, the external stimulus and fundamental nursing agitation management response. This last case is not true clinically, where the patient experiences a stimulus and receives treatment independent of

how they might be modelled.

Any model structure that fails to satisfy this requirement could not be considered adequate to model this system. Similarly, any model that did satisfy this requirement and showed improved performance in matching system responses would represent a superior model of the fundamental dynamics to those presented.

The method is outlined as follows:

- Assume the fundamental validity of the initial and predator-prey models as axioms.
- Generate the stimulus profile using the recorded standard bolus data as outlined in Section 4.3.
- Select basic PK parameters and K_T for both models based on observed simulations and information from the literature.
- Identify w_2 for a fixed value of w_1 for both models using the procedural bolus data. Note that w_1 is fixed to calibrate agitation to a 0-100 scale.
- Identify the nurse control model gains independently for ***both*** the initial and predator-prey models using optimisation-based deconvolution across entire patient records.
- Use the average nurse control gains across both models, if similar, to obtain a nurse control model that is independent of either model, yet fundamentally valid for both.

To summarize, in the method outlined the unknown elements, stimulus, S, PD parameters w_1/w_2 and nurse model gains, K_p and K_d, are identified using the recorded standard bolus and infusion data, the procedural bolus data, and the invariance condition of K_p and K_d with respect to the initial model and the predator-prey model.

Importantly, if the initial model structure were a self-fulfilling prophesy, one should be able to get another model with a different agitation mechanism and tune the parameters to get precisely the same or a better match to the data. By

showing that another independent model with a different agitation mechanism gives statistically significant, inferior results after optimally tuning the parameters, contradicts the self-fulfilling prophesy argument, and shows that the initial model structure, which provides the foundation for further improvements later in the thesis, is a real independent representation of agitation dynamics.

Therefore until a superior model structure is found, which can be assessed using the mathematically well-defined method in this chapter, the essential model structure presented in this thesis will provide the foundation for future work in this area. Furthermore, the model structure will provide the basis for launching more clinical studies once further measuring systems like agitation are developed.

6.1.2 Parameter Selection

Although more advanced parameter selection methods are presented for the physiologically-based model in Chapter 8, many parameters for the initial model are manually selected based upon observed performance of the model in simulations and information available in the literature. These parameters are selected to represent the long-term sedation dynamics in sedated ICU patients, and are more carefully evaluated for the physiological model in Chapter 7. Key components of the model such as sedative sensitivity, w_2, and the nurse model control gains, K_p and K_d, are the subject of a more rigorous identification procedure outlined in Sections 6.1.3 and 6.1.4.

The value of K_T is selected to give a drug effect decay rate approximately equivalent to the pharmacokinetic decay rates of Morphine and Midazolam. The relationship between half-life and rate constant K_T can be defined by:

$$K_T = \frac{\ln(2)}{t_{1/2}} \tag{6.1}$$

where $t_{1/2}$ is the desired half-life in minutes. Hence, K_T requires a known $t_{1/2}$ value.

The PK half-life of Morphine and Midazolam in ICU patients is commonly accepted to be longer than that in healthy patients. The half-life of Midazolam is approximately 2-8 hours [Fragen, 1997; Driessen et al., 1991; Malacrida et al.,

1992], and can be as long as 13 hours [Fragen, 1997]. Similarly, the half-life for Morphine also lies in the range 2-8 hours [Bion et al., 1986; Osborne et al., 1993; Aitkenhead et al., 1984; Volles and McGory, 1999], and can be up to 10.5 hours [Bion et al., 1986]. For the initial and predator-prey models, a half-life of 7.5 hours was chosen, corresponding to a K_T value of 0.0015. This value is in the reported range, nearer some of the average reported values. Near the higher end of the range, it also helps account for potential drug accumulation in the system and delayed clearance, for example from fatty tissue [Wagner and O'Hara, 1997; Crippen, 1990; Hughes et al., 1992; Arbour, 2000].

The remaining PK parameters are manually selected through observations of simulations and from data in the literature [Fragen, 1997; Driessen et al., 1991; Malacrida et al., 1992; Bion et al., 1986; Osborne et al., 1993; Aitkenhead et al., 1984; Volles and McGory, 1999; Chase et al., 2004a]. Identical time-invariant parameters are used for all 37 patients, for both the initial and the predator-prey models, and are listed in Table 6.2.

Table 6.2 Parameter values employed in the initial model

Parameter	Value	Unit
K_1	0.008	min^{-1}
K_2	0.0046	min^{-1}
K_3	0.005	min^{-1}
K_T	0.0015	min^{-1}
R	1	mg/mL
V_d	100	L

6.1.3 Obtaining Sedative Sensitivity from Recorded Procedural Bolus Data

The remaining parameters in the initial and predator-prey models, w_1 and w_2, or more specifically their ratio for a fixed w_1, are identified through observed simulation results and additional information contained in the recorded procedural bolus data described in Section 4.1. Selection of the values for parameters w_1 and w_2 relies on two fundamental principles:

- The desired patient agitation range is approximately 0–100, calibrating w_1. Note that this range is in arbitrary units and 100 offers acceptable resolution.

- Procedural boluses are delivered in advance of procedures with the intention to induce the same (mean agitation) state prior to, and in the long term steady state after, the procedure.

The first principle determines the magnitude of w_1, while the second principle leads to the identification of the specific value of w_2. Having selected a value for w_1, the sedative sensitivity, w_2, can then be identified, relative to that value, using the recorded procedural bolus data. In particular, the intent of the procedural bolus combined with recorded dose of delivered procedural bolus provides a method of identifying sedative sensitivity, w_2.

6.1.3.1 Selection of w_1

This section presents the method of identifying w_1, for the initial and predator-prey models, based on the principle that the desired patient agitation range is 0–100. Observations of simulation results using the previously selected PK parameters and the recorded drug delivery rate show that $w_1 \geq 0.03$ leads to agitation values commonly exceeding 100 for some patients, whereas $w_1 \leq 0.03$ leads to agitation values significantly lower than 100 for many patients. Therefore, as a compromise, patient agitation typically in the range 0–100 is achieved using a value of $w_1 = 0.03$. This value is used for both the initial and predator-prey models.

6.1.3.2 Identification of w_2 for the Initial Model

This section presents the method for identifying sedative sensitivity, w_2, for the initial and predator-prey models. The approach is based on the principle that procedural boluses are delivered in advance of procedures to induce the same mean agitation state prior to the procedure and in the steady state (long term) after the procedure. More specifically, clinical instructions indicate that proce-

dural boluses should be given 10–30 minutes prior to the procedure [Shaw et al., 2003b].

Substituting $\epsilon = K_T \int_0^t C_2(\tau) e^{-K_T(t-\tau)} d\tau$ into Equation (3.3) yields:

$$\frac{dA}{dt} = w_1 S - w_2 \epsilon \tag{6.2}$$

Integrating Equation (6.2) leads to:

$$A(t_2) = A(t_1) + w_1 \int_{t_1}^{t_2} S dt - w_2 \int_{t_1}^{t_2} \epsilon dt \tag{6.3}$$

Assuming that patient agitation at $t_2 = \infty$, a long time after the procedure, returns to the same level as at $t_1 = 0$, prior to the procedure, leads to:

$$A(0) = A(0) + w_1 \int_0^{\infty} S dt - w_2 \int_0^{\infty} \epsilon dt \tag{6.4}$$

where $t_1 = 0$ and $A(t_2) = A(t_1) = A(o)$, which can be simplified to:

$$w_1 \int_0^{\infty} S dt = w_2 \int_0^{\infty} \epsilon dt \tag{6.5}$$

Equation (6.5) states that the weighted areas of the stimulus, S, and net pharmacological drug effect, ϵ, must be equal. This equation expresses mathematically the principle behind the procedural bolus as clinically defined. Solving Equation (6.5) for w_2 gives:

$$w_2 = \frac{w_1 \int_0^{\infty} S dt}{\int_0^{\infty} \epsilon dt} \tag{6.6}$$

In this case, Equation (6.6) is independent of the mean agitation. However, note that for a general agitation mechanism in which $\frac{dA}{dt}$ in Equation (6.2) is a function of agitation, like the predator-prey model, the analogous expression for Equation (6.6) will be dependent on the mean agitation, as will be shown in section 6.1.3.3.

Assuming that a procedural bolus is delivered to a patient prior to a painful or uncomfortable procedure, it is possible to obtain the value on the right hand side of Equation (6.6). The recorded procedural bolus data provides the size of bolus delivered which, using the PK equations and previously selected parameters, leads

to $\epsilon(t)$ and the evaluation of the denominator of Equation (6.6). Similarly, the numerator can be evaluated if the intensity and duration of the stimulus profile of the procedure is known. Therefore, the identification of sedative sensitivity, w_2, uses the open-loop portion of the block diagram presented in Figure 4.5. Figure 6.1 presents the open-loop block diagram for the method used to identify w_2 using the procedural boluses.

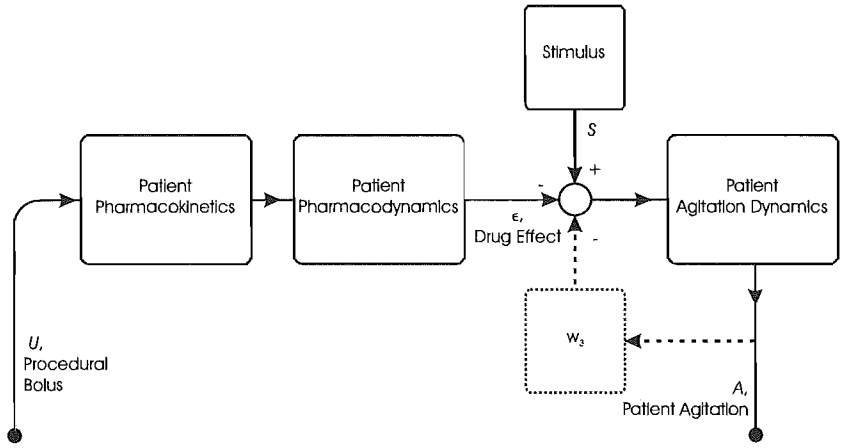

Figure 6.1 Block diagram for the identification of w_2 using procedural bolus data.

The intensity of the stimulus due to the procedure is assumed to be directly proportional to the dose of the stimulus in accordance with the stimulus generation method outlined in Section 4.3. Although the exact duration of the procedure is unknown, an estimate of 10–30 minutes is not unreasonable for the procedures outlined in Section 4.1. Therefore, by simulating the delivery of the procedural bolus and the presence of the stimulus during the painful procedure, all terms on the right hand side of Equation (6.6) can be evaluated.

Figure 6.2 shows an example of a procedural bolus of size 0.8mL delivered at time $t = 1$ hour, followed by a painful/uncomfortable procedure 20 minutes

later, of duration 20 minutes. This figure was generated using w_2 =0.4459. Note that although the procedural bolus causes an almost instantaneous rise in the drug concentration in compartment 1, the transport of the drug to compartment 2 takes further time. Furthermore, while the stimulus, representing the painful/uncomfortable procedure, has an immediate effect on patient agitation, the effect of the drugs is delayed and prolonged. This result occurs because the PK parameters in Section 6.1.2 were selected to represent the long-term sedation dynamics in sedated ICU patients. Importantly, the agitation a long time after the procedure returns to the same value as that prior to the procedure, in accordance with method and principle previously described. Although Figure 6.2 shows the situation where agitation begins at zero, agitation still returns to the initial value even if a non-zero initial agitation value is used. Finally, note that it is assumed the nurse delivers the procedural bolus based on how much a patient should be sedated to negate the effect of the procedure. Thus, in simulations the procedural bolus and procedure are assumed to be separate from other stimuli and drugs, and the initial drug concentrations are set to zero.

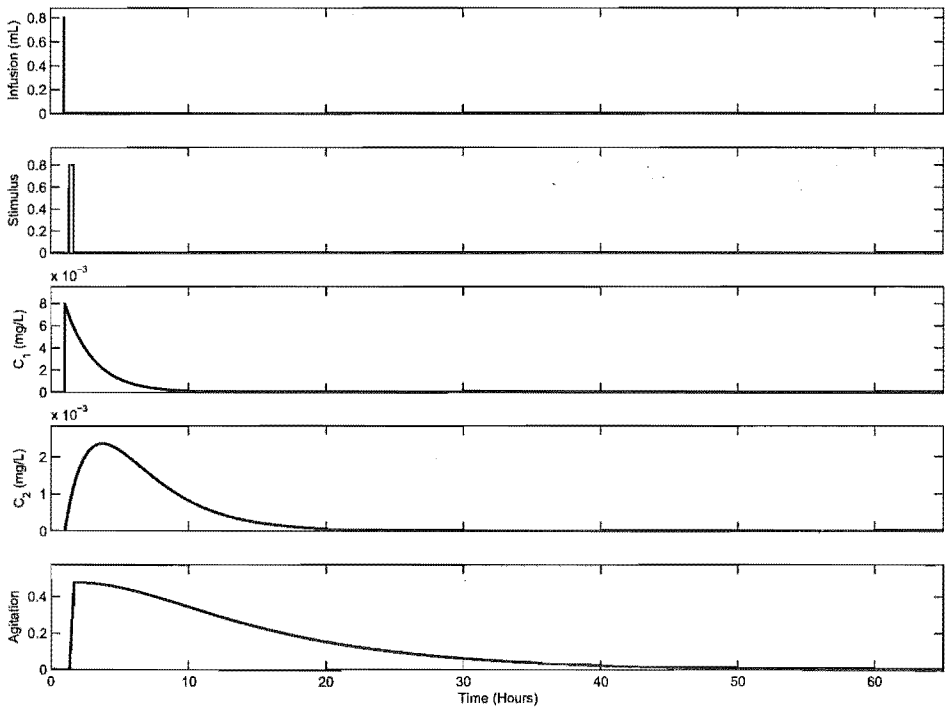

Figure 6.2 Example of a procedural bolus of size 0.8mL delivered at time $t = 1$ hour, followed by a painful/uncomfortable procedure 20 minutes later, of duration 20 minutes.

Note that identification of w_2 using Equation (6.6) is essentially independent

of the order and separation between the procedural bolus and the painful procedure. This feature exists because the key aspect is that the areas under the stimulus and pharmacological drug effect profiles are equal, thereby ensuring that agitation is the same before and after. Using values of 10–30 minutes for stimulus duration in Equation (6.6) yields a range of w_2 =0.23–0.67, and an average value of 20 minutes yields w_2 =0.4459. A value of w_2 =0.4459 is therefore employed in the initial model across all patients.

6.1.3.3 Identification of w_2 for the Predator-Prey Model

All the parameters previously identified are also applicable to the predator-prey model, with the exception of w_2. The procedure for identifying w_2 follows a similar methodology to section 6.1.3.2, but in this case the analogous form of Equation (6.6) for the predator-prey model cannot be written in closed form. However, the equation for w_2 can be formulated implicitly and solved numerically. The final equation of the predator-prey model can be written:

$$\frac{dA}{dt} = w_1 S - w_2 \epsilon A(t) \tag{6.7}$$

where $\epsilon = K_T \int_0^t C_2(\tau) e^{-K_T(t-\tau)} d\tau$. Equation (6.7) has the analytical solution:

$$A(t) = w_1 e^{-w_2 \overline{E}(t)} \int_0^t S(\tau) e^{w_2 \overline{E}(\tau)} d\tau + A_0 e^{-w_2 \overline{E}(t)} \tag{6.8}$$

where, $\overline{E} = \int_0^t \epsilon(\tau) d\tau, A_0 = A(0)$.

Assuming that the patient's agitation at $t = \infty$ a long time after the procedure, returns to the same level at $t = 0$, prior to the procedure, leads to:

$$A_0 = A(\infty) = w_1 e^{-w_2 \overline{E}(\infty)} \int_0^\infty S(\tau) e^{w_2 \overline{E}(\tau)} d\tau + A_0 e^{-w_2 \overline{E}(\infty)} \tag{6.9}$$

where $A_0 = A_{mean}$ is the mean patient agitation. Assuming that the stimulus occurs 20 minutes after the bolus and has a duration of 20 minutes gives:

$$\begin{aligned} S(t) &= S, \ 20 \leq t \leq 40 \\ &= 0, \text{ otherwise} \end{aligned} \tag{6.10}$$

Substituting Equation (6.10) into Equation (6.9) gives:

$$A_{mean} = w_1 e^{-w_2 \overline{E}(\infty)} S \int_{20}^{40} e^{w_2 \overline{E}(\tau)} d\tau + A_{mean} e^{-w_2 \overline{E}(\infty)} \tag{6.11}$$

The solution to Equation (6.11) is defined:

$$w_2 = F(S, A_{mean}) \tag{6.12}$$

where for a given stimulus magnitude, S, and mean agitation, A_{mean}, F is evaluated by numerically solving Equation (6.11) for w_2. Note that in this case the definition of w_2 depends on the average agitation, thus unlike the initial model it may change significantly from patient to patient. Also, a degree of uncertainty or noise on the patient's average agitation should be accounted for, thus the formula for w_2 is defined:

$$w_{2,pred-prey} = F(S, A_{mean,pred-prey} + \delta A_{std,pred-prey}) \tag{6.13}$$

where $A_{mean,pred-prey}$ and $A_{std,pred-prey}$ are the mean and standard deviation of the predator-prey model's simulated agitation and $-1 \leq \delta \leq 1$.

The full rigorous implementation of requires that Equation (6.13) is coupled to the optimisation procedure for finding K_p and K_d described later in Section 6.1.4. The goal can be achieved using the following procedure for each patient:

1. Set $i = 0$
2. Choose $\delta_i = -1 + 0.1i$
3. Approximate $A_{mean,pred-prey}$ and $A_{std,pred-prey}$ using $A_{mean,initial}$ and $A_{std,initial}$, which are the mean and standard deviation of the simulated agitation calculated from the initial model.
4. Calculate $w_{2,pred-prey}$ from Equation (6.13)
5. Find K_p and K_d that give the best RAND for the patient
6. Re-simulate predator-prey model and compute $A_{mean,pred-prey}$ and $A_{std,pred-prey}$
7. Continue steps (4)–(6) until $w_{2,pred-prey}$ converges (changes by less than 1%)

8. The final value of $w_{2,pred-prey}$ satisfies Equation (6.13)

9. Repeat steps (2)–(8) for $i = 1, ..., 20$ and choose the δ_i that gives the best RAND, therefore selecting the corresponding $w_{2,pred-prey}$

Although the above steps describe a general method that could be applied to any model, it was found that for simulations of the predator-prey model, steps (6)–(8) were not required, since convergence was achieved immediately. The reason for this is that the predator-prey model is itself a reasonable model for describing dynamics and as later sections show, gives results that are on average not too different from the initial model. Thus, the following approximation to Equation (6.13) for the case of the predator-prey model was found to be sufficiently accurate:

$$w_{2,pred-prey} = F(S, A_{mean,initial} + \delta A_{std,initial}) \tag{6.14}$$

However, note that for general models with a significantly poorer performance than the predator-prey and initial models this result may not hold. Thus, Equation (6.13) is a mathematically well-defined formula for w_2 based on the recorded procedural bolus data. This definition can be applied to all potential models, and the definition of w_2 is specific to each particular model and independent of all other models. In this case it is approximated by Equation 6.14 for the predator-prey model employed.

This resulting calibration of Equation 6.14 effectively adjusts patient-specific sedative sensitivity, w_2, in the predator-prey model to be essentially equivalent in the mid-range of the patient's agitation to the sedative sensitivity in the initial model, as might be expected. This is a reasonable approximation for the sedative sensitivity in the predator-prey model, and creates inherent equivalence between the initial and predator-prey models when patient agitation is close to the central value for each patient.

6.1.4 Identifying the Nurse Model

6.1.4.1 Invariance Hypothesis

Having selected the parameters for the initial model, the final component required for simulation is identification of the nurse control model parameters, K_p and K_d, outlined in Section 4.2. However, as highlighted in Table 6.1 and section 6.1.1, a third independent condition is required to identify the nurse control model. The nurse control gains K_p and K_d are identified in each of the initial and predator-prey models by requiring both high evaluation metrics and their invariance between the models with the same stimulus. This concept can be expressed in the general form:

Invariance Hypothesis: Given two independent patient models, axiomatically assumed to capture the fundamental agitation-sedation dynamics, an independent nurse control model will produce 'favourable' results in **both models** when implemented using an identical stimulus profile for both models.

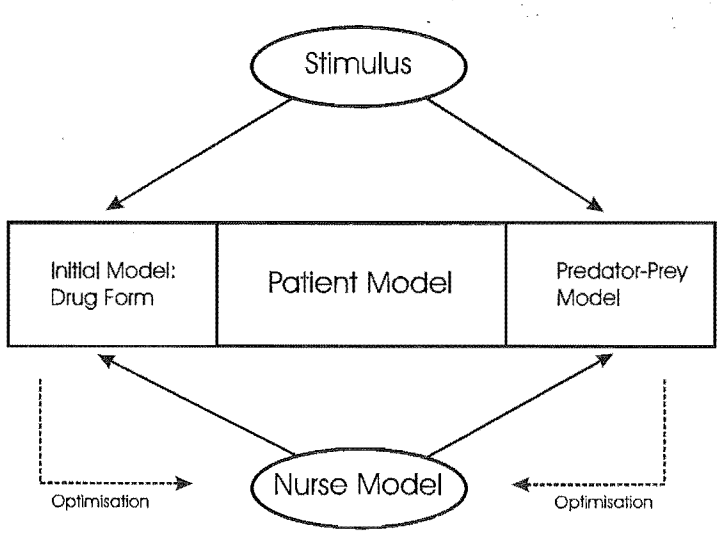

Figure 6.3 Schematic of the invariance hypothesis.

This invariance condition ensures that the nurse control gains cannot be adjusted to make up for a potentially poor agitation model and provides the third property required to make the model mathematically identifiable. Applied to the current situation, the two models are the initial model and the predator-prey model of patient-specific agitation-sedation dynamics. Both models have similar mechanisms at central levels of agitation and drug effect. More importantly, both models have similar overall structure and are representative of typical methods of modelling PD effects for other therapeutics [Carson and Cobelli, 2001; Hann et al., 2005; Doran et al., 2004; Aitkenhead et al., 1984; Chase et al., 2004a; Hughes et al., 1992; Lee et al., 2003, 2005; Persson et al., 1987; Wagner and O'Hara, 1997].

Therefore, both models are assumed, axiomatically, capable of modelling the fundamental dynamics of the agitation-sedation system. However, the initial model is linear in agitation, A, whereas the predator-prey is clearly non-linear. Specifically, the models incorporate different mechanisms for reducing agitation and different assumptions of behaviour, particularly at the extremes of drug effect and/or agitation level. Therefore the two models are independent representations of the fundamental patient dynamics.

The initial and predator-prey models are expected to capture the same PK and PD of the patient. Hence, the external stimulus, S, and nurse model gains, K_p and K_d must remain unaffected by the choice of model. Both models should therefore be expected to capture the patient dynamics using the same stimulus input and nurse response model across both models.

More specifically, given the same stimulus across both models, the identified nurse model gains over all patients and entire patient records should be the same for both models. They should also be largely invariant between patients. Such a result would indicate that the nurse control model is independent of the model any linear loop gain or other self-fulfilling argument.

If the identified nurse control model were different for each patient model, it would indicate that the nurse gains are in fact model-dependant, implying that one or both patient models did not accurately capture the dynamics in the data. Alternatively, it might equally well indicate an inaccurate model for nursing control response for that model. The latter result implies a model-dependent

nursing controller, and thus a failure of the modelled patient to be independent of the fundamental nursing agitation management response.

Any model structure that fails to satisfy this requirement could not be considered adequate to model this system. Similarly, any model that did satisfy this requirement and showed improved performance in matching system responses would represent a superior model of the fundamental dynamics to those presented.

6.1.4.2 Method for Identification of the Nurse Model

Identification of the nurse control parameters is achieved using optimisation-based deconvolution over entire patient records to achieve infusion profiles as close as possible to the average recorded infusion profiles, as indicated by the evaluation metrics TIB and RAND. In particular, a gradient descent search method, employing MATLAB's *FMINSEARCH* function, is used to optimise the nurse control gains for both models independently.

The gains are optimised to provide a constant set of gains over the entire record, rather than obtaining gains that vary each hour as exact deconvolution would provide. Such time-varying gains would not be representative of the average nursing response seen in each record and across all records. More specifically, each patient is treated over their stay by several nurse from the 100 nurses in the Christchurch hospital. Hence, each record represents an overall average clinical central bahaviour. Extreme hour-to-hour variation obtained from exact deconvolution would not accurately represent this situation. More importantly, it is important to discern whether this average response, while clinically accurate, can be effective for the two different axiomatically assumed model structures.

Two primary evaluation metrics are used to identify the nurse proportional-derivative control (PDC) gains for each model:

- Optimising the average RAND across all patients
- Optimising the average TIB across all patients

The gains in Equation (4.2) are optimised with no restriction placed on the possible gain values other than $K_p \geq 0$ and $K_d \geq 0$. Optimising for each metric for each model over all patient records results in four sets of nurse control gains as given in Table 6.3. These gains are optimised over all 37 patients.

Table 6.3 Optimised nurse control model gains

Model	Optimise RAND	Optimise TIB
Initial	K_p=0.000326	K_p=0.00033
	K_d=0.423	K_d=0.425
	Gain Ratio=1297	Gain Ratio=1287
	Median RAND=0.65	Median RAND=0.65
	Median TIB=0.79	Median TIB=0.79
Predator-Prey	K_p=0.000413	K_p=0.000416
	K_d=0.409	K_d=0.388
	Gain Ratio=990	Gain Ratio=933
	Median RAND=0.51	Median RAND=0.48
	Median TIB=0.61	Median TIB=0.61
Average Gains: $[K_p\ K_d]$=[0.00037 0.41]		

The optimised gain values are largely similar in all four cases, with an average value of $[K_p\ K_d]$=[0.00037 0.41], a Gain Ratio ($\frac{K_d}{K_p}$) of magnitude 1000 in each case. These results indicate that a derivative-focused PDC nurse model is appropriate for both the initial and predator-prey models. The inherent nature of a derivative-focused PDC imitate the observational sensing and feedback performed by bedside medical staff. Small changes over long periods (low derivative) have little effect on the control output, while large changes over shorter periods of time (large derivative) significantly affect the commanded sedation administration. Similarly, an absolute change in vital indications only invokes action once it reaches a threshold level. The nursing response equation is presented again here for clarity:

$$U = K_p A + K_d \dot{A} \tag{6.15}$$

where U is the feedback-controlled infusion rate, A is the agitation level, $\dot{A}$ is the rate of change of agitation, and K_p and K_d are the proportional and derivative gains, respectively.

Table 6.3 also presents the median RAND and TIB values for each of the optimised gain values for both models. The median RAND and TIB values for the initial model are 0.65 and 0.79 respectively for both optimisations. This indicates that optimising for TIB or RAND for the initial model makes very little difference in gain selection and evaluation metrics. The median RAND value for the predator-prey model is 0.51 and 0.48 for the RAND-optimised and TIB-optimised methods, and the median TIB is 0.61 for both optimisations. This indicates that optimising for TIB or RAND for the predator-prey model has only a small impact on gain selection and evaluation metrics.

It is clear in Table 6.3 that while both models capture the fundamental dynamics of the agitation-sedation system, the predator-prey model does not capture the dynamics as well as the initial model. The initial model is therefore selected for further analysis of inter-patient variability in the nursing response gains. In particular, the gradient descent search method is used to select patient-specific nurse gains, and observe the range and variability across the 37 patients. This scenario results in one specific PDC nurse model per patient record, resulting in 37 distinct 'nurses'. Table 6.4 presents the statistical summary of the resulting patient-specific nurse gains.

Table 6.4 Results summary for individual optimisation of nurse gains for the initial model

	RAND Optimised		TIB Optimised	
	K_p	K_d	K_p	K_d
Max	0.000400	0.475	0.000443	0.491
UQ	0.000360	0.443	0.000354	0.441
Mean	0.000328	0.427	0.000329	0.426
LQ	0.000310	0.410	0.000300	0.415
Min	0.000244	0.371	0.000243	0.331

Table 6.4 shows that the variation of between patients of the optimal gains is small, and in all cases the Gain Ratio has a value in the order of 1000. Further, the average nurse control gains obtained by optimising for each patient are very close to the gains obtained by optimising across all patients. Finally, it can be seen that optimising RAND or TIB has very little effect on the selection of the nurse control gains. The mean gain values obtained using this method provide a 'constant average nurse across all patients' representing the average ICU nurse and are thus similar to those in Table 6.3 optimised over all patients, as expected.

The feedback-controlled infusion, U, in Equation (6.15) represents the nursing response to agitation. Setting control gains to the rounded average values over both models and objective functions in Table 6.3 of $[K_p\ K_d]$=[0.0004 0.4] implements derivative-focused control. The derivative-focused approach to control focuses on controlling the shape of the agitation response rather than its magnitude, and in this case captures the fundamental nursing response to patient agitation. More importantly, these average nurse control gains represent an average of similar results across both models, are model-independent and thus implement the invariance hypothesis requirement in Section 6.1.4.1.

Derivative-focused control is not uncommon, and can be seen in other pharmaceutical PK/PD feedback controllers in systems similar to the agitation-sedation system [Lam et al., 2002; Doran et al., 2003; Chase et al., 2005b; Hann et al., 2005; Carson and Cobelli, 2001; Fisher, 1991; Furler et al., 1985; Lehman and Deutsch, 1996; Ollerton, 1989]. The controller described by Equation (6.15) with gains $[K_p\ K_d]$=[0.0004 0.4] is therefore selected as the candidate for the nursing response controller. Simulations using this nurse response model in conjunction with both the initial and predator-prey models are used to show the model-independence and of the nursing response.

Table 6.5 summarises the results of simulations for all patients using the same stimulus and independent nurse modelled response across both models, thus matching the hypothesized requirements. The median RAND and TIB values for the initial model are 0.56 and 0.71 respectively, whereas the median RAND and TIB for the predator-prey model are 0.52 and 0.62 respectively. The TIB values are high for both the initial and predator-prey models, although slightly lower for the predator-prey model than for the initial model. RAND values are lower than the TIB values, an indication of the stringency of the RAND values, but follow the same trend between models.

The RAND and TIB values for the initial model, combined with the observed simulated infusion profiles, indicate a very good fit between the recorded and simulated infusion profiles. Although the median RAND value of 0.51 for the predator-prey model is lower than that of the initial model, it is still greater than the 0.5 threshold, indicating a good fit between the recorded and simulated infusion profiles.

Table 6.5 Summary results for initial and predator-prey models using $[K_p\ K_d]$=[0.0004 0.4]

	Initial		Predator-Prey	
	RAND	TIB	RAND	TIB
Max	0.78	0.94	0.71	0.93
UQ	0.66	0.80	0.61	0.75
Med	0.56	0.71	0.51	0.64
LQ	0.51	0.64	0.43	0.52
Min	0.38	0.54	0.25	0.33

These results show that the nurse control model is effective in both the initial and the predator-prey models. Therefore, the nursing response model is shown to be model-independent and is supported by many other biological controllers in similar systems. The nursing response model defined in Equation (6.15) with gains $[K_p\ K_d]$=[0.0004 0.4] is therefore employed for all models throughout this thesis.

The initial model has higher RAND and TIB than the predator-prey model using the independent nurse model and in general, indicating that the initial model captures the fundamental dynamics of the agitation system better than the predator-prey model. This result is supported by clinical observations of patient behaviour and understanding of the agitation-sedation system. In particular, it is not an observation that the ability of drug therapy to reduce agitation is diminished during low agitation, as the predator-prey model depicts. The model development in the following chapters will therefore proceed with the form and structure of the initial model, and the predator-prey model will not be further developed.

In summary, identical time-invariant parameters are used across all 37 patients in the initial, and are summarised in Table 6.6.

6.1.5 Model Evaluation Summary

The initial model and the predator-prey model represent two independent models capturing the fundamental dynamics of the agitation-sedation system. The control gains of a PDC nursing response model were optimised for the initial and

Table 6.6 Parameter values employed in the initial model

Parameter	Value	Unit
K_1	0.008	min^{-1}
K_2	0.0046	min^{-1}
K_3	0.005	min^{-1}
K_T	0.0015	min^{-1}
R	1	mg/mL
V_d	100	L
w_1	0.03	-
w_2	0.4459	-
K_p	0.0004	mL/min
K_d	0.4	mL

predator-prey models independently. These gains were then averaged to create a model-independent nursing response, which can be used across a wider variety of models. Simulations implementing the nursing response in both the initial and predator-prey models showed that while both models produce favourable results, the initial model is a slightly better representation of the agitation-sedation system, particularly in the agitation troughs. The nursing response model is therefore selected for use throughout this thesis and across all patient models, and the initial model is selected for evaluation and further development.

Equations (3.1)–(3.3) can now be implemented in conjunction with the nurse control model developed in Section 6.1.4, the IIR filter, and patient-specific stimulus profile detailed in Chapter 4. This combination models the situation in the Christchurch ICU where the recorded infusion data used for model evaluation was obtained. More specifically, the IIR filter captures the InfuseRite device's impact on the 'raw' nursing sedation management response to patient agitation as captured by the nurse control model of Equation (4.2).

Each patient is simulated by solving the differential equations throughout the length of the recorded infusion, yielding drug concentration profiles, an agitation profile, and a simulated infusion profile for each patient. The simulated and recorded infusion profiles are then compared using the probability band described in Section 5.2 and the numerical metrics RTD, TIB and RAND.

6.2 Simulation Results and Discussion

Figure 6.4 illustrates how the three state variables for this model (C_1, C_2 and A) change over time in response to the simulated nurse infusion, U, and the presence of the stimulus, S. Similarities between the simulated and recorded infusion profiles are clear. In this figure, the solid dark lines represent the model responses to the simulated infusion using nurse control model and IIR filter, while the lighter filled area represents the actual recorded infusion profile.

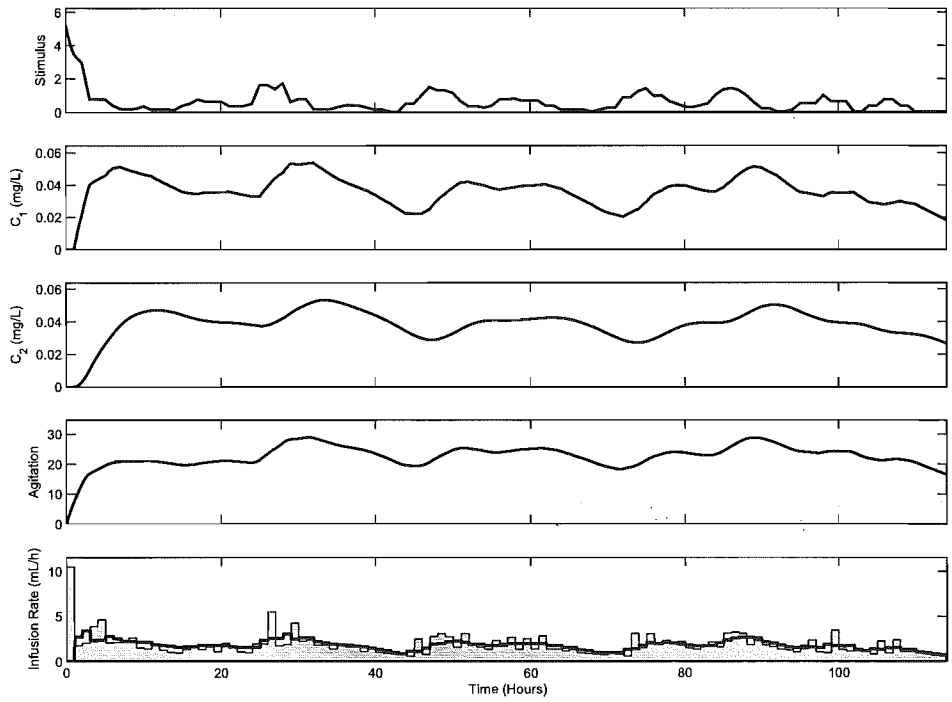

Figure 6.4 Example of modelled responses of recorded and simulated infusion profiles using the initial model for Patient 3.

Figure 6.5 presents three examples of the 99% probability band, with the simulated infusion overlaid. The grey area represents the probability band, the thin line represents the recorded infusion profile, and the solid dark line represents the simulated infusion profile. Again, the similarities between the clinical and simulated data are clear. The graphical nature of these probability bands and their ability to show areas of poorer performance is also evident.

The simulated infusion profiles are clearly smoother than the recorded infusion profiles. This is due to the fact that the recorded infusion profiles are the

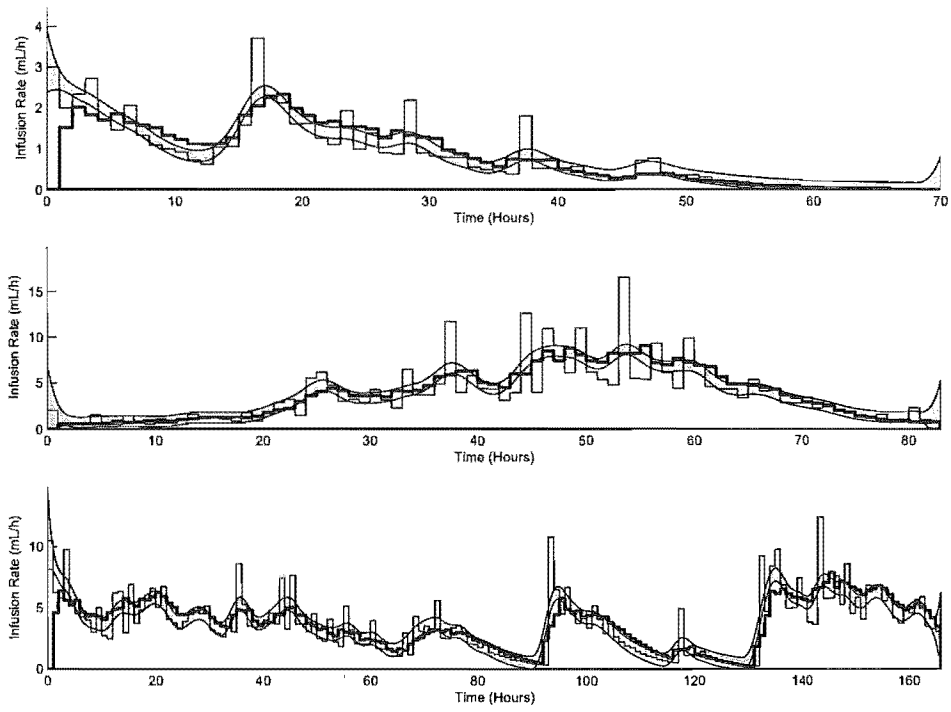

Figure 6.5 Examples of probability bands with simulated infusion profile using the initial model for three patients (Patients 7, 18 and 22 from top to bottom).

result of the response of bedside medical staff who periodically check on the patient, whereas the simulated infusion profile is the result of a consistent control protocol continuously observing patient agitation. In addition, the InfuseRite filter modifies the rate every hour yielding discrete clinical data. This discrete recording will also contribute to a small amount of poor correlation.

Figure 6.5 shows that the simulated infusion profile lies predominantly within the grey 99% probability band and tracks the mean recorded infusion rate closely, for these three patients. Similar graphs are observed for all 37 patients, as demonstrated by the median time within the band of 0.71 across all patients seen in Table 6.7. Due to size, Table 6.7 is located at the end of this Chapter for clarity and ease of use. The TIB has a median of 0.71 with a range of [0.54, 0.94], showing that while for most patients the simulated infusion rate lies predominantly within band, there are some patients where the simulated infusion rate leaves the probability band for approximately 30–40% of the time.

Importantly, a common reason for reduced total time within the probability band is a single, but lengthy, departure from the probability band, rather than

a consistently poor performance throughout the length of the simulation. This feature is observed in the upper plot of Figure 6.5 for Patient 7 between t=7 and t=14 hours. This result implies that, while performing well much of the time, the simulated infusion rate deviates from the recorded infusion rate over some particular period, and takes some time before tending towards the recorded infusion rate again. Equally importantly, these deviations are not visually dramatic and the inherent trends remain similar in both the simulated and clinical profiles.

The periods where the simulated infusion rate departs from the 99% probability band indicate the areas where the model may not capture certain dynamics. These periods may represent periods of particular distress or physiological change due to patient condition, or dynamics that are not captured by the model. In particular, a common reason for the departure of the simulated profile from the probability band is apparent time-delay, as observed in the upper plot of Figure 6.5.

Table 6.7 presents the evaluation metrics for the initial model. The RTD has a median value of 0.99 with a range of [0.92, 1.01], indicating that the simulated infusion rates are very close to the recorded infusion rates over the entire patient record. Ideally, the RTD should approach 1.0, representing identical equivalent doses. The RAND has a median of 0.56, with a range of [0.38, 0.78]. The low values for RAND are a combined result of the stringent criteria imposed by the RAND metric and the actual, overall capability of the initial model to capture all the observed dynamics. Visually, the simulated infusion rate clearly captures all the overall trends of the recorded infusion rate, as indicated by the median TIB=0.71. However, the RAND metric remains relatively low for many patients, highlighting the stringency of the RAND criteria.

Although there is a general correlation between the RAND, AND, TIB and RTD in Table 6.7, this is not always the case. Patient 21, for example, has a RTD of 0.98, which is close to the median RTD across all patients and very close to the ideal value of 1.0. However, the TIB and RAND for Patient 21 are 0.57 and 0.52, both of which are well below the median of 0.71 and 0.56. This result indicates that while RTD provides important information, it is a global variable only, and can be misleading. In contrast, there appears to be relatively good correlation between the TIB and RAND metrics for most patients, although the RAND values are consistently lower. This result is a consequence of the related

formulations of the probability band and the RAND metric, and the stringency of RAND. The evaluation metrics in Table 6.7 are a good illustration that a single metric alone is not a good indication of the model's ability to capture the observed dynamics.

Of the 37 patients, 7 patients have a RAND<0.5, of which two have RAND<0.45 and four 0.45<RAND<0.5. Inspection of the patients with low RAND values reveals that a common feature of these patients is an apparent time-delay between the recorded and simulated infusion rates. An example of this feature is shown in Figure 6.6 for Patient 21. Figure 6.6 shows the recorded and simulated infusion rates for Patient 21 with the probability band overlaid. This delay may be the result of excessive delayed drug distribution in the compartments. As the parameters for this model were manually selected, parameter selection is a likely cause of such differences between the recorded and simulated infusion rates.

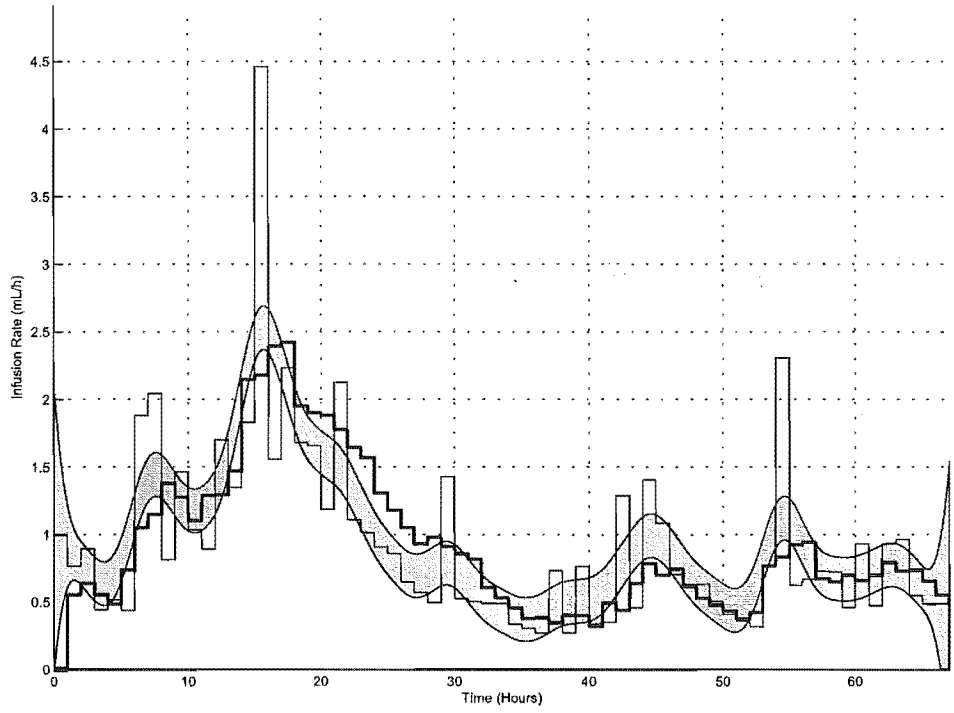

Figure 6.6 Example of the delay between the recorded and simulated infusion profiles using the initial model for Patient 21.

In addition to the apparent delay, there are examples of simulations where the simulated infusion rate lies well below the band at the peaks and troughs. This may be the result of the assumed linear PD relationship in the initial model.

The effect of the linear PD relationship has the most impact at high and low drug concentrations. The linear PD relationship typically over-estimates the PD effect, particularly at high concentrations. This effect may be a reason for the differences between the recorded and simulated infusion rates at the peaks and troughs, and may contribute to the low evaluation metrics.

It must be remembered that while stimulus profiles are specific to each patient, all simulations in this paper utilise identical parameters for all patients, including drug clearance and distribution. Later chapters in this thesis investigate patient-specific parameters. However, the results presented are a good indication that the proposed system model captures the *fundamental* underlying dynamics common to most patients, and generalisable, given the use of identical model parameters for all 37 patients.

6.3 Model Evaluation Summary

The use of two independent models and the invariance hypothesis have enabled evaluation and identification to the limit of the data available. The invariance condition takes account of the fact that the PK/PD equations model patient behaviour and must be independent of the stimulus and drug input. The results of independent optimisation-based deconvolution with a fixed stimulus, $S(t)$, delivered very similar nurse control models and a RAND-verified average nurse model that is model-independent and delivers high TIB.

Overall the results indicate that the simulations are a good representation of the essential fundamental dynamics captured in the recorded infusion profile, but that there are additional dynamics in the agitation-sedation system not captured by this initial model. Nonetheless, the model provides a platform for the testing and analysis of control strategies and protocols that may improve patient agitation management.

Table 6.7 Evaluation metrics for the initial model

	RAND	AND	TIB	RTD
1	0.70	0.65	0.94	0.92
2	0.65	0.52	0.71	0.98
3	0.61	0.52	0.90	0.96
4	0.54	0.49	0.78	0.96
5	0.55	0.42	0.71	1.00
6	0.73	0.61	0.81	0.95
7	0.48	0.37	0.66	0.97
8	0.49	0.37	0.64	0.99
9	0.52	0.41	0.64	0.98
10	0.56	0.45	0.69	1.00
11	0.61	0.50	0.68	0.98
12	0.52	0.42	0.70	0.98
13	0.51	0.42	0.66	0.95
14	0.47	0.40	0.86	0.98
15	0.67	0.49	0.78	0.99
16	0.43	0.33	0.55	0.99
17	0.50	0.43	0.59	0.99
18	0.78	0.63	0.82	1.00
19	0.75	0.56	0.84	0.99
20	0.69	0.56	0.79	0.99
21	0.52	0.39	0.57	0.98
22	0.55	0.43	0.70	0.99
23	0.57	0.48	0.72	1.01
24	0.55	0.44	0.76	0.99
25	0.50	0.38	0.56	1.00
26	0.55	0.43	0.61	0.98
27	0.44	0.35	0.54	0.98
28	0.63	0.48	0.72	0.99
29	0.38	0.32	0.68	0.94
30	0.68	0.53	0.84	1.01
31	0.75	0.59	0.84	0.99
32	0.56	0.43	0.71	0.99
33	0.72	0.56	0.80	0.99
34	0.45	0.35	0.56	0.99
35	0.64	0.52	0.71	0.98
36	0.60	0.50	0.62	0.99
37	0.61	0.55	0.81	0.98
Max	0.78	0.65	0.94	1.01
UQ	0.66	0.52	0.80	0.99
Med	0.56	0.45	0.71	0.99
LQ	0.51	0.41	0.64	0.98
Min	0.38	0.32	0.54	0.92
IQR	0.15	0.12	0.16	0.02

Chapter 7

Model Evaluation: Physiologically-based Model

This chapter employs the physiologically-based model, without the Endogenous Agitation Reduction (EAR) term of Equation (3.12), for evaluation. Section 7.1 outlines the procedure used in the simulations and presents the parameters used in the model. Section 7.2 presents the results of simulations using the physiologically-based model, and discusses their implications.

The model used in this chapter is presented again here for clarity:

I. Pharmacokinetics of Morphine:

$$V_c^a \frac{dC_c^a}{dt} = -(K_{CL}^a + K_{ce}^a + K_{cp}^a)C_c^a + R^a U + K_{ec}^a C_e^a + K_{pc}^a C_p^a \tag{7.1}$$

$$V_p^a \frac{dC_p^a}{dt} = -K_{pc}^a C_p^a + K_{cp}^a C_c^a \tag{7.2}$$

$$V_e^a \frac{dC_e^a}{dt} = -K_{ec}^a C_e^a + K_{ce}^a C_c^a \tag{7.3}$$

II. Pharmacokinetics of Midazolam:

$$V_c^s \frac{dC_c^s}{dt} = -(K_{CL}^s + K_{ce}^s + K_{cp}^s)C_c^s + R^s U + K_{ec}^s C_e^s \tag{7.4}$$

$$V_e^s \frac{dC_e^s}{dt} = -K_{ec}^s C_e^s + K_{ce}^s C_c^s \tag{7.5}$$

III. Pharmacodynamics of Morphine and Midazolam:

$$\frac{dA}{dt} = w_1 S - w_2 K_T \int_0^t E_{Comb}(\tau) e^{-K_T(t-\tau)} d\tau \tag{7.6}$$

where C_c, C_p and C_e are the drug concentrations (mg/L) in the central, peripheral and effect compartments, V_c, V_p and V_e are the distribution volumes (L) of the central, peripheral and effect compartments, U is the IV infusion rate (mL/min), A is an agitation index, S is the stimulus invoking agitation, K_{ij} is the transfer rate (L/min) from compartment i to compartment j, K_{CL} is the drug clearance (L/min), K_T is the effect time constant (min^{-1}), and R^a and R^s are the concentrations of Morphine ('o') and Midazolam ('s') in the infusion solution respectively (mg/mL). Time is represented by t (min), τ is the variable of integration, and the terms w_1 and w_2 are the stimulus and sedative sensitivities respectively. Finally, E_{Comb} is the combined PD effect of the individual effect site drug concentrations of Morphine and Midazolam, determined using response surface modelling displayed in the lower portion of Figure 3.3. Note that Equation (7.6) is missing the EAR term, $-w_3 A$, of Equation (3.12).

7.1 Model Evaluation Methods

Equations (7.1)–(7.6) are implemented in conjunction with the nurse control model, IIR filter for the InfuseRite device, and patient-specific stimulus profile detailed in Chapter 4. Each patient is simulated by solving the differential equations throughout the length of the recorded infusion, yielding drug concentration profiles, an agitation profile, and a simulated infusion profile for each patient. The simulated and recorded infusion profiles are then compared using the graphical probability band and numerical metrics RTD, TIB and RAND evaluated for each patient, as described in Chapter 5.

7.1.1 Patient Specific Parameters and Variability

In this chapter, the physiologically-based model is employed and time-invariant parameters are used for all patients. This agitation-sedation model consists of several PK and PD components. The PK parameters form the basis for the drug

distribution and elimination half-life, while the PD parameters define the shape of the response surface and drug sensitivities.

It is commonly accepted that significant inter-patient variability is observed in the pharmacology of sedatives in the critically ill and elderly [Barr and Donner, 1995; Young et al., 2000]. However, there is evidence that inter-patient variability appears to be due primarily to variations in PD parameters, such as drug sensitivity, rather than PK parameters, such as drug clearance or volume of distribution [Oldenhof et al., 1988; Vinik et al., 1983; Albrecht et al., 1999; Rudge et al., 2005b].

Therefore, identical PK parameters representative of a typical ICU patient were adapted from the literature [Meineke et al., 2002; Lötsch et al., 2002; Persson et al., 1987; Bolon et al., 2003] and applied across all patients. The general shape of the PD response surface in Figure 3.3 is approximated by information in the literature [Wagner and O'Hara, 1997; De Jonghe et al., 2003]. In particular, the response surface is defined to capture the synergistic sedative effects observed when Morphine and Midazolam are administered concomitantly [Wagner and O'Hara, 1997; De Jonghe et al., 2003], the mild sedative effect of Morphine alone [Barr and Donner, 1995; Levine, 1994], and saturation dynamics.

7.1.1.1 PK Parameters

The PK parameters required for the model described by Equations (7.1)–(7.6) are those for Morphine: K^a_{cp}, K^a_{ce}, K^a_{pc}, K^a_{ec}, K^a_{CL}, V^a_c, V^a_p, V^a_e; and those for Midazolam: K^s_{ce}, K^s_{ec}, K^s_{CL}, V^s_c, V^s_e. These parameters are selected based on an extensive literature search of PK parameters in both healthy and ICU patients. Standard PK studies typically record infusion and plasma concentration data, and use fitting techniques to select the PK parameters that result in the best fit to a proposed a PK model. Therefore, the PK parameters obtained in these studies are specific to the selected model, and are therefore not directly applicable to other model structures. However, in many cases conversion/translation of key parameters, such as volume of distribution, overall clearance rate, and internal transfer rates is possible by simple rearrangement of the model equations into similar forms. In many cases, this task simply requires multiplying or dividing by respective volumes of distribution or average weights of patients. The results

in this study, where necessary, have used this method to present parameters in a format suited to the model described by Equations (7.1)–(7.6).

As a result of the recent increased popularity of Midazolam, the literature contains more PK studies for Midazolam than for Morphine. However, for both Morphine and Midazolam, the majority of studies focus on the PK profiles of healthy subjects, rather than critically ill patients. Further, many studies are specifically designed to study the PK profiles of patients with a particular population, such as aged patients, or patients with critical illnesses such as ARF, or CRF, the latter two of which significantly impact drug clearance.

While the internal PK transport rates are important, the primary PK parameters in the compartmental model are the total volume of distribution, V_T, which is the sum of the volumes of the individual compartments, and the clearance rate, K_{CL}. Some studies also report a Minimum Effective Concentration (MEC) or a Observed Concentration Range (OCR), which provide information on the observed drug concentration levels. A summary of the PK studies, and their published PK values is presented for Morphine and Midazolam in Tables 7.1 and 7.2, respectively. In addition to the data presented in Table 7.1, Milne et al. [1996] presents a MEC range for Morphine of 0.0001–0.27mg/L. Similarly, Meineke et al. [2002] presents a OCR for Morphine of 0.2–0.4mg/L.

Table 7.1 General PK parameters in the literature for Morphine

Study	Population Type	n	V_T L	K_{CL} L/min
Milne et al. [1996]	n/a	n/a	125–238	1–2
Bion et al. [1986]	Healthy	8	-	1.1
Bion et al. [1986]	ARF	4	-	1.7
Osborne et al. [1993]	Healthy	10	232.2	1.97
Osborne et al. [1993]	RF	8	127.3	1.17
Aitkenhead et al. [1984]	Healthy	11	221.2	0.85
Aitkenhead et al. [1984]	CRF	9	169.4	0.721
Meineke et al. [2002]	Neuro ICU	9	302.7	1.84
Lötsch et al. [2002]	Healthy	8	304.1	1.26

After consideration of the values in Table 7.1, parameters V_T^a and K_{CL}^a for Morphine were selected to be 200L and 1.5L/min respectively. Similarly, after consideration of the values in Table 7.2, parameters V_T^s and K_{CL}^s for Midazolam

Table 7.2 General PK parameters in the literature for Midazolam

Study	Population Type	n	V_T L	K_{CL} L/min	OCR mg/L
Fragen [1997]	Healthy	8	73.1	0.456	0.35–0.74
Fragen [1997]	Elderly	10	152.6	0.285	-
Fragen [1997]	Young	10	159.6	0.427	-
Driessen et al. [1991]	ARF	6	159.0	0.132	-
Driessen et al. [1991]	ICU	33	106.0	0.198	-
Malacrida et al. [1992]	ICU	8	217.0	0.441	0.19–0.65
Malacrida et al. [1992]	Healthy	8	63.0	0.343	-
Oldenhof et al. [1988]	ICU	17	56–119	0.2-0.4	0.34
Mandema et al. [1992]	Healthy	8	60	0.523	-
Shafer [1998]	ICU	n/a	29–239	0.023–0.502	-
Vinik et al. [1983]	CRF	14	265.3	0.798	-
Vinik et al. [1983]	Healthy	14	152.6	0.471	-
Persson et al. [1987]	Healthy	15	135.8	0.483	0.317–1.25
Bolon et al. [2003]	ICU	30	28.14	0.537	0.0015–1.0

were selected to be 150L and 0.5L/min respectively. These values represent an average over a variety of studies, with particular emphasis on patient populations similar to the ICU population.

Of the studies in Table 7.1, both Meineke et al. [2002] and Lötsch et al. [2002] employ compartmental models for Morphine, and both present a good explanation of the model, including the compartmental diagram. Lötsch et al. [2002] develops a PK model of Morphine and M6G for healthy subjects. Their overall model employs a 3-compartment sub-model for the Morphine portion, and compares two different sub-models for the M6G portion of the overall model. Meineke et al. [2002] also presents a model of the PK of Morphine and its metabolites, but attempts to model the distribution of M3G and M6G in both the plasma and the CSF in neurological patients in an ICU. Like Lötsch et al. [2002], Meineke et al. [2002] employs a 3-compartment model to represent the basic Morphine PK, and adds compartments to represent the PK of M3G, M6G, and the additional CSF concentrations for Morphine and its metabolites. While there is significant debate over the activity and relevance of the Morphine metabolites, the PK of Morphine is more established. Therefore, a 3-compartment model is selected for use in this thesis, and the results from Lötsch et al. [2002] and Meineke et al. [2002], excluding the metabolite portions, are used as the basis for the selection of the

internal transfer rates (K^a_{cp}, K^a_{ce}, K^a_{pc}, K^a_{ec}, K^a_{CL}) and individual compartmental volumes (V^a_c, V^a_p, V^a_e), and are presented in Table 7.3.

Table 7.3 Compartmental PK parameters in the literature for Morphine

Parameter	Unit	Meineke et al. [2002]	Lötsch et al. [2002]
Population		Neuro ICU	Healthy
n		9	8
V_c	L	12.7	17.8
V_p	L	111.0	87.3
V_e	L	179.0	199.0
V_T	L	302.7	304.1
K_{CL}	L/min	1.84	1.26
K_{ce}	L/min	2.09	2.27
K_{cp}	L/min	0.18	0.33
K_{ec}	L/min	2.09	2.27
K_{pc}	L/min	0.18	0.33

Of the studies in Table 7.2, Persson et al. [1987] and Bolon et al. [2003] employ compartmental models for Midazolam, and both present the relevant parameters clearly. Persson et al. [1987] develops a PK model Midazolam for healthy subjects, employing 2-compartments. Bolon et al. [2003] also presents a 2-compartment model of the PK of Midazolam, but uses a PK Software package to determine the PK parameters for patients in an ICU. Therefore, a 2-compartment model is selected for use in this thesis, and the results from Persson et al. [1987] and Bolon et al. [2003] are used as the basis for the selection of the internal transfer rates (K^s_{ce}, K^s_{ec}, K^s_{CL}) and individual compartmental volumes (V^s_c, V^s_e), and are presented in Table 7.4.

Table 7.4 Compartmental PK parameters in the literature for Midazolam

Parameter	Unit	Bolon et al. [2003]	Persson et al. [1987]
Population		ICU	Healthy
n		30	15
V_c	L	28.14	32.97
V_e	L	0.0	102.83
V_T	L	28.14	135.8
K_{CL}	L/min	0.537	0.483
K_{ce}	L/min	0.464	0.610
K_{ec}	L/min	0.323	1.00

After consideration of the published model parameter values in Tables 7.3–7.4, the remaining model parameter values to be employed in this model were selected. These remaining parameters are presented in Table 7.6 and are representative of a typical ICU patient. Note that these PK parameter values are also applied across all patients.

7.1.1.2 PD Parameters

The general shape of the PD response surface in Figure 3.3 is approximated by information in the literature [Wagner and O'Hara, 1997; De Jonghe et al., 2003]. In particular, the response surface is defined to capture the synergistic sedative effects observed when Morphine and Midazolam are administered concomitantly [Wagner and O'Hara, 1997; De Jonghe et al., 2003], the mild sedative effect of Morphine alone [Barr and Donner, 1995; Levine, 1994], and saturation dynamics. The overall shape of the response surface is that of dual sigmoids, which are (individually) encountered frequently in this type of modelling.

The PD response surface methodology presented by Minto et al. [2000], and employed in this research, has 18 defining parameters, including 15 polynomial coefficients, $\beta_i(\theta)$, described in Section 3.3. Furthermore, of the small number of PD studies in the literature, there are few, if any, reporting PD parameters suitable for quantitative use. The fact that inter-patient PD variability is very large only compounds the difficulties associated with PD parameter estimation.

Minto et al. [2000] presented an example response surface that was defined by parameters obtained from fitting data from 400 subjects. However, the fitting procedure was completed using a comprehensive parameter estimation package, and the experimental conditions were strictly uniform. Unfortunately, neither the large data sets, nor the uniform experimental conditions are available in populations such as the critically ill, making precise fitting of the response surface to the empirical data difficult. Fortunately, the main purpose of the response surface in the agitation-sedation model is to capture the synergistic and saturation dynamics, which are features that pertain to the overall shape of the surface, rather than the particular parameters used to define it. Response surface parameter selection is, therefore, based upon the formation of a suitable response surface.

It is commonly accepted that while Morphine is primarily an analgesic, it is also a mild sedative [Berger and Waldhorn, 1995; Schmidt et al., 2004; Tverskoy et al., 1989]. Further, while there are some studies suggesting that the Morphine/Midazolam interaction is additive [Tverskoy et al., 1989], most agree that a synergistic sedative relationship exists between Morphine and Midazolam [Wagner and O'Hara, 1997; Barr and Donner, 1995; Fragen, 1997; Gilliland et al., 1996]. The response surface, therefore, must capture this synergism and the mild sedative effect of Morphine, when used alone, in its shape.

It is commonly accepted that the relationship between drug concentration and PD effect is non-linear [Minto et al., 2000; Fragen, 1997]. Further, one of the important aspects of the observed non-linearity is the saturation of effect at high concentrations. This dynamic creates the plateau in the concentration-effect curve, as seen in the sigmoid curve originally presented in Figure 1.2. The response surface must also capture this important saturation dynamic.

The parameters defining the PD response surface are manually selected to ensure that the surface captures each of these dynamics. In particular, the surface is defined such that the minimum effect is 0, the maximum effect approaches 100, the sedative potency of Morphine is half that of Midazolam, as an approximation of mild effect, and the steepness parameter, ψ, is in the range of example values presented in Minto et al. [2000]. The selected parameters are presented in Table 7.5, and together with patient-specific selection of C_{50}, define the response surface represented in Figure 7.1 for clarity.

Table 7.5 Parameters defining the PD response surface employed in the physiologically-based model

Parameter	Value
E_0	0
$E_{max}(\theta)$	$40 + 210 \cdot \theta - 210 \cdot \theta^2 + 40 \cdot \theta^3 + 0 \cdot \theta^4$
$U_{50}(\theta)$	$1 - 0.1 \cdot \theta + 0.1 \cdot \theta^2 + 0 \cdot \theta^3 + 0 \cdot \theta^4$
$\psi(\theta)$	$4 - \theta + \theta^2 + 0 \cdot \theta^3 + 0 \cdot \theta^4$

All parameters are time-invariant, and those applied across all patients are listed in Table 7.6. The remaining PD parameters, w_1 and K_T, are obtained using techniques similar to those described in Section 6.1 adapted for the physiological model. In particular, a K_T value of 0.0015 was chosen, corresponding to a half-life of 2.5 hours. This value is near the lower end of reported range of 2–8

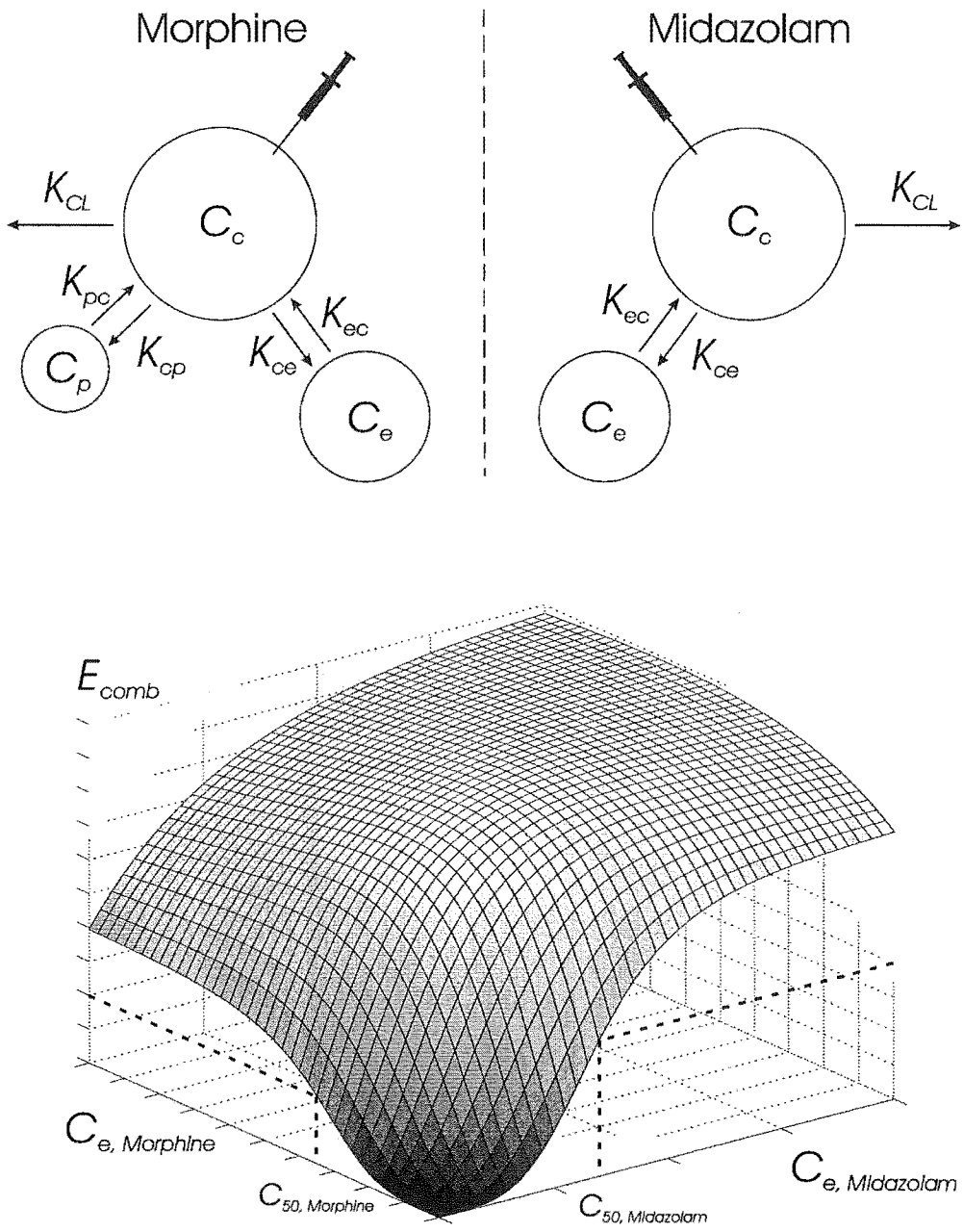

Figure 7.1 Schematic representation of the physiologically-based model, including the compartmental PKs (upper portion) and the PD response surface (lower portion).

hours described in Section 6.1.2 because the PK model now incorporates drug accumulation, which it did not in the initial model selection in Section 6.1.2. Hence, the lower value is now a better and still conservative choice.

Table 7.6 Constant parameter values employed in the physiologically-based model

Parameter	Value	Unit
V_c^a	10	L
V_p^a	70	L
V_e^a	120	L
K_{CL}^a	1.5	L/min
K_{ce}^a	2.1	L/min
K_{cp}^a	0.22	L/min
K_{ec}^a	2.1	L/min
K_{pc}^a	0.22	L/min
R^a	1	mg/mL
V_c^s	30	L
V_e^s	120	L
K_{CL}^s	0.5	L/min
K_{ce}^s	0.5	L/min
K_{ec}^s	0.7	L/min
R^s	0.5	mg/mL
w_1	0.0360	-
K_T	0.0046	min^{-1}
K_p	0.0004	mL/min
K_d	0.4	mL

While most parameters are both time-invariant and constant across all patients, some PD parameters in the physiological model, such as drug sensitivity, w_2, and concentration associated with 50% effect, C_{50}, are time-invariant but vary between patients. The C_{50} are manually selected based on individual recorded infusion profiles and w_2 values selected based on the principles described in Section 6.1.3. The values of C_{50}^a, C_{50}^s and w_2 used for each patient in the results in this chapter are presented in Table 7.7. Due to size, Table 7.7 is located at the end of this Chapter for clarity and ease of use. Time-varying parameters and their identification are discussed in Chapter 8.

7.2 Results and Discussion

Figure 7.2 illustrates, for Patient 3 how the six state variables for the model of Equations (7.1)–(7.6)(C_c^a, C_e^a, C_p^a, C_c^s, C_e^s and A) change over time in response to the simulated infusion, U, and the presence of the stimulus, S. In this figure, the solid lines represent the model responses to the simulated infusion using the nurse control model and IIR filter of Chapter 4, while the lighter filled areas represent the actual recorded infusion profile.

Similarities between the simulated and recorded infusion profiles are clear in this case. Figure 7.3 presents examples of the probability band, with the simulated infusion overlaid, for three patients. In Figure 7.3 the grey area represents the 99% probability band, the thin line represents the recorded infusion profile, and the solid dark line represents the simulated infusion profile. Again, the similarities between the recorded and simulated infusion rates are clear, and these figures can be directly compared to Figures 6.4–6.5 in Chapter 6 for the initial model.

The PK parameters selected in Section 7.1.1.1 determine the rates of distribution between the compartments and the overall clearance, and therefore the compartmental concentrations. The magnitudes of the simulated drug concentrations can therefore be compared to the magnitude of the MEC and OCR values observed in the PK studies presented in Section 7.1.1.1. Simulations for most patients resulted in average Morphine central compartment drug concentrations in the approximate range of 0.03–0.08mg/L, which lies within the minimum effective concentration range (0.0001–0.27) presented in the Morphine review by Milne et al. [1996], but lower than the OCR (0.2–0.4) presented by Meineke et al. [2002].

There are some patients in the cohort with large infusion rates whose simulated central compartment concentrations reached almost 0.2mg/L, nearing the upper end of observed concentrations in Milne et al. [1996]. One plausible reason that the simulated concentrations are not as high as those observed in Meineke et al. [2002] relates to the population of patients studied in Meineke et al. [2002] and the delivery method. Meineke et al. [2002] studied 9 neurological/neurosurgical ICU patients, and delivered the Morphine over a relatively short time intravenously. This infusion method may have resulted in initially

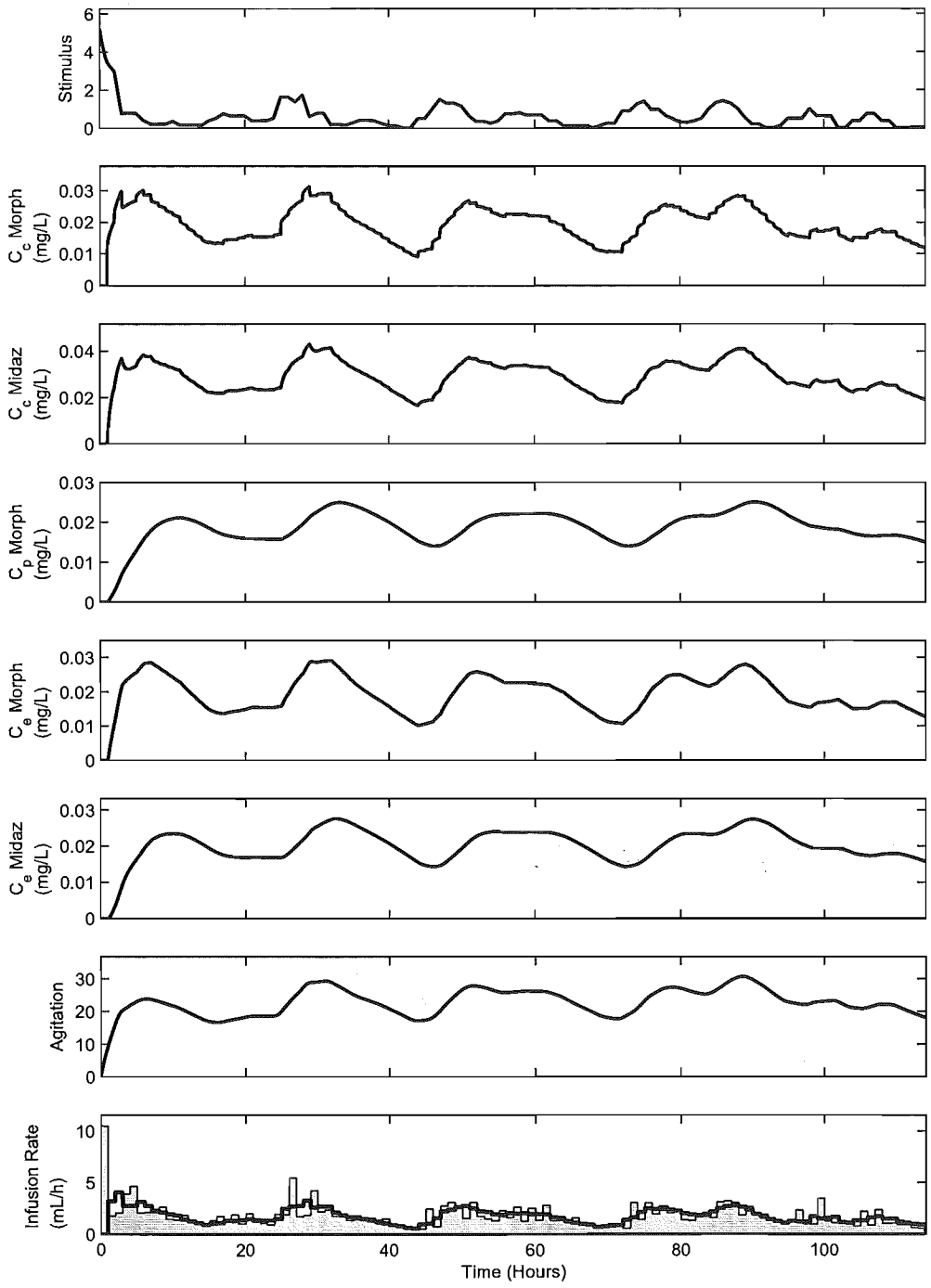

Figure 7.2 Example of modelled responses of recorded and simulated infusion profiles using the physiologically-based model for Patient 3.

high concentrations, or perhaps the dose required by the neurological ICU patients may be higher than general ICU patients. In general, the concentrations observed in the simulations are aligned with the concentrations observed and pre-

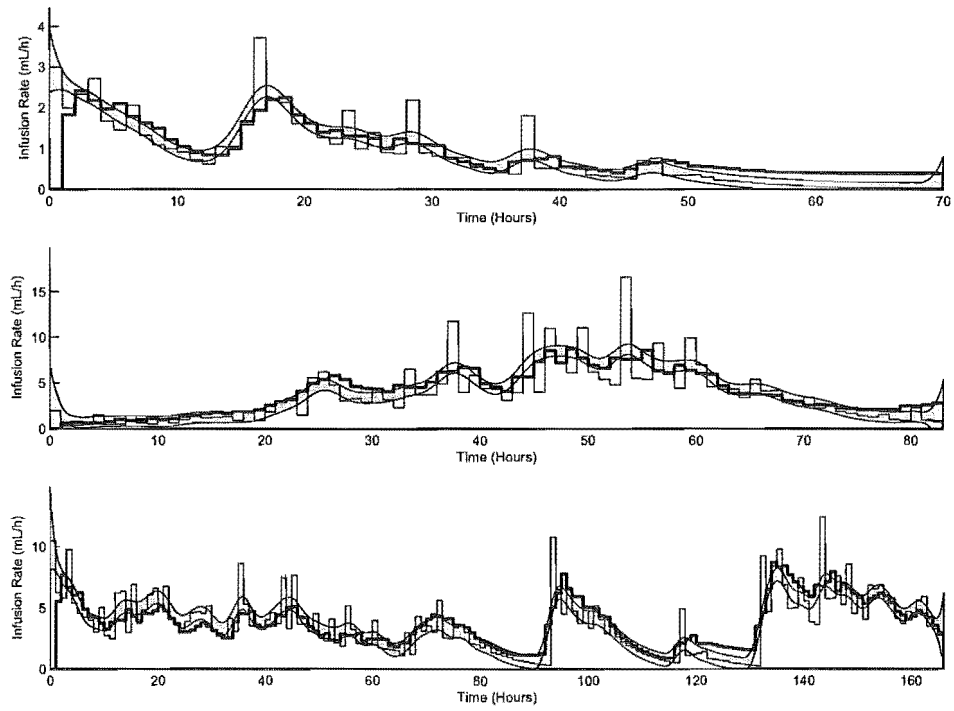

Figure 7.3 Examples of the probability bands with simulated infusion profile using the physiologically-based model for three patients (Patients 7, 18 and 22 from top to bottom).

sented in the available literature, confirming the selection of the PK parameters for Morphine.

Simulations for most patients resulted in Midazolam central compartment drug concentrations in the approximate range of 0.05-0.12mg/L, which is within the OCR (0.00015–1.0) presented in the Midazolam study on ICU patients by Bolon et al. [2003]. There are some patients in the cohort with large infusion rates whose simulated central compartment concentrations exceeded 0.2mg/L, which also falls within the observed OCR of ICU patients in Malacrida et al. [1992]. In general, the concentrations observed in the simulations are aligned with the concentrations observed and presented in the available literature, and in particular those studies on which the PK parameters were based. These results verify the selection of the PK parameters used for Midazolam.

Figure 7.3 shows that the simulated infusion profile lies predominantly within the grey 99% probability band, and tracks the mean recorded infusion rate closely for these three patients. Similar graphs are observed for all 37 patients, as demonstrated by the high median time within the band of 0.70 across all patients seen

in Table 7.8. Due to size, Table 7.8 is located at the end of this chapter for clarity and ease of use. The TIB has a median of 0.70 with a range of [0.39, 0.95], showing that while for most patients the simulated infusion rate lies predominantly within band, there are some patients where the simulated infusion rate leaves the probability band for approximately 40–50% of the time.

The RAND has a median of 0.57, with a range of [0.32, 0.84]. The low values for RAND are a combined result of the stringent criteria imposed by the RAND metric and the general capability of the physiologically-based model. Visually, the simulated infusion rate clearly captures all the overall trends of the recorded infusion rate. However, the RAND metric remains relatively low for many patients, highlighting the stringency of the RAND metric.

Upon inspection of the simulation profiles, it is clear that for most patients the simulated infusion rate remains within the probability band most of the time. However, there are periods of time for many patients where there is a distinct difference between the recorded and simulated infusion rates. In these specific regions the model does not appear to capture the observed patient dynamics.

In some cases this result occurs when absence of stimulus and low drug concentrations coincide with an agitation level that is decreasing, but not close to zero. In such situations, agitation remains at a constant non-zero level, per Equation (7.6), even though the recorded infusion rate drops to near-zero values. For other patients, often those with very long stays in the ICU, the observed difference between recorded and simulated infusion rate may be due to patient-specific parameters varying over the duration of the recorded data, as seen in Figure 7.4. For example, such an effect might be due to drug storage of Morphine and Midazolam in fatty tissues being released later [Crippen, 1990; Hughes et al., 1992; Arbour, 2000]. Simulations incorporating changes in these parameters over time are further investigated in Chapter 8.

The RTD has a median value of 1.01 with a range of [0.87, 1.16]. This result indicates that, across all patients, the simulated infusion rates are very close to the recorded infusion rates. This median RTD value is very close to the ideal value of 1.0, although it is slightly higher than the median RTD from the initial model of 0.99.

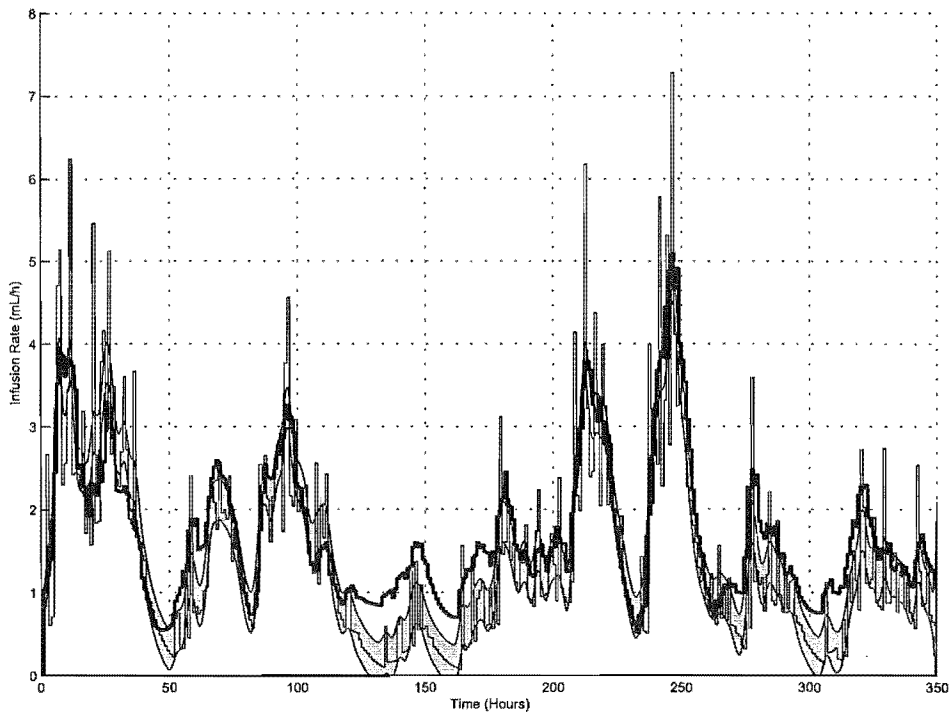

Figure 7.4 Example of the apparent changes in parameters over time for the physiologically-based model for Patient 10.

The physiologically-based model contains the physiological drug effect saturation dynamic, seen by the dual-sigmoid surface in Figure 3.3. However, at this stage Michaelis-Menton (MM) clearance saturation dynamics have not been implemented. Physiological metabolism and secretion of Morphine and Midazolam is limited by renal and hepatic clearance capacity. However, the maximum clearance rate and plasma concentrations at which the dynamics change from being first-order to zero-order kinetics are not easily obtained, particularly in the ICU population. A lack of available parameter values therefore makes the immediate implementation of MM kinetics difficult. However, the model still captures the fundamental agitation-sedation dynamics common to most ICU patients, and therefore provides a platform for the testing and analysis of control strategies and protocols that may improve patient agitation management.

It should be noted that the evaluation metrics in Table 7.8 were achieved using only a few patient-specific PD parameters and identical PK parameters across all patients. This agrees with published reports that inter-patient pharmacological variability is due primarily to PD differences rather than PK differences [Oldenhof et al., 1988; Vinik et al., 1983; Albrecht et al., 1999; Rudge et al., 2004b].

The subsequent fit of the model simulations using these parameter values further supports the model as an appropriate physiological representation of the agitation-sedation system.

Although the evaluation metrics for the physiologically-based model are only moderately improved over the initial model results in Table 6.7, the physiologically-based model is a more realistic representation of the physiology and is developed upon proven studies in the literature. In addition, it is clear from the plots of the simulation results that the physiologically-based model captures more of the fundamental dynamics most of the time, but lacks a dynamic that causes severe deviations from the recorded infusion rate for short, but distinct, periods of time. This result can be seen by the fact that for many patients the simulations using the physiologically-based model are a distinct improvement over those using the initial model (e.g. Patients 6, 17, 21, 23, 26, 36), while there are some patients for whom the results are worse (e.g. Patients 10, 11, 18, 22, 28, 31). The simulations for these patients show that most of the time the physiologically-based model performs much better, but for distinct periods of time in particular patients there is a particular deviation of the simulated infusion rate from the recorded infusion rate. This implies that while the physiologically-based model lacks some dynamics of the agitation-sedation system, it captures many of the important aspects and is a distinct improvement over the initial model.

Table 7.7 Patient-specific parameter values employed in the physiologically-based model

	w_2 $\times 10^{-4}$	C_{50}^a	C_{50}^s
		mg/L	mg/L
1	1.45	0.015	0.015
2	1.95	0.020	0.020
3	4.00	0.040	0.040
4	6.00	0.030	0.070
5	3.00	0.020	0.050
6	3.00	0.020	0.050
7	1.90	0.020	0.020
8	10.0	0.060	0.150
9	5.00	0.050	0.050
10	5.00	0.030	0.070
11	8.50	0.040	0.070
12	5.00	0.030	0.070
13	7.50	0.050	0.080
14	2.15	0.015	0.030
15	7.50	0.060	0.110
16	10.0	0.090	0.110
17	4.50	0.040	0.050
18	10.0	0.090	0.130
19	20.0	0.150	0.250
20	4.00	0.028	0.052
21	2.00	0.030	0.015
22	9.50	0.050	0.150
23	4.00	0.020	0.040
24	5.50	0.040	0.080
25	5.50	0.060	0.055
26	1.36	0.020	0.010
27	8.00	0.070	0.070
28	6.00	0.060	0.055
29	5.25	0.022	0.080
30	2.85	0.020	0.040
31	10.0	0.120	0.080
32	10.0	0.120	0.080
33	10.0	0.130	0.070
34	7.00	0.090	0.060
35	3.50	0.020	0.040
36	6.00	0.080	0.040
37	7.00	0.030	0.080

Table 7.8 Evaluation metrics for the physiologically-based model

	RAND	AND	TIB	RTD
1	0.79	0.73	0.95	0.96
2	0.59	0.48	0.72	1.02
3	0.72	0.61	0.92	0.97
4	0.58	0.52	0.79	0.97
5	0.65	0.49	0.73	1.04
6	0.84	0.71	0.88	1.01
7	0.37	0.28	0.48	1.07
8	0.55	0.41	0.65	1.01
9	0.52	0.42	0.64	1.01
10	0.32	0.25	0.39	1.16
11	0.40	0.33	0.54	0.87
12	0.66	0.53	0.83	0.96
13	0.44	0.36	0.68	1.01
14	0.61	0.52	0.91	1.00
15	0.58	0.42	0.70	1.04
16	0.48	0.37	0.67	1.02
17	0.70	0.59	0.71	0.99
18	0.57	0.46	0.67	1.05
19	0.62	0.46	0.70	1.00
20	0.66	0.54	0.83	1.03
21	0.69	0.52	0.75	1.02
22	0.44	0.34	0.59	1.01
23	0.82	0.70	0.91	0.98
24	0.55	0.44	0.71	1.07
25	0.56	0.43	0.71	1.03
26	0.84	0.66	0.82	1.00
27	0.51	0.41	0.62	1.03
28	0.40	0.30	0.46	1.08
29	0.46	0.39	0.75	0.91
30	0.78	0.60	0.85	0.99
31	0.49	0.39	0.60	1.04
32	0.48	0.37	0.56	1.02
33	0.34	0.26	0.44	1.07
34	0.46	0.35	0.55	1.01
35	0.45	0.37	0.51	0.99
36	0.65	0.53	0.66	1.03
37	0.57	0.52	0.82	0.99
Max	0.84	0.73	0.95	1.16
UQ	0.66	0.53	0.82	1.03
Med	0.57	0.44	0.70	1.01
LQ	0.46	0.37	0.60	0.99
Min	0.32	0.25	0.39	0.87
IQR	0.20	0.16	0.22	0.04

Chapter 8

Parameter Identification and Sensitivity Analysis

The physiologically-based model employed in Chapter 7 captures many of the fundamental observed dynamics in the agitation-sedation system. However, there are some periods in some patient profiles where it is clear that this physiologically-based model does not capture all the observed dynamics. Clinically, for control applications, these periods affect the model's ability to accurately predict ahead to stabilise a patient, requiring the addition of either extra dynamics or time-varying parameters. The importance of time-varying parameters to capture patient behaviour and predict ahead has been shown for similar and analogous glucose-insulin models [Hann et al., 2005], and has been demonstrated clinically in [Chase et al., 2005b]. Thus, for future clinical application, it is important to show that the agitation-sedation model and methods presented in this thesis can be readily extended to include time varying parameters whose real-time identification as the patient evolves will aid prediction and control.

This chapter introduces time-varying sensitivity parameters and the EAR dynamic to the physiologically-based model, and presents a parameter fitting method enabling the estimation of the potentially time-varying and critical model parameters. Note that the main purpose of this analysis is to provide a general way of dealing with unmodelled dynamics which will become important in future work once further sensors for objectively measuring agitation become available.

The integral-based parameter fitting method is adapted from Hann et al. [2005] for the model presented in Section 3.3. This method reduces the standard non-linear, recursive, least squares regression method typically employed [Carson and Cobelli, 2001] into a linear optimisation. This approach requires minimal

computation and allows significant scope to add further dynamics into the model to better match clinical data, due to its low computational intensity and ease of use. The minimal computation required in this method also makes it particularly suitable for clinical application. The model and fitting method are applied to the 37 ICU patient cohort, and parameter variability and sensitivity are analysed.

8.1 Methods

The aim of system identification in this context is to obtain the parameter values that lead to the best fit of the simulated infusion rates to the recorded infusion rates. This parameter fitting method uses identical parameters to those previously defined in Chapter 7, with the exception of C_{50}, w_2, and the introduction of w_3. The PD parameters, such as drug sensitivity, w_2, and concentration associated with 50% effect, C_{50}, are fitted and can vary widely between patients, whereas other PK parameters can be held constant, per the discussion in Section 7.1.1 [Oldenhof et al., 1988; Vinik et al., 1983; Albrecht et al., 1999]. Endogenous Agitation Reduction (EAR) is introduced into the model, and the selection of the EAR sensitivity parameter, w_3, is also presented.

8.1.1 Selection of C_{50}

The parameter C_{50} represents the concentration at which the drug, administered alone, would have 50% effect. Using the PK model parameters and employing the recorded infusion rate as the administered drug input, Equations (3.7)–(3.11) yield Morphine and Midazolam effect site concentration profiles for each patient. These profiles can be used to estimate patient-specific C_{50} values.

These estimated C_{50} values are based on the assumption that clinical effect site concentration rarely becomes completely saturated. Therefore, natural initial estimates for C_{50} would be either the average, or 50% of the maximum, effect site drug concentration from Equations (3.9) and (3.11). However, the synergistic nature of the effect surface means that the total combined effect of the drugs is higher than the simple sum of the individual drug effects, regularly causing saturation using these estimates. Setting C_{50} to be 80% of the max effect site

concentration provides an effective estimate based on the data currently available.

$$C_{50}^{i} = 0.8 \times max[C_{e}^{i}(t)_{openloop}] \tag{8.1}$$

where $C_{e}^{i}(t)_{openloop}$ represents the concentration profile resulting from the concentration profiles resulting from Equations (3.7)–(3.11) and employing the recorded infusion rate as the administered drug input.

8.1.2 Identifying Sedative Sensitivity, $w_2(t)$

An integral-based fitting method is adapted from Hann et al. [2005], and applied to the agitation-sedation model to obtain the patient-specific, time-varying, sedative sensitivity parameter, $w_2(t)$, and the patient-specific EAR parameter, w_3. The aim of the method is to obtain a time-varying w_2 profile and time-invariant w_3 for each patient that produces a close fit of the simulated infusion profile to the recorded infusion profile.

The literature supports high inter- and intra-patient variability of PD drug sensitivity [Barr and Donner, 1995; Young et al., 2000; Oldenhof et al., 1988; Vinik et al., 1983; Albrecht et al., 1999]. Therefore, the sedative drug sensitivity parameter w_2 is allowed to vary over time and between patients. On the other hand, the EAR sensitivity parameter, w_3, is allowed to vary only between patients, and not over time. This decision is based on several factors:

- Physiologically, the production rate of endorphins, the body's natural sedative, is not expected to change dramatically over time.
- Similar endogenous terms in other similar physiological systems have been shown to be time-invariant [Hann et al., 2005].
- The fitting method employed can compensate for small, time-varying changes in other parameters by changes in w_2 over time.

Defining $\epsilon(t) = K_T \int_0^t E_{Comb}(\tau)e^{-K_T(t-\tau)}$, and integrating both sides of Equation (3.12), the following expression holds for all time, t:

$$A(t) = \int_0^t (\{w_1 S - w_2(\tau)\epsilon(\tau)\}e^{-w_3(t-\tau)})dt \tag{8.2}$$

The nurse control model defined in Section 4.2 is presented again for clarity.

$$U(t) = K_p A + K_d \frac{dA}{dt} \tag{8.3}$$

Substituting Equations (3.12) and (8.2) into Equation (8.3) yields an expression for the bolus infusion rate $U(t)$.

$$\begin{aligned} U(t) &= K_p e^{-w_3 t} \int_0^t w_1 S e^{w_3 \tau} d\tau - K_p e^{-w_3 t} \int_0^t w_2(\tau)\epsilon(\tau) e^{w_3 \tau} d\tau + K_d w_1 S \\ &\quad - K_d w_2(t)\epsilon(t) - K_d w_3 e^{-w_3 t} \int_0^t w_1 S e^{w_3 \tau} d\tau \\ &\quad + K_d w_3 e^{-w_3 t} \int_0^t w_2(\tau)\epsilon(\tau) e^{w_3 \tau} d\tau \end{aligned} \tag{8.4}$$

Equation (8.4) can be simplified, yielding

$$\begin{aligned} U(t) &= (K_p e^{-w_3 t} - K_d w_3 e^{-w_3 t}) \int_0^t w_1 S e^{w_3 \tau} d\tau \\ &\quad -(K_p e^{-w_3 t} - K_d w_3 e^{-w_3 t}) \int_0^t w_2(\tau)\epsilon(\tau) e^{w_3 \tau} d\tau \\ &\quad + K_d w_1 S - K_d w_2(t)\epsilon(t) \end{aligned} \tag{8.5}$$

Because the recorded infusion data is updated hourly, Equation (8.5) is only satisfied hourly when used to fit model parameters to recorded clinical data. In between these points, the infusion rate remains constant creating a piecewise-constant profile. Given recorded bolus infusion data and the goal of matching recorded and simulated infusion rates, the recorded bolus infusion data, U_{rec}, can be used for fitting $w_2(t)$ in Equation (8.5). To accomplish this task, a piecewise-constant $w_2(t)$ is defined over time intervals of 1 hour:

$$w_2 = \sum_{i=1}^{n} w_2(i)\{H(t - 60(i-1)) - H(t - 60i)\} \tag{8.6}$$

$$H(t) = \begin{cases} 0 & \text{if } t < 0 \\ 1 & \text{if } t > 0 \end{cases} \tag{8.7}$$

where $H(t)$ is the Heaviside function, n is the number of hours of data available for the patient's stay, and $w_2(i)$ are constant values to be determined. Letting

t=60min in Equation (8.5) yields:

$$\begin{aligned} U_{rec}(60^+) &= (K_p e^{-60w_3} - K_d w_3 e^{-60w_3}) \int_0^{60} w_1 S e^{w_3 \tau} d\tau \\ &\quad -(K_p e^{-60w_3} - K_d w_3 e^{-60w_3}) w_2(1) \int_0^{60} \epsilon(\tau) e^{w_3 \tau} d\tau \\ &\quad + K_d w_1 S(60^-) - K_d w_2(1) \epsilon(60^-) \end{aligned} \tag{8.8}$$

where 60- and 60+ indicate the value immediately before or after the step change in value, respectively. Similarly, at t=120min, Equation (8.5) yields:

$$\begin{aligned} U_{rec}(120^+) &= (K_p e^{-120w_3} - K_d w_3 e^{-120w_3}) \int_0^{120} w_1 S e^{w_3 \tau} d\tau \\ &\quad -(K_p e^{-120w_3} - K_d w_3 e^{-120w_3}) \Big[w_2(1) \int_0^{60} \epsilon(\tau) e^{w_3 \tau} d\tau \\ &\quad + w_2(2) \int_{60}^{120} \epsilon(\tau) e^{w_3 \tau} d\tau \Big] + K_d w_1 S(120^-) \\ &\quad - K_d w_2(2) \epsilon(120^-) \end{aligned} \tag{8.9}$$

Hence, the general equation for the i^{th} hour is defined:

$$\begin{aligned} U_{rec}(60i^+) &= (K_p e^{-60iw_3} - K_d w_3 e^{-60iw_3}) \int_0^{60} w_1 S e^{w_3 \tau} d\tau \\ &\quad -(K_p e^{-60iw_3} - K_d w_3 e^{-60iw_3}) \Big[w_2(1) \int_0^{60} \epsilon(\tau) e^{w_3 \tau} d\tau \\ &\quad + w_2(2) \int_{60}^{120} \epsilon(\tau) e^{w_3 \tau} d\tau + \ldots + w_2(n) \int_{60(n-1)}^{60n} \epsilon(\tau) e^{w_3 \tau} d\tau \Big] \\ &\quad + K_d w_1 S(120^-) - K_d w_2(2) \epsilon(120^-) \end{aligned} \tag{8.10}$$

where the only unknown terms in Equation (8.10) are $w_2(1), w_2(2), ..., w_2(n)$ and w_3. However, if a value for w_3 is assumed, the unknown terms are reduced to $w_2(1), w_2(2), ..., w_2(n)$. Writing this equation for each hour in the patient's profile defines a set of n equations in n unknowns, $w_2(1), w_2(2), ..., w_2(n)$, which can be

written as a matrix system for each patient:

$$\mathbf{X} \begin{pmatrix} w_2(1) \\ w_2(2) \\ \vdots \\ w_2(n) \end{pmatrix} = \mathbf{b} \tag{8.11}$$

where $\mathbf{X}$ is a $(n \times m)$ matrix of variable coefficients from Equation (8.10) and $\mathbf{b}$ is a $(n \times 1)$ vector of resulting constants. Equation (8.11) is readily solved, for a given value of w_3, using any least squares solver for $[w_2(1), w_2(2), ..., w_2(n)]^T$. The trapezium rule is used to numerically evaluate the integrals for the known recorded bolus infusion, $U_{rec}(t)$, and stimulus, $S(t)$, to obtain $\mathbf{X}$ and $\mathbf{b}$. Selecting an array of w_3 values and solving the system of equations for each value of w_3 allows the patient-specific selection of w_3, with simultaneous identification of $w_2(t)$.

To reduce the effects of noise, pre- and post- three-point moving average smoothing steps are used in conjunction with upper and lower constraints on $w_2(t)$ to eliminate unrealistic high-frequency parameter changes. The constraints placed on $w_2(t)$ are $1e^{-6} < w_2 < 1e^{-2}$ to prevent non-physiological small (or negative) and large values, respectively.

The parameter fitting method described above is used to obtain the $w_2(t)$ parameter profile for the array of sedative sensitivity values $w_3 = [0 \quad 0.000001 \quad 0.00001 \quad 0.0001 \quad 0.001 \quad 0.01]$ for each patient. The resulting $w_2(t)$ vector, and the associated w_3 value, can then be used in a model simulation with the nurse control protocol and IIR filter, and the resulting simulated $U(t)$ compared to the recorded infusion data to verify the identified parameters.

To assess the sensitivity of the model to the time-varying $w_2(t)$, the fitted $w_2(t)$ profile is also smoothed using a 12-hour moving average. The results of the model are also observed when the sedative sensitivity, w_2, is set equal to the mean value of the central 50% of the fitted $w_2(t)$ profile. In all cases, the initial portion of the $w_2(t)$ profile for each patient remains as per the parameter-fitting, as the initial phase is influenced by the zero-value initial conditions. The overall set of three simulations (fitted, 12-hour smoothed, and constant w_2) provide insight as to how $w_2(t)$ actually varies with time and its impact on the model and results. The three levels of time-variance investigated are:

- Fitted $w_2(t)$ profile
- 12-hour smoothed $w_2(t)$ profile
- Constant w_2 profile

8.2 Results and Discussion

This section presents the results of the parameter fitting processes. In particular, the selected $C_{50}^{o,s}$ values are presented, and the summary statistics for the time-varying $w_2(t)$ are presented for each patient, along with figures displaying examples of the resulting fitted $w_2(t)$ profiles. The results of different w_3 are then presented. These selected parameters are then implemented in the model and the resulting evaluation metrics presented. Finally, the time variation of sedative sensitivity is investigated and the results presented.

8.2.1 C_{50} Parameter Selection

The C_{50} values for Morphine and Midazolam are evaluated for each patient using the method described in Section 8.1. The resulting selected values are presented in Table 8.1. Due to size, all tables in this chapter, including Table 8.1, are located at the end of this Chapter for clarity and ease of use. For Morphine, C_{50}^{a} has a range of [0.014, 0.143] across all patients, and a median value of 0.052 respectively. For Midazolam, C_{50}^{s} has a range of [0.013, 0.132] across all patients, and a median value of 0.042 respectively. The large range of both C_{50}^{s} and C_{50}^{a}, along with the high IQR, indicate a high inter-patient variability. This result is consistent with published results [Oldenhof et al., 1988; Vinik et al., 1983; Albrecht et al., 1999].

The method described to estimate the patient-specific, time-invariant C_{50} value for Morphine and Midazolam is simple and effective. Although the values are only an estimate, it is clear from the model formulation in Figure 3.3 that the system is not particularly sensitive to the C_{50} value. More specifically, if the C_{50} values are moderately altered, it shifts the locus of the simulation on the

response surface only a small amount. Note also that the fitting method used to fit sedative sensitivity is capable of compensating for minor discrepancies in C_{50}.

Table 8.1 shows that the IQR of the C_{50} values is large enough to indicate that while employing a time-invariant C_{50} may be satisfactory for a given patient, C_{50} is clearly not constant across all patients. If fixed values of C_{50} were used across all patients, some patients would remain high in the saturated plateau of the response curve of Figure 3.3, while others would be on the low portion where the drugs have little sedative effect, leading to poor model performance. Therefore, while the exact patient-specific determination of C_{50} is not important, these values are clearly patient-specific. This result indicates that each ICU patient has a different sensitivity to the drugs. For example, a plasma concentration of 0.02mg/L may have a significant effect on one patient, whereas it may have little effect on another. This last result is regularly observed and well accepted in clinical practice [Albrecht et al., 1999; Wagner and O'Hara, 1997].

8.2.2 Fitting Sedative Sensitivity, $w_2(t)$

The method for fitting $w_2(t)$ described in Section 8.1.2 requires the initial selection of a w_3 value. The specific results of w_3 selection are presented in Section 8.2.4. However, for Sections 8.2.2 and 8.2.3, the selected value of $w_3 = 0.0001$ is used without explanation. Implementing $w_3 = 0.0001$ for all patients and fitting $w_2(t)$ yields a time-varying sedative sensitivity profile for each patient. Examples of these profiles are presented in Figures 8.1–8.3, and the summary statistics of each patient's fitted $w_2(t)$ are presented in Table 8.2, located at the end of this Chapter for clarity and ease of use.

The parameter fitting method presented to identify $w_2(t)$ is seen to be effective, both in the high numerical evaluation metrics in Table 8.3 at the end of this chapter, and the close proximity of the simulated infusion rate to the probability band in the Figures 8.1–8.3. The parameter identification method employed is both effective at fitting the recorded data and computationally inexpensive, making it suited to real-time clinical applications

Table 8.2 highlights the importance of a time-varying, patient-specific sedative sensitivity. The median value across all patients of the median $w_2(t)$ has

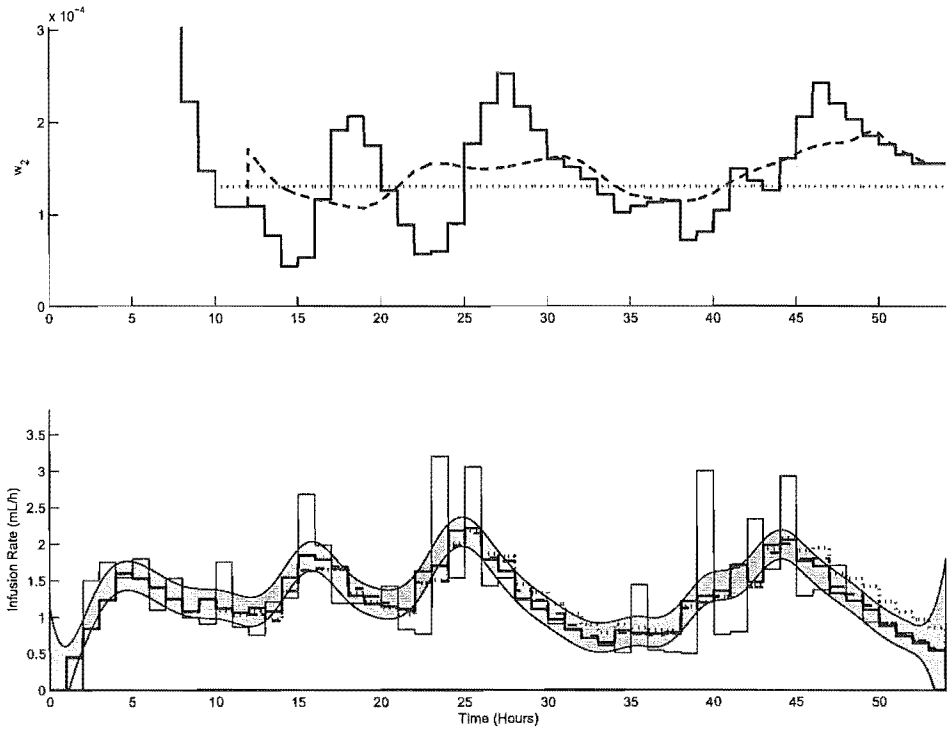

Figure 8.1 Plot showing the effect of time-invariance in $w_2(t)$ using the physiologically-based model for Patient 5.

a value of 4.60 $\times 10^{-4}$ and IQR=6.34 $\times 10^{-4}$. The final column of Table 8.2 presents the IQR of each patient's profile, and shows that the median and IQR are 2.96×10^{-4} and 5.79×10^{-4} respectively. The large median of the IQR column compared to the median of the median column indicates that there are important variations in sedative sensitivity throughout time for most patients. However, the lower quartile and minimum values of the IQR in the final column suggest that the time-varying nature of sedative sensitivity is not necessarily important for all patients.

Similarly, the large range in the first column and high IQR in the second column of Table 8.2 indicate that sedative sensitivity has significant inter-patient variability. These results agree with studies that have found that PD parameters vary significantly between patients [Oldenhof et al., 1988; Albrecht et al., 1999]. Therefore, identifying these changes is critical for understanding and optimising agitation management.

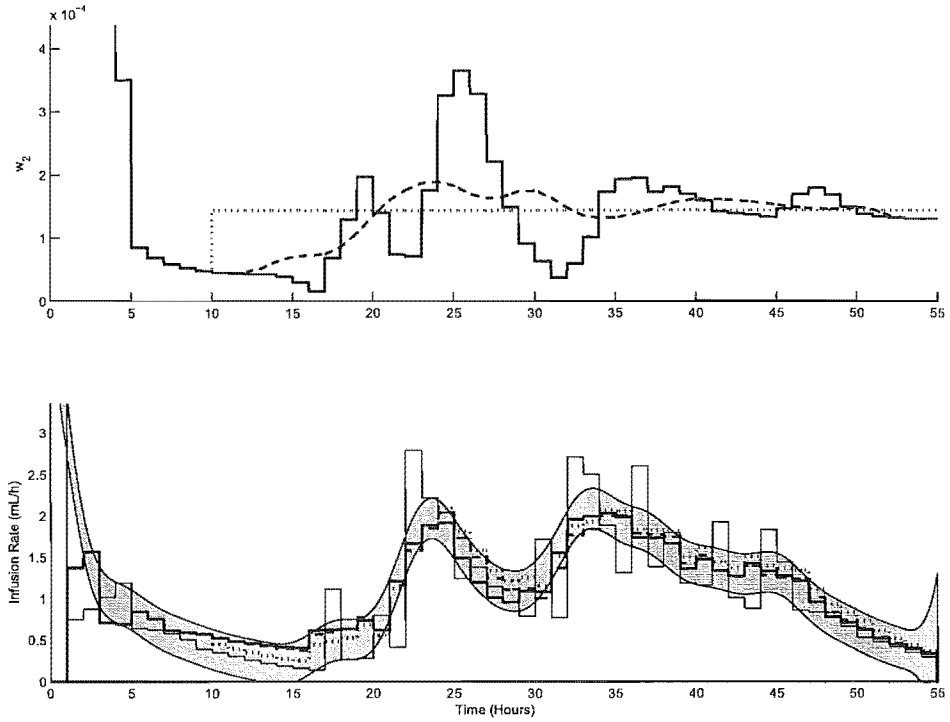

Figure 8.2 Plot showing the effect of time-invariance in $w_2(t)$ using the physiologically-based model for Patient 14.

8.2.3 Effect of Time-Variation on Model Evaluation Metrics

Tables 8.3–8.5, located at the end of this Chapter for clarity and ease of use, present the evaluation metrics RAND, AND, TIB and RTD for simulations with the fitted, smoothed and constant $w_2(t)$ for all patients with $w_3 = 0.0001$, comparing model performance with increasing levels of time-invariant drug sensitivity. Results are presented for three levels of time-variance:

- Fitted $w_2(t)$ profile
- 12-hour smoothed $w_2(t)$ profile
- Constant w_2 profile

Table 8.6 presents only the RAND for the fitted, smoothed and constant profiles for clear comparison, and is also located at the end of this chapter.

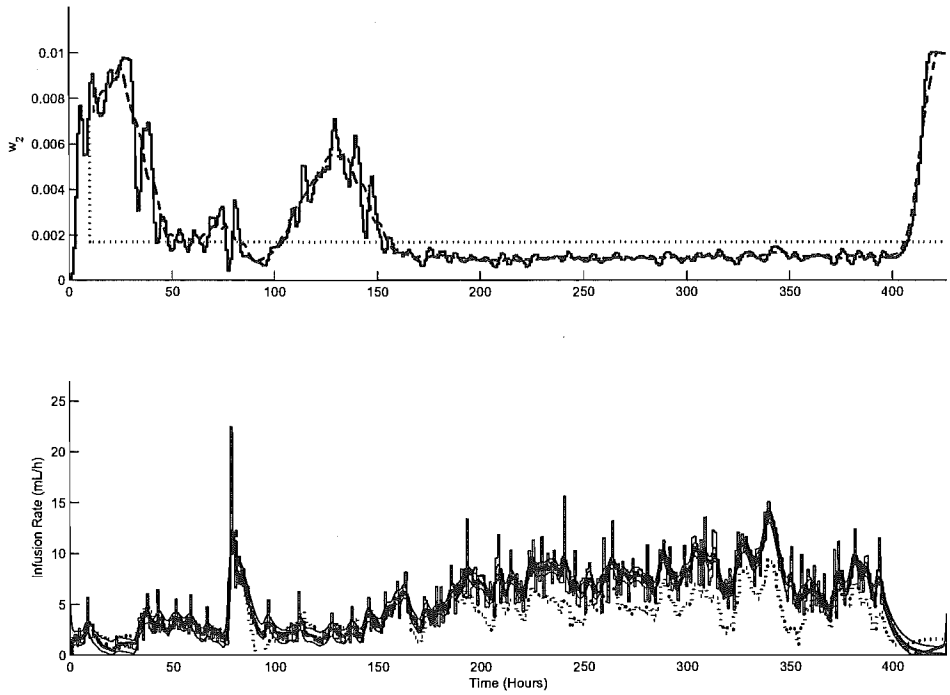

Figure 8.3 Plot showing the effect of time-invariance in $w_2(t)$ using the physiologically-based model for Patient 33.

The median and IQR of the RAND values with fitted $w_2(t)$ in Table 8.3 is 0.94 and 0.09 respectively, with range [0.65, 1.00]. The median and IQR of the TIB values with fitted $w_2(t)$ is 0.93 and 0.05 respectively, with range [0.87, 0.97]. The median and IQR of the RTD values with fitted $w_2(t)$ is 0.99 and 0.02 respectively, with range [0.93, 1.02].

The median and IQR of the RAND values with smoothed $w_2(t)$ in Table 8.4 is 0.78 and 0.08 respectively, with range [0.55, 0.91]. The median and IQR of the TIB values with smoothed $w_2(t)$ is 0.89 and 0.06 respectively, with range [0.81, 0.97]. The median and IQR of the RTD values with smoothed $w_2(t)$ is 0.99 and 0.03 respectively, with range [0.93, 1.01].

The median and IQR of the RAND values with constant $w_2(t)$ in Table 8.5 is 0.54 and 0.21 respectively, with range [0.18, 0.80]. The median and IQR of the TIB values with constant $w_2(t)$ is 0.68 and 0.25 respectively, with range [0.19, 0.93]. The median and IQR of the RTD values with constant $w_2(t)$ is 0.95 and 0.12 respectively, with range [0.48, 1.09].

Figures 8.1–8.3 present examples of the fitted, smoothed and constant $w_2(t)$ profiles, and the fit to the available recorded data when these $w_2(t)$ profiles are implemented in the model in with $w_3 = 0.0001$. In these figures, the upper plot presents the sedative sensitivity, $w_2(t)$, while the lower plot presents the associated simulated infusion profiles. In both the upper and lower plots, the dark solid line represents the fitted profile, the dashed line represents the smoothed profile, the dotted line represents the time-invariant profile and the shaded grey area indicates the 99% probability band overlaid on the thin-line recorded infusion profile.

Comparing the graphical results of the probability band and the RAND values, it is clear that RAND is a very stringent measure and is very sensitive to minor deviations. This result is particularly obvious when Figures 8.1 and 8.2 are compared to the numerical values of RAND in Tables 8.3–8.5 for Patients 5 and 14. Where these figures display a slightly worse fit to the recorded data in the case of the smoothed and time-invariant profiles, the RAND values for Patient 5 decreases from 1.00 to 0.84 for the 12-hour smoothed case, and further to 0.63 using a constant $w_2(t)$. Therefore, as previously mentioned, RAND > 0.5 is considered a reasonable model evaluation threshold.

The high median RAND of 0.94 and range [0.65, 1.00], as well TIB and RTD values with medians of 0.93 and 0.99, indicate that the fitting method produces a sedative sensitivity profile, $w_2(t)$, for each patient that produces simulated results closely fitting the recorded data. The $w_2(t)$ profile captures physiological changes in sedative sensitivity, as well as any other time-varying dynamics that may be present, including noise. These other dynamics can include things such as model shortfalls, transient dynamics not captured by the model, time-varying changes to the state of the patient, errors/inconsistancies in any of the other parameters, sensor error, and/or errors/subjectivity embedded in the recorded infusion data. Hence, some portion of the observed variation for a given patient may be due to any of these issues.

By increasing the time invariance of $w_2(t)$, the effect of many of these other influences is reduced. Using a 12-hour moving average filter smoothes out short-term changes in $w_2(t)$ to represent a more physiologically-realistic sedative sensitivity profile. The results can be seen graphically in Figures 8.1–8.3, and numerically in Table 8.6. The dashed lines in the upper plots of Figures 8.1–8.3

clearly show the small time-scale changes that are removed by 12-hour smoothing. As seen in the lower plots, the simulated infusion profile for the smoothed parameter is not drastically different from the unsmoothed version. Due to the greater stringency of the RAND value, the decrease in fit is more obvious in this metric. However, with a minimum RAND across all patients of 0.55, the fit is still acceptable by this standard.

For some patients, the removal of short term dynamics from the fitted $w_2(t)$ by smoothing has very little effect, as seen in Figures 8.1 and 8.2. For other patients, the variations are more important, at least for some portion of their stay. This impact would be more evident for those patients with noticeably decreased RAND. A good example of a case where there are distinct regions in which changes in $w_2(t)$ are important can be seen in Figure 8.3. From 0–50 hours, $w_2(t)$ remains relatively high. From 50-100 hours $w_2(t)$ is significantly reduced. From 100–150 hours, $w_2(t)$ returns to a high value. Finally, from 150 hours onward $w_2(t)$ is much lower again. In each region, the level of fluctuation around the smoothed line varies as well. While the exact cause for this feature is unknown, it may be a result of changes in the physiological status of the patient as their condition in the ICU evolves.

Figures 8.1–8.3 also display the sedative sensitivity profile and resulting infusion rate for time-invariant $w_2(t)$. In this case, $w_2(t)$ equals the mean of the central 50% of the fitted $w_2(t)$ values, as a representative value for the whole record. In some cases, the result has minimal effect, as seen in Table 8.6 for Patients 1–3 and 5, for example, and observed in Figure 8.1. For over half of the patients, constant sedative sensitivity still results in RAND values greater than 0.5. This result does not suggest that for the remaining nearly 50% of patients a time-invariant sedative sensitivity cannot result in a good fit, but rather that the particular sedative sensitivity value employed does not result in a good fit. In many of these cases, the poor fit is due to the specific selection of the time-invariant sedative sensitivity value. For example, in Figure 8.3 it is clear that a lower time-invariant sedative sensitivity value would result in a better fit, at least for the majority of the recorded period. Hence, experience and initial analysis indicate that significant improvements in fit can be made by utilising a very simple piecewise-constant sedative sensitivity with slow time variation.

Finally, it is clear that $w_2(t)$ is a patient-specific parameter relating to overall drug sensitivity, which is a critical parameter if sedation management is to be optimised for each patient. The results of smoothed and time-invariant forms of $w_2(t)$ indicate that the agitation-sedation system is insensitive to minor, short-term changes in this parameter. However, in many patients long term changes in sedative sensitivity over time are observed and are important features. These results contribute important insights toward understanding the agitation-sedation system, and the way patient parameters change over time.

8.2.3.1 Summary

The parameter identification method employed is both effective at fitting the recorded data and computationally inexpensive, making it suited to real-time clinical applications. RAND is seen to be an effective, statistically rigorous, and stringent evaluation metric for model assessment and evaluation. The parameter C_{50} is time-invariant but shown to have a high inter-patient variability. However, the model is reasonably insensitive to accurate selection of C_{50} for a given patient and the subsequent $w_2(t)$ fitting method is capable of adapting accordingly.

Acceptable RAND values for all 37 ICU patients resulted from the 12-hour smoothed sedative sensitivity and support the model as a sound platform for the development and testing of advanced control protocols for semi-automated sedation systems. Sedative sensitivity, $w_2(t)$, is found to be both patient-specific and time-varying. However, while the variation between patients can be as large as a factor of 10, the variation in time is smaller, and varies only slowly over a period of days rather than hours. This last result indicates that drug sensitivity is not likely to be regulated by hormonal action or patient condition (as might be expected), and instead may be due to the physiology surrounding the blood brain barrier. It may also vary, over days, as patient condition evolves.

Finally, the high evaluation metrics reported for RAND, TIB and RTD show that the extended agitation-sedation model explored in this chapter is capable of capturing the fundamental dynamics of the agitation-sedation system, particularly in comparison to prior models. While there are clearly observed dynamics that the model does not capture, many of the dynamics common to most patients are incorporated in the model. Overall the model captures the fundamental dy-

namics, both long and short term, seen in critical care patients.

8.2.4 Selecting w_3

This section presents the results of using the parameter fitting method presented in Section 8.1.2 to fit $w_2(t)$ for an array of values for w_3. The RAND values can then be used to select an optimal w_3 value for each patient. Table 8.7, located at the end of this chapter, presents the RAND values of the simulations resulting from the use of the smoothed $w_2(t)$ sedative sensitivity profiles for varying values of w_3 from Section 8.2.3. The w_3 value corresponding to the best fit between the simulated and recorded data for all patients was w_3=0.0001. The evaluation metrics in Table 8.7 shows high values for the model with the EAR dynamic (w_3=0.0001) and without (w_3=0).

The RAND values for simulations without EAR have a median of 0.77 with IQR 0.09 and range [0.51, 0.89]. Similarly, the RAND values for simulations including EAR have a median of 0.78 with IQR 0.08 and range [0.55, 0.91]. For w_3 =0.00001 (column 2) slightly lower values of the evaluation metrics are observed, and for w_3 = 0.001 (column 4) even lower values are observed, when compared to w_3 = 0.0001 (column 3).

These generally high evaluation metrics correspond to very close fits of the simulated infusion rate to the recorded infusion rate, as shown in Figures 8.4–8.6. In these figures, the upper plot shows the time-varying profile of the fitted $w_2(t)$, while the lower plot shows the resulting fit of the simulated and recorded infusion rates. In each of these figures, the dark solid line shows the results without the inclusion of EAR, and the dark dotted line shows the results including EAR. The light solid line in the lower plots shows the recorded infusion rate, and its 99% probability band is the grey band around it.

The best fit between the simulated and recorded data was obtained using w_3=0.0001 for all patients, which shows the low inter-patient variability and sensitivity of the EAR parameter. Although in many cases (e.g. Patients 1, 30) other values of w_3 produce similar performance and patient-specific values of w_3 may improve the fit for specific patients, an optimum value of w_3=0.0001 for all patients indicates that w_3 is relatively insensitive and can be assumed

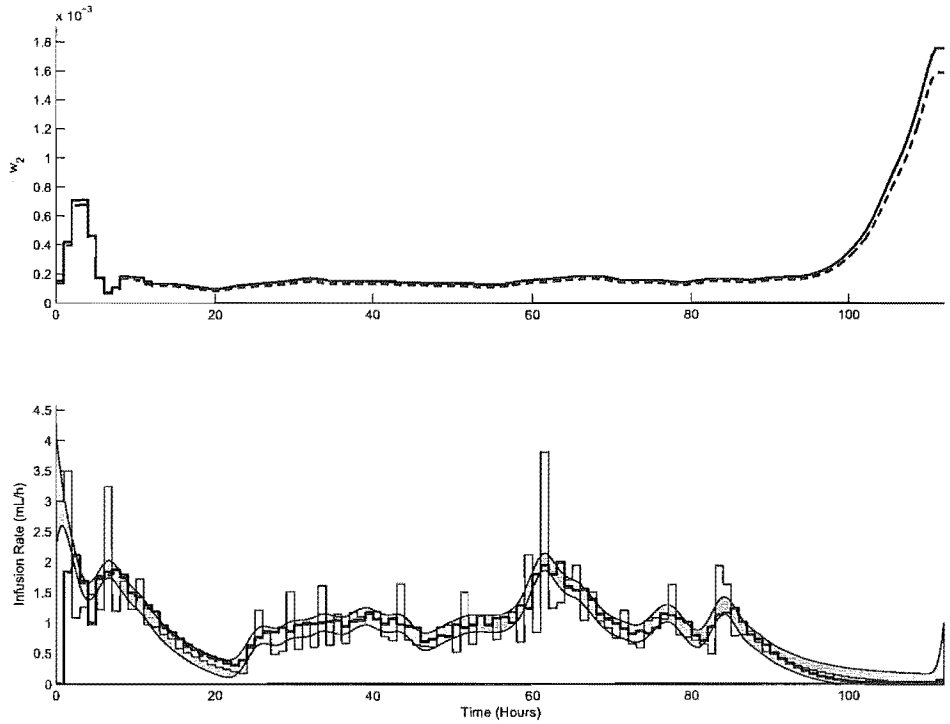

Figure 8.4 Plot of the effect of EAR using the physiologically-based model for Patient 2.

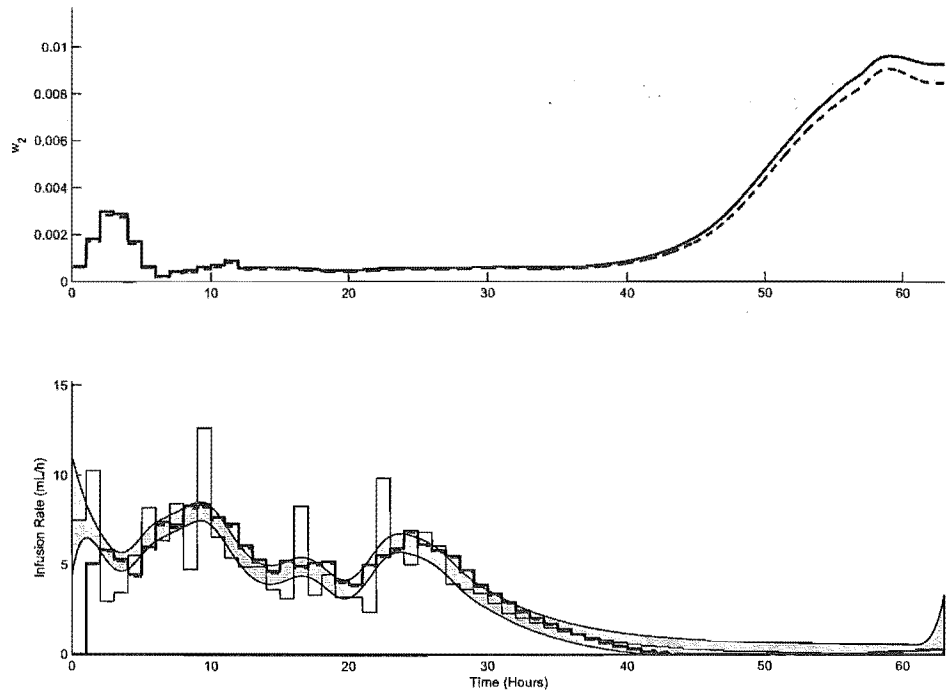

Figure 8.5 Plot of the effect of EAR using the physiologically-based model for Patient 36.

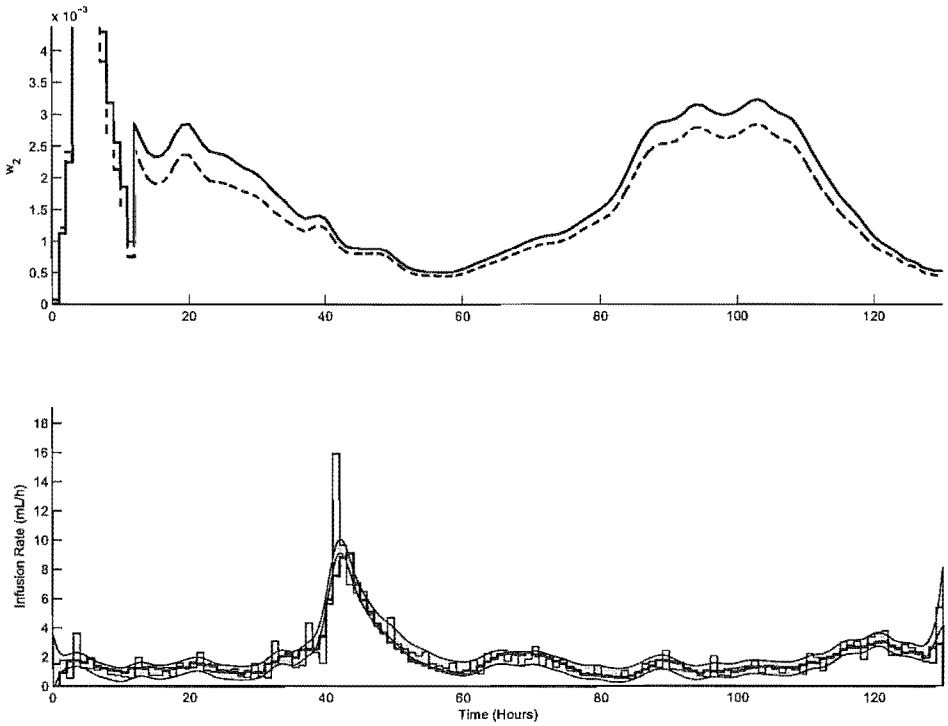

Figure 8.6 Plot of the effect of EAR using the physiologically-based model for Patient 37.

constant across all patients. The sensitivity of the model to the value of w_3 is reduced further by the fitting process for $w_2(t)$, which can compensate for slightly incorrect selection of w_3 [Hann et al., 2005].

This result indicates that while other PD parameters, such as C_{50}, are patient-specific and exhibit a high inter-patient variability, w_3 remains constant across all patients. This result is in contrast to most PD studies that support high inter-patient variability in PD dynamic parameters. One reason why the same value is optimal for all patients may be the fact that the resolution of the array of w_3 was too coarse. If an array $w_3 = [0 \;\; 0.0001 \;\; 0.0002 \;\; 0.0004 \;\; 0.0006 \;\; 0.0008]$ was used, more patient-specific w_3 values may result.

However, Table 8.7 shows that even with a selection of w_3 differing by orders of magnitude, the performance summary statistics are not drastically altered. Whether w_3 is patient-specific, time-varying, or non-existent, has only a mild effect on the resulting evaluation metrics across all the patients. These results show the insensitivity of the model to the w_3 parameter, as experienced in other similar physiological systems [Hann et al., 2005]. However, while the effect of the

EAR term is minimal across all patients, the dynamic is particularly important for some patients and/or clinical scenarios in particular.

The impact of EAR can be seen by comparing columns 1 and 3 in Table 8.7. The median and upper and lower quartiles of the RAND and TIB for the model including EAR are all higher than those without EAR, and the IQR of these metrics is reduced for the model including EAR. These results indicate that the addition of the EAR dynamic improves the ability of the model to capture the observed dynamics of the agitation-sedation system.

The upper plots in Figures 8.4–8.6 show that while the difference is small, the inclusion of EAR results in a slight decrease in $w_2(t)$ throughout the entire profile, especially where infusion rates in the lower plot are very low. Note that when infusion rates are very low the primary means of agitation reduction would be due to EAR. Hence, the EAR dynamic has the greatest effect during periods of low sedation infusion where there is less exogenous agitation reduction from sedative agents. Such periods would most notably include sedative weaning prior to extubation.

Visually, the lower plots on Figures 8.4–8.6 show that both models produce infusion profiles closely approximating the recorded infusion profiles. The fact that the solid and dotted dark lines on the bottom plot in these figures are difficult to distinguish indicates that the simulated infusion rates are very similar whether EAR is included or not. High median RAND values for both models of 0.77 (without EAR) and 0.78 (with EAR), support this visual finding with a statistically-based objective measure. Minimum RAND values of 0.51 and 0.55 for the two respective models reinforce this result. These results support both models as appropriate representations of the fundamental agitation-sedation dynamics present in a broad spectrum of ICU patients.

While the addition of the EAR dynamic increases the ability of the model to capture the observed dynamics of the agitation-sedation system, the improvement is relatively small. Further, the sensitivity of the model to the w_3 parameter is low. This feature is also found in non-drug mediated endogenous removal mechanisms in similar dynamic systems such as the glucose-insulin system [Hann et al., 2005; Chase et al., 2005b].

This last result offers the question of whether the EAR dynamic should be included at all. It may be possible that the errors and assumptions in the development of the model and the evaluation metrics are larger than the difference in performance between the model with and without EAR. Although this issue may represent a limitation of the model, it is important to note that the inclusion of EAR is important for accurately capturing periods of low, or no, sedative infusion that occur clinically, such as weaning.

The evaluation metrics summarised in Table 8.7 are achieved using very few patient-specific PD parameters and identical PK parameters across all patients. This result further supports the finding that inter-patient pharmacological variability is due primarily to PD differences rather than PK differences, as reported in the literature [Vinik et al., 1983; Albrecht et al., 1999]. However, the insensitivity of the w_3 parameter and its smaller impact on results indicate that EAR is not a significant PD parameter in this case. However, EAR becomes important when simulating low infusion rates, such as during weaning. Therefore, although EAR is not always a significant dynamic, it is important during specific clinical periods. Because it has no negative impact during other periods and introduces no additional parameter identification burden, it should be retained in the model.

For some patients high w_2 values are observed immediately after periods of relatively constant w_2, as seen in Figure 8.4–8.6. Although this feature is sometimes located centrally in recorded data, in many cases this feature is observed at the end of recorded data and may correspond to sedative weaning. More specifically these observations may be the result of an actual physiological change in sedative sensitivity as the patient's health improves prior to leaving the ICU. However, the magnitudes of the changes are in some cases quite large, which indicates that the change in observed sedative sensitivity may also be the result of an entirely separate dynamic.

One such dynamic could be the delayed release of drugs stored in fatty tissue [Hughes et al., 1992]. Although the peripheral compartment includes the fatty tissues into which these drugs and/or metabolites can be deposited, this dynamic may be considerably more prominent than currently modelled, requiring an additional separate storage compartment. Because benzodiazepines are lipid soluble, long-term infusions can lead to depositions of large amounts of the administered drug in fatty tissues [Arbour, 2000; Hughes et al., 1992; Kress et al., 2002]. When

the sedative administration stops, the stored drug is released back into circulation as concentrations fall [Kress et al., 2000; Barr and Donner, 1995; Arbour, 2000; Hughes et al., 1992]. If this dynamic was present during the clinical data recordings, the effect would be an inflated observed sedative sensitivity, w_2, at the end of the record due to "extra" drug availability in the system. It would also have the effect of lowering $w_2(t)$ through the middle of the record where there was actually less drug available due to this storage for later release. Further investigation is required to determine the effects of this storage dynamic.

Finally, the model incorporates physiological drug effect saturation dynamics, seen in the dual-sigmoid surface in Figure 3.3. Physiological metabolism and excretion of Morphine and Midazolam is limited by renal and hepatic clearance capacity. However, the maximum clearance rate and plasma concentrations at which the dynamics change from first-order to saturated zero-order kinetics are not easily obtained, particularly in the ICU population. A lack of available parameter values therefore makes the immediate implementation of more representative Michaelis-Menton saturation dynamics difficult, particularly with regard to drug clearance. Clinical trials with quantified agitation sensors [Chase et al., 2004c,b] and measured plasma drug concentrations could provide the data to improve these model parameters and add any necessary additional dynamics.

8.2.4.1 Summary

The physiologically-based model captures the essential dynamics of the agitation-sedation system, both with and without the EAR dynamic. High median RAND values of 0.77 (without EAR) and 0.78 (with EAR) and minimum RAND values of 0.51 and 0.55 for the two respective models show that both models are appropriate representations of the fundamental agitation-sedation dynamics present in a broad spectrum of ICU patients. While the addition of the EAR dynamic increases the ability of the model to capture the observed dynamics of the agitation-sedation system, the improvement is relatively small and the sensitivity of the model to the w_3 parameter is low. Although this may represent a limitation of the model, the inclusion of EAR is important for accurately capturing periods of low, or no, sedative infusion, such as weaning.

Table 8.1 Selected patient-specific C_{50} values employed in the physiologically-based model

	C_{50}^{a}	C_{50}^{s}
1	0.025	0.018
2	0.018	0.014
3	0.030	0.022
4	0.065	0.050
5	0.019	0.016
6	0.073	0.061
7	0.018	0.016
8	0.107	0.091
9	0.045	0.042
10	0.041	0.035
11	0.122	0.096
12	0.041	0.034
13	0.086	0.066
14	0.017	0.016
15	0.055	0.049
16	0.085	0.078
17	0.050	0.035
18	0.085	0.074
19	0.116	0.111
20	0.041	0.036
21	0.021	0.017
22	0.063	0.060
23	0.040	0.029
24	0.052	0.038
25	0.052	0.049
26	0.014	0.013
27	0.091	0.082
28	0.030	0.028
29	0.053	0.041
30	0.025	0.020
31	0.104	0.094
32	0.143	0.132
33	0.113	0.111
34	0.063	0.053
35	0.045	0.039
36	0.071	0.057
37	0.070	0.054
Max	0.143	0.132
UQ	0.085	0.066
Med	0.052	0.042
LQ	0.030	0.028
Min	0.014	0.013
IQR	0.055	0.038

Table 8.2 Summary of the fitted patient-specific $w_2(t)$ values employed in the physiologically-based model

	$w_2(t)(\times 10^{-4})$	
	Median	IQR
1	2.07	2.25
2	1.37	0.64
3	2.16	1.07
4	5.86	6.20
5	1.55	1.08
6	12.2	8.07
7	1.79	2.96
8	9.13	4.55
9	3.88	1.75
10	4.60	7.18
11	15.5	47.0
12	3.17	1.39
13	10.4	14.6
14	1.38	1.11
15	4.53	2.53
16	7.17	3.09
17	3.47	1.31
18	8.53	18.2
19	10.4	3.67
20	4.13	2.12
21	1.69	1.24
22	5.68	2.66
23	3.88	3.96
24	3.74	1.48
25	4.50	2.06
26	1.20	0.57
27	10.4	11.8
28	2.79	1.11
29	4.79	3.55
30	1.88	1.11
31	10.4	6.74
32	13.2	7.52
33	11.5	15.3
34	5.04	2.28
35	5.02	3.33
36	6.74	22.4
37	13.3	16.2
Max	15.5	47.0
UQ	9.13	7.18
Med	4.60	2.96
LQ	2.79	1.39
Min	1.20	0.57
IQR	6.34	5.79

Table 8.3 Evaluation metrics for the physiologically-based model employing the fitted $w_2(t)$

	RAND	AND	TIB	RTD
1	0.82	0.75	0.97	1.00
2	0.94	0.75	0.94	0.98
3	0.87	0.73	0.96	1.00
4	0.72	0.65	0.88	0.94
5	1.00	0.76	0.92	0.98
6	0.89	0.75	0.94	0.99
7	0.96	0.74	0.91	0.95
8	1.00	0.76	0.92	0.99
9	0.94	0.75	0.91	1.00
10	0.99	0.80	0.95	0.99
11	0.87	0.71	0.92	1.02
12	0.89	0.71	0.95	0.98
13	0.90	0.74	0.91	0.97
14	0.65	0.56	0.94	0.96
15	0.97	0.71	0.95	1.00
16	0.99	0.76	0.94	0.99
17	0.96	0.81	0.94	0.97
18	0.93	0.75	0.90	0.99
19	1.00	0.77	0.96	1.00
20	1.00	0.82	0.96	0.99
21	0.94	0.70	0.90	0.98
22	0.89	0.69	0.88	0.99
23	0.79	0.67	0.89	0.93
24	0.95	0.76	0.94	0.99
25	0.82	0.62	0.88	1.00
26	1.00	0.79	0.96	0.99
27	0.96	0.76	0.91	0.99
28	0.94	0.72	0.93	1.00
29	0.66	0.56	0.93	0.94
30	0.96	0.74	0.94	0.99
31	1.00	0.80	0.95	1.00
32	1.00	0.77	0.93	0.99
33	0.98	0.76	0.95	1.00
34	0.94	0.72	0.90	0.99
35	0.89	0.73	0.87	1.01
36	0.89	0.72	0.87	0.99
37	0.84	0.75	0.90	0.96
Max	1.00	0.82	0.97	1.02
UQ	0.98	0.76	0.95	1.00
Med	0.94	0.75	0.93	0.99
LQ	0.89	0.71	0.90	0.98
Min	0.65	0.56	0.87	0.93
IQR	0.09	0.05	0.05	0.02

Table 8.4 Evaluation metrics for the physiologically-based model employing the 12-hour smoothed $w_2(t)$

	RAND	AND	TIB	RTD
1	0.79	0.73	0.97	1.00
2	0.84	0.67	0.92	0.98
3	0.74	0.63	0.95	1.00
4	0.69	0.62	0.89	0.96
5	0.84	0.64	0.86	0.97
6	0.83	0.70	0.92	0.99
7	0.79	0.61	0.86	0.93
8	0.77	0.58	0.85	0.99
9	0.75	0.60	0.82	1.01
10	0.82	0.66	0.89	0.98
11	0.75	0.62	0.89	1.01
12	0.76	0.61	0.91	0.98
13	0.82	0.68	0.88	0.97
14	0.55	0.47	0.90	0.97
15	0.77	0.56	0.88	1.01
16	0.73	0.56	0.84	1.00
17	0.86	0.73	0.89	0.98
18	0.84	0.68	0.84	0.98
19	0.89	0.66	0.94	1.00
20	0.91	0.74	0.94	0.99
21	0.81	0.60	0.85	0.96
22	0.72	0.57	0.83	0.98
23	0.76	0.65	0.89	0.93
24	0.78	0.62	0.91	0.99
25	0.69	0.53	0.81	1.01
26	0.88	0.68	0.92	0.99
27	0.77	0.61	0.83	0.97
28	0.82	0.62	0.88	1.00
29	0.70	0.59	0.94	0.93
30	0.87	0.68	0.90	0.99
31	0.86	0.68	0.93	1.00
32	0.79	0.61	0.87	0.99
33	0.81	0.63	0.89	0.99
34	0.77	0.59	0.84	1.00
35	0.78	0.64	0.84	1.00
36	0.74	0.60	0.84	0.97
37	0.76	0.68	0.89	0.96
Max	0.91	0.74	0.97	1.01
UQ	0.83	0.68	0.91	1.00
Med	0.78	0.62	0.89	0.99
LQ	0.75	0.60	0.85	0.97
Min	0.55	0.47	0.81	0.93
IQR	0.08	0.08	0.06	0.03

Table 8.5 Evaluation metrics for the physiologically-based model employing the constant w_2

	RAND	AND	TIB	RTD
1	0.66	0.61	0.86	0.86
2	0.64	0.52	0.75	1.01
3	0.75	0.63	0.93	0.94
4	0.54	0.48	0.75	1.02
5	0.63	0.48	0.71	1.02
6	0.63	0.53	0.72	0.86
7	0.28	0.22	0.32	0.90
8	0.33	0.25	0.46	0.87
9	0.56	0.45	0.66	1.02
10	0.27	0.22	0.36	0.48
11	0.18	0.15	0.19	0.80
12	0.71	0.57	0.89	0.97
13	0.37	0.30	0.57	0.96
14	0.51	0.43	0.89	1.00
15	0.71	0.52	0.83	1.00
16	0.55	0.42	0.71	0.97
17	0.70	0.59	0.75	0.96
18	0.47	0.38	0.50	0.82
19	0.58	0.43	0.62	1.08
20	0.65	0.53	0.74	0.92
21	0.59	0.44	0.67	0.94
22	0.43	0.34	0.51	0.90
23	0.65	0.56	0.80	0.91
24	0.58	0.47	0.76	0.98
25	0.53	0.40	0.55	1.09
26	0.80	0.62	0.83	0.99
27	0.29	0.23	0.36	0.87
28	0.62	0.47	0.75	0.97
29	0.43	0.36	0.76	0.91
30	0.60	0.46	0.71	1.07
31	0.32	0.25	0.36	0.86
32	0.42	0.32	0.50	0.97
33	0.19	0.15	0.24	0.74
34	0.53	0.41	0.64	0.95
35	0.45	0.37	0.55	0.99
36	0.35	0.28	0.38	0.94
37	0.45	0.41	0.68	0.78
Max	0.80	0.63	0.93	1.09
UQ	0.63	0.52	0.75	0.99
Med	0.54	0.43	0.68	0.95
LQ	0.42	0.32	0.50	0.87
Min	0.18	0.15	0.19	0.48
IQR	0.21	0.20	0.25	0.12

Table 8.6 Comparison of RAND for the physiologically-based model employing the fitted, 12-hour smoothed, and constant $w_2(t)$

	Fitted	Smoothed	Const
1	0.82	0.79	0.66
2	0.94	0.84	0.64
3	0.87	0.74	0.75
4	0.72	0.69	0.54
5	1.00	0.84	0.63
6	0.89	0.83	0.63
7	0.96	0.79	0.28
8	1.00	0.77	0.33
9	0.94	0.75	0.56
10	0.99	0.82	0.27
11	0.87	0.75	0.18
12	0.89	0.76	0.71
13	0.90	0.82	0.37
14	0.65	0.55	0.51
15	0.97	0.77	0.71
16	0.99	0.73	0.55
17	0.96	0.86	0.70
18	0.93	0.84	0.47
19	1.00	0.89	0.58
20	1.00	0.91	0.65
21	0.94	0.81	0.59
22	0.89	0.72	0.43
23	0.79	0.76	0.65
24	0.95	0.78	0.58
25	0.82	0.69	0.53
26	1.00	0.88	0.80
27	0.96	0.77	0.29
28	0.94	0.82	0.62
29	0.66	0.70	0.43
30	0.96	0.87	0.60
31	1.01	0.86	0.32
32	1.00	0.79	0.42
33	0.98	0.81	0.19
34	0.94	0.77	0.53
35	0.89	0.78	0.45
36	0.89	0.74	0.35
37	0.84	0.76	0.45
Max	1.00	0.91	0.80
UQ	0.98	0.83	0.63
Med	0.94	0.78	0.54
LQ	0.89	0.75	0.42
Min	0.65	0.55	0.18
IQR	0.09	0.08	0.21

Table 8.7 Comparison of RAND for physiologically-based model employing the 12-hour smoothed $w_2(t)$ and varying w_3

w_3	0	1×10^{-5}	1×10^{-4}	1×10^{-3}	Max
1	0.79	0.79	0.79	0.55	0.79
2	0.80	0.81	0.84	0.35	0.84
3	0.69	0.69	0.74	0.23	0.74
4	0.69	0.69	0.69	0.47	0.69
5	0.83	0.83	0.84	0.21	0.84
6	0.82	0.82	0.83	0.40	0.83
7	0.77	0.78	0.79	0.44	0.79
8	0.74	0.75	0.77	0.18	0.77
9	0.73	0.73	0.75	0.22	0.75
10	0.78	0.78	0.82	0.41	0.82
11	0.71	0.71	0.75	0.49	0.75
12	0.73	0.74	0.76	0.21	0.76
13	0.79	0.79	0.82	0.41	0.82
14	0.51	0.51	0.55	0.28	0.55
15	0.76	0.76	0.77	0.18	0.77
16	0.71	0.71	0.73	0.15	0.73
17	0.86	0.86	0.86	0.25	0.86
18	0.80	0.80	0.84	0.42	0.84
19	0.88	0.88	0.89	0.15	0.89
20	0.89	0.89	0.91	0.39	0.91
21	0.79	0.79	0.81	0.31	0.81
22	0.69	0.69	0.72	0.28	0.72
23	0.75	0.75	0.76	0.51	0.76
24	0.77	0.77	0.78	0.24	0.78
25	0.67	0.67	0.69	0.14	0.69
26	0.86	0.86	0.88	0.33	0.88
27	0.70	0.71	0.77	0.45	0.77
28	0.79	0.80	0.82	0.25	0.82
29	0.60	0.62	0.70	0.24	0.70
30	0.87	0.87	0.87	0.30	0.87
31	0.83	0.84	0.86	0.34	0.86
32	0.77	0.77	0.79	0.17	0.79
33	0.78	0.79	0.81	0.30	0.81
34	0.73	0.74	0.77	0.18	0.77
35	0.75	0.75	0.78	0.39	0.78
36	0.64	0.65	0.74	0.59	0.74
37	0.73	0.74	0.76	0.48	0.76
Max	0.89	0.89	0.91	0.59	0.91
UQ	0.80	0.80	0.83	0.41	0.83
Med	0.77	0.77	0.78	0.30	0.78
LQ	0.71	0.71	0.75	0.22	0.75
Min	0.51	0.51	0.55	0.14	0.55
IQR	0.09	0.09	0.08	0.19	0.08

Part III

Control

Chapter 9

Control Specifications

Parts I–II of this thesis presented and evaluated the developed models of agitation-sedation dynamics. Each of these models are used in turn as a platform for the development and evaluation of sedative infusion protocols to minimise agitation and total dose. Simple derivative-focused control approaches are explored and optimal and non-linear control strategies that offer additional potential and insight are also investigated. Rather than analysing the impact of various controllers on the physiological model only, controllers are evaluated on each of the models consecutively. This approach allows assessment of the impact of the various dynamics captured by each of the models on control, and helps to identify the clinically important aspects of each model. Contrasting and comparing the impact of various controllers on each of the models enables analysis of:

- The impact of various control approaches on the initial model, thereby understanding the capabilities of controllers in the absence of saturation limits.

- The impact of various control approaches on the physiological model, thereby understanding the ability of controllers to manage agitation in a non-linear model with physiological factors, such as saturation, limit the effectiveness of control.

- The performance of the same control approach across different models, hence identifying dynamics of the agitation-sedation system that have important consequences for controller development, such as saturation.

Therefore, each of the models presented in Parts I-II of this thesis are analysed with various control approaches, allowing contrasts and comparisons between control protocols and across models.

9.1 Goals of Sedation

The goal of sedation in the ICU is to reduce anxiety, control agitation, and produce a patient who is calm, cooperative, and preferable able to communicate [Fragen, 1997]. Therefore, the ideal sedative infusion protocol administers the optimal dose of drug at the optimal time to effectively control agitation and create a comfortable patient, while at the same time ensuring that the patient is able to communicate and co-operate by preventing over-sedation. Therefore, there is a trade-off between minimising agitation and minimising drug dose. Either goal alone is relatively simple to achieve — minimal agitation achieved via excessive drug dose or minimal drug dose at the cost of patient anxiety and agitation.

In many control applications, actuation is bi-directional, such as the ability to push or pull a cart, or increase or decrease an input force. However, in the case of the agitation-sedation system, drugs may be administered to the patient, but are not readily removed or reversed. An alternative to drug removal is the use of antagonists such as the Midazolam antagonist, Flumazenil [Young and Prielipp, 2001], and Morphine antagonist, Naloxone [Bridges and Grimm, 1982]. Although these drugs may hold significant potential for agitation management and the prevention of over-sedation in the future [Young and Prielipp, 2001; Ritz et al., 1990; Geller et al., 1988], they are not commonly used in the ICU and are not considered in this thesis. More directly, these effects, while broad, would not likely offer the fine measure of control required. Finally, this problem is generic to almost all physiological drug infusion management control problems.

The saturation dynamic in the physiologically-based model also restricts the capacity of the controller to reduce instantaneous agitation when drug levels are moderate to high. Even employing an approach which simply delivers additional drug in response to agitation, the efficacy of the drug in the body is limited by the upper plateau on the saturation curve. Therefore, if the instantaneous stimulus invoking agitation outweighs the maximum achievable cumulative PD effect of

the drugs, the control capacity is removed and patient agitation will increase. This characteristic of the agitation-sedation system has important implications for agitation management and controller design. More specifically, it means that a desired target agitation level is not always necessarily achievable. Hence, a more appropriate objective of the ideal controller might be to minimise overall agitation, rather than achieve a pre-set level at any moment in time.

9.2 Controller Specifications

An infusion protocol for use in a semi-automated sedative administration controller should meet the following minimax cost-benefit criteria:

- Minimise patient agitation (benefit)
- Minimise over-sedation (cost)

Safety is also a critical factor, so the protocol should also maintain infusion rates within clinically specified safety limits to minimise cardiopulmonary depression and other critical side-effects. Hence, this cost/benefit trade-ff is constrained by safety limits. This definition is logical and has been described as "the quandary that faces clinicians daily" [Kress et al., 2002]. The important concept, therefore, is to employ an optimal drug delivery strategy. The goal of an optimal sedation control protocol is therefore to use the same drugs and similar dose, but deliver the drug in a way that improves outcome.

9.3 Performance Metrics

Objective performance metrics are necessary to evaluate the performance of any proposed sedative infusion protocol. Clearly, if an infusion protocol does not provide advantages over the current practice, then its implementation offers little outcome benefit for significant added complexity. Therefore, the simulations using the nurse control protocol, presented in Sections 6.2, 7.2, and Chapter 8.2.4 are used as the benchmark for comparison. The nurse control protocol

is a representation of current clinical practice that is both easily repeated and previously verified. The control protocol specifications in Section 9.2 form the backbone of the sedative protocol performance metrics. Four performance metrics are proposed:

RTD Relative Total Dose is defined as the total simulated dose of the proposed control protocol, relative to the total recorded dose. RTD is an important global performance metric because it is a general indication of drug usage, which has both financial and healthcare implications. In general, the use of excessive drugs leads to increased costs, and is an indication of over-sedation, especially compared to clinical practice. Therefore, from both a healthcare and financial perspective, a low RTD is desirable.

RPIR Relative Peak Infusion Rate is defined as the maximum infusion rate of a proposed control protocol, relative to the maximum recorded infusion rate. RPIR is a particularly important parameter in ICU sedation, as high infusion rates can be damaging to patient health and are associated with cardiopulmonary depression, among other side-effects [Barr and Donner, 1995]. For this reason, maximum recorded infusion rates exist, and a low RPIR is desirable.

RMA Relative Mean Agitation is defined as the mean simulated agitation employing the proposed control protocol, relative to the mean simulated agitation employing the nurse control protocol. RMA is one of the most important global performance metrics for both the patient and the medical staff. High average agitation levels can hinder the recovery process by preventing rest and healing. Periods of inflated average agitation levels are uncomfortable and dangerous for patients, and difficult and time-consuming for bedside medical staff. Therefore, for both patients and medical staff, a low RMA is desirable.

RPA Relative Peak Agitation is defined as the maximum modelled agitation employing the proposed control protocol, relative to the maximum modelled agitation employing the nurse control protocol. RPA is a local metric that represents the point in time at which the patient is most likely to attempt to remove their life-support systems (such as removing the ET tube), or resist staff. These actions are both damaging to patient health and a concern for

staff safety. Therefore, for both patients and medical staff, a low RPA is desirable.

These metrics represent both local and global measures of the inputs and outputs of agitation management. RTD is a global measure of the sedative drug input while RPIR represents a local measure of the sedative drug input. These measures of input represent the control effort required, and hence represent the cost of agitation management.

In contrast, RMA and RPA are measures of output. In particular, RMA represents a global performance measure, and RPA represents a local performance measure. These output measures represent the result of the control protocol employed, and hence the benefits obtained. In this application, lower output metrics are desirable.

Therefore, a combination of each of these metrics provides an indication of the relative cost-benefit ratio of a particular control protocol. The output metrics provide an indication of the benefit obtained through a particular protocol, and the input metrics provide and indication of the cost of those benefits. In this case, RTD and RMA represent the global cost-benefit trade-off, and RPIR and RPA represent the local const-benefit trade-off.

Chapter 10

Control of the Initial Model

Having established the initial model as a platform for developing control protocols, the results of the simulated nurse control protocol in Section 6.2 can be used as a benchmark for assessing the effects of different infusion control protocols. In particular, the effect of removing the IIR filter and increasing the derivative-focused control gains is investigated. Model parameters identical to those used in Section 6.2 are used for all patients. Performance metrics from Section 9.3 indicate the improvement in agitation management achieved through direct feedback control of agitation. Without the filter, this approach tests the impact of a quantified agitation measurement system and simple control protocols. Eliminating the filter also removes an artificial, forced decay rate of drug dose that is only optimal if agitation-sedation requirements decay at the same rate.

10.1 Methods

This chapter investigates the impact of removing the IIR filter of Section 4.2 and replacing the nurse control protocol with an alternative sedative infusion protocol. In particular, the impact of a constant infusion rate throughout the entire profile is investigated, as well as the impact of increased control gains. Finally, the impact of placing upper and lower limits on the infusion rate is investigated.

The impact of a constant continuous sedative infusion protocol on patient agitation is assessed through the simulated delivery of a constant infusion at a rate equivalent to the average recorded infusion rate. By definition, this case ensures that the total recorded dose and total simulated dose are equal, resulting

in RTD=1.0 for all patients. This protocol therefore delivers a patient-specific, constant infusion rate throughout the entire recorded profile. The impact of this protocol on patient agitation has important clinical applications, as some traditional sedation administration protocols employ similar continuous infusions [Kress et al., 2000; Barr and Donner, 1995; Fragen, 1997; Kress et al., 2002]. In clinical practice the protocol is easily implemented using electronic infusion pumps, and is hassle-free for bedside medical staff because minimal effort is required. However, there are obvious disadvantages with such a protocol, in particular the risk of over-sedation, or insufficient sedation [Fragen, 1997; Barr and Donner, 1995; Arbour, 2000]. In particular, if a rate is kept constant such that most or all agitation is eliminated it will also likely be too high for a large majority of the patient's stay.

Several biological control systems employ simple forms of feedback control [Carson and Cobelli, 2001]. Studies have shown that artificial controllers in first order systems similar to the agitation-sedation system models defined in Chapter 3 have benefited from derivative-focused control [Lam et al., 2002; Doran et al., 2004; Rudge et al., 2004a, 2005a]. Hence, an infusion rate, U, in the form of a proportional-derivative control protocol using agitation, A, as the feedback quantity can be readily defined:

$$U = K_p A + K_d \dot{A} \tag{10.1}$$

where K_p and K_d are the proportional and derivative gains respectively. Choosing control gains such that $K_d \gg K_p$ implements a derivative-focused agitation feedback control protocol that focuses on controlling the shape of the agitation response rather than the specific magnitude. Note that methods to objectively measure agitation are emerging [Chase et al., 2004c,a; Lam et al., 2003; Starfinger et al., 2003; Agogué, 2005; Lam, 2003; Starfinger, 2003]. The sedative infusion rate is updated hourly, matching the nurse control protocol in Section 4.2. Because of the stimulus generation procedure, there are no dynamics faster than approximately one hour in the stimulus profile, representing a limitation of the model evaluation method. However, the same fundamental trends resulting from the use of these control protocols should be expected for smaller time-scales.

Substitution of Equation (10.1) into Equation (3.1) creates a feedback loop and is used to investigate the benefits of direct derivative-focused control on agi-

tation management. Using this derivative-focused approach, sedative agents are typically not administered while agitation is falling to avoid over-sedation. The control gains employed by the nurse control protocol, and obtained in chapter 6 are K_p=0.0004 and K_d=0.4. In this chapter, these control gains are multiplied by a Gain Factor (GF) to equally increase both the proportional and derivative gain, maintaining a ratio of 1:1000 between them. The gain factor acts as a magnification factor to compensate for the increased mean infusion removed with the removal of the IIR filter. The impact of increasing the control gains is investigated using four control protocols with increasing gain factor:

GF3 This protocol employs proportional and derivative control gains multiplied by a factor of three. It has similar performance metrics to that of the nurse control protocol, and therefore represents a good comparison between direct controllers and the filtered nurse control protocol.

GF4 This protocol employs proportional and derivative control gains multiplied by a factor of four. It shows the impact of increased control gains on infusion profiles and agitation levels.

GF5 This protocol employs proportional and derivative control gains multiplied by a factor of five.

GF6 This protocol employs proportional and derivative control gains multiplied by a factor of six. It explores any advantage of a very strong reaction to rising and/or falling agitation response.

In all sedative control protocols the IIR filter of Section 4.1 is removed, creating four direct derivative-focused control protocols. In all cases, the only restriction placed on the controlled infusion rate is that negative infusion rates are not allowed. These protocols investigate the impact of increasing the control gains, without any other limitations.

Finally, in an attempt to capitalise on the benefits of the GF6 protocol, but eliminate the negative consequences of excessively high infusion rates, several variations on the GF6 protocol are analysed. The impact of imposing upper and lower limits on the controlled infusion rate is investigated by comparing the GF6 protocol with protocols employing exactly the same gain factor, but with infusion limits. In particular, two protocols are investigated:

CappedGF6 This approach employs the GF6 protocol and places an upper limit on the infusion rate, capping it to the maximum recorded infusion rate for any given patient. This approach represents an example of a protocol that inherently protects against excessively high infusion rates. The maximum infusion rate is set to the maximum of the recorded infusion rate because it represents a conservative indication of clinical practice.

BoundGF6 This approach employs the GF6 protocol and places upper and lower limits on the infusion rate. The maximum infusion rate is set to the maximum recorded infusion rate and the minimum infusion rate is set to 50% of the average recorded infusion rate for any given patient. This protocol attempts to combine the advantages of the bolus-oriented derivative-focused approach to sedation, and a constant continuous infusion. It also inherently protects against excessively high infusion rates. The minimum infusion rate was selected somewhat arbitrarily, but provides an indication of the impact of such a protocol. This protocol has important clinical implications because many clinical sedation administration protocols employ a combination of boluses and continuous infusion [Kress et al., 2002].

Finally, note that imposing the maximum infusion rate limit results in a maximum possible RPIR=1.0 by definition. These protocols are designed to investigate the impact of increasing gain factor combined with infusion limits on agitation management. Hence they focus more on the outcome benefits of improved agitation performance metrics rather than the input, dose-related, performance metrics.

10.2 Results and Discussion

10.2.1 Constant Infusion Protocol

Figure 10.1 presents the results of the constant continuous infusion protocol for a typical patient using the initial model. The upper plot shows the infusion rates, and the lower plot shows the resulting agitation profile. In these plots, the lighter solid line represents the constant infusion protocol, and the darker solid line represents the nurse control protocol as a benchmark for comparison. Figure 10.1 shows that the constant infusion protocol initially struggles to reduce

agitation levels, but eventually overcomes agitation and delivers excessive drug when the agitation levels are low. This result is a common feature throughout many patients. For portions of the profile the constant infusion protocol provides adequate sedation, but for a majority of the profile the infusion rate is either too small or too great, which may indicate insufficient sedation or over-sedation, respectively. In particular, this protocol typically results in excessive variations in agitation throughout the profile.

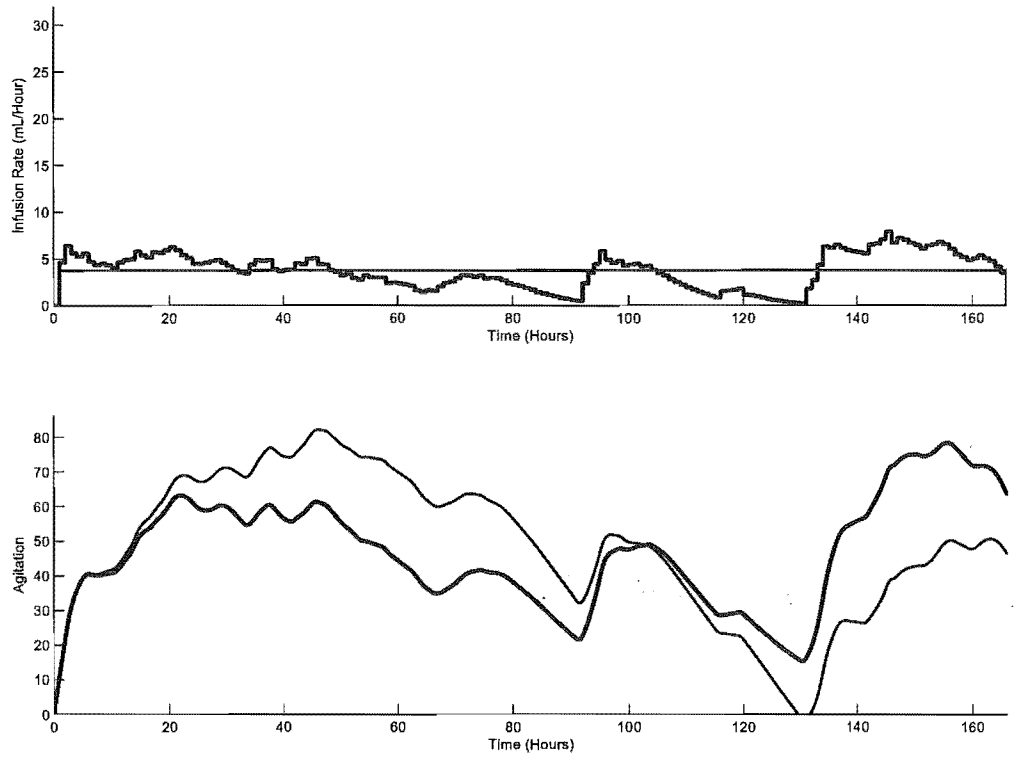

Figure 10.1 Example of the simulated results employing the constant infusion protocol in the initial model.

The implementation of the constant continuous infusion protocol results in a RTD=1.0 by definition, and RPIR is no longer relevant. Table 10.1, located at the end of this chapter for clarity and ease of use, presents the summary statistics of the performance metrics across all 37 patients for the 7 control protocols analysed in this chapter. The constant infusion protocol results in median values of RMA=1.02 and RPA=0.98, as seen in Table 10.1. Although these values represent patient agitation similar to that achieved by the nurse control protocol, the constant protocol is ineffective for many patients, as seen by the large variance of RMA and RPA between patients, indicated by the high IQR in the first

portion of Table 10.1. Specifically, the IQRs for the constant infusion protocol are considerably higher than that of any other protocol, reflecting the extreme variability of performance across a wide range of patients.

Note also the negative value for the minimum RMA, indicating that for at least one patient, the protocol delivered drug when it was unnecessary resulting in 'negative agitation levels'. This feature over-uses drugs, and may indicate over-sedation. Note that this drawback typically occurs in protocols that administer a component of the infusion rate independent of patient agitation levels, such as the constant infusion protocol. The direct derivative-focused protocols, by their defined agitation feedback response, rarely result in negative agitation values. More importantly, if agitation falls below zero, a derivative-focused control protocol typically cuts the infusion rate, quickly returning agitation above zero and reducing drug consumption and preventing over-sedation

The result of the constant infusion protocol is a wide range of metrics across patients, with overall poor performance. Although some particular patients benefit dramatically from the protocol, most do not. The main feature of the protocol is its inability to tailor sedative infusion rates to current patient agitation. The result is large variability in agitation management between patients and, over time, for any given patient. In particular, its tendency to deliver too much drug when unnecessary makes it undesirable.

However, these results do shed some light on the success in the U.S. of sedative interruption protocols [Kress et al., 2000]. In the U.S. constant infusions are often used. Thus, daily interruption would ease total dose to manageable levels and produce at least some of the reduced over-sedation and LOS observed.

All of these results are only relevant for a constant infusion rate equal to the mean recorded infusion. If a different constant infusion rate were selected, it may be more effective. In this research, previously recorded infusion data provides a simple method of approximating this constant rate. However, prospective determination in clinical practice is considerably more difficult, as inter-patient variability and time-varying parameters make the selection of this ideal rate extremely difficult. More importantly, the consequences of incorrect selection of the infusion rate are either extreme over-sedation or elevated levels of agitation, both of which are damaging to patient health. This makes the clinical application

of constant continuous infusion protocols difficult, although adaptive titration methods or boluses may be more effective [Chase et al., 2005b].

If sedative drugs are administered when agitation is near, or at, zero, the drugs administered will likely contribute to extended length of stay and over-sedation. Feedback control protocols employing direct or capped proportional-derivative controllers prevent this scenario by definition. However, a direct consequence of any infusion protocol that determines the infusion rate independent of patient agitation is the risk of insufficient sedation and/or excessive delivery of unnecessary drug. Both of these outcomes are damaging to patient health and contribute to rising healthcare costs, and represents a significant disadvantage of the constant infusion approach in general.

10.2.2 GF3–GF6 Protocols

Table 10.1, located at the end of this chapter for clarity and ease of use, presents the performance metrics of the direct derivative-focused control protocols, GF3–GF6. For the GF3 protocol, the median performance metrics are RTD=0.97, RPIR=0.96, RMA=0.97 and RPA=0.96. These metrics show that the GF3 protocol represents a direct derivative-focused control protocol with similar drug dose characteristics to the nurse control protocol of Section 4.2. More specifically, the three-fold increase in gains is seen to compensate for the removal of the IIR filter, delivering a similar total dose, and resulting in overall similar performance metrics. This result is largely due to a gain greater than 1.0 in the IIR filter design at lower frequencies.

However, while the GF3 protocol delivers similar total dose, the timing of the drug delivery is distinctly different to that delivered by the nurse control protocol, as seen in Figure 10.2. This figure presents the results of the direct derivative-focused control protocols, GF3–GF6, for a typical patient using the initial model. The upper plot shows the infusion rates, and the lower plot shows the resulting agitation profile. In these plots, the lighter solid line represents the GF3 infusion protocol, the dashed line represents the GF4 infusion protocol, the dash-dotted line represents the GF5 infusion protocol, the dotted line represents the GF6 infusion protocol, and the darker solid line represents the nurse control protocol as a benchmark for comparison.

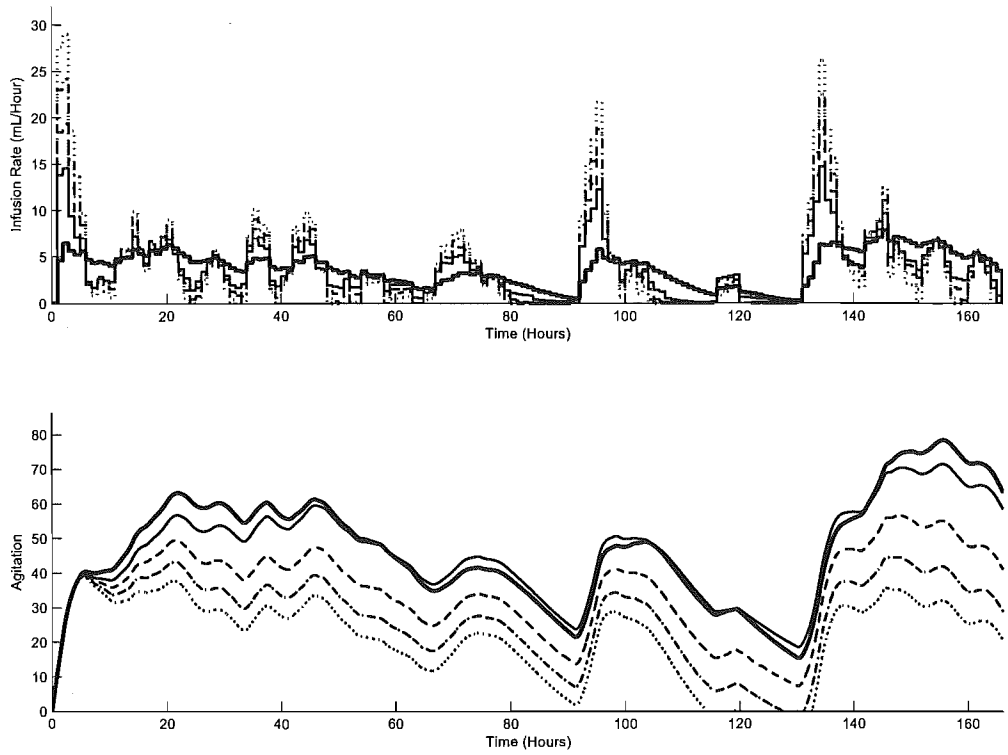

Figure 10.2 Example of the simulated results employing the GF3–GF6 infusion protocols in the initial model.

The direct derivative-focused control protocols result in bolus-oriented infusion profiles with gradually increasing peaks and reducing troughs with increasing gain factor. Similarly, the agitation profiles gradually reduce with increasing gain factor. Although the agitation profiles resulting from increasing gain factor follow a clear downward trend, the agitation profile from the nurse control protocol does not always follow the trend. This feature is seen in many patients and is a result of the presence of the IIR filter employed by the nurse control protocol, and its absence in the direct control protocols. Where the nurse control protocol (incorporating the IIR filter) produces a more consistent delivery profile, the GF3 protocol produces a more bolus-oriented approach, as seen in Figure 10.2. This approach is seen to employ higher infusion rates when agitation is either high or increasing, and lower infusion rates when agitation is low or decreasing.

The GF4 protocol represents an increase in sensitivity to agitation levels, and to the rate of change of agitation, compared to GF3. As a consequence of the increase in gains, the infusion profile becomes even more bolus-oriented, with higher peaks and lower troughs, as observed in Figure 10.2. Increasing the gain

factor to GF=4 has minimal effect on the median RTD, but increases the RPIR to 1.25, as seen in Table 10.1. Although this increase is potentially less desirable, the advantage of this protocol is its ability to further lower the median RMA from 0.97 for GF3 to 0.75 for GF4, and the median RPA from 0.96 to 0.81.

Therefore, with similar overall drug dose, the GF4 protocol is capable of reducing mean agitation 25% and peak agitation 19% compared to the nurse control protocol. In some cases, the mean and peak agitation levels are reduced by as much as 33% and 28% respectively. However, these benefits come at the cost of an increased peak infusion rate of 25% across all patients, and in some instances as much as a 69% increase. Although this protocol is not necessarily an ideal sedation protocol, it indicates that very simple controllers can provide significant benefits to agitation management.

Further increasing the gains of the direct derivative-focused control protocol yields control protocols GF5 and GF6. Table 10.1 shows that increasing the gains increases the median RTD slightly to 1.04 and 1.06 respectively, while the median RPIR increases to 1.50 and 1.75. However, in some cases the peak infusion rates are much higher with a maximum RPIR of 2.54 for GF6. These excessive infusion rates may be unacceptably high for clinical implementation. However, the benefit of such protocols is the large reduction in agitation metrics and reduced total dose. The median RMA for GF5 and GF6 is only 0.60 and 0.47, respectively, and the median RPA is 0.71 and 0.64. These reductions in both mean and peak agitation have desirable implications for both patients and medical staff. For example, some patients experienced a reduction in mean and peak agitation of up to 80% and 50%, respectively, under the GF6 protocol. Even the patients who benefited least from this protocol had mean and peak agitation levels reduced to 58% and 95% of those under the nurse control protocol.

The agitation profiles for GF5 and GF6 are seen in Figure 10.2 to drop below zero for a short period. This occasionally occurs in some patients for whom agitation is kept low by the GF5 and GF6 infusion protocols. These instances represent very low levels of agitation, and hence periods where no further sedative drug is required for managing agitation. As previously mentioned, a control protocol that delivers drug during these periods risks over-sedation and unnecessary use of drugs. However, the inherent design of derivative-weighted control protocols, such as the GF5 and GF6 protocols, typically prevent such action.

Therefore, although patient agitation occasionally drops below zero under these protocols, it remains near zero and quickly returns to positive values. Hence, in model terms it should be interpreted as effectively zero agitation.

Increasing the control gain factor yields a bolus-oriented approach to sedation management which is particularly sensitive to both absolute agitation and changes in agitation. This bolus-oriented approach responds to increasing agitation with short, sharp boluses in an attempt to douse agitation before it increases. This approach results in periods of very high infusion rates during periods of agitation, and periods during which there is no infusion at all. However, it is noted that during the periods of zero infusion, the concentration in compartment 2 is usually non-zero. This non-zero concentration means that there is still a small PD effect, and is a result of the transport delay of the drug between the first and second compartment, and the elimination rate of the drug. More importantly, this approach means that drug is not administered when it is unnecessary. Therefore, although the RTD is similar, the drugs are delivered at completely different times, and results in clearly improved performance metrics.

Whereas Target Controlled Infusion (TCI) systems deliver drugs to maintain constant drug concentrations, the protocols described in Section 10.1 deliver drugs to maintain low agitation. This distinction is important, as one of the primary objectives of ICU sedation is to appropriately manage agitation. Therefore, it is important that the feedback quantity for a control protocol is the intended quantity being regulated. In this application, because the stimulus varies between patients and with time, a constant concentration of drugs will not necessarily provide suitable sedation to keep agitation low. The infusion rates therefore respond to patient agitation, leading to drug concentrations, and hence PD effect, that vary in response to patient requirements.

The relationship between concentration and PD effect is assumed to be linear in the initial model. This assumption creates a linear relationship between drug concentration and its PD effect on agitation, and means that it is theoretically possible to reduce agitation to any desired level, with the appropriate drug delivery profile. However, as observed in this chapter, the drug dose and/or infusion rates required to achieve those goals may be unrealistically high, or in the case of very high gains, the system may become unstable, or respond in ways not captured by the model.

As the gains are increased, the agitation performance metrics are all reduced, whereas the RPIR increases and RTD remains almost unchanged. The RPIR increases as a direct consequence of the increased gains causing sharper responses to changes in agitation, and hence the higher infusion rates. The RTD remains almost unchanged because although increased drug is delivered in the high peaks of bolus delivery, less drug is used in the trough immediately following. This result is potentially desirable, as the drug is delivered only during periods when it is really necessary, and not at all when it is unnecessary. As the effect of the drug is directly proportional to the concentration, it appears to be more effective to use short-term large doses of drug in direct response to agitation, rather than long-term lower doses.

The results in Table 10.1 clearly show that all patients experience lower levels of agitation throughout their stay under these direct derivative-focused protocols, compared with the nurse control protocol. More importantly, these improvements in agitation metrics are achieved using similar doses. The primary drawback of these protocols is the resulting high infusion rates. However, a fundamental outcome of these results is that simply through changing the timing of drug delivery, it is possible to dramatically influence the agitation profile. Although these protocols are not ideal, they indicate that very simple control protocols may provide significant benefits to agitation management in comparison to current clinical practice.

10.2.3 CappedGF6 and BoundGF6 Protocols

Applying an upper limit of the maximum recorded infusion rate to the simulated infusion rate results in a maximum RPIR=1.0 by definition. Table 10.1, located at the end of this chapter, shows the performance metrics for the GF6, CappedGF6, and BoundGF6 protocols. The median RTD remained almost unchanged at 1.05 for the CappedGF6 protocol. The median RMA increased slightly from 0.47 for GF6 to 0.52 for CappedGF6, and similarly the median RPA increased from 0.64 to 0.66. Hence, little is lost in agitation management for a major reduction in peak infusion rate and similar total dose.

Imposing a maximum limit to the infusion rate of the GF6 protocol ensures that the infusion rate for each patient does not exceed the maximum recorded

infusion rate. This approach is conservative, as safe peak infusion rates may be higher. However, this protocol shows the effect of this limit on the benefits otherwise achieved. Therefore, the bolus-oriented approach of the GF6 protocol is maintained, but potentially undesirable large infusion rates are prevented.

Figure 10.3 presents the results of the derivative-focused control protocols with infusion limits for a typical patient using the initial model. The upper plot shows the infusion rates, and the lower plot shows the resulting agitation profile. In these plots, the lighter solid line represents GF6, the dashed line represents CappedGF6, the dotted line represents BoundGF6, and the darker solid line represents the nurse control protocol, as a benchmark for comparison.

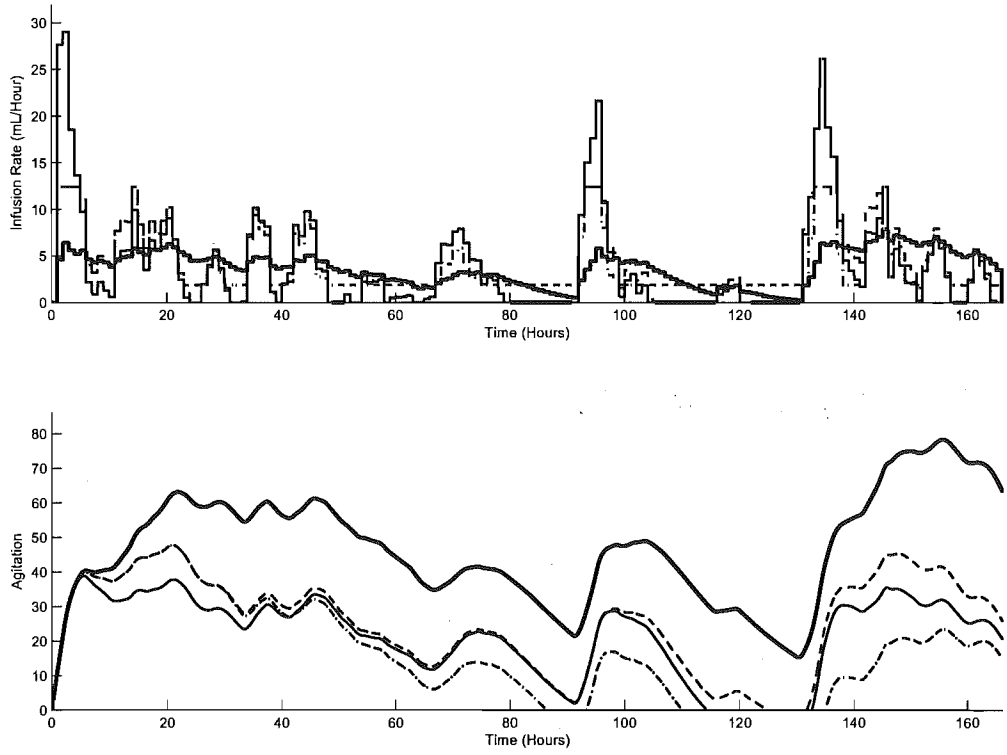

Figure 10.3 Example of the simulated results employing the CappedGF6 and BoundGF6 infusion protocols in the initial model.

The CappedGF6 protocol results in an infusion profile very similar to the GF6 protocol. However, where the infusion rate would have exceeded the maximum limit, the infusion rate remains at the maximum level for a little longer before dropping below the maximum level. Because the rapid response of the control protocol to increases in agitation is limited by the capped infusion rate, its ability

to reduce the mean agitation and peak agitation levels is restricted, and leads to the small increases reported for RMA and RPA.

However, a median reduction of 48% and 34% in mean and peak agitation levels, respectively, represents a significant improvement for both patients and medical staff. Although mean and peak agitation is only reduced by 30% and 2% in some patients, the protocol represents an improvement for all patients, in some cases reducing mean and peak agitation by 63% and 47%, respectively. More importantly, these benefits are achieved with a total dose approximately equal to that of the recorded dose, and without exceeding the infusion rate limits. This control protocol therefore represents a significant improvement in agitation management. It also clearly shows the impact of drug dose timing on agitation, as the total doses are essentially the same, but the resulting agitation is much different.

Imposing minimum and maximum limits on the infusion rate of the GF6 protocol represents a bolus-oriented approach combined with a low constant continuous infusion, as seen in Figure 10.3. The advantage of this protocol is its ability to reduce average agitation through consistently higher concentrations than the CappedGF6 protocol. Table 10.1 shows that the BoundGF6 protocol results in an increase in median RTD from 1.05 for GF6 to 1.14 for BoundGF6. By definition, RPIR cannot exceed 1.0 for either CappedGF6 or BoundGF6. The median RMA is reduced from 0.52 for CappedGF6 to 0.39 for BoundGF6, and similarly the median RPA is reduced from 0.66 to 0.61.

Initially, these performance metrics appear very desirable. In particular, the performance metrics show that across all patients, a 61% reduction of mean agitation and 39% reduction in peak agitation is possible. Additionally, these benefits are achieved at the expense of only 14% more drug and without exceeding maximum infusion rates. However, the very low value for the minimum RMA indicates that for at least one patient, the protocol delivered drug when it was unnecessary, likely due to the constant infusion portion of the protocol. This feature over-uses drugs, and the results indicate that some over-sedation occurs. Note that this drawback primarily occurs in protocols that administer a component of the infusion rate independent of the patient state, such as the constant infusion protocol or the BoundGF6 protocol. The derivative-focused protocols, by definition, rarely let agitation fall below zero, and more importantly prevent

over-sedation by delivering minimal drug in these instances.

10.2.4 Summary

Constant infusion protocols are shown to provide poor agitation management as a result of failing to tailor drug delivery to patient requirements. This blanket approach to sedation can be seen in the constant and BoundGF6 protocols, and often results in excessive drug delivery and over-sedation, or inadequate drug delivery and insufficient sedation. In contrast, this analysis of the various control protocols using the initial model has shown that very simple control protocols can provide effective agitation management. More importantly, these simple control protocols offer considerable improvements over current clinical practice.

In particular, direct derivative-focused feedback control of agitation is shown to produce a bolus-oriented approach to sedation that tailors sedative delivery rates to patient agitation, resulting in improved agitation management. This approach is seen in the control protocols GF3–GF6, in which median reductions of up to 53% and 36% are achieved for mean and peak agitation respectively. Importantly, these reductions in agitation are achieved without only a minimal increase in total drug dose. Finally, capping the maximum allowable infusion rate not only eliminates the higher infusion rates produced by the GF3–GF6 protocols but has minimal effect on the considerable improvements on these protocols.

Table 10.1 Agitation performance metrics for all sedative infusion protocols using the initial model.

	RTD	RPIR	RMA	RPA
Constant				
Max	1.00	0.41	2.54	2.24
UQ	1.00	0.30	1.34	1.21
Med	1.00	0.24	1.02	0.98
LQ	1.00	0.20	0.74	0.81
Min	1.00	0.12	-0.50	0.51
IQR	0.00	0.10	0.60	0.40
GF3				
Max	1.07	1.33	1.00	1.01
UQ	0.98	1.11	0.98	0.98
Med	0.97	0.96	0.97	0.96
LQ	0.95	0.84	0.95	0.93
Min	0.90	0.65	0.92	0.88
IQR	0.03	0.26	0.04	0.05
GF4				
Max	1.23	1.69	0.80	0.97
UQ	1.03	1.40	0.76	0.84
Med	1.00	1.25	0.75	0.81
LQ	0.99	1.09	0.74	0.79
Min	0.97	0.79	0.67	0.72
IQR	0.04	0.31	0.02	0.05
GF5				
Max	1.37	2.12	0.68	0.96
UQ	1.08	1.68	0.62	0.75
Med	1.04	1.50	0.60	0.71
LQ	1.01	1.28	0.56	0.67
Min	1.00	0.94	0.40	0.57
IQR	0.07	0.39	0.06	0.08
GF6				
Max	1.49	2.54	0.58	0.95
UQ	1.12	1.96	0.52	0.70
Med	1.06	1.75	0.47	0.64
LQ	1.03	1.53	0.42	0.57
Min	1.00	1.09	0.20	0.50
IQR	0.09	0.43	0.10	0.13
CappedGF6				
Max	1.31	1.00	0.70	0.98
UQ	1.10	1.00	0.58	0.76
Med	1.05	1.00	0.52	0.66
LQ	1.03	1.00	0.49	0.60
Min	1.00	1.00	0.37	0.53
IQR	0.08	0.00	0.09	0.16
BoundGF6				
Max	1.43	1.00	0.66	0.98
UQ	1.24	1.00	0.48	0.72
Med	1.14	1.00	0.39	0.61
LQ	1.08	1.00	0.32	0.56
Min	1.03	1.00	0.03	0.48
IQR	0.16	0.00	0.16	0.16

Chapter 11

Control of the Physiologically-based Model

11.1 Methods

The methods described in Section 10.1 are used in this chapter, but with the physiologically-based model of Chapter 7. In particular, the model employed in this chapter includes the PD response surface, but does not incorporate the EAR dynamic. The same sedative infusion protocols (Constant, GF3, GF4, GF5, GF6, CappedGF6, BoundGF6) are used. The use of the physiologically-based, more non-linear, model seeks to determine whether the saturation and synergy dynamics limit the benefits observed in the previous chapter.

11.2 Results and Discussion

11.2.1 Constant Protocol

Figure 11.1 presents the results of the constant continuous infusion protocol for a typical patient using the physiologically-based model. The upper plot shows the infusion rates, and the lower plot shows the resulting agitation profile. In these plots, the lighter solid line represents the constant infusion protocol, and the darker solid line represents the nurse control protocol as a benchmark for comparison. Figure 11.1 shows that the constant infusion initially struggles to reduce agitation levels, but eventually overcomes agitation, and delivers excessive drug delivery when the agitation levels are low.

Again, this is a common feature throughout many patients. For part of the profile the constant infusion provides adequate sedation, but for most of the profile the infusion rate is either too small or too great, which may indicate insufficient or over-sedation, respectively. In particular, the protocol typically results in excessive variations in agitation levels throughout the profile, in many cases becoming very high or very low and over-using drug.

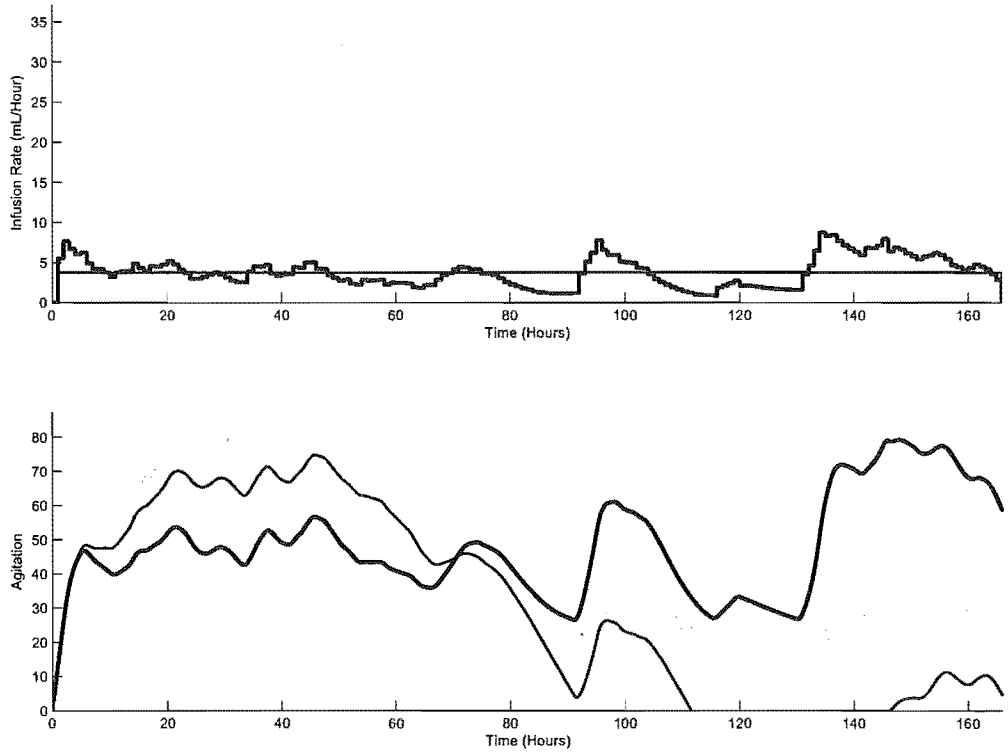

Figure 11.1 Example of the simulated results employing the constant infusion protocol in the physiologically-based model.

The implementation of the constant continuous infusion protocol results in a RTD=1.0 by definition, and RPIR is no longer important. Table 11.1, located at the end of this chapter for clarity and ease of use, presents the summary statistics of the performance metrics across all 37 patients for the 7 control protocols analysed in this chapter. The constant infusion protocol results in median values of RMA=0.84 and RPA=0.96, as seen in Table 11.1. Although these values represent an improvement over the nurse control protocol, the constant protocol is once again ineffective for many patients, as seen by the large variance between patients in RMA and RPA in the first portion of Table 11.1. Specifically, the IQR for the constant infusion protocol are considerably higher than that of any other

protocol, reflecting the extreme variability of performance across a wide range of patients.

Note that the negative value for the minimum RMA indicates that for at least one patient this protocol delivered drug when it was unnecessary, resulting in 'negative agitation levels'. This control protocol is therefore associated with all the risks of insufficient sedation and potential over-sedation discussed in Sections 10.2.1 and 10.2.3. These risks have important clinical implications and are significant considerations for clinical sedative infusion protocols.

11.2.2 GF3–GF6 Protocols

As seen from results using the initial model, the GF3 control protocol represents a direct derivative-focused control protocol with similar performance metrics to the nurse control protocol. Again, the additional drug delivered via the IIR filter in the nurse control protocol is compensated for by the increase in gains. However, while the GF3 protocol delivers similar total dose, the timing of the drug delivery is distinctly different to that delivered by the nurse control protocol, as seen in Figure 11.2. This figure presents the results of the direct derivative-focused control protocols, GF3–GF6, for a typical patient using the physiologically-based model. The upper plot shows the infusion rates, and the lower plot shows the resulting agitation profile. In these plots, the lighter solid line represents the GF3 infusion protocol, the dashed line represents the GF4 infusion protocol, the dash-dotted line represents the GF5 infusion protocol, the dotted line represents the GF6 infusion protocol, and the darker solid line represents the nurse control protocol, as a benchmark for comparison.

Like the infusion profiles resulting from using the initial model, the infusion profiles in the physiologically-based model display increased peaks and reduced troughs with increasing gain factor. In addition, the agitation profiles reduce with increasing the gain factor. Further, to a greater extent than seen in the initial model, clear differences exist in agitation profiles between the GF protocols and the nurse control protocol. In particular, the agitation profile resulting from the nurse control protocol differs from the trend between the direct derivative-focused protocols. This result is due, as in the initial model, to the presence of the IIR filter in the nurse control protocol, and its absence from the direct derivative-

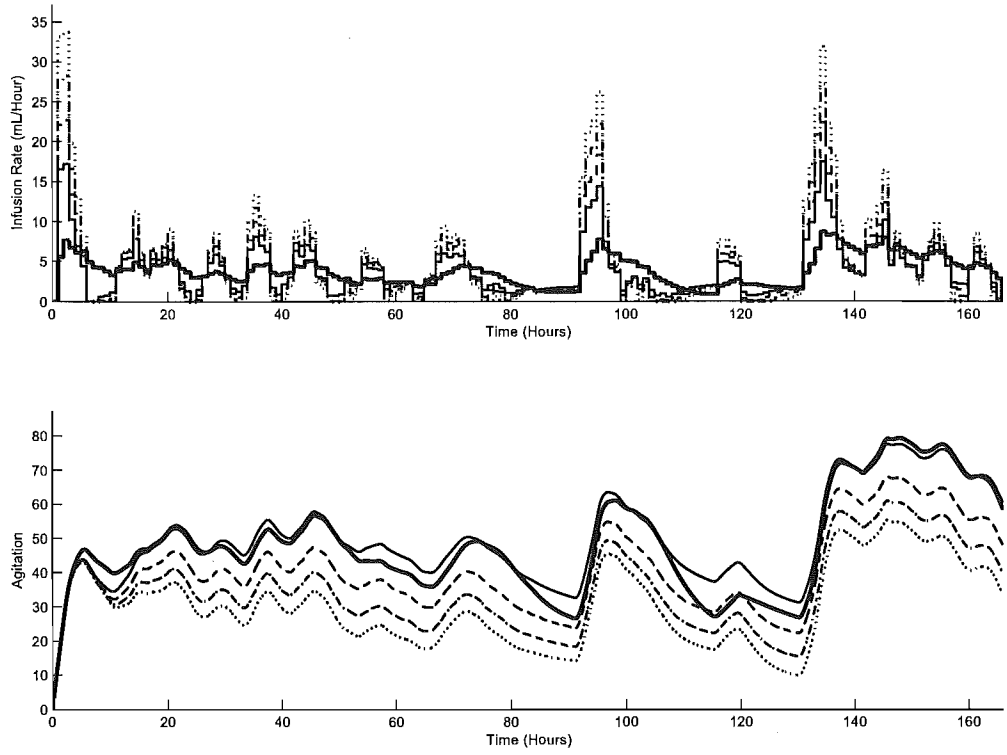

Figure 11.2 Example of the simulated results employing the GF3–GF6 infusion protocols in the physiologically-based model.

focused protocols. A likely reason for the enhanced difference observed in the physiologically-based model is the effect of the non-linear PD response surface.

Figure 11.2 shows that the GF3 protocol produces a bolus-oriented approach to sedation administration by delivering short, sharp timely boluses of sedative agents in response to rising agitation. Table 11.1, located at the end of the chapter, shows that the median RTD and RPIR across all patients for the GF3 protocol is 1.05 and 1.11, respectively. This result shows that although the GF3 protocol delivers a similar total dose of drug, the timing of the delivery is distinctly different. In particular, where the nurse control protocol has a more significant continuous component, the GF3 protocol has more peaks and troughs.

The GF4 protocol produces an even more bolus-oriented infusion profile than the GF3 protocol, with higher peaks and lower troughs, as seen in Figure 11.2. The agitation profile is lower than that of the GF3 protocol, and peaks are reduced. The GF4 protocol reduces the mean and peak agitation levels for all patients, but at the expense of increases in both dose and peak infusion rate.

The median RTD increases from 1.05 for GF3 to 1.14 for GF4, and the median RPIR increases from 1.11 to 1.35. These increases are accompanied by reductions in the agitation performance metrics. The median RMA is reduced from 1.02 for GF3 to 0.82 for GF4, and the median RPA is reduced from 0.99 for GF3 to 0.87 for GF4. Overall, while some patients' agitation levels are reduced without an increase in drug dose and peak rate, most patients experience lowered agitation levels at the expense of increased dose and/or peak infusion rates.

This result is in contrast to the results of the initial model, where the GF4 protocol achieved improvements in the agitation performance metrics with almost no change in RTD. This difference between the two models is probably due to the saturation dynamic incorporated in the response surface of the physiologically-based model. This dynamic restricts the maximum agitation-reducing effect of the drugs at high concentrations. This effect corresponds to rendering the peak effect concentrations produced by the GF4 protocol less effective. In some cases, this reduction means that additional drug is delivered beyond saturation point, which essentially contributes to excessive drug use, but does not reduce agitation. For similar reasons, the RPIR is higher in the physiologically-based model than for the initial model.

Increasing the control gains further to GF=5 and GF=6 accentuates the trends observed in the GF3 and GF4 protocols. Like results from the initial model, the physiologically-based model results in improved agitation metrics with increasing gain factor. However, unlike the results from the initial model, these benefits are achieved at the expense of increased RTD and RPIR, as seen in Table 11.1. This feature is attributed primarily to the saturation dynamic in the PD response surface. It may also be due, in part, to the somewhat arbitrary selection of C_{50}. The manual selection of C_{50} values may result in concentrations in the saturated plateau region of the response surface, reducing the enhanced effectiveness of additional drug, and thereby increasing the demand for additional drug administration. Alternatively, the selected C_{50} values may result in concentrations in the lower plateau region of the response surface, yielding only minimal effect and thereby demanding additional drug. In either case, the manual selection of C_{50} also contributes to this increase in RTD and RPIR.

The GF5 and GF6 protocols in the physiologically-based model result in a distinct bolus-oriented approach to sedation, similar to that seen in the initial

model. However, the profiles observed using the physiologically-based model are even more bolus-oriented with higher peaks and lower troughs, as seen by the higher RPIR values in Table 11.1 and displayed in Figure 11.2. The median RPIR for the GF6 protocol using the physiologically-based model is 1.89, compared to 1.75 for the initial model. Similar statistics are observed for the GF3–GF5 protocols. The sharper responses in the physiologically-based model are a likely result of the non-linear relationship between concentration and PD effect, or perhaps the slight delay between drug administration and effect. More specifically, the bolus peaks grow as saturation dynamics blunt the response of the entire bolus. This effect occurs because agitation is not reduced as much in the physiologically-based model as with the initial model that does not include effect saturation. Therefore, the limiting effect of saturation outweighs the enhanced effects of synergistic interaction. In both cases, the instantaneous PD effect is reduced, leading to an increase in agitation, and therefore leading to higher peak infusion rates.

As seen in the initial model, the direct derivative-focused control protocols result in a bolus-oriented approach to sedation. This feature can be seen in Figure 11.2, where the infusion rate is high during periods of high agitation and rapid increases of agitation, but low, or zero, during periods of relative calm or decline in agitation. This approach has the benefit of delivering substantial drug when needed, and preserving drug when it is unnecessary, avoiding oversedation and minimising drug consumption. However, it should be noted that even though the infusion may stop for short periods, the effect concentration does not usually drop to zero. Because of the transport and storage of drug from the other compartments, the effect site concentration is not typically not zero even if there is no drug delivery at that time. Hence, a small PD effect remains even during periods of zero infusion.

The fundamental outcome of these results is that the saturation dynamic in the physiologically-based model restricts the control protocol's ability to reduce agitation when the effect concentrations are in, or near, the saturated plateau of the response surface. Therefore, if a strong stimulus invoking agitation occurs at the same time as saturated effect concentrations, the mechanism through which any control protocol can reduce agitation is disabled. In clinical practice, where it is assumed that everything has been done to remove and alleviate all known sources of stimulus, this result has important implications. Fundamentally, these

results imply that for any given patient, it is not always possible to achieve a given target level of agitation. At the point of saturation, additional delivery of drug simply results in unused drug and creates potential for over-sedation and prolonged effect through drug storage and accumulation. Hence, other alternatives should be considered if this condition is detected, or estimated from the model.

This outcome represents an important consideration for clinical agitation management. Rather than attempting to reduce agitation to a target value, which is not always possible due to saturation, the goal of good agitation management should be to minimise agitation in the face of unknown stimulus, and simultaneously minimise unnecessary over-use of sedative drugs. This approach to agitation management aims to minimise agitation through timely delivery of sedative drugs, but recognises saturation and minimises drug delivery by ceasing drug administration during periods of saturation. Unfortunately, clinical implementation of this approach is not easy. There is currently, unfortunately, no simple method of knowing when saturation has been reached, except via model estimation. Although the careful medical staff can notice a lack of additional effect to additional drug, the saturation point is still not easily observed.

11.2.3 CappedGF6 and BoundGF6 Protocols

Imposing a maximum limit on the infusion rate of the GF6 protocol ensures that the infusion rate for each patient does not exceed the maximum recorded infusion rate. Therefore, the bolus-oriented approach of the GF6 protocol is maintained, but the undesirable large infusion rates are prevented. Figure 11.3 presents the results of the derivative-focused control protocols with infusion limits for a typical patient using the physiologically-based model. The upper plot shows the infusion rates, and the lower plot shows the resulting agitation profile. In these plots, the solid line represents GF6, the dashed line represents CappedGF6, the dotted line represents BoundGF6, and the darker solid line represents the nurse control protocol as a benchmark for comparison. Imposing this upper limit to the infusion rate results in a maximum RPIR=1.0 by definition. Table 11.1, located at the end of this chapter for clarity and ease of use, shows the performance metrics for the GF6, CappedGF6, and BoundGF6 protocols.

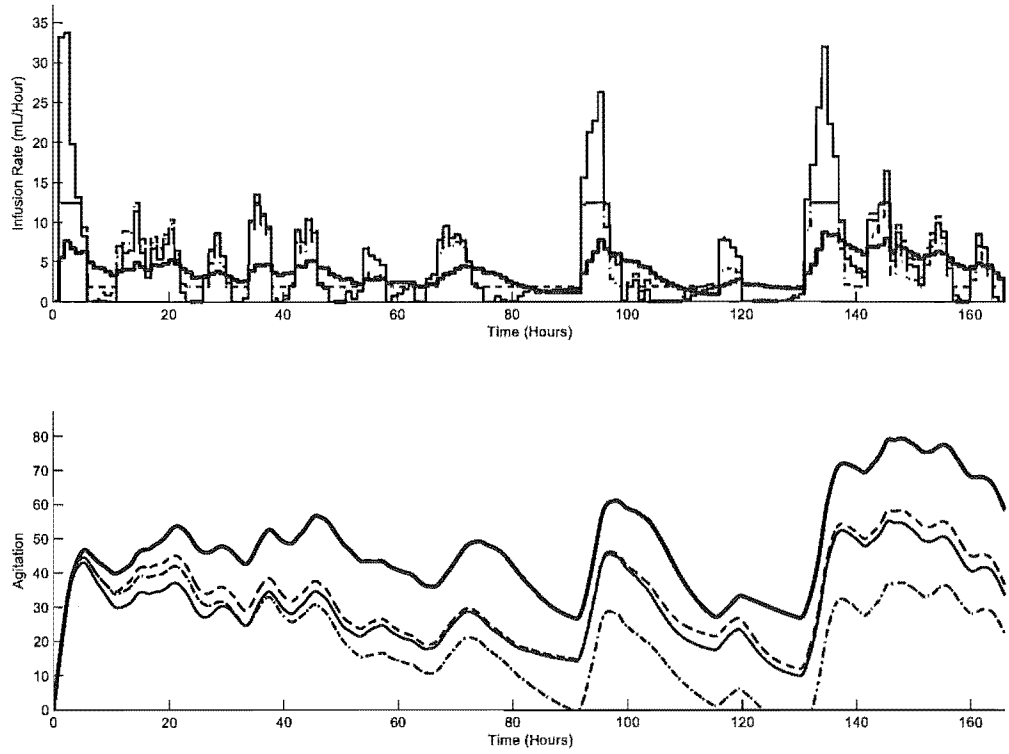

Figure 11.3 Example of the simulated results employing the CappedGF6 and BoundGF6 infusion protocols in the physiologically-based model.

As can be seen in Table 11.1, the RTD decreased from 1.34 for the GF6 protocol to 1.24 for the capped GF6 protocol. This reduction of RTD is probably the result of the elimination of the high peaks observed in the GF6 protocol, which results in less drug use. In contrast to the initial model where this reduction in dose is compensated by an increased duration of maximum infusion, the infusion rate in the physiologically-based model decreases. The infusion profile for CappedGF6 in Figure 11.3 is therefore more similar to that of the GF6 protocol, with the exception of a limit on the upper infusion rate.

Further, the RMA only increases from 0.62 to 0.64 by the implementation of the capped rate, and the RPA is not affected at all. These differences are probably due to the non-linear PD response surface employed by the physiologically-based model, and the selection of C_{50}. Although the dose that was delivered in the high peaks of the GF6 protocol is eliminated, its effect appears to be negligible. This result may be due to the fact that drug delivered in the high peaks of the GF6 protocol has almost no effect because the concentrations were in the saturated zone. Therefore, when they are eliminated in the CappedGF6 protocol,

the difference in PD effect is minimal, resulting is reduced RTD, no change in RPA and minimal change in RMA. Importantly, the reduction of RTD is a more significant gain than the negative impact of a slightly lower agitation reduction.

Imposing maximum and minimum limits on the infusion rate of the GF6 protocol has a similar effect in the physiologically-based model to that of the initial model. Because of increased effect site concentrations resulting from the continuous infusion, the PD effect reducing agitation is increased, thereby reducing the median RMA from 0.62 for CappedGF6 to 0.45 for BoundGF6 and the median RPA from 0.74 to 0.68. These reductions represent a decrease of 27.4% and 8% in RMA and RPA respectively. However, in contrast to the initial model, the median RTD did not increase. Rather, the RTD decreased slightly from 1.24 in the CappedGF6 protocol to 1.23 for the BoundGF6 protocol. This result is probably due to the fact that the constant infusion maintains the effect site concentrations in the central portion of the PD response surface so the increased drug doses are more effectively utilised, reducing the demand for drug, and hence reducing RTD.

11.2.4 Summary

Constant infusion protocols are shown, once again, to provide poor agitation management, often resulting in excessive drug delivery and over-sedation, or inadequate drug delivery and insufficient sedation. This analysis of the various control protocols using the physiologically-based model has again shown that very simple control protocols can provide considerably improved agitation management over current clinical practice. However, this chapter has highlighted the limiting effect of the saturation curve on the ability of control protocols to reduce agitation.

In particular, the presence of the saturation dynamic in the response curve incorporated in the physiologically-based model restricts the capacity of control protocols to reduce agitation. This limitation represents an important consideration for clinical agitation management. It suggests that instead of reducing agitation to a target value, which is not always possible due to saturation, the aim of good clinical agitation management should be to minimise agitation, and simultaneously minimise over-sedation. This approach to agitation management

minimises agitation using timely bolus delivery of sedative drugs, but recognises saturation limits and minimises drug delivery by ceasing drug administration during these periods of saturation. Unfortunately, no simple method of knowing when saturation has been reached, making clinical implementation difficult. However, a potential solution could be to estimate saturation limits using PKPD models, and limit doses accordingly [Chase et al., 2005b].

The limit of the saturation dynamic means that improved benefits (reduced agitation) come only at the expense of increased costs (drug dose). However, in spite of this trade-off, considerable improvements over current clinical practice are achieved through the use of direct derivative-focused feedback control protocols GF3–GF6. In particular, median reductions of up to 40% and 36% are achieved for mean and peak agitation respectively. However, these benefits were achieved at the cost of a 34% increase in median total drug dose and 89% increase in peak infusion rate. Capping the infusion rate results in the CappedGF6 protocol achieving median reductions of up to 40% and 36% are achieved for mean and peak agitation respectively, at the expense of 24% more drug. These reductions represent considerable benefit to critically ill patients and medical staff, for relatively small cost. However, these costs and benefits must be weighed appropriately to determine the advantages of such a protocol to clinical agitation management.

Table 11.1 Agitation performance metrics for all sedative infusion protocols using the physiologically-based model.

	RTD	RPIR	RMA	RPA
Constant				
Max	1.00	0.41	3.38	2.53
UQ	1.00	0.30	1.13	1.12
Med	1.00	0.24	0.84	0.96
LQ	1.00	0.20	0.44	0.65
Min	1.00	0.12	-2.82	0.10
IQR	0.00	0.10	0.69	0.47
GF3				
Max	1.22	1.56	1.10	1.07
UQ	1.08	1.34	1.04	1.01
Med	1.05	1.11	1.02	0.99
LQ	1.01	0.92	0.98	0.96
Min	0.91	0.73	0.93	0.87
IQR	0.07	0.42	0.06	0.05
GF4				
Max	1.46	2.03	0.95	1.00
UQ	1.19	1.76	0.85	0.89
Med	1.14	1.35	0.82	0.87
LQ	1.10	1.20	0.80	0.82
Min	1.04	0.89	0.74	0.77
IQR	0.09	0.56	0.05	0.07
GF5				
Max	1.69	2.54	0.88	0.98
UQ	1.30	2.16	0.73	0.84
Med	1.23	1.63	0.69	0.78
LQ	1.19	1.44	0.66	0.73
Min	1.07	1.07	0.58	0.63
IQR	0.11	0.72	0.07	0.11
GF6				
Max	1.91	3.04	0.83	0.98
UQ	1.41	2.55	0.64	0.80
Med	1.34	1.89	0.60	0.74
LQ	1.28	1.65	0.56	0.67
Min	1.10	1.24	0.46	0.54
IQR	0.13	0.90	0.08	0.13
CappedGF6				
Max	1.50	1.00	0.88	0.99
UQ	1.27	1.00	0.72	0.80
Med	1.24	1.00	0.62	0.74
LQ	1.20	1.00	0.57	0.68
Min	1.09	1.00	0.50	0.57
IQR	0.07	0.00	0.15	0.12
BoundGF6				
Max	1.58	1.00	0.76	0.99
UQ	1.30	1.00	0.56	0.75
Med	1.23	1.00	0.45	0.68
LQ	1.17	1.00	0.41	0.60
Min	1.10	1.00	0.28	0.49
IQR	0.13	0.00	0.15	0.15

Chapter 12

Control of the Extended Physiological Model

12.1 Methods

The methods described in Section 10.1 are used in this chapter, but with the extended physiologically-based model of Section 8.2.4. In particular, the model employed in this chapter includes the PD response surface and the EAR dynamic, as well as the parameter identification techniques presented in Chapter 8. The same sedative infusion protocols (Constant, GF3, GF4, GF5, GF6 CappedGF6, BoundGF6) are used. The use of the extended physiologically-based model seeks to determine the effects parameter identification techniques employed and the EAR dynamic.

The differences between the physiologically-based model of Chapter 7 and the extended physiologically-based model include:

1. The inclusion of the EAR dynamic, $-w_3 A$, from Section 8.2.4.
2. The time-varying, fitted $w_2(t)$, from Section 8.1.2.
3. The consistent selection of C_{50}, as seen in Section 8.1.1.

The EAR dynamic is likely to reduce the amount of drug required to achieve a particular agitation level, or for a given agitation level reduce the drug requirements, as a result of the combined endogenous and exogenous agitation reduction. The time-varying fitted $w_2(t)$ is expected to affect the capacity of the control protocol to reduce agitation by the time-varying nature of the sedative sensitivity. Because $w_2(t)$ is fitted using the procedure in Section 8.1.2, the time-varying $w_2(t)$ is likely to reduce agitation levels through increased sedative

sensitivity where required. The consistent selection of C_{50} creates more consistent PD response surface between patients, and reduces over-saturation and under-utilisation due to any associated model error. This, in turn, alters the PD response surface and saturation dynamic to be more patient-specific.

12.2 Results and Discussion

12.2.1 Constant Protocol

Figure 12.1 presents the results of the constant continuous infusion protocol for a typical patient using the extended physiologically-based model. The upper plot shows the infusion rates, and the lower plot shows the resulting agitation profile. In these plots, the lighter solid line represents the constant infusion protocol, and the darker solid line represents the nurse control protocol as a benchmark for comparison. As with the initial model and the physiologically-based model, Figure 12.1 shows that while the constant infusion initially struggles to reduce agitation levels, it eventually overcomes agitation, and delivers excessive drug delivery when the agitation levels are low. Again, this is a common feature throughout many patients. For part of the profile the constant infusion provides adequate sedation, but for most of the profile the infusion rate is either too great or too small, which may indicate insufficient or over-sedation. In particular, the protocol typically results in excessive variations in agitation levels throughout the profile, in many cases becoming very high or very low and over-using drug.

The implementation of the constant continuous infusion protocol results in a relative total dose of 1.0 by definition, and RPIR is no longer relevant. Table 12.1, located at the end of this chapter, presents the summary statistics of the performance metrics across all 37 patients for the 7 control protocols analysed in this chapter. The constant infusion protocol results in median values of RMA=0.45 and RPA=0.91, as seen in Table 12.1. Although these values represent a significant improvement over the nurse control protocol and appear to produce desirable results, the constant protocol is once again ineffective for many patients resulting in severe over-use of sedative drugs. This feature is seen by the large variance between patients in the IQR of RMA and RPA in the first portion of Table 12.1. Specifically, the IQR for the constant infusion protocol is considerably higher

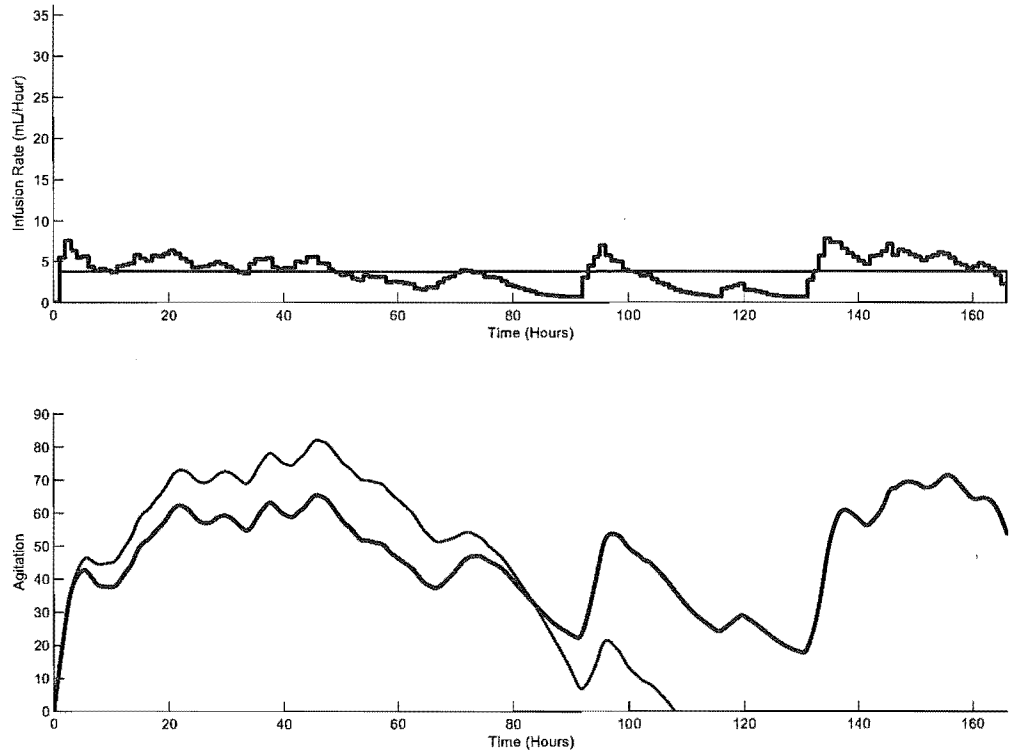

Figure 12.1 Example of the simulated results employing the constant infusion protocol in the extended physiologically-based model.

than that of any other protocol, reflecting the extreme variability of performance across a wide range of patients. Specifically, agitation values regularly fall below zero, and the protocol the continues to deliver unnecessary drugs.

Note that the multiple negative values for the RMA column of Table 12.1 indicate that for many patients this protocol delivered drug when it was unnecessary resulting in 'negative agitation levels'. This control protocol is therefore associated with all the risks of insufficient sedation and potential over-sedation discussed in Section 10.2.1 and 10.2.3. These risks have important clinical implications and are significant considerations for clinical sedative infusion protocols.

It is interesting to note that this protocol results in an exceptionally high number of patients with 'negative agitation levels' for this model. This result is probably primarily due to the PD response surface and the selection method for C_{50}. During the constant infusion the effect site concentrations will remain at a constant elevated level. Because of the C_{50} selection criteria, the constant effect site concentration will correspond to a relatively high PD effect, accentuated by

the synergistic nature of Morphine and Midazolam. Further to this effect, the EAR dynamic may also contribute to the increased reductions in agitation and thus the increased negative agitation results.

12.2.2 GF3–GF6 Protocols

As seen from results using the initial and physiologically-based models in Chapters 10 and 11, the GF3 control protocol represents a direct derivative-focused control protocol with similar performance metrics to the nurse control protocol, but with a distinctly bolus-oriented approach. Figure 12.2 presents the results of the direct derivative-focused control protocols, GF3–GF6, for a typical patient using the physiologically-based model. The upper plot shows the infusion rates, and the lower plot shows the resulting agitation profile. In these plots, the lighter solid line represents the GF3 infusion protocol, the dashed line represents the GF4 infusion protocol, the dash-dotted line represents the GF5 infusion protocol, the dotted line represents the GF6 infusion protocol, and the darker solid line represents the nurse control protocol as a benchmark for comparison.

Table 12.1, located at the end of the chapter, shows that the median RTD and RPIR across all patients for the GF3 protocol is 0.97 and 1.03, respectively. This result shows that although the GF3 protocol delivers a very similar total dose of drug, the timing of the delivery is distinctly different. In particular, whereas the nurse control protocol has a more significant continuous component, the GF3 protocol has more peaks and troughs. This dose is also lower than in Chapter 11, likely due to the EAR dynamic.

Like in the initial and physiologically-based models, the GF4 protocol in the extended physiologically-based model produces a more bolus-oriented approach to sedation administration. The median RTD increased from 0.97 for GF3 to 1.05 for GF4. This increase of RTD is also seen in the physiologically-based model, but in this extended model the change is not as large. Similarly, the median RPIR increased from 1.03 for the GF3 protocol to 1.30 for the GF4 protocol, which is also observed in the physiologically-based model. The median RMA dropped from 0.96 for GF3 to 0.78 for GF4, and the median RPA dropped from 0.95 to 0.84.

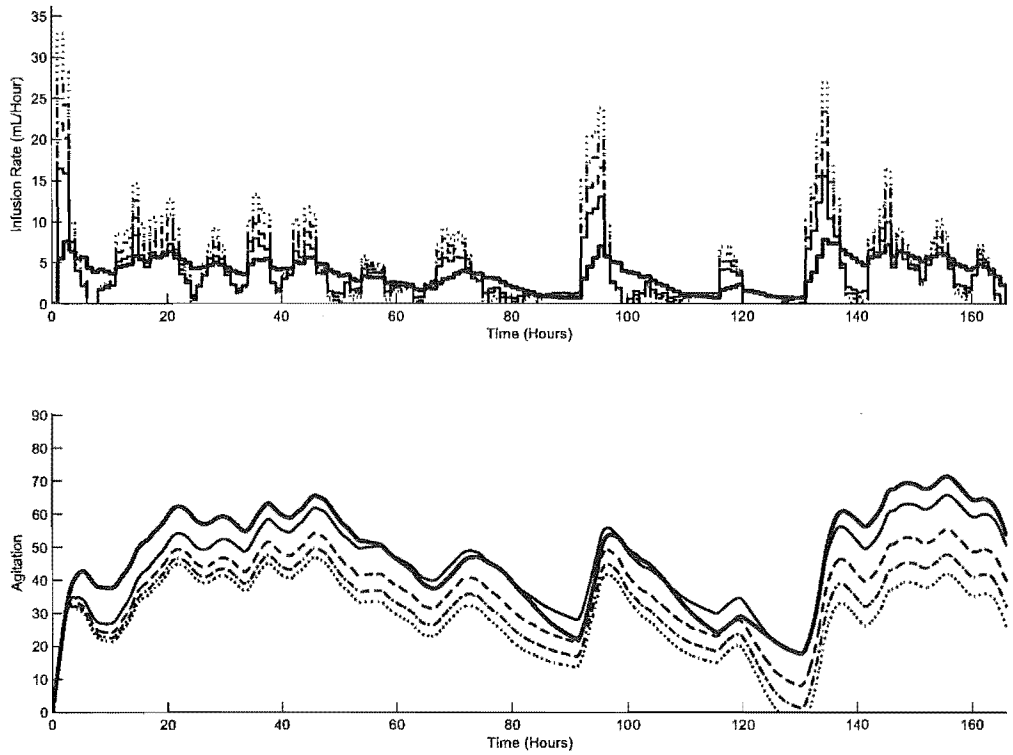

Figure 12.2 Example of the simulated results employing the GF3–GF6 infusion protocols in the extended physiologically-based model.

These performance metrics show that while the extended physiologically-based model exhibits the same trends as the physiologically-based model of Chapter 11, some of the changes are not as severe, and the trends tend to lie between those of the initial model and physiologically-based model. This result is a direct consequence of the combination of the EAR dynamic, the time-varying $w_2(t)$ and the C_{50} selection. This more patient-specific model with added agitation reduction dynamics better suits the feedback control approach and its ability to customise sedation to agitation response.

Similar trends in the extended physiologically-based model for performance metrics are observed when the gain factor is increased to 5 and 6, as those in the physiologically-based model. The median RTD increases to 1.08 and 1.10 for GF5 and GF6 protocols, and the RPIR increases to 1.57 and 1.83, respectively. Like the results from both the initial and physiologically-based model, the median RMA is reduced to 0.64 and 0.55 for GF5 and GF6 respectively, and the median RPA is reduced to 0.77 and 0.72. Like the physiologically-based model, the RTD and RPIR increase with increasing gain factor because the saturation curve

limits the effectiveness of the additional drug. However, the time-varying $w_2(t)$ and EAR dynamic in the extended model mediate the effect of the saturation dynamic. Therefore, although the RTD increases with increasing gains, as in the physiologically-based model, the increase is not as dramatic, while the agitation management improvements are retained.

These reductions in mean and peak agitation levels using the GF5 and GF6 protocols are significant. The median reduction in mean agitation is 45%, with some patients experiencing a reduction of up to 90%. Similarly, peak agitation levels are dramatically reduced, with the median reduction of 28%, and maximum reduction of 67%. Although these improvements are clinically desirable, these benefits are achieved at the expense of an increase in total dose and peak infusion rate. However, the increase in total dose is relatively small, and not as important as the increase in peak infusion rate. The GF6 protocol, although showing significant agitation reduction, results in a median increase in peak infusion rates of 83%, and in some cases up to 203%. These high infusion rates are likely to be unacceptable for clinical practice, and are also likely to be minimally effective due to saturation.

As previously discussed in Chapter 11, the saturation dynamic in the extended physiologically-based model is a major factor limiting the performance of any sedative infusion protocol. This feature is highlighted by the fact that the initial model, which does not incorporate the saturation dynamic, is capable of significantly improved reductions in both mean and peak agitation for any given control protocol. However, in spite of this issue, the GF6 protocol shows potential for improved agitation management if the high infusion rates are reduced.

12.2.3 CappedGF6 and BoundGF6 Protocols

Imposing a maximum limit on the infusion rate of the GF6 protocol ensures that the infusion rate for each patient does not exceed the maximum recorded infusion rate. Therefore, the bolus-oriented approach of the GF6 protocol is maintained, but the undesirable large infusion rates are prevented. Figure 12.3 presents the results of the derivative-focused control protocols with infusion limits for a typical patient using the extended physiologically-based model. The upper plot shows the infusion rates, and the lower plot shows the resulting agitation

profile. In these plots, the lighter solid line represents GF6, the dashed line represents CappedGF6, the dotted line represents BoundGF6, and the darker solid line represents the nurse control protocol as a benchmark for comparison. Imposing this upper limit on the infusion rate results in a maximum RPIR=1.0 by definition.

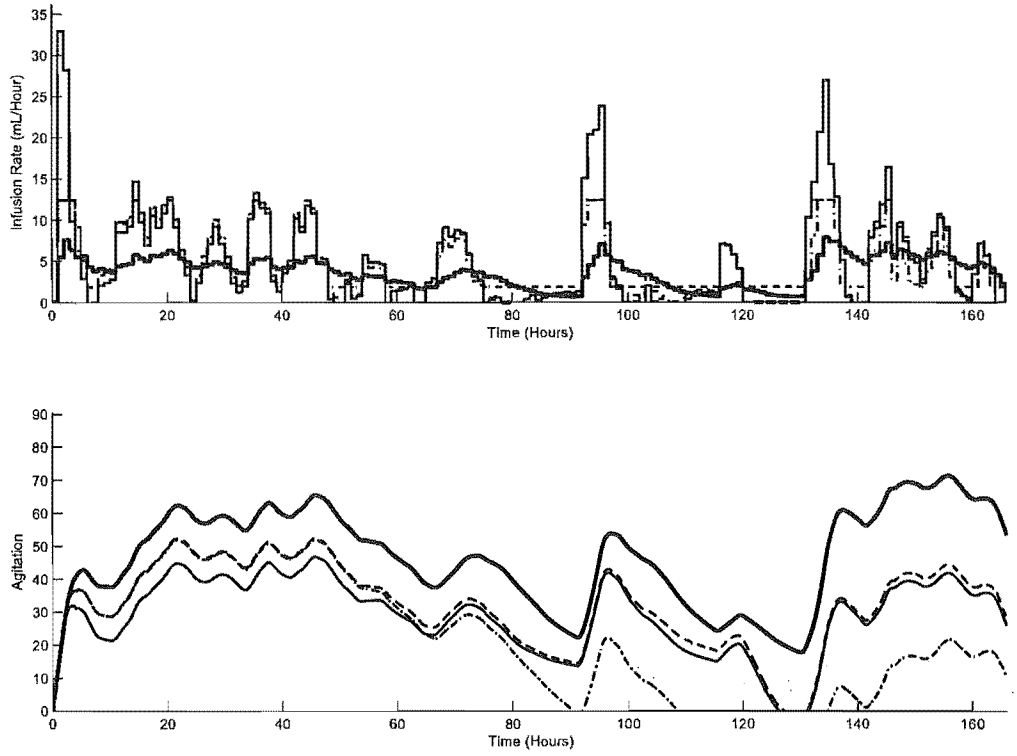

Figure 12.3 Example of the simulated results employing the CappedGF6 and BoundGF6 infusion protocols in the extended physiologically-based model.

Table 12.1 shows the performance metrics for the GF6, CappedGF6, and BoundGF6 protocols. Like the physiologically-based model, the median RMA increases slightly from 0.55 to 0.57, and RPA increases slightly from 0.72 to 0.74, as seen in Table 12.1. However, in contrast to the physiologically-based model, and more like the initial model, the extended model shows an increase in RTD from 1.10 to 1.21. This is most likely due to the increased time that the infusion rate is at peak value, and may differ from the physiologically-based model because of the different C_{50} selection and values.

However, for approximately 20% more drug dose and no increase in peak infusion rates, the CappedGF6 protocol results in a median reduction of mean

agitation of 43%. Further, some patients experience a mean agitation reduction of up to 90%. Similarly, the median reduction in peak agitation is 26%, and in some cases a reduction of up to 66% is observed. These results show that the Capped GF6 protocol is an effective protocol all round, and emphasises again how a simple control protocol can be extremely effective.

Applying maximum and minimum limits to the infusion rate of the GF6 protocol has a similar effect in the extended model to that of the initial and physiologically-based models. Because of increased effect site concentrations resulting from the continuous infusion, the PD effect reducing agitation is increased, thereby reducing the median RMA from 0.57 for CappedGF6 to 0.38 for BoundGF6 and the median RPA from 0.74 to 0.67. Unlike the physiologically-based model, the RTD increased slightly from 1.21 in the CappedGF6 protocol to 1.23 for the BoundGF6 protocol. However, the dominating feature of the results of the BoundGF6 in the extended model is the fact that, once again, the continuous infusion causes some patients to experience 'negative agitation levels'. This once again highlights the point that protocols that deliver a component of the infusion rate independent of patient agitation run the risk of over-sedation or insufficient sedation.

12.2.4 Summary

This analysis of the various control protocols using the extended physiologically-based model has reiterated the results of the previous chapter. In particular, the results indicate that constant infusion protocols provide poor agitation management, while very simple control protocols can provide improved agitation management over current clinical practice. Further, this chapter has once again emphasised the limiting effect of the saturation dynamic on the capacity of any given control protocol to reduce agitation.

Although the patient-specific identification of PD parameters and the effect of the EAR dynamic are shown to mediate the effect of the saturation dynamic, the saturation curve still represents the dominant feature restricting the capacity of control protocols to reduce agitation. However, in spite of this restriction, considerable improvements over current clinical practice are achieved. In particular the CappedGF6 protocol achieved median reductions of up to 63% and 28%

for mean and peak agitation, respectively. More importantly these benefits are achieved without exceeding conservative safety infusion limits, and at the expense of only 21% more total drug dose. The important feature of this bolus-oriented approach to agitation management is the use of timely boluses of sedatives in response to patient agitation, rather than a continuous infusion rate. The result of this bolus-oriented approach is a reduction in the unnecessary over-use of drugs, and reductions in both mean and peak agitation.

These reductions represent considerable benefit to critically ill patients and medical staff. However, the presence of the saturation dynamic means that these benefits (reduced agitation) come only at the expense of increased costs (drug dose). This trade-off between benefits and costs makes agitation management a complex issue involving the value of reduced agitation levels and improved healthcare, compared to the cost of increased drug dose.

Table 12.1 Agitation performance metrics for all sedative infusion protocols using the extended physiologically-based model.

	RTD	RPIR	RMA	RPA
Constant				
Max	1.00	0.41	1.31	1.64
UQ	1.00	0.30	0.93	1.14
Med	1.00	0.24	0.45	0.91
LQ	1.00	0.20	-0.30	0.52
Min	1.00	0.12	-7.85	0.05
IQR	0.00	0.10	1.23	0.62
GF3				
Max	1.09	1.53	1.01	1.05
UQ	0.99	1.29	0.98	0.99
Med	0.97	1.03	0.96	0.95
LQ	0.94	0.94	0.90	0.92
Min	0.80	0.71	0.75	0.81
IQR	0.05	0.35	0.08	0.07
GF4				
Max	1.20	2.02	0.85	0.93
UQ	1.08	1.63	0.80	0.88
Med	1.05	1.30	0.78	0.84
LQ	0.98	1.21	0.71	0.82
Min	0.80	0.90	0.47	0.61
IQR	0.10	0.42	0.09	0.06
GF5				
Max	1.29	2.52	0.78	0.85
UQ	1.16	1.99	0.69	0.80
Med	1.08	1.57	0.64	0.77
LQ	0.97	1.46	0.55	0.74
Min	0.63	1.07	0.25	0.44
IQR	0.19	0.53	0.14	0.06
GF6				
Max	1.39	3.03	0.73	0.81
UQ	1.22	2.39	0.62	0.74
Med	1.10	1.83	0.55	0.72
LQ	0.93	1.73	0.44	0.69
Min	0.41	1.22	0.10	0.33
IQR	0.29	0.66	0.18	0.05
CappedGF6				
Max	1.42	1.00	0.84	0.88
UQ	1.26	1.00	0.67	0.76
Med	1.21	1.00	0.57	0.74
LQ	1.12	1.00	0.52	0.70
Min	0.96	1.00	0.10	0.34
IQR	0.14	0.00	0.15	0.06
BoundGF6				
Max	1.54	1.00	0.67	0.88
UQ	1.30	1.00	0.50	0.71
Med	1.23	1.00	0.38	0.67
LQ	1.15	1.00	0.15	0.60
Min	1.04	1.00	-0.11	0.24
IQR	0.15	0.00	0.35	0.11

Chapter 13

H_∞ Control of the Physiologically-based Model

H_∞ control is selected over other approaches for formal control systems analysis based on its ability to minimise the transfer function between an unknown stimulus and the resulting patient agitation. H_∞ applications are more common in the pharmacokinetically similar glucose-insulin system, where it has been used in simulations studies to regulate blood glucose in diabetes [Kienitz and Yoneyama, 1993; Ruiz-Velazquez et al., 2004]. In agitation management, the primary advantage of H_∞ methods is that the input disturbance need not be explicitly known to control steady state response, offering a significant advantage in this case. This chapter develops an H_∞ methodology using the physiologically-based model of Chapter 7.

13.1 Linearity Assumptions

Using the physiologically-based agitation-sedation model of Chapter 7, a linear matrix inequality (LMI) H_∞ static output feedback control design methodology is developed. By optimally reducing the maximum magnitude of the transfer function between the unknown stimulus input, S, and the measured patient agitation output, A, H_∞ control doesn't require the stimulus, S, to be known.

First, a linear version of the agitation-sedation system presented in Equations (7.1)–(7.6) is required. The non-linear Equation (7.6) can be expanded into two

separate differential equations. Equation (7.6) can be re-written:

$$\begin{aligned}\epsilon &= K_T \int_0^t E_{Comb} e^{-K_T(t-\tau)} d\tau \\ &= K_T e^{-K_T t} \int_0^t E_{Comb} e^{K_T \tau} d\tau \\ &= f(t)g(t) \end{aligned} \tag{13.1}$$

where $f(t) = K_T e^{-K_T t}$ and $g(t) = \int_0^t E_{Comb} e^{K_T \tau} d\tau$.

Differentiating Equation 13.1 using the product rule and the fundamental theorem of calculus yields:

$$\begin{aligned}\frac{d\epsilon}{dt} &= f'(t)g(t) + f(t)g'(t) \\ &= -K_T^2 e^{-K_T t} \cdot \left[\int_0^t E_{Comb} e^{K_T \tau} d\tau \right] + K_T e^{-K_T t} \cdot [E_{Comb} e^{K_T t}] \\ &= -K_T \cdot \left[K_T e^{-K_T t} \int_0^t E_{Comb} e^{K_T \tau} d\tau \right] + K_T \cdot E_{Comb} \\ &= -K_T \epsilon + K_T E_{Comb} \end{aligned} \tag{13.2}$$

Note that this form of the PD effect equation indicates that the pharmacologically active drug is transported to the effect site via a diffusion process, in this case presumed to be the diffusion across the blood brain barrier into the brain and central nervous system. Substituting Equation (13.1) into Equation (7.6) yields a linear form of Equation (7.6) in terms of ϵ.

$$\frac{dA}{dt} = w_1 S - w_2 \epsilon \tag{13.3}$$

Next, the non-linear effect response surface in Figure 3.3 is replaced by the linear surface shown in Figure 13.1. The dark flat surface represents the linear response surface, and the line-mesh white curved surface represents the non-linear surface for comparison. This linear surface is defined:

$$E_{Comb} = \kappa^a C_e^a + \kappa^s C_e^s \tag{13.4}$$

where κ^a and κ^s are chosen to ensure the centre of the non-linear and linear surfaces coincide. Hence, Figure 13.1 is a linear approximation of the net slope of the sigmoid in Figure 3.3, rather than its middle slope, capturing an average

type of response.

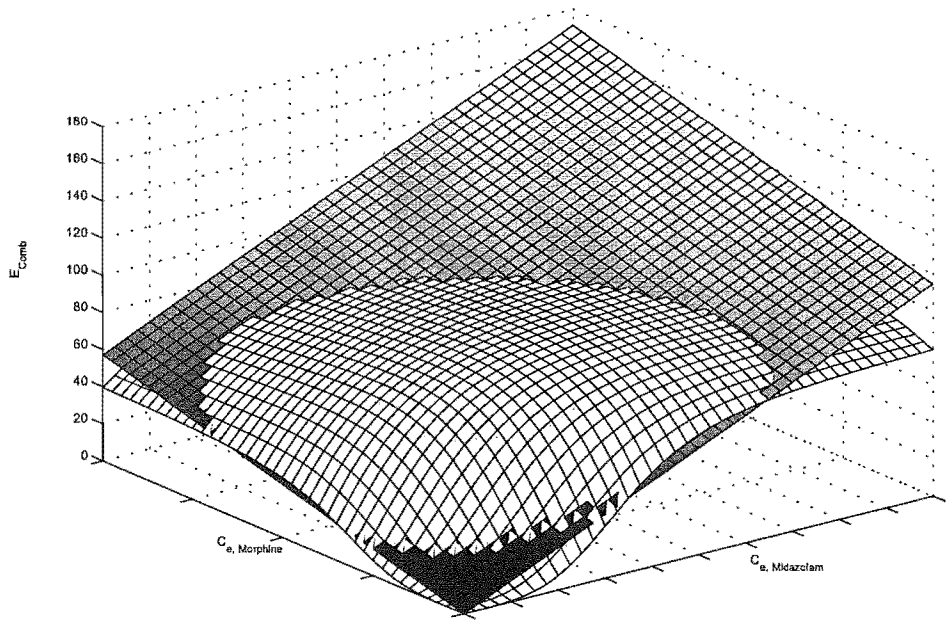

Figure 13.1 Schematic of the linearised PD response surface.

13.2 H_∞ Control Methodology

Equations (7.1)–(7.5) and (13.2)–(13.3), incorporating the linear response surface in Equation (13.4), forms a simplified linear state-space model of the agitation-sedation system.

$$\begin{bmatrix} \dot{C}_c^a \\ \dot{C}_p^a \\ \dot{C}_e^a \\ \dot{C}_c^s \\ \dot{C}_e^s \\ \dot{\epsilon} \\ \dot{A} \end{bmatrix} = \begin{bmatrix} a_{11} & a_{12} & a_{13} & 0 & 0 & 0 & 0 \\ a_{21} & a_{22} & 0 & 0 & 0 & 0 & 0 \\ a_{31} & 0 & a_{33} & 0 & 0 & 0 & 0 \\ 0 & 0 & 0 & a_{44} & a_{45} & 0 & 0 \\ 0 & 0 & 0 & a_{54} & a_{55} & 0 & 0 \\ 0 & 0 & a_{63} & 0 & a_{65} & a_{66} & 0 \\ 0 & 0 & 0 & 0 & 0 & a_{76} & 0 \end{bmatrix} \begin{bmatrix} C_c^a \\ C_p^a \\ C_e^a \\ C_c^s \\ C_e^s \\ \epsilon \\ A \end{bmatrix} + \begin{bmatrix} R^a \\ 0 \\ 0 \\ R^s \\ 0 \\ 0 \\ 0 \end{bmatrix} U + \begin{bmatrix} 0 \\ 0 \\ 0 \\ 0 \\ 0 \\ 0 \\ w_1 \end{bmatrix} S$$

$$\dot{\mathbf{x}} = \mathbf{A}\mathbf{x} + \mathbf{B}_1 U + \mathbf{B}_2 S \tag{13.5}$$

where

$$\mathbf{A} = \begin{bmatrix} \frac{-K^a_{CL}-K^a_{ce}-K^a_{cp}}{V^a_c} & \frac{K^a_{pc}}{V^a_c} & \frac{K^a_{ec}}{V^a_c} & 0 & 0 & 0 & 0 \\ \frac{K^a_{cp}}{V^a_p} & -\frac{K^a_{pc}}{V^a_p} & 0 & 0 & 0 & 0 & 0 \\ \frac{K^a_{ce}}{V^a_e} & 0 & -\frac{K^a_{ec}}{V^a_e} & 0 & 0 & 0 & 0 \\ 0 & 0 & 0 & \frac{-K^s_{CL}-K^s_{ce}}{V^s_c} & \frac{K^s_{ec}}{V^s_c} & 0 & 0 \\ 0 & 0 & 0 & \frac{K^s_{ce}}{V^s_e} & -\frac{K^s_{ec}}{V^s_e} & 0 & 0 \\ 0 & 0 & \kappa^a K_T & 0 & \kappa^s K_T & -K_T & 0 \\ 0 & 0 & 0 & 0 & 0 & -w_2 & 0 \end{bmatrix}$$

The measured output, $\mathbf{y}$, is defined as a 2-signal vector of the patient agitation, A, and its rate of change, $\dot{A}$, both of which are becoming available from newly developed agitation sensing methods [Chase et al., 2004c,a; Lam et al., 2003; Starfinger et al., 2003; Agogué, 2005; Lam, 2003; Starfinger, 2003; Chase et al., 2004b]:

$$\begin{aligned} \mathbf{y} &= \begin{bmatrix} A \\ \dot{A} \end{bmatrix} \\ &= \begin{bmatrix} x_7 \\ w_2 x_6 + w_1 S \end{bmatrix} \\ &= \begin{bmatrix} 0 & 0 & 0 & 0 & 0 & 0 & 1 \\ 0 & 0 & 0 & 0 & 0 & -w_2 & 0 \end{bmatrix} \begin{bmatrix} x_1 \\ x_2 \\ x_3 \\ x_4 \\ x_5 \\ x_6 \\ x_7 \end{bmatrix} + \begin{bmatrix} 0 \\ w_1 \end{bmatrix} S \\ &= \mathbf{C_1 x} + \mathbf{D_1} S \end{aligned} \tag{13.6}$$

A static output feedback controller for determining the sedation input to this system is therefore a proportional-derivative controller.

$$\begin{aligned} U &= -\begin{bmatrix} K_p & K_d \end{bmatrix} \begin{bmatrix} A \\ \dot{A} \end{bmatrix} \\ &= -\mathbf{K}\mathbf{y} \end{aligned} \tag{13.7}$$

The derivative-focused proportional-derivative control protocol employing $\mathbf{K} = [-0.0004 - 0.4] \times 3$ in Section 11.2.2 provides an essentially bolus-driven management approach, which is shown in Chapter 11 to be effective in managing patient agitation given a consistent agitation measurement. Adopting the simple approach of increasing the original control gains by a factor of six (GF6 protocol) reduced mean patient agitation by 40% across all patients, and by as much as 54% for some patients, in comparison to the infusion methods currently employed. These ideas are further investigated and validated using H_∞ control methods as a formal means of control systems analysis.

The closed-loop system state space equations are defined:

$$\dot{\mathbf{x}} = [\mathbf{A} - \mathbf{B_1}\mathbf{K}\mathbf{C_1}]\mathbf{x} + [\mathbf{B_2} - \mathbf{B_1}\mathbf{K}\mathbf{D_1}]S = \mathbf{A_{cl}}\mathbf{x} + \mathbf{B_{cl}}S \tag{13.8}$$

where $\mathbf{A_{cl}}$ and $\mathbf{B_{cl}}$ represent the closed-loop plant and external disturbance mapping matrices, respectively.

To derive H_∞ optimality conditions, a quadratic Lyapunov function can also be defined [Vidyasagar, 1993] :

$$\mathbf{v} = \mathbf{x}^\mathbf{T}\mathbf{P}\mathbf{x} \tag{13.9}$$

where $\mathbf{P} = \mathbf{P}^\mathbf{T}$ is assumed. Differentiating Equation (13.9) and substituting Equation (13.8) yields:

$$\dot{\mathbf{v}} = \mathbf{x}^\mathbf{T}[\mathbf{A_{cl}}\mathbf{P} + \mathbf{P}\mathbf{A_{cl}}]\mathbf{x} + [\mathbf{B}_\mathbf{cl}^\mathbf{T}\mathbf{P}\mathbf{x} + \mathbf{x}^\mathbf{T}\mathbf{P}\mathbf{B_{cl}}]S \tag{13.10}$$

If $\mathbf{P} = \mathbf{P}^\mathbf{T} > 0$ can be found such that $\dot{\mathbf{v}} < 0, \forall x \neq 0$ then stability is ensured via standard Lyapunov stability theory. This stability criterion can be augmented

to include an H_∞ bound criteria [Boyd and Ghaoui, 1993]:

$$\dot{\mathbf{v}} + \mathbf{z}^\mathbf{T}\mathbf{z} - \gamma^2\mathbf{w}^\mathbf{T}\mathbf{w} \leq \mathbf{0}, \quad \forall x \neq 0 \tag{13.11}$$

where the regulated output, z, is defined as patient agitation for this case:

$$z = A = [0 \;\; 0 \;\; 0 \;\; 0 \;\; 0 \;\; 0 \;\; 1]\mathbf{x} = \hat{\mathbf{C}}_\mathbf{1}\mathbf{x} \tag{13.12}$$

Note that this metric will be reduced in an l_2 or rms sense, similar to the average agitation metrics of Chapters 10–12.

Substituting Equations (13.10) and (13.12) into Equation (13.11) and simplifying yields:

$$\mathbf{x}^\mathbf{T}[\mathbf{A}_\mathbf{cl}^\mathbf{T}\mathbf{P} + \mathbf{P}\mathbf{A}_\mathbf{cl} + \hat{\mathbf{C}}_\mathbf{1}^\mathbf{T}\hat{\mathbf{C}}_\mathbf{1}]\mathbf{x} + \mathbf{w}^\mathbf{T}\mathbf{B}_\mathbf{cl}^\mathbf{T}\mathbf{P}\mathbf{x} + \mathbf{x}^\mathbf{T}\mathbf{P}\mathbf{B}_\mathbf{cl}\mathbf{w} - \gamma^2\mathbf{w}^\mathbf{T}\mathbf{w} \leq \mathbf{0} \tag{13.13}$$

However, Equation (13.13) is not easily simplified, but is clearly valid [Chase and Smith, 1996; Chase et al., 2005a] if:

$$\mathbf{x}^\mathbf{T}[\mathbf{A}_\mathbf{cl}^\mathbf{T}\mathbf{P} + \mathbf{P}\mathbf{A}_\mathbf{cl} + \hat{\mathbf{C}}_\mathbf{1}^\mathbf{T}\hat{\mathbf{C}}_\mathbf{1}]\mathbf{x} + \mathbf{w}^\mathbf{T}\mathbf{B}_\mathbf{cl}^\mathbf{T}\mathbf{P}\mathbf{x} + \mathbf{x}^\mathbf{T}\mathbf{P}\mathbf{B}_\mathbf{cl}\mathbf{w} - \gamma^2\mathbf{w}^\mathbf{T}\mathbf{w} + \Gamma^T\Gamma \leq 0 \tag{13.14}$$

where a careful selection of Γ yields:

$$\Gamma = \frac{1}{\gamma}(\mathbf{B}_\mathbf{cl}^\mathbf{T}\mathbf{P}\mathbf{x} - \gamma\mathbf{w}) \tag{13.15}$$

Substituting Equation (13.15) into Equation (13.14) and simplifying yields a more readily solved matrix condition to find a matrix $\mathbf{P} = \mathbf{P}^\mathbf{T} > 0$ that also satisfies Equation (13.11):

$$\mathbf{x}^\mathbf{T}\left[\mathbf{A}_\mathbf{cl}^\mathbf{T}\mathbf{P} + \mathbf{P}\mathbf{A}_\mathbf{cl} + \frac{1}{\gamma}\mathbf{P}\mathbf{B}_\mathbf{cl}\mathbf{B}_\mathbf{cl}^\mathbf{T}\mathbf{P} + \hat{\mathbf{C}}_\mathbf{1}^\mathbf{T}\hat{\mathbf{C}}_\mathbf{1}\right]\mathbf{x} \leq \mathbf{0} \tag{13.16}$$

Equation (13.16) is satisfied when the matrix is negative definite, or negative semi-definite:

$$\left[\mathbf{A}_\mathbf{cl}^\mathbf{T}\mathbf{P} + \mathbf{P}\mathbf{A}_\mathbf{cl} + \frac{1}{\gamma}\mathbf{P}\mathbf{B}_\mathbf{cl}\mathbf{B}_\mathbf{cl}^\mathbf{T}\mathbf{P} + \hat{\mathbf{C}}_\mathbf{1}^\mathbf{T}\hat{\mathbf{C}}_\mathbf{1}\right] \leq \mathbf{0} \tag{13.17}$$

Finally, using Schur complements, Equation (13.17) can be expressed as a Linear

Matrix Inequality (LMI):

$$\begin{bmatrix} \mathbf{A}_{\mathbf{cl}}^{\mathbf{T}}\mathbf{P} + \mathbf{P}\mathbf{A}_{\mathbf{cl}} + \hat{\mathbf{C}}_{\mathbf{1}}^{\mathbf{T}}\hat{\mathbf{C}}_{\mathbf{1}} & \mathbf{P}\mathbf{B}_{\mathbf{cl}} \\ \mathbf{B}_{\mathbf{cl}}^{\mathbf{T}}\mathbf{P} & -\gamma^2 \end{bmatrix} \leq 0 \tag{13.18}$$

If a positive definite symmetric matrix $\mathbf{P}$ can be found to satisfy Equation (13.18) for a given value of $\gamma > 0$, then the linear system H_∞ norm is bound by γ [Chase and Smith, 1996]. Note that $\mathbf{A_{cl}}$ and $\mathbf{B_{cl}}$ both contain the gain matrix $\mathbf{K}$, making this LMI non-convex in the variables $\mathbf{P}$, $\mathbf{K}$ and γ. It is therefore not possible to directly use semi-definite programming tools to simultaneously find the gain matrix $\mathbf{K}$, the minimum γ, and $\mathbf{P}$.

However, for a given gain matrix $\mathbf{K}$, semi-definite programming can be used to find $\mathbf{P}$ and minimise γ. Repeating this process over a grid of gains K_p and K_d yields a γ-surface. SDPSOL, a LMI matrix optimisation software package was used for this process [Wu and Boyd, 2000]. In this section, these values are termed linear H_∞ bounds, γ_{linear}.

Clinical H_∞ norms, γ_{clin}, can also be calculated for each patient from the non-linear simulation data generated using the agitation-sedation model of Chapter 7 and nurse control protocol.

$$\gamma_{clin} = \frac{\| A \|_2}{\| S \|_2} \tag{13.19}$$

These γ_{clin} values represent the best available assessment of current clinical practice. Non-linear simulations implementing the derivative-focused GF3 and GF6 control protocols enable the calculation of the H_∞ norms, γ_{GF3} and γ_{GF6}, for comparison with the clinical γ_{clin} values and the linear bounds. These H_∞ norms represent the non-linear equivalent of the linear H_∞ bounds, γ_{linear}.

The non-linear H_∞ norms, γ_{GF6}, can then be compared to the linear values γ_{linear}, obtained using the linear system to determine the impact of non-linearities. In addition, γ_{clin} can then be compared to non-linear results obtained using the H_∞ optimal control gains to determine whether these optimal control gains provide enhanced performance. Finally, the overall grid search of control gains enables the analysis of which gain balance (derivative-focused or propor-

tional focused) is optimal.

This last point is clinically relevant because derivative-focused methods lead to bolus-based delivery and proportional-focused methods lead to more continuous infusion oriented delivery. Hence, this analysis compares and contrasts these two approaches formally. It also provides a measure of analytical proof, given the optimal H_∞ approach chosen for this analytical exercise. In summary, five different H_∞ norms are calculated:

Clinical: γ_{clin} Based upon simulated results generated in Chapter 7.

GF3: γ_{GF3} Based upon simulated results generated using the direct derivative-focused GF3 control protocol representing the direct derivative-focused protocol with total dose similar to the nurse control protocol.

GF6: γ_{GF6} Based upon simulated results generated using the direct derivative-focused GF6 control protocol, representing an improved control protocol.

Linear: γ_{linear} Based upon H_∞ analysis using linear system.

Optimal: γ_{H_∞} Based upon simulated results generated using the H_∞ optimal control gains.

13.3 Results and Discussion

Lyapunov stability analyses show that the linear open-loop system is borderline-stable, and the closed-loop system is asymptotically stable for all values of the patient-specific parameters. These results are confirmed by checking the eigenvalues of the plant matrix **A**. The stability characteristics of the open and closed-loop systems are not unexpected. Inspection of the system described by Equations (7.1)–(7.5) and (13.2)–(13.3) reveals that the open-loop system is inherently borderline stable. Similarly, inspection of the closed-loop system matrix, $\mathbf{A_{cl}}$, reveals an inherently stable, or at least full rank, plant matrix. Note that the inclusion of the $-w_3 A$ EAR dynamic would make the open loop matrix, **A**, stable, as might be expected.

The effect of changing the control gains on the H_∞ norm is displayed in Table 13.1, where the normalised H_∞ bounds are presented in a grid of control gains K_p

and K_d. Note that the values are normalised to the average linear system γ from all patients using the gain values $\mathbf{K} = [0.0004 \quad 0.4]$, shown by the normalised γ value of unity. No value indicates instability in the linear model for at least 1 of the 37 patients. The thin lines in the diagram represent the boundary between regions of improved and degraded average H_∞ norm relative to the gain values $\mathbf{K} = [0.0004 \quad 0.4]$ of the linear system. Areas with values less than 1.0 are gains that might provide improved performance. Finally, note that proportional-weighted ($K_p \gg K_d$) or equal-weighted ($K_p \approx K_d$) gain combinations are in the unstable gain region. This last result might be expected given the results from Chapters 10–12 for constant infusions.

As the magnitude of the control gains increases, the linear system becomes increasingly less stable, where stability is defined as a bound output in response to a bound input. Table 13.1 shows the regions of instability by regions with no values, which clearly represent unsuitable choices for the control gains. This rapid progression toward instability is probably a result of the linear simplification, as previous simulations have shown that some of these regions remain stable in the non-linear model. If saturation dynamics are included, the agitation abating effect of the drugs at high concentrations is significantly reduced, lessening the tendency for instability, but still resulting in a higher γ value.

The development of the H_∞ design LMI in this paper is based upon the linear approximation of the non-linear system presented in Equations (7.1)–(7.6). To obtain a linear system, the non-linear response surface presented in Figure 3.3 is replaced by a linear response surface, defined in Equation (13.4), and shown in Figure 13.1. This linear approximation removes the saturation dynamics at higher doses. The lower results using the linear model, γ_{linear}, compared to results from the non-linear analysis, are therefore a result of these non-linear saturation dynamics.

The consequence of removing the effect saturation dynamic from the drug response surface is that the drugs become more effective at higher effect site concentrations, much like the initial results in Chapter 10. Therefore, by Equation (7.6), for a given stimulus profile, the agitation levels will be more greatly reduced in the linear model, resulting in lower H_∞ bounds. To compensate, the gains are increased by a factor of 3, yielding the GF3 protocol which is shown to provide similar agitation management to the nurse control protocol in Chapters 10–12.

Table 13.1 can be used to find an improved set of control gains over the GF6 protocol, shown to provide enhanced agitation management in Chapters 10–12. Using the information gained from the H_∞ based grid-search, an improved control gain matrix, $\mathbf{K} = [0.0005 \;\; 0.5]$, is obtained. These control gains in the linear model correspond to what is termed the GF7.5 protocol for the non-linear model.

The non-linear clinical H_∞ norms, γ_{clin}, non-linear H_∞ norms using the GF3 control protocol of Section 10.1, γ_{GF3}, non-linear H_∞ norms using the GF6 control protocol, γ_{GF6}, linear H_∞ bounds, γ_{linear}, and non-linear H_∞ norms using the optimal H_∞ control gain protocol GF7.5, determined via grid search, are presented for all 37 patients in Table 13.2. The γ_{clin} values have a mean value of 28.13, and the γ_{GF3} values have a mean value of 28.16. The γ_{linear} values have a mean value of 10.20, whereas the γ_{GF6} values have a mean value of 17.79, where the difference between γ_{GF6} and γ_{linear} is due to the impact of drug effect saturation limiting the effect of the drugs infused in the non-linear case, and the increase in gains. The result of implementing the H_∞ optimal control protocol, GF7.5, produced H_∞ values with a mean value of 15.34. Finally, these improvements are achieved at the expense of increased median drug dose of 34% and 47% for the GF6 gains and optimal H_∞ control gains respectively. These higher doses would lead to RTD values closer to 1.0 if the inputs were capped to avoid excessive saturation at the high end where the controller demands input.

Table 13.2 shows that the derivative-focused GF3 control protocol has an average γ_{GF3} across all patients of 28.26, compared to an average of 28.13 for the nurse control protocol. This result highlights the similar agitation management provided by the nurse control protocol and the GF3 protocol. In contrast, the mean γ_{GF6} across all patients is 17.79, showing that the simple derivative-focused GF6 control protocol is capable of reducing the transfer of stimulus to patient agitation. Implementing the optimal control protocol, GF7.5, resulted in a reduced average H_∞ of 15.34 using non-linear simulations, compared to 17.79 using the previous control gains. Hence, H_∞ analysis and control design yielded over 14% improvement over prior manual control design, and an over 45% improvement versus current clinical practice. Equally importantly, these results show that while specific differences between results from the linear and non-linear systems exist, general trends in the linear system are reflected in the non-linear system and provide useful information for gain selection.

The clinical H_∞ norms, γ_{clin}, are an indication of the non-linear transfer from stimulus to modelled agitation obtained clinically. The range of γ_{clin} from 15.54–38.16 is a direct result of the selected w_1 value used in the model. In both the linear and non-linear cases, the stimulus profiles used in these simulations range in magnitude from approximately 1-10 units, whereas the agitation levels typically range from 10-100 units. The benefit of γ_{clin} is that it provides a benchmark against which non-linear simulations of improved controllers may be evaluated. The wide range may also be indicative of the wide range of clinical practice and effectiveness using a coarse subjective agitation assessment scale, as well.

The region in Table 13.1 with values less than 1.0 indicates control gains that reduce the transfer from stimulus to patient agitation below that of the control gains developed by trial and error in Section 10.1. However, reducing patient agitation is not the sole aim of automated sedative infusion systems, as reduced levels of agitation may be simply achieved through the administration of excessive drug dose. The aim of an effective automated sedative infusion system is to minimise patient agitation using minimal drug dose. Therefore, control gain selection must be based not only on the direct impact on patient agitation, but also on the resulting control effort, or total dose, required to achieve reduced agitation levels.

Simple techniques, such as placing upper limits on the commanded infusion rate, were shown to reduce agitation levels in Section 11.2.2. However, if the methodology presented here were enhanced to minimise control effort, as well as patient agitation, then further insight into H_∞ control gain selection may be obtained. This goal can be achieved by changing the regulated output, z, to include effect site concentrations $\mathbf{C}_e^{a,s}$, which reflect control effort, by redefining the matrix $\hat{\mathbf{C}}_1$ in Equation (13.6).

13.3.1 Summary

This formal analysis approach using optimal control theory confirms the results of Chapters 10–12. In particular, this H_∞ analysis has provided optimal control gains corresponding to the lowest magnitude of the transfer function from any given stimulus to patient agitation. Although the linear assumptions of the analysis lead to discrepancies between the simulated non-linear results and the linear

theoretical results, the trends observed hold.

Importantly, the results of the H_∞ analysis show that the optimal control gains represent a derivative-focused agitation feedback controller and agree with the results of Chapters 10–12. A derivative-focused control protocol produces sedative infusion profiles with high infusion rates during increasing agitation, and low infusion rates during periods of low agitation. More importantly, this bolus-oriented approach to sedation is shown in Chapters 10–12 to provide considerable improvements in agitation management over current clinical methods.

Table 13.1 Normalised H_∞ bounds

K_p	0.000004	0.00004	0.0001	0.0002	0.0003	0.0004	0.0005	0.0006	0.0007	0.0008	0.0009	0.001	0.002	0.004
K_d														
0.000004	92.36	9.24	4.15	3.85	5.04									
0.00004	92.36	9.24	4.15	3.85	5.04									
0.0004	92.36	9.24	4.13	3.82	4.99									
0.004	92.36	9.24	4.03	3.62	4.56	88.03								
0.04	92.36	9.24	3.70	2.39	2.61	3.16	4.24	143.66						
0.1	92.36	9.24	3.70	1.85	1.58	1.75	2.02	2.40	58.58	3.92	6.41			
0.2	92.36	9.24	3.70	1.84	1.25	1.11	1.21	1.33	1.48	1.69	1.90	2.21		
0.3	92.36	9.24	3.70	1.84	1.25	1.01	0.98	1.05	1.13	1.22	1.32	1.45		
0.4	92.36	9.24	3.70	1.84	1.25	1.00	0.96	0.95	1.00	1.06	1.13	1.21	130.63	
0.5	92.36	9.24	3.70	1.84	1.25	1.00	0.92	0.93	0.96	1.00	1.07	1.11	65.44	
0.6	92.36	9.24	3.70	1.84	1.25	1.02	0.93	0.92	0.95	0.99	1.03	1.07	1.95	
0.7	92.36	9.24	3.70	1.84	1.26	1.03	0.95	0.94	0.96	1.00	1.03	1.07	1.78	
0.8	92.36	9.24	3.70	1.85	1.28	1.06	0.98	0.97	0.99	1.03	1.06	1.10	1.75	
0.9	92.36	9.24	3.70	1.86	1.30	1.10	1.03	1.01	1.04	1.07	1.11	1.14	1.77	
1	92.36	9.24	3.70	1.87	1.34	1.15	1.10	1.07	1.10	1.13	1.17	1.21	1.87	
1.2	92.36	9.24	3.70	1.94	1.44	1.28	1.24	73.12	1.28	1.32	1.36	1.41	2.75	
1.6	92.36	9.53	4.38	151.11	73.70	85.66								
2														

Table 13.2 H_∞ norms

	γ_{clin}	γ_{GF3}	γ_{linear}	γ_{GF6}	γ_{H_∞}
1	15.54	14.83	8.74	9.38	8.10
2	26.40	27.26	8.75	16.63	14.43
3	27.25	27.85	8.76	16.24	13.54
4	23.11	23.13	9.64	15.81	14.06
5	26.49	25.59	13.75	15.13	12.51
6	22.82	23.12	13.75	17.52	16.25
7	22.82	23.94	8.78	17.59	16.46
8	29.75	30.47	12.38	19.01	16.30
9	32.97	32.96	8.76	19.13	15.86
10	34.41	35.21	11.56	20.01	16.45
11	25.09	26.31	8.83	20.20	18.80
12	27.45	28.44	11.56	18.05	15.70
13	22.41	23.74	8.86	16.64	14.74
14	24.20	22.73	11.55	15.37	13.26
15	31.43	30.95	12.16	18.38	14.88
16	31.95	33.25	9.16	18.19	14.53
17	25.11	26.11	9.25	18.11	16.18
18	32.06	31.12	10.29	17.49	13.90
19	35.30	34.84	10.37	18.41	14.31
20	28.38	29.74	10.78	18.18	15.47
21	26.36	24.98	9.29	14.97	12.90
22	28.24	28.97	12.98	18.22	15.35
23	19.26	18.61	8.59	11.94	10.37
24	30.60	31.26	12.04	18.03	14.84
25	31.17	29.12	8.78	19.63	17.45
26	29.86	28.02	9.32	21.98	21.03
27	27.31	29.19	8.90	18.45	15.73
28	36.25	35.79	8.86	16.88	12.51
29	18.45	19.02	12.47	16.12	15.60
30	28.31	27.47	11.62	16.42	13.82
31	35.32	35.78	9.12	21.48	18.40
32	35.19	36.07	9.12	23.42	20.54
33	38.16	38.77	9.45	23.14	19.85
34	31.41	31.23	9.00	16.78	13.70
35	31.93	32.63	9.46	20.73	17.88
36	24.66	23.82	9.60	20.64	20.20
37	23.57	23.47	9.42	13.85	11.55
Mean	28.13	28.26	10.20	17.79	15.34

Chapter 14

Robustness Analysis

The intra- and inter-patient parameter variations observed in Section 8.2 have important implications for patients, medical staff, systems modelling, and control design. Parameter variability may be a marker of clinical outcome or of therapy, and knowledge of parameter variations over time and between patients can be used to improve patient care. From a modelling and control systems perspective, changes in parameters are an important consideration. If parameter changes between patients or over time are unaccounted for, the usefulness of the model is limited. More importantly, the clinical effectiveness of a given control protocol depends on its ability to manage agitation in the face of changing parameters.

The sedative infusion control protocols in Section 10.1 represent protocols that, upon clinical implementation in conjunction with quantitative agitation sensors [Lam et al., 2003; Lam, 2003; Starfinger et al., 2003; Starfinger, 2003; Shaw et al., 2003b; Chase et al., 2004a], could result in improved clinical agitation management. However, clinical implementation of such control protocols introduces many additional complicating factors that were not accounted for in the previous simulations. Two examples include noise in the feedback signal, and unpredictable, immeasurable changes in patient parameters over time. While many of these factors cannot be properly analysed in simulations and require clinical trials, some simple aspects of them may be analysed through simulations before clinical trials begin.

In particular, the robustness of a control protocol against the time-varying nature of patient parameters is of clinical importance. Specifically, prior to clinical implementation of a control protocol, the protocol's response to stochastic, immeasurable changes in patient parameters must be analysed. Control proto-

cols that become unstable or produce undesirable outcomes as a result of such variation in patient parameters may put patients and/or medical staff at risk. Preferably, control protocols should be robust against such changes in parameters, either continuing to function effectively, or at least remaining safe and stable.

This chapter employs statistical ARMA models to capture the parameter changes in the fitted sedative sensitivity profiles, $w_2(t)$, from Chapter 8 and uses these models to generate virtual sedative sensitivity profiles, $\tilde{w}_2(t)$. These virtual profiles are then used to evaluate the CappedGF6 protocol for robustness and sensitivity to realistic parameter variations in the extended physiologically-based model evaluated in Chapter 8. In particular, the robustness of the CappedGF6 control protocol against the stochastic, immeasurable time-variation of sedative sensitivity, $w_2(t)$, is compared to the robustness of current clinical practice, the nurse control protocol of Section 4.2.

14.1 Methods

14.1.1 Modelling Parameter Trends

The generation of virtual sedative sensitivity profiles, $\tilde{w}_2$, for each patient, requires a method of modelling the trends and patterns in the patient's fitted sedative sensitivity profile, $w_2(t)$. Since the values of $w_2(t)$ do not change independently from one time step to the next, $w_2(t)$ is a correlated time series, and an Auto Regressive Moving Average (ARMA) model is used.

An ARMA(p,q) model, in general, has the form:

$$\begin{aligned} x(k) &= a_1x(k-1) + a_2x(k-2) + ... + a_px(k-p) + \\ &\quad +z(k) + b_1z(k-1) + b_2z(k-2) + ... + b_qz(k-q) \end{aligned} \tag{14.1}$$

where $x(1), x(2), ...$ is the time series being modelled, $z(1), z(2), ...$ are random terms, $a_1, a_2, ..., a_p$ are the coefficients of the AR component of the model, $b_1, b_2, ..., b_q$ are the coefficients of the MA component of the model, and p and q are the AR and MA model orders, respectively.

For agitation-sedation models of the sedative sensitivity, $w_2(t)$, as an ARMA process, Equation (14.1) is written:

$$\begin{aligned} w_2(k) &= a_1 w_2(k-1) + a_2 w_2(k-2) + ... + a_p w_2(k-p) + \\ &\quad + z(k) + b_1 z(k-1) + b_2 z(k-2) + ... + b_q z(k-q) \end{aligned} \tag{14.2}$$

Equation (14.2) assumes that the random terms, z, take the form of a normally distributed, independent random variable with zero mean. For a complete description of the ARMA model representing the $w_2(t)$ profile for any given patient, the orders p and q must be selected and the coefficients $a_1, a_2, ..., a_p$ and $b_1, b_2, ..., b_q$ that best represent the stochastic time series $w_2(1), w_2(2), ..., w_2(n)$ from Chapter 8 determined.

MATLAB's System Identification Toolbox is designed for building accurate, simplified models of complex systems from noisy time-series data. It provides general tools for creating mathematical models of dynamic systems based on observed input/output data. The identification techniques provided with this toolbox are useful for applications ranging from control system design and signal processing to time-series analysis and vibration analysis. However, there are some tools required for the complete identification of ARMA models that are lacking from the standard System Identification Toolbox. The MATLAB ARMASel toolbox is specifically designed for ARMA analysis, and contains some tools for ARMA models not available in the standard MATLAB system identification toolbox. It is a program capable of generating a time-series model from a stationary stochastic signal with unknown characteristics [Broersen, 2002]. It is written by P. Broersen [2002], and is available on MATLAB Central in MATLAB's open file exchange platform [Mathworks, 2005]. Thus, the MATLAB system identification toolbox, and associated ARMASel toolbox, are used to find the ARMA model parameters which most closely model the observed sedative sensitivity profiles obtained via the fitting process developed in Chapter 8.

More specifically, the MATLAB toolbox is found to have excellent tools for creating ARMA models, but lacks a tool for the selection of the order to the AR and MA polynomials. ARMASel has useful tools for selecting the model orders, but its model estimation methods are not as robust as those found in MATLAB. The ARMASel toolbox is therefore used for order selection, and the System Identification Toolbox used to create the ARMA model by determining the coefficients

$a_1, a_2, ..., a_p$ and $b_1, b_2, ..., b_q$. The model is then checked by evaluating the auto-correlation of the residuals for various lags using the *RESID* command found in the System Identification Toolbox.

The automatic selection of AR and MA orders is based on statistical criteria, designed to select the order with the smallest expectation of the prediction error. The AR order, p, is selected using the Combined Information Criteria (CIC), which combines the asymptotic balance between under- and over-fit and the finite sample resistance against the selection of model orders that are too high [Broersen, 2000, 2002]. The MA order is selected using the generalised information criteria (GIC), obtaining a compromise between over-fit and under-fit [Broersen, 2000, 2002].

ARMASel selects model orders, p and q, given a stochastic input time series and an order difference, $d = p - q$. Therefore, to select the best combination of coefficient orders, an array of order differences $d = 1, 2, ..., l$ is tested and the orders resulting in models with minimum residual are selected. The MATLAB command *ARMAX* creates an ARMA model from an input data set and model orders p and q. *ARMAX* creates a full ARMA model including the coefficients $a_1, a_2, ..., a_p$ and $b_1, b_2, ..., b_q$, as well as the variance and noise structure. MATLAB's *ARMAX* function minimises a robustified quadratic prediction error criterion using an iterative search algorithm. A stability test of the predictor is performed to ensure that only models corresponding to stable predictors are tested [Ljung, 1999]. The System Identification toolbox also provides the model evaluation tool *RESID*, which can be used to check fit by testing whether the residuals are uncorrelated. However, this test provides necessary but not sufficient evidence for an appropriate model. Models failing the residual test are therefore rejected, while models passing the residual test are kept for further analysis.

The numerical output of *RESID* also provides a useful method for selecting a model from various models that have all passed the residual test. When deciding between two models that have passed the residual test, the model with lowest sum of absolute residuals is selected. Although this selection method does not necessarily guarantee the ideal model, it eliminates failed models and provides an objective selection criterion. All models are manually checked after this selection process, and their resulting outputs evaluated against the original input data set.

Therefore, the ARMA model creation process for each patient includes:

1. The patient's w_2 profile is passed to ARMASel to select the best orders p and q from an array of order differences $d = [0, 1, 2, ..., 10]$.
2. The selected combinations of p and q for each order difference are used to create an ARMA model using *ARMAX*.
3. Each p/q combination model is tested using *RESID*.
4. Models that fail the residual test are rejected, while models that pass are kept.
5. The sum of absolute values of the residuals is evaluated for each p/q combination model.
6. The p/q combination resulting in the lowest sum of absolute residual terms is selected.
7. The selected p and q orders are used with the *ARMAX* command to create the ARMA model.

This process is used to create an ARMA model for each patient in MATLAB. The resulting model structure contains the coefficients $a_1, a_2, ..., a_p$ and $b_1, b_2, ..., b_q$, as well as the variance and noise structure. The process is based on the hourly fitted $w_2(t)$ profile described in Chapter 8. For all patients the first 12 hours and the final 12 hours of the fitted w_2 profile is not used in the model estimation step due to the impact of boundary conditions on ARMA model estimation. In addition, some small portions of the $w_2(t)$ profiles of some patients are manually excluded to obtain an ARMA model that passes the residual test. The structure can then be used to generate a time-series based on this model for each patient.

14.1.2 Generating Virtual Patient Parameter Profiles

The ARMA model structures created using the process defined in Section 14.1.1 enable the generation of *'virtual'* sedative sensitivity profiles, $\tilde{w}_2(t)$, for each

patient. The process simply employs the equation defining the ARMA process:

$$\begin{aligned}\tilde{w}_2(k) &= a_1\tilde{w}_2(k-1) + a_2\tilde{w}_2(k-2) + ... + a_p\tilde{w}_2(k-p) + \\ &\quad +z(k) + b_1z(k-1) + b_2z(k-2) + ... + b_qz(k-q) \end{aligned} \tag{14.3}$$

where $\tilde{w}_2(1), \tilde{w}_2(2), ...$ is the generated stochastic time-series, $z(1), z(2), ...$ are the random terms, $a_1, a_2, ..., a_p$ are the AR coefficients, $b_1, b_2, ..., b_q$ are the MA coefficients, and p and q are the AR and MA model orders, respectively. The model coefficients are contained in the model structure generated using *ARMAX*, along with information about the nature of the random terms, $z(1), z(2), ...$, in particular, their standard deviation, σ.

The initial values of the series, $\tilde{w}_2(1), \tilde{w}_2(2), ..., \tilde{w}_2(p)$, are set to the average value of the fitted $w_2(12), w_2(13), ..., w_{36}(p)$ series which ensures that the $\tilde{w}_2$ profile is initialised, and enables the generation of a complete $\tilde{w}_2(t)$. Reflective boundaries are applied to the virtual parameter generator, set at the upper and lower limits of the fitted w_2 profile. These boundaries cause a reflection of the generated $\tilde{w}_2$ term if it approaches one of the limits, thereby ensuring that the virtual profiles generated remain in similar range to that of the fitted w_2.

14.1.3 Control Protocol Robustness Analysis

Section 14.1.2 outlines a procedure for generating patient-specific virtual sedative sensitivity profiles, $\tilde{w}_2(t)$, based on ARMA models developed from the fitted $w_2(t)$ profiles from Section 8.2.2. Therefore, while the changes observed in the patient-specific virtual sedative sensitivity profiles are physiologically realistic and characteristic of the original fitted $w_2(t)$ profiles, they are clearly stochastic and uncorrelated to the patient-specific recorded time-series data. Therefore, the stochastic changes in the virtual sedative sensitivity profiles represent potential changes in a patient's sedative sensitivity that may be observed clinically, but are immeasurable to a real-time controller.

These virtual profiles are therefore employed to assess the response of a control protocol to these unpredictable changes in $w_2(t)$ that are anticipated in clinical implementation. More specifically, no controller can accurately and consistently predict what change this parameter might take in the forthcoming time

frame. Hence, its ability to control agitation is reduced by this stochastic variation, which can also impact robustness. A similar problem arises with insulin control of glucose and insulin sensitivity [Chase et al., 2005b].

This chapter employs the virtual profiles in the physiologically-based agitation-sedation model described in Section 3.3. All parameters used in this chapter are identical to those employed in the evaluation of the physiologically-based model in Section 8.2, except that the fitted sedative sensitivity profiles, $w_2(t)$, are replaced by the virtual sedative sensitivity profiles, $\tilde{w}_2(t)$. Note that the virtual profiles are generated from the fitted $w_2(t)$ profiles, and are therefore smoothed using the 12-hour smoothing filter to create physiologically-realistic changes, as in Section 8.2.3. In addition, the initial 12 hours of the virtual profiles, $\tilde{w}_2(t)$, are replaced by the initial 12 hours of the fitted sedative sensitivity profile, $w_2(t)$, for the same initialisation reasons mentioned in Section 8.2.3.

Ten patients are randomly selected from the 37 patients in the study cohort. For each of these ten patients, 50 virtual $\tilde{w}_2(t)$ profiles are generated using the procedure in Section 14.1.2. A virtual trial is simulated using each of the 50 corresponding virtual sedative sensitivity profiles, yielding 50 simulation results per patient. Performance metrics, representing the effectiveness of the control protocol, are evaluated for each virtual trial and summary statistics of the performance metrics are then calculated for each patient. The performance metrics are defined:

TD Total Dose is defined as the total simulated dose of the proposed control protocol. TD is an important global performance metric because it is a general indication of drug usage, which has both financial and healthcare implications. In general, the use of excessive drugs leads to increased costs, and may be an indication of over-sedation. Therefore, from both a healthcare and financial perspective, a low TD is desirable.

PIR Peak Infusion Rate is defined as the maximum infusion rate of a proposed control protocol. PIR is a particularly important parameter in ICU sedation, as high infusion rates can be damaging to patient health and are associated with cardiopulmonary depression and other side-effects [Barr and Donner, 1995]. For this reason, a low PIR is desirable.

MA Mean Agitation is defined as the mean simulated agitation employing the

proposed control protocol. MA is one of the most important global performance metrics for both the patient and the medical staff. High average agitation levels can hinder the recovery process by preventing rest and healing. Periods of inflated average agitation levels are uncomfortable and dangerous for patients, and difficult and time-consuming for bedside medical staff. Therefore, for both patients and medical staff, a low MA is desirable.

PA Peak Agitation is defined as the maximum simulated agitation employing the proposed control protocol. PA is a local metric that represents the point in time at which the patient is most likely to attempt to remove their life-support systems (such as removing the ET tube), or resist staff. These actions are damaging to patient health and a concern for staff safety. Therefore, for both patients and medical staff, a low PA is desirable.

STDA Standard Deviation of Agitation is defined as the standard deviation of the agitation profile resulting from employing the proposed control protocol. This global metric is a general measure of the size of the oscillations in the resulting agitation profile. It is limited because it fails to recognise the agitation profile as a correlated time-series, and instead treats it as selection of independent values. However, STDA is an important metric, as large oscillations between sedation and agitation may be dangerous to patients' health.

The simulation process described above is followed for both the nurse control protocol incorporating the IIR filter, described in Section 4.2, and the CappedGF6 protocol described in Section 10.1. For both of these control protocols the same ten patients with the same 50 virtual profiles are used. This process yields summary performance metrics across the 50 virtual trials for each of the ten patients for both control protocols. Comparing the summary performance metrics resulting from use of the CappedGF6 protocol to those resulting from the nurse control protocol provides an indication of the performance ability of the CappedGF6 protocol.

14.2 Results and Discussion

The ten randomly selected patients used in this chapter are patients 1, 3, 8, 16, 19, 20, 21, 26, 30, 32. The results of three of the fifty virtual trial simulations, including the virtual $\tilde{w}_2(t)$ profiles, for Patient 3 are presented in Figures 14.1–14.3. The upper plot of these figures presents the sedative sensitivity profile, the middle plot presents the infusion rate, and the lower plot presents the agitation profile. In the upper plot, the lighter solid line represents the virtual sedative sensitivity profile, $\tilde{w}_2(t)$, and the darker solid line represents the smoothed sedative sensitivity profile identified in Section 8.2.3. In the middle and lower plots, the dashed lines represent the modelled responses of the CappedGF6 protocol in the virtual trial, the dotted lines represent the modelled responses of the nurse control protocol in the virtual trial, and the dark solid line represents the modelled responses of the nurse control protocol using the smoothed $w_2(t)$ profile from the model evaluation procedure in Section 8.2.3.

Note that the virtual sedative sensitivity profiles, $\tilde{w}_2(t)$, in the upper plots of Figures 14.1–14.3 have similar characteristics to the corresponding original smoothed sedative sensitivity, $w_2(t)$, from Section 8.2.3, yet are distinctly different. This difference results from the fact that ARMA models used to generate the virtual profiles are based on these original profiles, but are generated using a stochastic process. Note also in these figures that the initial 12 hours of both the smoothed and virtual profiles are identical.

In the middle plots of Figures 14.1–14.3 the difference between the bolus-oriented approach of the CappedGF6 protocol and the approach of the nurse control protocol should be noted. The CappedGF6 protocol employs a bolus-oriented approach, whereas the nurse control protocol delivers drug in a more uniform approach. This feature is also seen in the earlier results of Section 12.2.3.

Finally, note in the lower plots of Figures 14.1–14.3 the effect of the $\tilde{w}_2(t)$ on modelled agitation. Figure 14.2 highlights the result of a decrease in $\tilde{w}_2(t)$, and Figure 14.3 highlights the result of an increase in $\tilde{w}_2(t)$. A decrease in $\tilde{w}_2(t)$ corresponds to an unpredictable decrease in a patient's sedative sensitivity, which leads to decreased effect of the sedative drug. Decreased effect leads to increasing patient agitation, as seen in the lower plot of Figure 14.2. Conversely, an increase in $\tilde{w}_2(t)$ corresponds to an unpredictable increase in a patient's sedative sensitiv-

ity, which leads to lower patient agitation, as seen in Figure 14.3. The important aspect in these results is the way that the sedative infusion protocols deal with these changes in parameters, and hence agitation– i.e. controller robustness.

A summary of the performance metrics across all 50 virtual trials is shown in Table 14.1 for each of the ten patients. These values are the summary performance metrics of the CappedGF6 protocol relative to the summary performance metrics of the nurse control protocol. The values in Table 14.1 therefore provide a comparative indication of the performance of the CappedGF6 protocol compared to the nurse control protocol, under the same virtual conditions. A value greater than 1.00 indicates a higher value for the CappedGF6 control protocol than for the nurse control protocol, whereas a value less than 1.00 indicates a lower value for the CappedGF6 control protocol than for the nurse control protocol.

For example, the median value of TD=1.20 for Patient 1 indicates that the median total dose across all 50 virtual trials for the CappedGF6 protocol is 20% higher than the median total dose across all 50 virtual trials for the nurse control protocol. Similarly, the IQR of TD=0.89 for Patient 1 indicates that the inter-quartile range of total dose across all 50 virtual trials for the CappedGF6 protocol is 11% lower than the inter-quartile range of total dose across all 50 virtual trials for the nurse control protocol. Because the values in this table are those of the CappedGF6 protocol relative to the nurse control protocol, some apparently confusing numbers result. In particular, the fact that the maximum TD for Patient 1 is smaller than the minimum TD seems odd. However, this result can be understood by simply recognising that the values in Table 14.1 are relative. Thus, the maximum value of TD=1.20 for Patient 1 shows that maximum TD of the fifty virtual simulations for Patient one using the CappedGF6 protocol is 20% higher than the maximum TD of the fifty virtual simulations for Patient 1 using the nurse control protocol. Similarly, the minimum value of TD=1.28 for Patient 1 shows that minimum TD of the fifty virtual simulations for Patient 1 using the CappedGF6 protocol is 28% higher than the minimum TD of the fifty virtual simulations for Patient one using the nurse control protocol.

Table 14.1 shows that the performance of the CappedGF6 protocol, relative to the nurse control protocol, varies between patients. For example, for Patient 1, the median TD=1.20, whereas for Patient 3, the median TD=1.49 compared to the nurse control protocol. This result shows that the median performance of

the CappedGF6 protocol differs between patients. However, the overall summary statistics in Table 14.1 provide an indication of how much the median TD varies between patients. The median TD of the virtual trials has a median of 1.21 with an inter-quartile range of 0.09 across all ten patients. The median value of 1.21 indicates that, in response to stochastic time-variance in patient sedative sensitivity, the CappedGF6 protocol delivers a total dose 21% higher than the nurse control protocol, across all patients. The inter-quartile range of 0.09 indicates that this increased dose varies a small amount between patients.

Because a higher total dose is less desirable, this result implies that the CappedGF6 protocol performs worse than the nurse control protocol in regard to total dose, under the stochastic time-variance of sedative sensitivity. However, the results in Table 12.1 of Section 12.2.3 indicate that even under well-defined conditions, the Capped GF6 protocol delivers a total dose 21% higher than the nurse control protocol. Therefore, based on these results, the total increase in dose delivered by the CappedGF6 control protocol over the nurse control protocol is unaffected by the volatile, time-varying changes in sedative sensitivity that may encountered be in clinical applications.

Table 14.1 shows that the median PIR of the virtual trials has a median of 1.66 with an inter-quartile range of 0.49 across all ten patients. The median value of 1.66 indicates that, in response to stochastic changes over time in patient sedative sensitivity, the CappedGF6 protocol delivers peak infusion rates 66% higher than the nurse control protocol across all patients. However, the high IQR of 0.49 suggests that this comparative value varies considerably between patients. The high PIR indicates that the CappedGF6 protocol results in significantly higher peak infusion rates than the nurse control protocol under the time-varying conditions seen in clinical practice. Further, in contrast to the total dose, this value is also considerably higher than RPIR=1.0, obtained under well-defined conditions and presented in Table 12.1.

However, it must be remembered that the definition of the CappedGF6 protocols includes a maximum limit on the infusion rate equal to the maximum recorded dose. This leads to the RPIR in Table 12.1 of 1.0, and means that although the peak infusion rate for the CappedGF6 protocol is considerably higher than that of the nurse control protocol, the rates are still within conservative clinical safety limits. Therefore, although the PIR in Table 14.1 indicates that

the peak infusion rates of the CappedGF6 protocol are higher than the nurse control protocol, they are still within the conservative clinical safety limits, and are therefore acceptable.

The median MA of the virtual trials has a median of 0.54 with an inter-quartile range of 0.20 across all ten patients, as seen in Table 14.1. The median value of 0.54 indicates that, in response to stochastic changes in patient sedative sensitivity over time, the CappedGF6 protocol results in mean agitation levels 46% lower than the nurse control protocol across all patients. The inter-quartile range of 0.20 suggests that this comparative value varies between patients. Further, this value is similar to the mean agitation value of RMA=0.57 in Table 12.1, which is the result of simulations under well-defined conditions. Therefore, based on these results, the reduction in mean agitation achieved by the CappedGF6 control protocol over the nurse control protocol is only mildly affected by the stochastic time-variance in sedative sensitivity that may be encountered in clinical applications.

Note the negative minimum value that appears in the mean agitation column of the summary results for Patients 1 and 21 in Table 14.1. These negative values indicate that the CappedGF6 protocol, for at least one of the virtual sedative sensitivity profiles, reduced agitation below zero for a significant proportion of the total profile. This result has not yet been observed in simulations for a derivative-focused control protocol, even the CappedGF6 protocol, and is a direct result of the combination of a particular virtual sedative sensitivity profile, $\tilde{w}_2(t)$, and the CappedGF6 protocol. Figure 14.4 shows an example of one such profile for Patient 21. In this figure, the upper plot presents the sedative sensitivity profile, the middle plot presents the infusion rate, and the lower plot presents the agitation profile. In the upper plot, the lighter solid line represents the virtual sedative sensitivity profile, $\tilde{w}_2(t)$, and the darker solid line represents the smoothed sedative sensitivity profile from Section 8.2.3. In the middle and lower plots, the dashed lines represent the modelled responses of the CappedGF6 protocol in the virtual trial, the dotted lines represent the modelled responses of the nurse control protocol in the virtual trial, and the dark solid line represents the modelled responses of the nurse control protocol using the smoothed $w_2(t)$ profile from the evaluation procedure in Section 8.2.3.

Figure 14.4 shows that the small negative mean agitation value typically

results from two features:

1. A large initial bolus resulting in initially low agitation, that continues for a considerable proportion of the profile. This dynamic may also be accompanied by an initially high sedative sensitivity.

2. Continuously high w_2 values

The first feature, a large initial bolus accompanied by a high sedative sensitivity, is seen in the first portion of the upper plot of Figure 14.4. These features sometimes result in agitation levels below zero for a period at the beginning of a profile. For profiles with relatively short total time, this dynamic can have a significant impact on the mean agitation, and result in a negative mean agitation value. This feature, primarily due to initialisation, is not expected to present a problem in clinical implementation of the control protocol.

The second feature, continuously high w_2 values, can be seen for hours 15–34 in the upper plot of Figure 14.4. High w_2 corresponds to a high patient sensitivity to sedatives, and results in low patient agitation, as seen for hours 25–40 in the lower plot of Figure 14.4. Although the modelled agitation is below zero during hours 25–40, there are some points within this period where the CappedGF6 delivers drug. This drug delivery occurs because although the agitation level may be below zero, the rate of change may in fact be positive. If this positive rate of change of agitation, combined with the control gains employed, is greater than the negative component contributed by the absolute agitation level, then a positive infusion rate results, as per Equation (10.1). The delivery of sedative drugs during periods of negative agitation is an undesirable feature not only in the CappedGF6 protocol, but all the derivative-focused control protocols. A simple, yet effective, method of preventing this is to apply an additional rule to CappedGF6 requiring zero infusion when $A \leq 0$. This additional condition requires further investigation, and is briefly investigated in Chapter 15.

Peak agitation observed in the virtual trials, as seen in Table 14.1, has a median value of 0.73 with an inter-quartile range of 0.09 across all ten patients. This result shows that, in response to stochastic changes in sedative sensitivity, peak agitation is reduced using the CappedGF6 protocol compared to the nurse control protocol. In particular, the peak agitation resulting from the CappedGF6

protocol is reduced by a median value of 27% across all ten patients compared to the nurse control protocol. The inter-quartile range of 0.09 suggests that this reduction varies between patients. Again, this median value is similar to the peak infusion rate of 0.74, resulting from simulations under well-defined conditions presented in Table 12.1 Therefore, with regard to the peak infusion rate, the CappedGF6 control protocol is almost unaffected by the time-varying nature of sedative sensitivity encountered in clinical application.

The standard deviation of agitation is a limited measure of the size of the oscillations in the agitation profile. However, it does correlate with observed oscillations and fluctuations in the agitation profiles and is therefore an approximate measure of the cyclic nature of agitation-sedation dynamics. As seen in Table 14.1, the median STDA of the virtual trials has a value of 0.93 with an inter-quartile range of 0.12 across all ten patients. The median value of 0.93 indicates that the oscillations and fluctuations resulting from use of the CappedGF6 protocol are less than those resulting from use of the nurse control protocol in circumstances of stochastically varying sedative sensitivity. However, the relatively high IQR reduces the strength of this argument. Nonetheless, an important outcome of this result is that, based on these results, the CappedGF6 protocol does not induce increased oscillations or fluctuations in the agitation profile. This result has important clinical implications, as larger oscillations in agitation can be dangerous to patients' health.

14.3 Summary

The fundamental outcome of these virtual trial results points to the robustness of the CappedGF6 protocol, and its ability to provide tight control of agitation in spite of the unpredictable, immeasurable time-variation of sedative sensitivity encountered in clinical practice. The fact that the CappedGF6 protocol is still capable of improved reductions in mean and peak agitation over the nurse control protocol, in spite of the stochastic changes in sedative sensitivity, shows that the CappedGF6 protocol is robust to these changes. The results of this chapter show that in spite of the clinical time-variance of the sedative sensitivity, the CappedGF6 protocol achieves median reductions of 46% and 27% in mean and peak agitation, respectively. Further, these improvements in agitation per-

formance metrics are achieved without exceeding maximum infusion rate safety requirements, and at the relatively small cost of approximately 20% more total drug dose. These results highlight the robustness of the CappedGF6 to unpredictable changes in the sedative sensitivity parameter.

In addition to its robustness, the CappedGF6 protocol is shown to provide effective agitation management through a bolus-oriented approach. This approach employs short, sharp timely boluses during periods of agitation and reduces overuse of drugs through minimal delivery during periods of low agitation. This protocol therefore offers significant advantages for clinical agitation management, and has the potential to improve healthcare for critically ill patients.

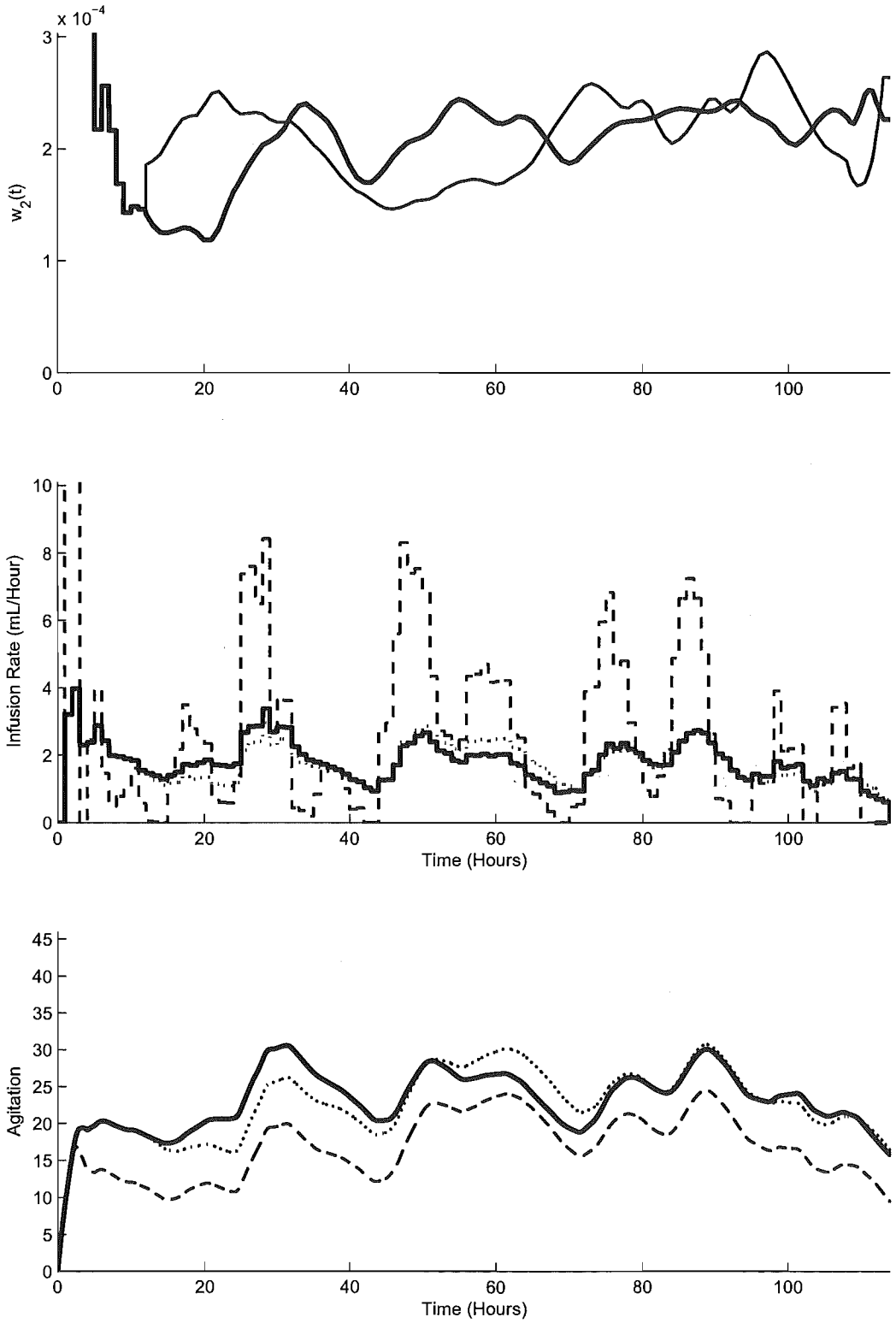

Figure 14.1 Results of one virtual trial for Patient 3

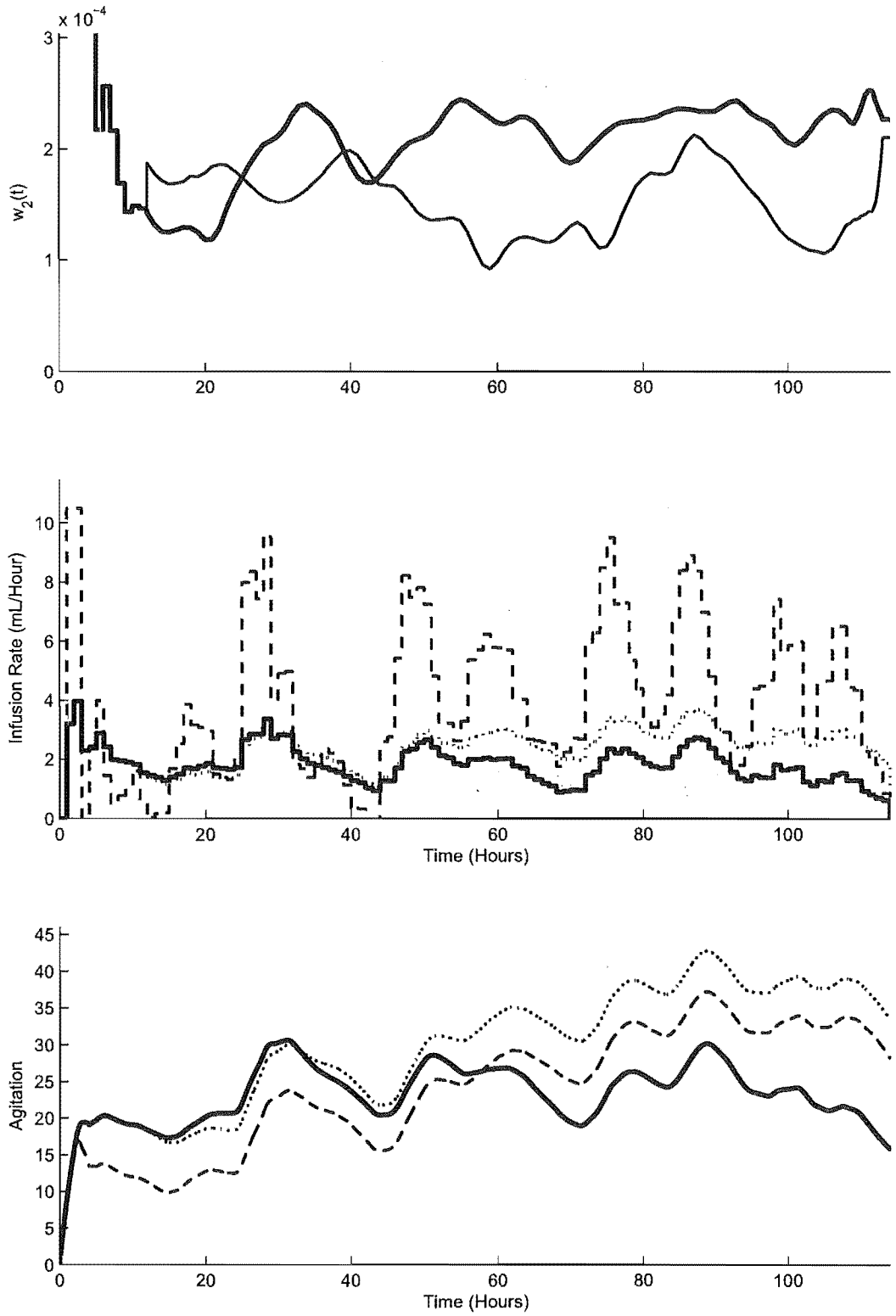

Figure 14.2 Results of one virtual trial for Patient 3 showing the effect of low overall sedative sensitivity

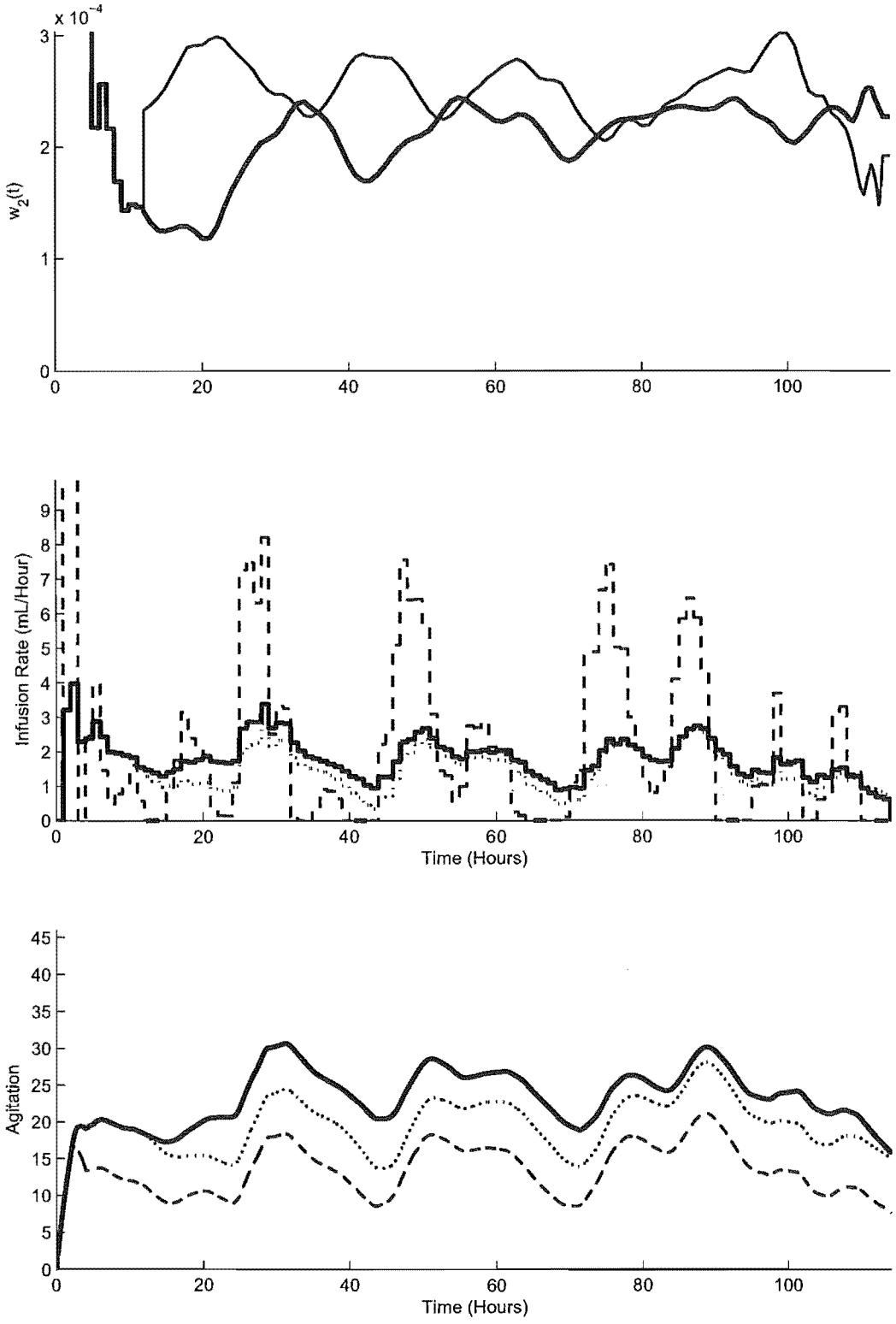

Figure 14.3 Results of one virtual trial for Patient 3 showing the effect of high overall sedative sensitivity

Table 14.1 Virtual trial summary statistics of the CappedGF6 control protocol, relative to the summary statistics of the nurse control protocol.

	TD	PIR	MA	PA	STDA	TD	PIR	MA	PA	STDA
			Patient 1					Patient 20		
Max	1.20	1.50	0.16	0.74	1.09	1.45	1.61	0.73	0.84	0.95
UQ	1.18	1.63	0.10	0.73	1.16	1.36	1.73	0.65	0.77	0.95
Med	1.20	1.71	0.05	0.73	1.17	1.35	1.99	0.61	0.75	0.95
LQ	1.23	1.92	0.00	0.73	1.20	1.30	2.17	0.52	0.70	0.82
Min	1.28	2.28	-0.12	0.60	1.24	1.27	2.28	0.40	0.68	0.70
IQR	0.89	0.00	1.01	0.78	0.95	1.55	0.00	1.08	1.00	1.15
			Patient 3					Patient 21		
Max	1.66	2.52	0.83	0.89	1.01	1.13	1.68	0.37	0.57	0.94
UQ	1.52	2.64	0.77	0.83	0.99	1.07	1.82	0.29	0.43	0.86
Med	1.49	2.64	0.76	0.82	0.96	1.05	1.86	0.25	0.39	0.86
LQ	1.45	2.64	0.73	0.80	0.93	1.08	1.99	0.15	0.36	0.81
Min	1.41	2.64	0.69	0.76	0.92	1.06	2.14	-0.03	0.28	0.72
IQR	1.92	0.00	0.97	0.97	1.12	1.01	0.00	1.05	1.51	1.13
			Patient 8					Patient 26		
Max	1.22	0.97	0.62	0.81	0.93	1.26	1.40	0.68	0.75	0.82
UQ	1.19	1.07	0.57	0.78	0.94	1.22	1.45	0.62	0.68	0.80
Med	1.18	1.17	0.53	0.77	0.92	1.22	1.48	0.59	0.66	0.80
LQ	1.17	1.24	0.50	0.75	0.89	1.20	1.49	0.55	0.66	0.76
Min	1.16	1.50	0.38	0.65	0.72	1.17	1.49	0.51	0.63	0.69
IQR	1.37	0.00	1.28	0.90	1.10	1.29	0.00	0.95	0.93	1.12
			Patient 16					Patient 30		
Max	1.31	1.06	0.70	0.85	1.01	1.27	1.57	0.48	0.72	1.02
UQ	1.27	1.29	0.64	0.78	0.98	1.19	1.84	0.42	0.68	1.05
Med	1.24	1.42	0.57	0.74	0.93	1.19	2.02	0.38	0.65	1.04
LQ	1.21	1.58	0.51	0.70	0.88	1.20	2.23	0.31	0.59	1.02
Min	1.19	1.68	0.43	0.67	0.81	1.18	2.91	0.23	0.56	1.07
IQR	1.60	0.00	1.40	1.14	1.44	1.15	0.00	0.88	1.08	1.14
			Patient 19					Patient 32		
Max	1.33	1.25	0.70	0.81	0.90	1.16	1.06	0.59	0.80	0.90
UQ	1.31	1.44	0.66	0.77	0.86	1.12	1.26	0.52	0.70	0.83
Med	1.29	1.60	0.64	0.73	0.82	1.11	1.39	0.48	0.66	0.79
LQ	1.27	1.67	0.63	0.70	0.80	1.10	1.53	0.43	0.61	0.79
Min	1.22	1.80	0.57	0.68	0.73	1.07	2.13	0.30	0.47	0.69
IQR	1.68	0.00	1.02	1.14	1.13	1.36	0.00	1.22	1.16	1.01

Summary Statistics

	TD		PIR		MA		PA		STDA	
	Med	IQR	Med	IQR	Med	IQR	Med	IQR	Med	IQR
Max	1.26	0.12	1.45	0.49	0.65	0.19	0.80	0.09	0.94	0.10
UQ	1.20	0.12	1.54	0.47	0.60	0.20	0.75	0.09	0.94	0.13
Med	1.21	0.09	1.66	0.49	0.54	0.20	0.73	0.09	0.93	0.12
LQ	1.20	0.08	1.80	0.59	0.50	0.20	0.70	0.10	0.85	0.12
Min	1.18	0.09	2.13	0.57	0.39	0.24	0.64	0.10	0.73	0.19
IQR	1.37	0.41	0.00	0.00	1.03	0.20	1.04	0.20	1.13	0.04

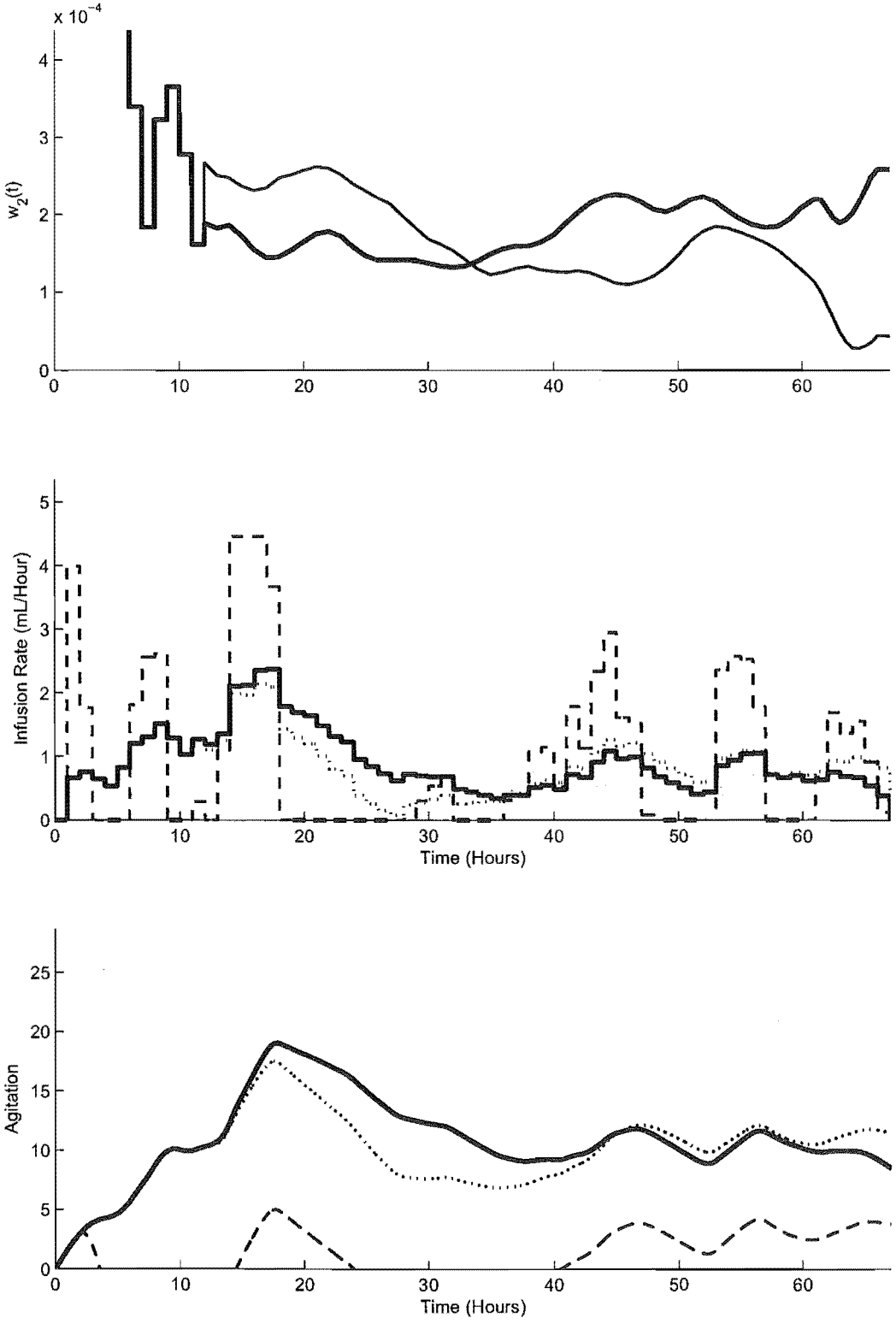

Figure 14.4 Results of one virtual trial for Patient 21 showing the features contributing to negative mean agitation values.

Chapter 15

Non-linear Control Protocols

Chapters 9–13 assessed the performance of several derivative-focused and constant infusion-based agitation feedback control and sedation management protocols. In particular, Chapters 9–12 assessed the performance of these direct controllers through simulations, and Chapter 13 employed a more formal theoretical analysis, confirming the results of the earlier chapters. All of these control protocols are linear, in which the feedback quantities, agitation and its derivative, appear linearly in the agitation feedback law of Equation 10.1, or not at all for a constant infusion protocol. This chapter goes a step further to analyse the impact of non-linear control protocols on agitation-sedation management using the extended physiologically-based model employed in Chapters 8 and 12.

15.1 Methods

This chapter employs an identical method to that of Section 12.1 to analyse five non-linear control protocols. The extended physiologically-based model is used, incorporating the EAR dynamic, smoothed time-varying sedative sensitivity profile, $w_2(t)$, and patient-specific C_{50} selection. The performance metrics of Section 9.3 are once again used as a measure of the ability of the non-linear control protocols to meet the goals outlined in Sections 9.1–9.2.

The non-linear feedback control laws investigated are all of the form:

$$U = K_p A + K_d \dot{A} + \widetilde{K}_p A \times abs(A^{\pi}) + \widetilde{K}_d \dot{A} \times abs(\dot{A}^{\delta}) \qquad (15.1)$$

where K_p and K_d are the proportional and derivative gains respectively, π and

δ are the powers of agitation and rate of change of agitation terms, respectively, $\widetilde{K}_p$ and $\widetilde{K}_d$ are gains of the non-linear terms, and $abs(\cdot)$ indicates the absolute value. The gain values, K_p and K_d, employed in this chapter are those of the GF6 protocol in Chapters 9–12. The use of the $abs(\cdot)$ in Equation (15.1) preserves the sign of the original feedback quantity in the overall non-linear terms. Three limits are placed on the non-linear protocols investigated in this chapter:

Maximum Infusion Rate The infusion rate is capped to a maximum limit of twice the maximum recorded infusion rate. This maximum infusion limit is set twice as high as the previous value to investigate the effects of higher peak infusion rates. Although this increased maximum infusion limit may have a negative impact on some patients, it is not expected to have negative effects on most patients, because the recorded infusion rate is typically a somewhat conservative, clinical indication [Shaw et al., 2003a].

Minimum Infusion Rate Negative infusion rates are not allowed. This limit results from the discussion in Section 9.1 regarding the difficulty of removing drug from a patient once delivered.

Zero Infusion Condition The infusion rate is set to zero if modelled agitation becomes negative. This condition explicitly prevents the delivery of drugs during periods of clearly low agitation, preventing the unnecessary delivery, and subsequent over-use, of sedative drugs.

The specific control protocols investigated in this chapter are not selected for completeness or optimality but to sample the possibilities for analysis. The specific control laws are defined:

GF6A^2 This protocol employs parameter values: $\widetilde{K}_p$=K_p, $\pi = 1$, $\widetilde{K}_d = 0$ and $\delta = 0$.

$$U = K_p A + K_d \dot{A} + K_p A \times abs(A^1) \tag{15.2}$$

This protocol investigates the impact of the additional non-linear agitation term, A^2, on agitation management. This term increases the continuous proportional control of sedation through a component of the infusion rate that increases with the square of agitation.

GF6$\dot{A}^2$ This protocol employs parameter values: $\widetilde{K}_p$=0, $\pi = 0$, $\widetilde{K}_d = 1000K_d$ and $\delta = 1$.

$$U = K_pA + K_d\dot{A} + 1000K_d\dot{A} \times abs(\dot{A}^1) \tag{15.3}$$

This protocol investigates the impact of the additional non-linear agitation derivative term, $\dot{A}^2$, on agitation management. This term significantly enhances the derivative focus of the protocol through a component of the infusion rate that increases with the square of agitation derivative, where the last term ensures it has the proper sign.

GF6$A^2\dot{A}^2$ This protocol employs parameter values: $\widetilde{K}_p$=K_p, $\pi = 1$, $\widetilde{K}_d = 1000K_d$ and $\delta = 1$.

$$U = K_pA + K_d\dot{A} + K_pA \times abs(A^1) + 1000K_d\dot{A} \times abs(\dot{A}^1) \tag{15.4}$$

This protocol is a combination of the previous two protocols, and investigates their combined impact.

GF6A^3 This protocol employs parameter values: $\widetilde{K}_p$=K_p, $\pi = 2$, $\widetilde{K}_d = 0$ and $\delta = 0$.

$$U = K_pA + K_d\dot{A} + K_pA \times abs(A^2) \tag{15.5}$$

This protocol investigates the impact of increasing the power of the non-linear agitation term, yielding the term A^3, significantly increasing the continuous proportional feedback of sedation.

GF6$A^3\dot{A}^2$ This protocol employs parameter values: $\widetilde{K}_p$=K_p, $\pi = 2$, $\widetilde{K}_d = 1000K_d$ and $\delta = 1$.

$$U = K_pA + K_d\dot{A} + K_pA \times abs(A^2) + 1000K_d\dot{A} \times abs(\dot{A}^1) \tag{15.6}$$

This protocol is a combination of the GF6A^3 and GF6$\dot{A}^2$ protocols, and investigates their combined impact.

Overall, these five control laws seek to examine non-linear enhancements that would enable more rapid automated, or semi-automated, response to patient agitation. In essence, they seek to add non-linearity to enhance the results seen with derivative-focused methods.

15.2 Results and Discussion

Figures 15.1–15.2 present the results of the non-linear control protocols with infusion limits for a typical patient using the extended physiologically-based model. Figure 15.1 presents the results for protocols GF6A^2, GF6$\dot{A}^2$, and GF6$A^2\dot{A}^2$. The first three plots show the infusion profiles, and the lower plot shows the resulting agitation profiles. In these plots the GF6A^2 protocol is represented by the lighter solid line, the GF6$\dot{A}^2$ protocol is represented by the dashed line, the GF6$A^2\dot{A}^2$ protocol is represented by the dotted line, and the nurse control protocol is represented by the darker solid line as a benchmark for comparison. Similarly, Figure 15.2 presents the results for protocols GF6A^2, GF6A^3, and GF6$A^3\dot{A}^2$. The first three plots show the infusion profile, and the lower plot shows the resulting agitation profiles. In these plots the GF6A^2 protocol is represented by the lighter solid line, the GF6A^3 protocol is represented by the dashed line, the GF6$A^3\dot{A}^2$ protocol is represented by the dotted line, and the nurse control protocol is represented by the darker solid line as a benchmark for comparison.

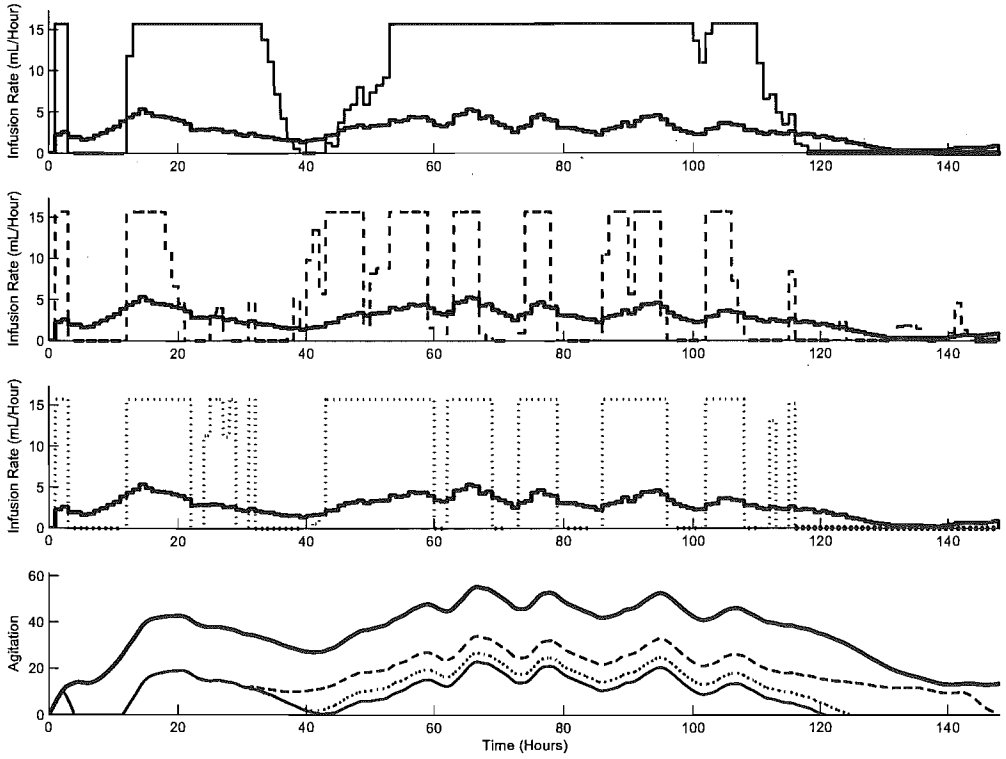

Figure 15.1 Example of the impact of non-linear control protocols GF6A^2 (top), GF6$\dot{A}^2$ (middle), and GF6$A^2\dot{A}^2$ (bottom) on agitation (lower plot).

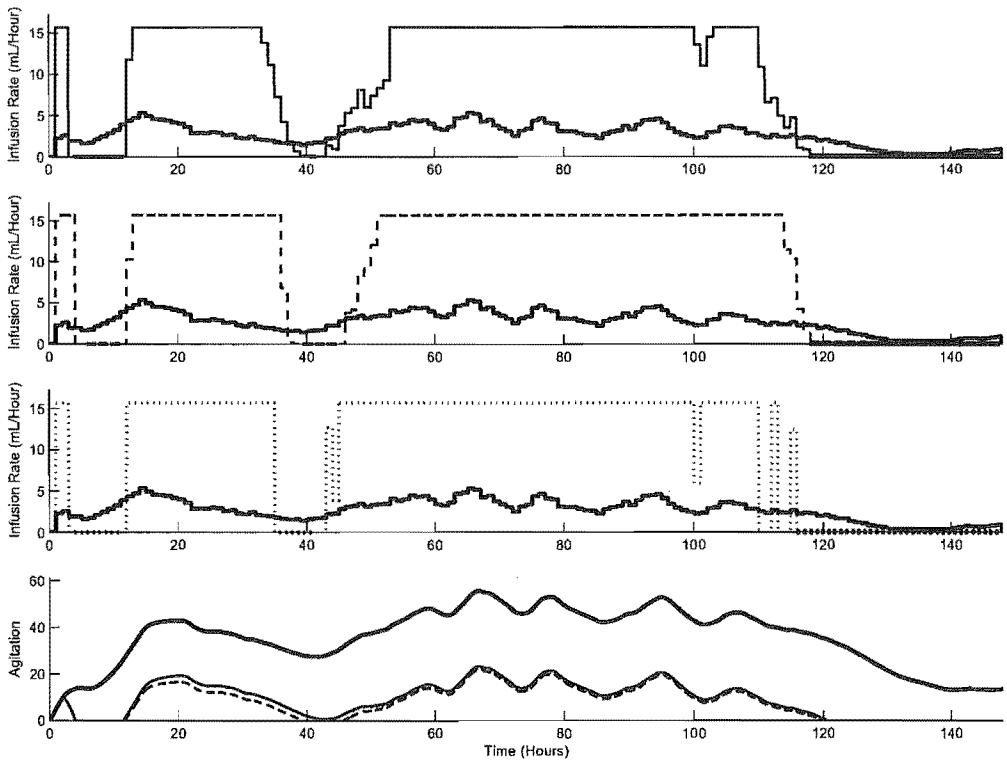

Figure 15.2 Example of the impact of non-linear control protocols GF6A^2 (top), GF6$\dot{A}^3$ (middle), and GF6$A^3\dot{A}^2$ (bottom) on agitation (lower plot)

The GF6A^2 protocol produces an infusion profile with very high infusion rates during periods of high agitation, and very low infusion rates in periods of low agitation, as seen in the top plot of Figure 15.1, as expected. In many cases, this protocol is capped by the maximum infusion limit, and remains at the maximum infusion rate for long periods. The lighter solid line in the bottom plot of the same figure shows that this approach to sedation management reduces agitation considerably. The effect of the Zero Infusion Condition is seen after t =120 hours in these plots. However, in spite of zero infusion rate during this period, the agitation drops and continues to fall below zero. This is not the result of current sedative infusion, rather the effect of significant drug doses in the previous hours arriving at the effect site as the patient was effectively over-loaded and over-sedated. These results occur despite an infusion profile that looks qualitatively like a sedation-interruption algorithm was applied.

In contrast, the GF6$\dot{A}^2$ protocol yields a strong bolus-oriented approach to sedation, as seen in the second plot of Figure 15.1. However, in contrast to the

earlier results of the linear derivative-focused protocols, this non-linear protocol has such a strong derivative focus that the infusion profile begins to look like that of a 'bang-bang' controller. This approach tends to employ a '*completely on or completely off*' approach, by delivering either the maximum infusion rate, or none at all. The dashed line in the bottom plot shows that while the GF6$\dot{A}^2$ protocol does not reduce agitation as low as the GF6A^2 protocol, it certainly provides considerably improved agitation management over current clinical practice represented by the nurse control protocol. An advantage of the GF6$\dot{A}^2$ protocol is the fact that it does not deliver excessive drugs resulting in agitation below zero, as observed in the GF6A^2 results.

The infusion protocol that combines these two approaches, GF6$A^2\dot{A}^2$, results in an infusion profile with features from each of its constituent protocols. In particular, the profile in the third plot of Figure 15.1 again shows a heavy bolus-oriented approach, but with more extended periods at maximum infusion rate. This profile looks even more like the output of a 'bang-bang' controller, and is almost always either at maximum or zero infusion. This protocol reduced agitation to levels between that of the two previous protocols, but closer to that of the GF6A^2 protocol. Once again, the previously high infusion rates near the end of the profile cause agitation to fall below zero in spite of the Zero Infusion Condition.

Although these first three protocols (GF6A^2, GF6$\dot{A}^2$, and GF6$A^2\dot{A}^2$) are seen to produce considerably reduced agitation, it is clear that the dose they employ to achieve that benefit is also considerable. Table 15.1, located at the end of this chapter, presents the summary statistics of the performance metrics across all 37 patients for the 5 control protocols analysed in this chapter. Note that imposing the upper limit on the infusion rate results in a maximum RPIR=2.0 by definition. The GF6A^2 protocol results in median reductions of over 80% and 45% in mean and peak agitation, respectively, while the GF6$\dot{A}^2$ protocol results reductions of 75% and 43%. The combined protocol, GF6$A^2\dot{A}^2$, results in median reductions in mean and peak agitation of 87% and 48%, respectively. These improvements over current clinical practice are of great potential benefit, but come at the cost of increased dose.

Although the infusion rates are capped, the total dose for these non-linear protocols is much larger than those of the linear protocols earlier investigated.

In particular, the median RTD for the GF6A^2 protocol is 3.48, with a maximum RTD of 8.09. Although the median RTD values for the GF6$\dot{A}^2$ (1.96) and GF6$A^2\dot{A}^2$ (2.54) protocols are lower, they all represent a considerable increase in the dosage and cost of reduced agitation.

Figure 15.2 shows the impact of increasing the exponent of the non-linear agitation term from two to three. Comparing the top three infusion profile plots, it is seen that, for this patient, while there are some differences between them, they are all similar and dominated by large infusion rates capped by the maximum limit. More importantly, the bottom plot of this figure shows that, for this patient, these changes result in minimal reductions of agitation. However, the median RMA values for these protocols in Table 15.1 indicate that across all patients there is a significant reduction in mean agitation (97%) for the further increase in total drug (up to 284%).

15.2.1 Summary

These results have briefly explored the impact on non-linear control protocols on agitation management. The results indicate that non-linear control offers potential benefits to agitation management in the form of reduced mean agitation levels, but at the expense of considerable increases in total drug dose. Once again, these results show a trade-off between cost and benefit. Importantly, the results of this chapter highlight the relatively small improvement in benefits versus the linear control protocols for increased cost and complexity of the non-linear control protocols. Hence, they further emphasise the considerable benefits of the simple linear derivative-focused control protocols presented in Chapters 9–13.

Table 15.1 Performance metrics for all non-linear protocols using the extended physiologically-based model.

	RTD	RPIR	RMA	RPA
GF6A^2				
Max	8.09	2.00	0.45	0.82
UQ	4.26	2.00	0.31	0.62
Med	3.48	2.00	0.19	0.54
LQ	2.58	2.00	0.02	0.47
Min	1.60	2.00	-0.68	0.39
IQR	1.68	0.00	0.29	0.15
GF6$\dot{A}^2$				
Max	3.26	2.00	0.63	0.82
UQ	2.25	2.00	0.42	0.63
Med	1.96	2.00	0.25	0.57
LQ	1.61	2.00	-0.20	0.53
Min	0.71	2.00	-1.39	0.09
IQR	0.64	0.00	0.62	0.11
GF6$A^2\dot{A}^2$				
Max	6.12	2.00	0.46	0.82
UQ	3.21	2.00	0.32	0.59
Med	2.54	2.00	0.13	0.52
LQ	2.04	2.00	-0.20	0.50
Min	0.71	2.00	-1.41	0.09
IQR	1.17	0.00	0.52	0.10
GF6A^3				
Max	10.65	2.00	0.44	0.82
UQ	4.60	2.00	0.23	0.61
Med	3.84	2.00	0.03	0.54
LQ	2.97	2.00	-0.23	0.45
Min	1.27	2.00	-1.44	0.13
IQR	1.63	0.00	0.47	0.17
GF6$A^3\dot{A}^2$				
Max	10.01	2.00	0.44	0.82
UQ	4.25	2.00	0.25	0.61
Med	3.62	2.00	0.03	0.52
LQ	2.44	2.00	-0.27	0.46
Min	0.83	2.00	-1.40	0.09
IQR	1.81	0.00	0.53	0.15

Part IV

Conclusions and Future Work

Chapter 16

Conclusions

Agitation management via effective sedation management is an important and fundamental activity in the ICU. However, in clinical practice a lack of understanding of the underlying dynamics, combined with subjective assessment tools, makes effective and consistent clinical agitation management difficult. Quantitative models and control protocol studies developed in this research provide the ability to gain insight into the underlying dynamics of the physiological system, and enable the development and evaluation of improved control strategies. Further, these models and control studies, coupled with emerging quantified agitation sensors, are a first step toward enabling the development of semi-automated sedative delivery methods for improved agitation management.

The primary goal of ICU sedation is to control agitation, while preventing over-sedation and over-use of drugs. Current clinical practice employs subjective agitation/sedation assessment scales, combined with medical staff experience and intuition, to deliver appropriate sedation. This approach typically leads to largely continuous infusions that lack a bolus-focused approach, and commonly result in either over-sedation, or insufficient sedation and agitation.

This thesis has developed quantitative models of the observed agitation-sedation dynamics using compartmental PK and PD response surface modelling. The initial model creates a good platform for adding additional physiological dynamics and assessing the effect of no saturation limit. The physiologically-based model incorporates more advanced dynamics, such as separate compartmental modelling, effect saturation, drug effect synergism, and endogenous agitation reduction. These models are fundamentally based on observed dynamics and physiology, and are subsequently evaluated against recorded infusion data.

A fundamental conclusion of this thesis is that the essential dynamics of the agitation-sedation system are linear. This conclusion can be seen by the ability of the initial model to capture the fundamental dynamics of the system, and highlights that linear systems of differential equations are adequate representations of the basic dynamics. While the addition of saturation, and other more complex non-linear dynamics, adds significant improvements they do not alter the fact that the underlying dynamics of the agitation-sedation system are linear in nature.

The models developed are employed as platforms for developing and evaluating several sedative control protocols for managing patient agitation. In particular, constant infusion rates, direct derivative-focused agitation feedback control protocols, and non-linear feedback protocols are investigated. Significant improvements over the current clinical practices are achieved through the use of very simple control protocols, indicating the potential for more automated approaches to sedation management.

Constant infusion protocols are shown to provide poor agitation management across a range of ICU patients, because they fail to deliver sedation based on the current patient requirements. While the constant infusion protocol can be effective for some patients if the correct rate is selected, in general it results in poor performance and often results in over-sedation or insufficient sedation. More importantly, the correct infusion rate is difficult to select a priori, may change over time during a patients stay, and the consequences of an incorrect selection are potentially severe.

The derivative-focused protocols represent simple approaches to agitation management, and are shown to be effective at reducing both mean and peak agitation, at the expense of increased total dose and peak infusion rate. Imposing simple upper limits on the infusion rates of these protocols eliminates peak infusion rates, and helps prevent over-sedation. These protocols produce a bolus-oriented approach to sedation that responds rapidly to increasing agitation with bolus drug delivery, and minimises over-sedation through minimal drug delivery during periods of low agitation. In particular, one protocol is shown to achieve median reductions of up to 63% and 28% for mean and peak agitation, respectively. More importantly these benefits are achieved without exceeding conservative safety infusion limits, and at the expense of only 21% more total drug dose.

Furthermore, this protocol is shown to be robust against unpredictable changes in patient parameters, which makes it suitable for clinical implementation.

The physiological saturation effect observed in sedative drugs, and incorporated in the physiological model, restricts the capacity of sedative controllers to reduce agitation. A clinical implication of this feature is that it is not always possible to achieve a specific target level of agitation. It also means that in some cases more sedation will not be the solution for patient agitation. Hence, the ability to identify these situations using model estimation would alert clinical staff to consider other treatment options.

A fundamental result is that agitation management represents a trade-off between the benefits of low patient agitation versus the cost of higher infusion rates and increased total dose requirements. However, in contrast to the 'stiff' nature of many engineering systems in which value can often be measured in dollars, the 'soft' nature of biological systems precludes a formal cost/benefit analysis. As a result of the trade-off identified, this thesis suggests that the aim of a good protocol is to minimise patient agitation and over-sedation, seeking an optimal clinical balance. This clinical balance is, however, not a direct function of strict linear or non-linear cost per unit agitation controlled. Instead, it is trade-off in which the bounds are less rigorously defined and where smaller relative variations, for example in total drug dose, may have no effective cost compared to the improved agitation management achieved. The derivative-focused, bolus-based sedation approach is shown to be highly effective in achieving good clinical balance, and via H_∞ analysis, is essentially optimal. Thus, more complex controllers may not be necessary, in the context of the models developed, to achieve good clinical outcomes.

Overall, the research presented shows that it is possible to create and evaluate models of the agitation-sedation system and use them to develop and evaluate control protocols for improved agitation management. This thesis shows that a bolus-oriented approach works best, which matches anecdotal longer term experience. However, for a given dose of drug, agitation management is highly variable, and is dependant on the delivery strategy employed. This thesis clearly shows significant evidence to support the idea that it is not the drug class or drug dose that is important, but rather the drug administration strategy employed is the most important factor in agitation management.

Chapter 17

Future Work

The models presented in this thesis represent the beginning of quantitative modelling of agitation-sedation dynamics. While they incorporate many of the fundamental dynamics observed in critically ill patients, there remain many aspects that would benefit from additional research. Similarly, the simple control protocols investigated in this thesis are only a small portion of the potentially applicable control protocols. This chapter presents areas of research which would benefit from future work.

17.1 Model Development

17.1.1 Drug Storage Dynamic

The effect of adding a separate compartment representing the accumulation of drug in fatty tissue may enhance the clinically observed over-sedation effect. This effect is partially seen in Section 3.3 for the added PK compartments in the drug kinetics. An additional compartment would increase the number of differential equations and parameters, but may have an important impact on the resulting pharmacokinetics. In particular, slow transfer rates to and from the storage compartment may model the storage, and delayed release, of drugs.

17.1.2 Stimulus Profiles

Fechner contributed to the field of psychology through developing a quantitative relationship between a stimulus, such as source of light, or temperature, and the sensation a person feels [Mackay, 1963]. Perhaps, with additional experiments, a more robust form of stimulus profile can be obtained for use in the model. Another option that may be worth investigating is the generation of surrogate stimulus profiles from emerging agitation sensor recordings from patients.

17.1.3 Michaelis-Menton Dynamic

The incorporation of the Michaelis-Menton dynamic is limited by the lack of published data from which parameters can be identified. Physiological estimates of the maximum physiological clearance rates would assist in determining the appropriate parameters. The Michaelis-Menton dynamics could then be added to the model, and the impact on drug accumulation and over-sedation analysed.

17.1.4 Metabolite Compartments

Although the pharmacological activity of many of the metabolites of Morphine and Midazolam is not yet fully quantified, there may be some benefit in investigating the impact of including metabolites into the agitation-sedation model. This analysis would include the addition of compartments for the concentrations of the various metabolites, and additional effect compartments representing the pharmacodynamic activity of the metabolites. Incorporating the PD effect of the metabolites would require the creation of a PD response surface that is a function of more than two drugs.

However, the complexity of the model would be greatly increased by the addition of metabolites, as will the number of parameters. This increased complexity and additional parameters, may not provide significantly improved results. Therefore, a preliminary study to determine the impact of the inclusion of metabolites is suggested. If there is enough improvement from the increased complexity, then these aspects should be retained. However, if the benefit is small, then not including the effect of metabolites may represent an adequate model.

17.2 Model Applications, Clinical Trials, and Evaluation

This research has proceeded with retrospective data and without the aid of quantitative agitation sensors. With ethical consent, clinical trials and experiments would further validate the models developed in this thesis, and further enhance control protocols. In particular, as quantitative agitation sensors become available, clinical trials become more feasible and should be undertaken.

17.2.1 Agitation Verification

The emergence of quantified agitation sensors enable direct verification of the agitation-sedation models developed in this thesis. Although agitation sensors are not yet commercially available, they may already provide some indication of agitation, which can be correlated to modelled agitation retrospectively. Agitation verification trials would further validate the models in this thesis.

17.2.2 Model Estimation of Saturation

Estimating saturation has been identified as a major factor limiting the capacity of control protocols to reduce agitation. Saturation points determined, or estimated in real-time, could be used in clinical practice to prevent additional infusions which may result in over-sedation. Although this task is difficult clinically, model estimation of the saturation points could be used as an approximate indicator, and sedative delivery rates capped accordingly.

17.2.3 Blood Concentration Study

The pharmacokinetic portion of the models in this thesis can be verified independently through simple clinical studies investigating the concentrations of drugs in critically ill patients over time. Drug concentrations recorded with drug infusion rates could be compared to modelled concentrations, and the PK parameters of the model adjusted accordingly. However, because the patient-specific parameters in these models lie primarily in the PD components, the improved parameters resulting from such a study may not significantly change the results.

17.3 Control Systems Considerations

17.3.1 Alternative Lyapunov Control Formulation

The current H_∞ methodology employs $\mathbf{v} = \mathbf{x}^\mathbf{T}\mathbf{P}\mathbf{x}$ as the general Lyapunov equation. However, other equations which satisfy the role of the Lyapunov equation exist. A common Lyapunov equation used in stable compartment systems is $\mathbf{v} = \mathbf{e}^\mathbf{T}\mathbf{x}$, which is valid for positive systems. This could be used in the H_∞ analysis to see what effect it has on the optimal gains obtained.

17.3.2 Include $\dot{A}$ in H_∞ Methodology

The current H_∞ methodology employs agitation, A, as the regulated feedback quantity. The addition of the rate of change of agitation, $\dot{A}$, into the regulated output vector may produce control gains that reduce agitation as well as its rate of change. This approach may improve agitation management.

17.3.3 Simulate Published Results

The models developed may be used to simulate the results published by Kress et al. [2000]. In this study the interruption of continuous sedative infusions lead to a reduction in over-sedation. By directly simulating the protocol employed in this study, similar results may be obtained.

17.4 Summary

In addition to the ideas mentioned in this chapter, there are many others that could improve or contribute to this research. However, some areas will have a greater impact than others. In all cases it is important to ensure that the future work is relevant to the advancement of the model and control protocols, and has clinical implications. The areas of greatest clinical and research potential identified in this chapter are:

1. Predator-Prey model investigation
2. Clinical validation using quantified agitation sensors
3. Clinical saturation determination using model estimation

Appendix A

Proof 1

Proposition. $Ex(\hat{\mu}_t)$ and $Var(\hat{\mu}_t)$ can be estimated by:

$$\hat{Ex}(\hat{\mu}_t) = \sum_{i=-m}^{m} \omega_{t,i}\hat{\mu}_{t+i} \tag{A.1}$$

$$\begin{aligned} \hat{Var}(\hat{\mu}_t) &= \hat{\sigma}_0^2 \sum_{i=-m}^{m} \omega_{t,i}^2 + 2\hat{\sigma}_1^2 \sum_{i=-m}^{m-1} \omega_{t,i}\omega_{t,i+1} + 2\hat{\sigma}_2^2 \sum_{i=-m}^{m-2} \omega_{t,i}\omega_{t,i+2} + ... \\ &\quad ... + 2\hat{\sigma}_{2m}^2 \omega_{t,-m}\omega_{t,m} \end{aligned} \tag{A.2}$$

respectively, where $\hat{\sigma}_\lambda^2$ is defined:

$$\hat{\sigma}_\lambda^2 = \frac{1}{n-\lambda} \sum_{k=1}^{n-\lambda} (U_k - \hat{\mu}_k)(U_{k+\lambda} - \hat{\mu}_{k+\lambda}) \quad \forall \ \lambda = 0, 1, ..., 2m \tag{A.3}$$

Proof:

$$Ex(\hat{\mu}_t) = Exp\left(\sum_{i=-m}^{m} \omega_{t,i} U_{t+i} \right) = \sum_{i=-m}^{m} \omega_{t,i} Ex(U_{t+i}) = \sum_{i=-m}^{m} \omega_{t,i}\mu_{t+i} \tag{A.4}$$

and so, estimating μ_{t+i} by $\hat{\mu}_{t+i}$, an estimate for $Ex(\hat{\mu}_t)$ is

$$\hat{Ex}(\hat{\mu}_t) = \sum_{i=-m}^{m} \omega_{t,i}\hat{\mu}_{t+i} \tag{A.5}$$

Next,

$$Var(\hat{\mu}_t) = Exp[(\hat{\mu}_t - Ex(\hat{\mu}_t))^2] \tag{A.6}$$

and

$$\hat{\mu}_t - Ex(\hat{\mu}_t) = \sum_{i=-m}^{m} \omega_{t,i}(U_{t+i} - \mu_{t+i}) = \sum_{i=-m}^{m} \omega_{t,i}\epsilon_{t+i} \tag{A.7}$$

and so

$$(\hat{\mu}_t - Ex(\hat{\mu}_t))^2 = \sum_{i=-m}^{m} \omega_{t,i}^2 \epsilon_{t+i}^2 + 2 \sum_{i=-m}^{m-1} \sum_{i<j\leq m} \omega_{t,i}\omega_{t,j}\epsilon_{t+i}\epsilon_{t+j} \quad \text{(A.8)}$$

Therefore,

$$\begin{aligned} Ex[(\hat{\mu}_t - Ex(\hat{\mu}_t))^2] &= \sum_{i=-m}^{m} \omega_{t,i}^2 Ex(\epsilon_{t+i}^2) \\ &\quad +2 \sum_{i=-m}^{m} \sum_{i<j\leq m} \omega_{t,i}\omega_{t,j} Ex(\epsilon_{t+i}\epsilon_{t+j}) \end{aligned} \quad \text{(A.9)}$$

Let σ_λ^2 be the lag λ covariance for ϵ. Then

$$\begin{aligned} Ex[(\hat{\mu}_t - Ex(\hat{\mu}_t))^2] &= \sigma_0^2 \sum_{i=-m}^{m} \omega_{t,i}^2 + 2\sigma_1^2 \sum_{i=-m}^{m-1} \omega_{t,i}\omega_{t,i+1} \\ &\quad +2\sigma_2^2 \sum_{i=-m}^{m-2} \omega_{t,i}\omega_{t,i+2} + ... + 2\sigma_{2m}^2 \omega_{t,-m}\omega_{t,m} \end{aligned} \quad \text{(A.10)}$$

and it remains to compute σ_λ^2 for $\lambda = 0, 1, ..., 2m$. Using the observations, $U_{1:n}$, and the estimates, $\hat{\mu}_{1:n}$, let

$$\hat{\varepsilon}_t = U_t - \hat{\mu}_t \quad \text{(A.11)}$$

for t = 1, 2, ..., n. Then for $\lambda = 0, 1, ..., 2m$, estimate σ_λ^2 by

$$\hat{\sigma}_\lambda^2 = \frac{1}{n-\lambda} \sum_{i=1}^{n-\lambda} (\hat{\varepsilon}_i \hat{\varepsilon}_{i+\lambda}) \quad \text{(A.12)}$$

Finally, $Var(\hat{\mu}_t)$ can be estimated by

$$\begin{aligned} Var(\hat{\mu}_t) &= \hat{\sigma}_0^2 \sum_{i=-m}^{m} \omega_{t,i}^2 + 2\hat{\sigma}_1^2 \sum_{i=-m}^{m-1} \omega_{t,i}\omega_{t,i+1} + 2\hat{\sigma}_2^2 \sum_{i=-m}^{m-2} \omega_{t,i}\omega_{t,i+2} + ... \\ &\quad ... + 2\hat{\sigma}_{2m}^2 \omega_{t,-m}\omega_{t,m} \end{aligned} \quad \text{(A.13)}$$

where Equation (A.13) is the same as Equation (5.12).

■

Appendix B

Proof 2

Theorem. Let $Ex(\tilde{f}_t)$ and $Var(\tilde{f}_t)$ be the mean and variance of $\tilde{f}_t$. Then

$$Ex(\tilde{f}_t) = \hat{Ex}(\hat{\mu}_t) \tag{B.1}$$

and

$$Var(\tilde{f}_t) = \alpha_t^2[s_t^2 + \sum_{i=-m}^{m} \omega_{t,i}\hat{\mu}_{t+i}^2 - \hat{Ex}(\hat{\mu}_t)^2] \tag{B.2}$$

Proof:

$$\begin{aligned}
Ex(\tilde{f}_t) &= \int \hat{\mu}\tilde{f}_t(\hat{\mu})d\hat{\mu} \\
&= \sum_{i=-m}^{m} \omega_{t,i} \int \hat{\mu}\phi[\hat{\mu}|\alpha_t\hat{\mu}_{t+i} + (1-\alpha_t)\hat{Ex}(\hat{\mu}_t), \alpha_t^2 s_t^2]d\hat{\mu} \\
&= \sum_{i=-m}^{m} \omega_{t,i}[\alpha_t\hat{\mu}_{t+i} + (1-\alpha_t)\hat{Ex}(\hat{\mu}_t)] \\
&= \alpha_t \sum_{i=-m}^{m} \omega_{t,i}\hat{\mu}_{t+i} + (1-\alpha_t)\hat{Ex}(\hat{\mu}_t) \\
&= \hat{Ex}(\hat{\mu}_t)
\end{aligned} \tag{B.3}$$

and

$$\begin{aligned}
Var(\tilde{f}_t) &= \int \hat{\mu}^2 \tilde{f}_t(\hat{\mu}) d\hat{\mu} - Ex(\tilde{f}_t)^2 \\
&= \sum_{i=-m}^{m} \omega_{t,i} \int \hat{\mu}^2 \phi[\hat{\mu}|\alpha_t \hat{\mu}_{t+i} + (1-\alpha_t)\hat{Ex}(\hat{\mu}_t), \alpha_t^2 s_t^2] d\hat{\mu} - \hat{Ex}(\hat{\mu}_t)^2 \\
&= \sum_{i=-m}^{m} \omega_{t,i} [\alpha_t^2 s_t^2 + (\alpha_t \hat{\mu}_{t+i} + (1-\alpha_t)\hat{Ex}(\hat{\mu}_t))^2] - \hat{Ex}(\hat{\mu}_t)^2 \\
&= \alpha_t^2 s_t^2 + \alpha_t^2 \sum_{i=-m}^{m} \omega_{t,i} \hat{\mu}_{t+i}^2 + 2\alpha_t(1-\alpha_t)\hat{Ex}(\hat{\mu}_t) \sum_{i=-m}^{m} \omega_{t,i} \hat{\mu}_{t+i} + \\
&\quad + (1-\alpha_t)^2 \hat{Ex}(\hat{\mu}_t)^2 - \hat{Ex}(\hat{\mu}_t)^2 \\
&= \alpha_t^2 [s_t^2 + \sum_{i=-m}^{m} \omega_{t,i} \hat{\mu}_{t+i}^2 - \hat{Ex}(\hat{\mu}_t)^2] \qquad \text{(B.4)}
\end{aligned}$$

The mean of $\tilde{f}_t$ is automatically equal to $\hat{Ex}(\tilde{f}_t)$. The next theorem shows that the variance of $\tilde{f}_t$ can be made equal to $\hat{Var}(\tilde{f}_t)$ through appropriate choice of α_t and s_t. First, a practical choice of the kernel bandwidth, $\alpha_t s_t$ is selected. Let m_t be the actual number of points within the support of the regression kernel, so that $m_t \leq 2m+1$, and let $\omega_{t,(1)}, ..., \omega_{t,(m_t)}$ be the weights corresponding to those m_t points. Define the *effective number of points* for $\tilde{f}_t$ as [Liu and Chen, 1995]

$$\tilde{m}_t = \left(\sum_{i=1}^{m_t} \omega_{t,(i)}^2 \right)^{-1} \qquad \text{(B.5)}$$

The use of $\tilde{m}_t$ rather than m_t for a weighted (dependent) collection of points is a simple way to account for dependence. Notice that $\tilde{m}_t = m_t$ if the points are actually independent. Therefore, a simple practical choice of bandwidth for the density kernel is [Scott, 1992]

$$\alpha_t s_t = \tilde{m}_t^{-\frac{1}{5}} \sqrt{\hat{Var}(\hat{\mu}_t)} \qquad \text{(B.6)}$$

■

Theorem. Let

$$\hat{W}_t = \sum_{i=-m}^{m} \omega_{t,i} \hat{\mu}_{t+i}^2 - \hat{Ex}(\mu_t)^2 \qquad \text{(B.7)}$$

If

$$\alpha_t^2 s_t^2 = \hat{Var}(\hat{\mu}_t)\tilde{m}_t^{-\frac{2}{5}} \tag{B.8}$$

and

$$\alpha_t^2 = (1 - \tilde{m}_t^{-\frac{2}{5}})\frac{\hat{Var}(\hat{\mu}_t)}{\hat{W}_t} \tag{B.9}$$

then

$$Var(\tilde{f}_t) = \hat{Var}(\hat{\mu}_t) \tag{B.10}$$

Proof:

$$Var(\tilde{f}_t) = \alpha_t^2(s_k^2 + \hat{W}_t) = \hat{Var}(\hat{\mu}_t)\tilde{m}_t^{-\frac{2}{5}} + (1 - \tilde{m}_t^{-\frac{2}{5}})\hat{Var}(\hat{\mu}_t) = \hat{Var}(\hat{\mu}_t) \tag{B.11}$$

■

References

ADRAC (2004). Propofol: danger of prolonged and high infusion rates in icu. *Australian Adverse Drug Reactions Bulletin.*, 23(6):23–24.

Agogué, F. (2005). *Objective measurements of patient agitation in critical care using physiological signals and fuzzy systems.* Phd thesis, University of Canterbury.

Aitkenhead, A. R., Vater, M., Achola, K., Cooper, C. M., and Smith, G. (1984). Pharmacokinetics of single-dose i.v. morphine in normal volunteers and patients with end-stage renal failure. *Br J Anaesth*, 56(8):813–9.

Albrecht, S., Ihmsen, H., Hering, W., Geisslinger, G., Dingemanse, J., Schwilden, H., and Schuttler, J. (1999). The effect of age on the pharmacokinetics and pharmacodynamics of midazolam. *Clin Pharmacol Ther*, 65(6):630–9.

Anderson, K. and Kenny, G. (2003). Total intravenous anaesthesia (tiva) ii. *Bulletin on the Royal College of Anaesthetists*, Buletin 17:831–834.

Arbour, R. (2000). Sedation and pain management in critically ill adults. *Crit Care Nurse*, 20(5):39–56; quiz 57–8.

Arendt, R. M., Greenblatt, D. J., deJong, R. H., Bonin, J. D., Abernethy, D. R., Ehrenberg, B. L., Giles, H. G., Sellers, E. M., and Shader, R. I. (1983). In vitro correlates of benzodiazepine cerebrospinal fluid uptake, pharmacodynamic action and peripheral distribution. *J Pharmacol Exp Ther*, 227(1):98–106.

Azzalini, A., Bowman, A. W., and Hardle, W. (1989). On the use of nonparametric regression for model checking. *Biometrika*, 76(1):1–11.

Barr, J. and Donner, A. (1995). Optimal intravenous dosing strategies for sedatives and analgesics in the intensive care unit. *Crit Care Clin*, 11(4):827–47.

Bates, J. J., Foss, J. F., and Murphy, D. B. (2004). Are peripheral opioid antagonists the solution to opioid side effects? *Anesth Analg*, 98(1):116–22, table of contents.

Berger, I. and Waldhorn, R. E. (1995). Analgesia, sedation and paralysis in the intensive care unit. *Am Fam Physician*, 51(1):166–72.

Bergman, R. N., Finegood, D. T., and Ader, M. (1985). Assessment of insulin sensitivity in vivo. *Endocr Rev*, 6(1):45–86.

Bion, J. F., Logan, B. K., Newman, P. M., Brodie, M. J., Oliver, J. S., Aitchison, T. C., and Ledingham, I. M. (1986). Sedation in intensive care: morphine and renal function. *Intensive Care Med*, 12(5):359–65.

Bolon, M., Bastien, O., Flamens, C., Paulus, S., Salord, F., and Boulieu, R. (2003). Evaluation of the estimation of midazolam concentrations and pharmacokinetic parameters in intensive care patients using a bayesian pharmacokinetic software (pks) according to sparse sampling approach. *J Pharm Pharmacol*, 55(6):765–71.

Boyd, S. and Ghaoui, L. E. (1993). Method of centers for minimizing generalized eigenvalues. *Linear Algebra and Its Applications*, 188-89:63.

Brattebo, G., Hofoss, D., Flaatten, H., Muri, A. K., Gjerde, S., and Plsek, P. E. (2002). Effect of a scoring system and protocol for sedation on duration of patients' need for ventilator support in a surgical intensive care unit. *BMJ*, 324(7350):1386–9.

Bridges, R. S. and Grimm, C. T. (1982). Reversal of morphine disruption of maternal behavior by concurrent treatment with the opiate antagonist naloxone. *Science*, 218(4568):166–8.

Broersen, P. (2000). Finite sample criteria for autogressive order selection. *IEEE Transactions on Signal Processing*, 48(12).

Broersen, P. (2002). Automatic spectral analysis with time series models. *IEEE Transactions on instrumentation and measurement*, 51(2).

Brook, A. D., Ahrens, T. S., Schaiff, R., Prentice, D., Sherman, G., Shannon, W., and Kollef, M. H. (1999). Effect of a nursing-implemented sedation protocol on the duration of mechanical ventilation. *Crit Care Med*, 27(12):2609–15.

Burns, A. M., Shelly, M. P., and Park, G. R. (1992). The use of sedative agents in critically ill patients. *Drugs*, 43(4):507–15.

Carrasco, G. (2000). Instruments for monitoring intensive care unit sedation. *Crit Care*, 4(4):217–25.

Carson, E. and Cobelli, C. (2001). *Modelling methodology for physiology and medicine*. Academic Press, London.

Chase, J., Rudge, A., Shaw, G., Wake, G., Lee, D., Hudson, I., and Johnston, L. (2004a). Modeling and control of the agitation-sedation cycle for critical care patients. *Medical Engineering & Physics*, 26(6):459–471.

Chase, J., Starfinger, C., Lam, Z.-H., Agogue, F., and Shaw, G. (2004b). Quantifying agitation in sedated ICU patients using heart rate and blood pressure. *Physiological Measurement*, Accepted 1/04, to appear.

Chase, J. G., Agogue, F. A., Starfinger, C., Lam, Z., Shaw, G. M., Rudge, A. D., and Sirisena, H. (2004c). Quantifying agitation in sedated icu patients using digital imaging. *Computer Methods and Programs in Biomedicine*.

Chase, J. G., Rudge, A. D., Lee, D. S., and Shaw, G. M. (2005a). H-infinity control analysis of patient agitation management in the critically ill. *Intl Journal of Intelligent Systems Technologies and Applications (IJISTA)*, accepted September 04 to appear.

Chase, J. G., Shaw, G. M., Lin, J., Doran, C. V., Hann, C., Robertson, M. B., Browne, P. M., Lotz, T., Wake, G. C., and Broughton, B. (2005b). Adaptive bolus-based targeted glucose regulation of hyperglycaemia in critical care. *Med Eng Phys*, 27(1):1–11.

Chase, J. G. and Smith, H. A. (1996). Robust h-infinity control considering actuator saturation part 1: Theory. *Journal of Engineering Mechanics, ASCE*, 122(10):976–983.

Cohen, I. (2002). Management of the agitated intensive care unit patient. *Crit Care Med*, 30(2 Supp):S97–S123.

Cousins, M. and Mather, L. (1984). Intrathecal and epidural administration of opiods. *Anesthesiology*, 61:276–310.

Crippen, D. W. (1990). The role of sedation in the icu patient with pain and agitation. *Crit Care Clin*, 6(2):369.

Crippen, D. W. (1994). Pharmacologic treatment of brain failure and delirium. *Crit Care Clin*, 10(4):733–66.

Dar, R., Ariely, D., and Frenk, H. (1995). The effect of past-injury in pain threshold and tolerance. *Pain*, 60:189–93.

De Deyne, C., Struys, M., Decruyenaere, J., Creupelandt, J., Hoste, E., and Colardyn, F. (1998). Use of continuous bispectral eeg monitoring to assess depth of sedation in icu patients. *Intensive Care Med*, 24(12):1294–8.

De Jonghe, B., Bastuji-Garin, S., Fangio, P., Lacherade, J. C., Jabot, J., Appere-De-Vecchi, C., Rocha, N., and Outin, H. (2005). Sedation algorithm in critically ill patients without acute brain injury. *Crit Care Med*, 33(1):120–7.

De Jonghe, B., Cook, D., Griffith, L., Appere-de Vecchi, C., Guyatt, G., Theron, V., Vagnerre, A., and Outin, H. (2003). Adaptation to the intensive care environment (atice): development and validation of a new sedation assessment instrument. *Crit Care Med*, 31(9):2344–54.

Devlin, J. W., Holbrook, A. M., and Fuller, H. D. (1997). The effect of icu sedation guidelines and pharmacist interventions on clinical outcomes and drug cost. *Ann Pharmacother*, 31(6):689–95.

Doran, C., Chase, J., Shaw, G., Moorhead, K., and Hudson, N. (2004). Automated insulin infusion trials in the ICU. *Diabetes Technology & Therapeutics*, Accepted 1/04, to appear 4/04 6(2).

Doran, C., Moorhead, K., Hudson, N., Chase, J., and Shaw, G. (2003). Derivative weighted active insulin control modelling and clinical trials for ICU patients. *Medical Engineering & Physics*.

Driessen, J. J., Vree, T. B., and Guelen, P. J. (1991). The effects of acute changes in renal function on the pharmacokinetics of midazolam during long-term infusion in icu patients. *Acta Anaesthesiol Belg*, 42(3):149–55.

Ely, E. W., Shintani, A., Truman, B., Speroff, T., Gordon, S. M., Harrell, F. E., J., Inouye, S. K., Bernard, G. R., and Dittus, R. S. (2004). Delirium as a predictor of mortality in mechanically ventilated patients in the intensive care unit. *Jama*, 291(14):1753–62.

Faura, C. C., Collins, S. L., Moore, R. A., and McQuay, H. J. (1998). Systematic review of factors affecting the ratios of morphine and its major metabolites. *Pain*, 74(1):43–53.

Fidler, M., Egan, T., and Kern, S. (2003). A new approach to modeling pharmacodynamic interactions with response surfaces. In *World Congress on Physics in Medicine and Biomedical Engineering*, Sydney, Australia.

Fisher, M. E. (1991). A semiclosed-loop algorithm for the control of blood glucose levels in diabetics. *IEEE Trans Biomed Eng*, 38(1):57–61.

Fragen, R. J. (1997). Pharmacokinetics and pharmacodynamics of midazolam given via continuous intravenous infusion in intensive care units. *Clin Ther*, 19(3):405–19; discussion 367–8.

Fraser, G. L. and Riker, R. R. (2001a). Advances and controversies in sedating the adult critically ill. *The New York Health-System Pharmacist*, 20(3):17–24.

Fraser, G. L. and Riker, R. R. (2001b). Monitoring sedation, agitation, analgesia, and delirium in critically ill adult patients. *Crit Care Clin*, 17(4):967–87.

Furler, S. M., Kraegen, E. W., Smallwood, R. H., and Chisholm, D. J. (1985). Blood glucose control by intermittent loop closure in the basal mode: computer simulation studies with a diabetic model. *Diabetes Care*, 8(6):553–61.

Geller, E., Halpern, P., Barzelai, E., Sorkine, P., Lewis, M. C., Silbiger, A., and Nevo, Y. (1988). Midazolam infusion and the benzodiazepine antagonist flumazenil for sedation of intensive care patients. *Resuscitation*, 16(Suppl):S31–9.

Gentilini, A., Frei, C. W., Glattfedler, A. H., Morari, M., Sieber, T. J., Wymann, R., Schnider, T. W., and Zbinden, A. M. (2001). Multitasked closed-loop control in anesthesia. *IEEE Eng Med Biol Mag*, 20(1):39–53.

Gentilini, A., Schaniel, C., Morari, M., Bieniok, C., Wymann, R., and Schnider, T. (2002). A new paradigm for the closed-loop intraoperative administration of analgesics in humans. *IEEE Trans Biomed Eng*, 49(4):289–99.

Gilbert, T. T., Wagner, M. R., Halukurike, V., Paz, H. L., and Garland, A. (2001). Use of bispectral electroencephalogram monitoring to assess neurologic status in unsedated, critically ill patients. *Crit Care Med*, 29(10):1996–2000.

Gilliland, H. E., Prasad, B. K., Mirakhur, R. K., and Fee, J. P. (1996). An investigation of the potential morphine sparing effect of midazolam. *Anaesthesia*, 51(9):808–11.

Greenfield, K., Dove, R., and Shaw, G. (2001). Optimisation of sedation therapy within an intensive care setting. In *Proc. of Engineering and Physical Sciences in Medicine*, Fremantle, Australia.

Guyton, A. C. and Hall, J. E. (1996). *Textbook of medical physiology.* ninth edition.

Hann, C. E., Chase, J. G., Lin, J., Lotz, T., Doran, C., and Shaw, G. M. (2005). Integral-based parameter identification for long-term dynamic verification of a glucose-insulin model. *Computer Methods and Programs in Biomedicine*, 77(3):pp. 259–270.

Hardle, W. (1990). *Applied Nonparametric Regression.* Cambridge university press.

Helson, H. (1959). *Psychology: A study of a science*, volume 1. McGraw-Hill, New York.

Hughes, M., Glass, P., and Jacobs, J. (1992). Context-sensitive half-time in multicompartment pharmacokinetic models for intravenous anesthetic drugs. *Anesthesiology*, 76(3):334–41.

Jaarsma, A. S., Knoester, H., van Rooyen, F., and Bos, A. P. (2001). Biphasic positive airway pressure ventilation (pev+) in children. *Crit Care*, 5(3):174–7.

Kang, T. M. (2002). Propofol infusion syndrome in critically ill patients. *Ann Pharmacother*, 36(9):1453–6.

Kenny, G. N. and Mantzaridis, H. (1999). Closed-loop control of propofol anaesthesia. *Br J Anaesth*, 83(2):223–8.

Kienitz, K. and Yoneyama, T. (1993). A robust controller for insulin pumps based on h_∞ theory. *IEEE Trans. Biomed. Eng.*, 40(11):1133–1137.

Knoester, P. D., Jonker, D. M., Van Der Hoeven, R. T., Vermeij, T. A., Edelbroek, P. M., Brekelmans, G. J., and de Haan, G. J. (2002). Pharmacokinetics and pharmacodynamics of midazolam administered as a concentrated intranasal spray. a study in healthy volunteers. *Br J Clin Pharmacol*, 53(5):501–7.

Koopmans, R., Dingemanse, J., Danhof, M., Horsten, G. P., and van Boxtel, C. J. (1988). Pharmacokinetic-pharmacodynamic modeling of midazolam effects on the human central nervous system. *Clin Pharmacol Ther*, 44(1):14–22.

Kreek, M. J. (2002). *The Genomic Revolution: Unveiling the Unity of Life.* Joseph Henry Press, Washington D.C.

Kress, J. P., Pohlman, A. S., and Hall, J. B. (2002). Sedation and analgesia in the intensive care unit. *Am J Respir Crit Care Med*, 166(8):1024–8.

Kress, J. P., Pohlman, A. S., O'Connor, M. F., and Hall, J. B. (2000). Daily interruption of sedative infusions in critically ill patients undergoing mechanical ventilation. *N Engl J Med*, 342(20):1471–7.

Lam, Z., Starfinger, C., Chase, J. G., Shaw, G. M., and Agogue, F. A. (2003). Movement quantification for use in agitation quantification in icu patients. In *World congress on medical physics and biomedical engineering*, Sydney, Australia.

Lam, Z.-H. (2003). *Agitation measurement and signal processing of physiological variables for sedated subjects.* Masters thesis, University of Canterbury.

Lam, Z.-H., Lee, J.-Y., Hwang, K.-S., Chase, J., and G.C., W. (2002). Active insulin infusion using optimal and derivative-weighted control. *Journal of Medical Engineering and Physics*, 24(10):663–672.

Lee, D., Rudge, A., Chase, J., Hudson, N., Shaw, G., Johnston, L., and Wake, G. (2003). Dynamic model assessment using a probability band for local linear kernel regression, with an application in agitation-sedation modeling. In *Proc. of New Zealand Statistical Association 54th Annual Conference*, Massey University, Palmerston North, New Zealand.

Lee, D. S., Rudge, A. D., Chase, J. G., and Shaw, G. M. (2005). A new model validation tool using kernel regression and density estimation. *Computer Methods and Programs in Biomedicine*, In press.

Lehman, E. and Deutsch, T. (1996). Computer assisted diabetes care: a 6-year retrospective. *Computer Methods and Programs in Biomedicine*, 50:209–230.

Levine, R. L. (1994). Pharmacology of intravenous sedatives and opioids in critically ill patients. *Crit Care Clin*, 10(4):709–31.

Liu, J. and Chen, R. (1995). Blind deconvolution via sequential imputations. *Journal of the American Statistical Association*, 90(430):567–576.

Ljung, L. (1999). *System identication.* Prentice-Hall., Upper Saddle River, NJ, 2nd edition edition.

Lötsch, J., Skarke, C., Schmidt, H., Liefhold, J., and Geisslinger, G. (2002). Pharmacokinetic modeling to predict morphine and morphine-6-glucuronide plasma concentrations in healthy young volunteers. *Clin Pharmacol Ther*, 72(2):151–62.

Mackay, D. M. (1963). Psychophysics of perceived intensity: A theoretical basis for fechner's and stevens' laws. *Science*, 139:1213–1216.

MacLaren, R., Plamondon, J. M., Ramsay, K. B., Rocker, G. M., Patrick, W. D., and Hall, R. I. (2000). A prospective evaluation of empiric versus protocol-based sedation and analgesia. *Pharmacotherapy*, 20(6):662–72.

Malacrida, R., Fritz, M. E., Suter, P. M., and Crevoisier, C. (1992). Pharmacokinetics of midazolam administered by continuous intravenous infusion to intensive care patients. *Crit Care Med*, 20(8):1123–6.

Mandema, J. W., Tuk, B., van Steveninck, A. L., Breimer, D. D., Cohen, A. F., and Danhof, M. (1992). Pharmacokinetic-pharmacodynamic modeling of the central nervous system effects of midazolam and its main metabolite alpha-hydroxymidazolam in healthy volunteers. *Clin Pharmacol Ther*, 51(6):715–28.

Mathworks (2005). www.mathworks.com/matlabcentral/fileexchange.

McKeage, K. and Perry, C. M. (2003). Propofol: a review of its use in intensive care sedation of adults. *CNS Drugs*, 17(4):235–72.

Meineke, I., Freudenthaler, S., Hofmann, U., Schaeffeler, E., Mikus, G., Schwab, M., Prange, H. W., Gleiter, C. H., and Brockmoller, J. (2002). Pharmacokinetic modelling of morphine, morphine-3-glucuronide and morphine-6-glucuronide in plasma and cerebrospinal fluid of neurosurgical patients after short-term infusion of morphine. *Br J Clin Pharmacol*, 54(6):592–603.

Milne, R. W., Nation, R. L., and Somogyi, A. A. (1996). The disposition of morphine and its 3- and 6-glucuronide metabolites in humans and animals, and the importance of the metabolites to the pharmacological effects of morphine. *Drug Metab Rev*, 28(3):345–472.

Minto, C. F., Schnider, T. W., Short, T. G., Gregg, K. M., Gentilini, A., and Shafer, S. L. (2000). Response surface model for anesthetic drug interactions. *Anesthesiology*, 92(6):1603–16.

Nasraway, S. A., J. (2005). The bispectral index: expanded performance for everyday use in the intensive care unit? *Crit Care Med*, 33(3):685–7.

Nasraway, S. A. J., C., W. E., Kelleher, R. M., Yasuda, C. M., and Donnelly, A. M. (2002). How reliable is the bispectral index in critically ill patients? a prospective, comparative, single-blinded observer study. *Crit Care Med*, 30(7):1483–7.

Oldenhof, H., de Jong, M., Steenhoek, A., and Janknegt, R. (1988). Clinical pharmacokinetics of midazolam in intensive care patients, a wide interpatient variability? *Clin Pharmacol Ther*, 43(3):263–9.

Ollerton, R. (1989). Application of optimal control theory to diabetes mellitus. *Internation Journal of Control*, 50(6):2503–2522.

Osborne, R., Joel, S., Grebenik, K., Trew, D., and Slevin, M. (1993). The pharmacokinetics of morphine and morphine glucuronides in kidney failure. *Clin Pharmacol Ther*, 54(2):158–67.

Persson, P., Nilsson, A., Hartvig, P., and Tamsen, A. (1987). Pharmacokinetics of midazolam in total i.v. anaesthesia. *Br J Anaesth*, 59(5):548–56.

Platten, H. P., Schweizer, E., Dilger, K., Mikus, G., and Klotz, U. (1998). Pharmacokinetics and the pharmacodynamic action of midazolam in young and elderly patients undergoing tooth extraction. *Clin Pharmacol Ther*, 63(5):552–60.

Pol, H., Hijman, R., Baare, W., and J.M., v. R. (1998). Effects of context on judgements of odor intensities in humans. *Chemical Senses*, 23:131–135.

Ramsay, M. A., Savege, T. M., Simpson, B. R., and Goodwin, R. (1974). Controlled sedation with alphaxalone-alphadolone. *Br Med J*, 2(920):656–9.

Riker, R., Picard, J., and Fraser, G. (1999). Prospective evaluation of the sedation-agitation scale for adult critically ill patients. *Crit Care Med*, 27(7):1325–9.

Ritz, R., Zuber, M., Elsasser, S., and Scollo-Lavizzari, G. (1990). Use of flumazenil in intoxicated patients with coma. a double-blind placebo-controlled study in icu. *Intensive Care Med*, 16(4):242–7.

Romberg, R., Olofsen, E., Sarton, E., den Hartigh, J., Taschner, P. E., and Dahan, A. (2004). Pharmacokinetic-pharmacodynamic modeling of morphine-6-glucuronide-induced analgesia in healthy volunteers: absence of sex differences. *Anesthesiology*, 100(1):120–33.

Rorabaugh, C. (1998). *DSP Primer*. McGraw-Hill, New York.

Rudge, A., Chase, J., Shaw, G., and Wake, G. (2003a). Improved agitation management in critically ill patients via feedback control of sedation administration. In *Proc. of World Congress on Medical Physics and Biomedical Engineering (WC2003)*, Sydney, Australia.

Rudge, A. D., Chase, J. G., Shaw, G. M., Johnston, L., and Wake, G. C. (2003b). Modelling and control of the agitation-sedation cycle. In *5th IFAC Symposium on Modelling and Control in Biomedical Systems*, pages pp. 89–95, Melbourne, Australia.

Rudge, A. D., Chase, J. G., Shaw, G. M., Lee, C., Wake, G. C., Hudson, I. L., and Johnston, L. (2005a). Impact of control on agitation-sedation dynamics. *Control Engineering Practice (CEP)*, accepted June 04 to appear.

Rudge, A. D., Chase, J. G., Shaw, G. M., and Lee, D. S. (2004a). Automated agitation management accounting for saturation dynaimcs. In *26th International Conf of IEEE Engineering in Med and Biology Society (EMBS 2004)*, pages pp. 3459–3462, San Francisco, CA.

Rudge, A. D., Chase, J. G., Shaw, G. M., and Lee, D. S. (2004b). Physiologically-based minimal model of agitation-sedation dynamics. In *26th International Conf of IEEE Engineering in Med and Biology Society (EMBS 2004)*, pages pp. 774–777, San Francisco, CA.

Rudge, A. D., Chase, J. G., Shaw, G. M., and Lee, D. S. (2005b). Physiological modelling of agitation-sedation dynamics. *Medical Engineering and Physics*, accepted 3/05 to appear.

Ruiz-Velazquez, E., Femat, R., and Campos-Delgado, D. (2004). Blood glucose control for type i diabetes mellitus: a robust tracking h_∞ problem. *Control Engineering PRactice*, 12:1179–1195.

Schmidt, G. N., Bischoff, P., Standl, T., Lankenau, G., Hilbert, M., and Schulte Am Esch, J. (2004). Comparative evaluation of narcotrend, bispectral index, and classical electroencephalographic variables during induction, maintenance, and emergence of a propofol/remifentanil anesthesia. *Anesth Analg*, 98(5):1346–53.

Schwilden, H., Stoeckel, H., and Schuttler, J. (1989). Closed-loop feedback control of propofol anaesthesia by quantitative eeg analysis in humans. *Br J Anaesth*, 62(3):290–6.

Scott, D. (1992). *Multivariate desnisty Estimation: Theory, Practice and Visualization.* Wiley-Interscience.

Sessler, C. N., Gosnell, M. S., Grap, M. J., Brophy, G. M., O'Neal, P. V., Keane, K. A., Tesoro, E. P., and Elswick, R. K. (2002). The richmond agitation-sedation scale: validity and reliability in adult intensive care unit patients. *Am J Respir Crit Care Med*, 166(10):1338–44.

Shafer, A. (1998). Complications of sedation with midazolam in the intensive care unit and a comparison with other sedative regimens. *Crit Care Med*, 26(5):947–56.

Shaw, G., Dove, R., Greenfield, K. M., Rudge, A., and Chase, J. (2003a). A computerised approach to sedation administration in critically ill patients. In *Proc. of ANZICS/ACCCN 28th Australia and New Zealand ASM on Intensive Care*, Dunedin, New Zealand.

Shaw, G. M., Chase, J. G., Lee, D. S., Hooper, E., Rudge, A. D., and Agogue, F. (2005). Emerging methods for sedation and agitation management in critical illness. *Critical Care Medicine*, 32(12):A97.

Shaw, G. M., Chase, J. G., Rudge, A. D., Starfinger, C., Lam, Z., Lee, D. S., Wake, G. C., Greenfield, K., and Dove, R. (2003b). Rethinking sedation and agitation management in critical illness. *Critical care and resuscitation*, 5:198–206.

Silverman, B. (1986). *Density estimation for statistics and data analysis.* Chapman & Hall.

Simmons, L. E., Riker, R. R., Prato, B. S., and Fraser, G. L. (1999). Assessing sedation during intensive care unit mechanical ventilation with the bispectral index and the sedation-agitation scale. *Crit Care Med*, 27(8):1499–504.

Smith, B. and Reves, J. (1995). *Computer-assisted Continuous Infusion of Intravenous Anesthesia Drugs*, volume 33 of *International Anesthesiology Clinics*. Little, Brown and Company, Boston.

Smyrnios, N., Connolly, A., Wilson, M., Curley, F., French, C., Heard, S., and Irwin, R. (2002). Effects of a multifaceted, multidisciplinary, hospital-wide quality improvement program on weaning from mechanical ventilation. *Crit Care Med*, 30(6):1224–30.

Starfinger, C. (2003). *Measurement of agitation in sedated ICU patients using biomedical signal processing*. Dipl. inform. med. thesis, Universität Heidelberg/FH Heilbronn.

Starfinger, C., Lam, Z.-H., Chase, J., Shaw, G., and Agogue, F. (2003). Measurement of agitation in sedated ICU patients using adaptive signal processing and fuzzy mathematics. In *Proc. of World Congress on Medical Physics and Biomedical Engineering (WC2003)*, Sydney, Australia.

Szokol, J. and Vender, J. (2001). Anxiety, delirium, and pain in the intensive care unit. *Crit Care Clin*, 17(4):821–42.

Tonner, P. H., Wei, C., Bein, B., Weiler, N., Paris, A., and Scholz, J. (2005). Comparison of two bispectral index algorithms in monitoring sedation in postoperative intensive care patients. *Crit Care Med*, 33(3):580–4.

Tuk, B., van Oostenbruggen, M. F., Herben, V. M., Mandema, J. W., and Danhof, M. (1999). Characterization of the pharmacodynamic interaction between parent drug and active metabolite in vivo: midazolam and alpha-oh-midazolam. *J Pharmacol Exp Ther*, 289(2):1067–74.

Tverskoy, M., Fleyshman, G., Ezry, J., Bradley, E. L., J., and Kissin, I. (1989). Midazolam-morphine sedative interaction in patients. *Anesth Analg*, 68(3):282–5.

Vidyasagar, M. (1993). *Nonlinear systems analysis*. Prentice-hall, Englewood cliffs, New Jersey.

Vinik, H. R., Reves, J. G., Greenblatt, D. J., Abernethy, D. R., and Smith, L. R. (1983). The pharmacokinetics of midazolam in chronic renal failure patients. *Anesthesiology*, 59(5):390–4.

Volles, D. F. and McGory, R. (1999). Pharmacokinetic considerations. *Crit Care Clin*, 15(1):55–75.

Wagner, B. and O'Hara, D. (1997). Pharmacokinetics and pharmacodynamics of sedatives and analgesics in the treatment of agitated critically ill patients. *Clin Pharmacokinet*, 33(6):426–53.

Wallach, H. (1963). The perception of neutral colors. *Scientific American*, 208:107–116.

Wand, M. and Jones, M. (1995). *Kernel Smoothing*. Monographs on Statistics and Applied Probability. Chapman & Hall, London.

Weinert, C. R., Chlan, L., and Gross, C. (2001). Sedating critically ill patients: factors affecting nurses' delivery of sedative therapy. *Am J Crit Care*, 10(3):156–65; quiz 166–7.

West, M. (1993). Approximating posterior distributions by mixtures. *Journal of the royal Statistical Society*, 55:409–422.

Wood, M. and Wood, A. (1990). *Drugs and Anesthesia, Pharmacology for Anesthesiologists*. Williams & Wilkins, Baltimore, Maryland.

Wu, S. and Boyd, S. (2000). *A parser/solver for semidefinite programs with matrix structure*. Recent advances in LMI methods for control, SIAM.

Young, C., Knudsen, N., Hilton, A., and Reves, J. G. (2000). Sedation in the intensive care unit. *Crit Care Med*, 28(3):854–66.

Young, C. C. and Prielipp, R. C. (2001). Benzodiazepines in the intensive care unit. *Crit Care Clin*, 17(4):843–62.